THE INFLUENCE OF TERRAIN PARAMETERS ON THE SPATIAL VARIABILITY OF POTENTIAL AVALANCHE TRIGGER LOCATIONS IN COMPLEX AVALANCHE TERRAIN

by

Zachary Mark Guy

A thesis submitted in partial fulfillment
of the requirements for the degree

of

Master of Science

in

Earth Sciences

MONTANA STATE UNIVERSITY
Bozeman, Montana

November, 2011

APPROVAL

of a thesis submitted by

Zachary Mark Guy

This thesis has been read by each member of the thesis committee and has been found to be satisfactory regarding content, English usage, format, citation, bibliographic style, and consistency and is ready for submission to the Division of Graduate Education.

Dr. Stephan G. Custer
(Co-Chair)

Dr. Karl W. Birkeland
(Co-Chair)

Approved for the Department of Earth Sciences

Dr. Stephan G. Custer

Approved for The Graduate School

Dr. Carl A. Fox

STATEMENT OF PERMISSION TO USE

In presenting this thesis in partial fulfillment of the requirements for a master's degree at Montana State University, I agree that the Library shall make it available to borrowers under rules of the Library.

If I have indicated my intention to copyright this thesis by including a copyright notice page, copying is allowable only for scholarly purposes, consistent with "fair use" as prescribed in the U.S. Copyright Law. Requests for permission for extended quotation from or reproduction of this thesis in whole or in parts may be granted only by the copyright holder.

Zachary Mark Guy

November, 2011

ACKNOWLEDGEMENTS

This research would not have been possible without all of the support that I received along the way. I would like to thank my advisor, Karl Birkeland, for his wisdom and assistance through the entire research process. I'd also like to thank my other committee members, Stuart Challendar and Steve Custer and also Jordy Hendrikx for their involvement in my research.

Moonlight Basin, Big Sky, and Jackson Hole Ski Patrols were incredibly supportive in allowing access to their terrain, their weather data, and for looking out for the safety of sampling teams. I'd especially like to thank Brad Carpenter, Nick Armitage, Chelan Babineau-Z, and Bob Comey.

I am grateful for research grants from the American Avalanche Association, Mazamas, the American Alpine Club, and the Association of American Geographers. LiDAR data was provided by Brian McGlynn and the MSU Watershed Hydrology Laboratory with support from the U.S. National Science Foundation (BCS #0518429) and from the Bridger Teton National Forest Avalanche Center.

I'd like to thank all of my field assistants for putting up with cold, windy, and long days on exposed terrain, especially Jordan Mancey, who was always far too eager to help out. I'd also like to thank Lucy Marshall and Jim Robison-Cox for their statistical counsel, Diana Cooksey for her assistance with the GPS units, Alex Marienthal and Leila Sterman for peer reviews, and everyone else who offered advice along the way.

Lastly, I am most grateful to my close friends and family for supporting me through my graduate studies.

TABLE OF CONTENTS

TABLE OF CONTENTS - CONTINUED

LIST OF FIGURES

Figure Page

LIST OF FIGURES - CONTINUED

Figure Page

LIST OF FIGURES - CONTINUED

Figure Page

LIST OF FIGURES - CONTINUED

Figure Page

LIST OF TABLES

Table Page

LIST OF TABLES - CONTINUED

Table Page

LIST OF TABLES - CONTINUED

ABSTRACT

More winter recreationists are venturing into steep avalanche chutes and "extreme" terrain each year, and avalanche fatalities are increasing. The slope-scale spatial variability of weak layers and slabs and how it relates to this complex terrain is of critical importance but poorly understood. In this study, I use terrain parameters to model potential trigger locations (PTLs) of slab avalanches, which are defined based on slab thicknesses and presence of weak layers.

In a sample couloirs and chutes in Montana and Wyoming, field teams tracked and mapped persistent weak layers and slabs with probe sampling. Terrain parameters derived from a one meter DEM were used to explore the relationships between PTLs and terrain. Exploratory analysis, multi-model classification trees, and logistic regression models support strong relationships between terrain and PTLs.

Modeling of PTLs was highly successful for individual couloirs, with terrain-based model success rates frequently exceeding 70% for depth hoar PTLs and 85% for near-surface weak layers. However, models varied widely from couloir to couloir, with generally poor cross-validation results between couloirs, suggesting that the relationships between terrain and PTLs in each couloir are unique and highly complex. For these 21 couloirs in steep alpine terrain, parameters relating to wind deposition and scouring have the strongest association with PTLs.. Parameters with the greatest ability to discriminate PTLs are distance from the edge of a couloir, relative elevation, degree of wind exposure, and degree of terrain exposure. The influences of these and other terrain parameters vary, depending on broader-scale terrain characteristics, prior weather patterns, and seasonal trends.

Practical implications from this study are numerous. With an understanding of the broader scale influences and physical processes involved, we can use terrain to optimize stability test locations, explosive placements, or route selection. The unique nature of each couloir means that simple rules relating terrain to PTLs will not apply, although couloirs in the same cirque generally share similarities. This work increases our understanding of how each parameter relates to the physical processes causing PTLs and how these relationships can vary. This information will help to improve practical decision-making ability as well as future modeling efforts.

1. INTRODUCTION

Avalanches pose a serious threat to human life and infrastructure in mountainous areas worldwide. In the United States, avalanches kill more people on average annually than earthquakes, landslides, or other mass movement phenomena (Voight et al., 1990). Last winter season, 25 people were killed in avalanches in the United States (avalanche.org, 2011). One of the best ways to mitigate avalanche deaths is an increased understanding of avalanches and the snowpack.

The majority of avalanche fatalities are the result of slab avalanches (McClung and Schaerer, 2006). Slab avalanches occur when a more cohesive slab of snow overlies a less cohesive weak layer and the conditions in the snowpack are conducive to weak layer fracture across a slope (Schweizer et al., 2003). Snow accumulates and metamorphoses in layers that may or may not be continuous at various scales, from centimeters to kilometers, and are often difficult to predict. A crucial element for improving avalanche prediction and mitigation is understanding the structure and spatial pattern of weak layers and slabs as they interact with the terrain.

Numerous studies in the past half century have characterized the spatial variability of snow properties such as penetration resistance, shear strength, and stability test scores. Results vary tremendously due to differences in scale triplets (support size, spacing, and extent of measurements), field methods, analysis methods, and natural variability. Schweizer et al. (2008) provide a comprehensive review of this previous work. There has been limited success in predicting and explaining the observed variability, particularly with regards to terrain. Furthermore, due to the challenging

nature of working in steep, avalanche terrain, these previous studies typically characterize the snowpack on uniform slopes less than 35^{o}. Few snow scientists have attempted to characterize or predict the snowpack in the highly variable and complex terrain that many skiers, snowboarders, climbers, and snowmobilers now venture into on a regular basis. The present study is unique in that it looks at spatial patterns of snowpack characteristics in complex alpine terrain by sampling patterns of weak layers and slabs in steep, snow-filled gullies, chutes, or couloirs bounded on either side by rock or trees (hereafter referred to as couloirs for consistency).

There are two primary objectives for this study. The first is to describe the spatial patterns and variability of various weak layers and slabs in couloirs. Second, I explore how terrain parameters relate to snow weaknesses and which terrain parameters are most influential for predicting weaknesses in this complex terrain. The practical implications of this research will be more effective avalanche control at ski areas, safer route selection in steep terrain, more effective selection of snow pit sites for assessing avalanche danger, and improved modeling capabilities for avalanche forecasting.

This study examines the spatial variability of depth hoar, surface hoar, near-surface facets, and slabs in a sample of 21 couloirs from the Madison Range of Montana and the Teton Range of Wyoming collected over two winters. Avalanche probe profiles at numerous points describe the stratification in the snowpack. Based on presence of weak layers and slabs, the snow observations are used to define "Potential Trigger Locations" (PTLs) within each couloir. Exploratory statistical analysis, classification

trees, and logistic regression show how PTLs are related to a number of terrain predictors derived from a one meter digital elevation model (DEM).

2. LITERATURE REVIEW

The release of a slab avalanche requires the failure of a weak layer or weak interface underneath a snow slab (Schweizer et al., 2003). Weak layers form through various processes, and a distinction is made between short-term weaknesses in the storm snow that occur as the new snow accumulates and persistent weaknesses. The latter, termed persistent weak layers, are characterized by snow grains with weak structures that endure relatively long periods of time (McClung and Schaerer, 2006). Because of their long-lived and fragile nature, persistent weak layers or the interface above them are often difficult to detect and are the causes of most avalanche fatalities. From a sample of 186 avalanches, Schweizer and Jamieson (2001) found that 82% failed on a persistent weak layer. Persistent weak layers, which are the focus of this study, are classified into three main types depending on the processes that cause their formation and the resulting grain type: depth hoar, facets, and surface hoar.

Weak Layers

Depth hoar forms near the base of the snowpack as a result of strong temperature and vapor gradients and relatively warm temperatures near the ground. Metamorphism of grains in shallow, early season snowpacks with strong temperature gradients can result in the growth of poorly bonded and weak faceted or cupped grains. Numerous studies have described the formation processes, rates of growth, and properties of depth hoar (e.g., Akitaya, 1974; Bradley et al., 1977; Giddings and LaChapelle, 1962; Sturm and Benson, 1997). Near-freezing temperatures near the ground and much colder air

temperatures at the snow surface are the driving forces behind depth hoar formation, and research has shown that depth hoar preferentially forms near shallowly buried rocks (Arons et al., 1998; Birkeland et al., 1995). In a study of 90 human-triggered avalanches in Switzerland, approximately 20% failed in depth hoar or at the interface above depth hoar (Schweizer and Lütschg, 2001). From a sample of 46 fatal avalanches in Canada, 22% failed on depth hoar (Jamieson and Johnston, 1992). Birkeland (1998) reported that 6% of large backcountry avalanches investigated in southwest Montana over a five-year period failed on depth hoar.

Facets often form another dangerous persistent weak layer. Numerous laboratory, field, and theoretical studies have demonstrated that facets typically form from rapid metamorphism near the surface of the snow caused by extreme temperature gradients (e.g., Armstrong, 1985; Fukuzawa and Akitaya, 1993; Morstad et al., 2007). Birkeland (1998) describes the dominant processes for near-surface faceting: diurnal recrystallization, melt-layer recrystallization, and radiation recrystallization, all of which require a strong temperature flux near the surface of the snow. Because crusts act as barriers against upward moving water vapor, faceting is typically enhanced below various crusts (Colbeck, 1991). Facets are also frequently found above crusts because of the latent heat released from freezing wet or moist layers. The faceting process is likely enhanced due to low thermal conductivity of the faceted layer in relation to the crust (Colbeck and Jamieson, 2001). Jamieson and Langevin (2004) showed that faceting associated with melt-freeze crusts can be favored at certain elevation bands with the optimal combination of freezing levels for subsequent storms. Short-wave and long-

wave radiation, as well as snow density and thermal conductivity, are linked to facet formation (Slaughter, 2010), and aspects where crusts are thicker due to greater solar radiation favor facet development because more latent heat is released from the freezing crusts (Jamieson and Langevin, 2004). Cooperstein (2008) found that southern aspects favored diurnal recrystallization in a field study from southwestern Montana. Larger, more developed facets are expected to persist longer and take longer to gain strength (Colbeck, 1998). Failure on a facets account for over 30% of the human triggered avalanches in the Swiss avalanche dataset (Schweizer and Lütschg, 2001), 59% of the avalanches from the Montana dataset (Birkeland, 1998), and 28% of the fatal Canadian avalanches (Jamieson and Johnston, 1992).

Surface hoar also forms an extremely fragile persistent weak layer. The winter equivalent of dew, these feathery crystals form when water vapor sublimates directly from the air to the snow surface. The conditions necessary for surface hoar formation have been the focus of many studies. Lang et al. (1984) demonstrated that the crystal growth is associated with significantly cooler snow surface temperatures than the overlying air, which is typical during clear, cold nights. Light air turbulence and humidity are required for grain growth (Colbeck, 1988; Hachikubo and Akitaya, 1997). Cooperstein (2008) showed that aspect affects the growth of surface hoar, which was more prevalent on north aspects in southwest Montana due to differences in radiation supply. In addition to validating previous findings, Slaughter et al. (2011) showed that incoming long-wave radiation and snow surface temperatures are significant factors in surface hoar formation. Surface hoar is easily destroyed by significant winds, and

because of the difficulty in modeling air turbulence in complex terrain with respect to both formation or destruction of surface hoar, it is nearly impossible to forecast for the presence of surface hoar remotely (Feick et al., 2007). However, in wind sheltered forested openings, both Shea and Jamieson (2010) and Lutz and Birkeland (2011) were able to successfully model surface hoar growth based on skyview and its relationship to incoming and outgoing radiation. Trees and terrain features shield longwave radiation emittance and prevent the rapid cooling of snow surface at night; thus inhibiting surface hoar growth (Shea and Jamieson, 2010). Surface hoar accounted for 31% of the backcountry avalanches in the Montana dataset (Birkeland, 1998), 41% of the fatal avalanches in Canada (Jamieson and Johnston, 1992), and approximately 20% of the human-triggered avalanches studied in Switzerland (Schweizer and Lütschg, 2001).

Spatial Variability

The spatial distribution of weak layers and snow strength is a primary concern for avalanche prediction and mitigation. Spatial variability of the snowpack at various scales is a primary source of uncertainty in avalanche forecasting (Hageli and McClung, 2004). Wind during or after deposition of snow is a major agent in causing variability (Sturm and Benson, 2004), as well as precipitation, sublimation, radiation, temperature, and snow metamorphism as they interact with terrain. These processes act on or over a range of various scales, from micro-structure to slope to mountain range, adding to the complexity of the problem (Schweizer et al., 2008).

Conway and Abrahamson (1984) spurred an interest in slope scale spatial variability with a benchmark paper analyzing shear strength measurements in a spatial

context. Based on highly variable shear strengths measured across crown walls and un-fractured slopes, they suggested that weak zones (or deficit zones) of sufficient size may cause tensile failure, and depending on the distribution of strong zones (or pinning zones), the fracture could propagate across the slope to cause an avalanche. Furthermore, the average strength of the slope may not be as critical as the minimum strength or the size of the deficit zones. The research of Conway and Abrahamson (1984) brought to question the validity of point stability tests for assessing avalanche danger, and numerous studies followed exploring the variability of different snow strength or stability tests at the slope scale.

Jamieson and Johnston (1993) performed a series of evenly spaced Rutschblock tests on six uniform slopes, free of rock outcrops or abrupt slope changes. They found no large deviations from the median score (+/- 3 scores) from 277 tests, and showed that 97% of their tests fell within +/- 1 score of the median. In highly contrasting results, Landry et al. (2004) compared stability indices on eleven uniform slopes and found 25% to 39% of their sites were not statistically representative of the stability of the slope.

A number of other studies describe the spatial variability of point stability tests on relatively uniform slopes, typically ranging from 25^{o} to 40^{o} (Campbell and Jamieson, 2007; Föhn, 1988; Hendrikx et al., 2009; Jamieson, 1995; Kronholm and Schweizer, 2003; Stewart and Jamieson, 2002). Disparate results can be attributed to natural variability and different field and analysis techniques. Many studies have used different scale triplets: the support size of each measurement, spacing between measurements, and spatial extent of all of the measurements are not consistent and cause further variability in

results (Schweizer et al., 2008). The effects of ground surface irregularities, terrain geometry, depth to failure layer, slope angle, solar radiation, proximity to the tops of slopes, trees, and "tree bombs" (snow falling from tree branches) are all cited as potential sources of variability (Campbell and Jamieson, 2007; Föhn, 1989; Jamieson, 1995).

To further understand the causes of spatial variability in the snow, Harper and Bradford (2003) traced snow stratigraphy on a flat glacier in an attempt to isolate densification and layering processes from the influences of vegetation, topography, and a variable basal boundary. They noted little variability across tens of meters in layers recorded in snowprofiles, but observed discontinuities using higher resolution tools (a permittivity probe and radar imaging). The variability in layers less than 1 cm thick was credited to primary processes such as wind gusts and changing snowfall rates or crystal form. Because these primary layers were well preserved, Harper and Bradford (2003) suggested that "the high spatial variability in snow stratigraphy commonly cited is typically due to the influence of local boundary conditions rather than feedbacks between primary and secondary densification processes alone." This reinforced the idea that spatial variability on avalanche slopes is driven by topography and ground cover.

As the character of spatial variability became an important parameter in avalanche release models (Schweizer, 1999), more studies attempted to quantify spatial variability using spatial statistics. Kronholm and Schweizer (2003) and Kronholm et al. (2004) applied geostatistical techniques to characterize the spatial variability of stability tests on eight slopes and penetrometer profiles on one slope. In nearly half of their samples, they found large slope-scale trends accounted for half of the variability in test scores, which

was partly attributed to slab thickness. All of the layers analyzed with a penetrometer showed significant linear trends across the slopes. The slope trends imply selection of stability site location is critical. All of the weak layers tracked with the penetrometer could be modeled with semivariograms, but showed a wide range of model parameters. Like previous studies, their data supports the inference that the spatial structure of a weak layer or slab is not an inherent property, but rather a product of its location in space. Other spatial variability studies have had varying geostatistical results, again a product of natural variability, layer type, method, and scale, but autocorrelation lengths were frequently on the order of 10 m (Guy and Birkeland, 2010; Logan et al., 2007; Lutz and Birkeland, 2011) or poorly defined (Shea and Jamieson, 2010).

With inconclusive results on the spatial variability of snow and weak layers, the problem of representative pit selection for assessing slope stability remains. Birkeland and Chabot (2006) documented a 10% to 15% "false-stable" rate from a database of 3500 stability tests. In other words, one out of ten slopes that were deemed safe by a stability test was actually unstable, an unacceptable rate when human lives are at stake. Birkeland and Chabot (2006) recommend digging more widely spaced pits to improve backcountry users' probability of finding weaknesses, but also note that there can be large areas of strong snow and relatively small weak zones; thus a second pit may only slightly improve the chances of finding the weak zone. This concept is supported by field research (e.g., Hendrikx et al., 2009; Stewart and Jamieson, 2002) in which clusters of high strength and low strength have been observed. Birkeland et al. (2010) used a statistical approach on 25 previous spatial variability datasets and found that there is no

optimal test spacing for minimizing the probability of choosing two relatively strong pit locations, even when layer type, stability test type, or spatial layout are considered. Thus, it is critical to target weak areas for pit site selection. While the presence of a weak layer doesn't necessarily indicate instability, targeting locations with weak layers improves the probability of finding instability and a better representation of the slope.

Terrain Influences

Nearly all of the spatial variability research points towards terrain as one of the best, and perhaps only, tools for targeting weaknesses. While potential environmental causes for the observed spatial variability patterns at the slope scale are frequently discussed, statistical testing or modeling of these influences has been limited. Exceptions include Birkeland et al. (1995), Lutz and Birkeland (2011), and Shea and Jamieson (2010).

Birkeland et al. (1995) explained the spatial variations in snow strength surveyed on two inclined slopes, one uniform and one with a more complex substrate. The latter showed a complicated pattern of resistance, but the presence of rocks underlying the snow was found to significantly decrease resistance in a multiple linear regression model, although the relationship was statistically weak.

Shea and Jamieson (2010) used Google Earth land cover images to model the effect of trees impinging on sky view and surface hoar growth. Using several surface hoar events from sparsely forested slopes, they used a scaled linear relationship between averaged grayscale values and surface hoar size to model surface hoar crystal size after a surface hoar event and achieved reasonable results. They tested their model on a similar

slope for a different event, and found that it correctly predicted size within 1.5 mm 60% of the time.

Lutz and Birkeland (2011) used the relationship between incoming radiation and terrain to spatially model surface hoar strength and size. They used a survey station to construct a 0.5 m digital elevation model (DEM) of topography and vegetation of the field site prior to the first snowfall. A sky visibility model and meteorological parameters modeled incoming longwave and shortwave radiation. Surface hoar size had significant linear correlations with all of the radiation parameters calculated, and shear strength was correlated with shortwave radiation. Smaller, stronger surface hoar crystals were observed and predicted on the portion of the slope where: (1) incoming longwave radiation was greater due to re-radiation from trees (preventing cooling of the snow surface at night and crystal growth), and (2) incoming shortwave radiation was greater (inhibiting persistence by warming of the snow surface during the day).

Also noteworthy is Birkeland's (2001) work, which modeled the relationships of terrain (coordinates, elevation, distance from ridge, radiation, and slope angle) with snowpack and stability data at the mountain range scale. This study found surprisingly weak correlations with terrain on the first sampling day in February. However, on the second sampling day in April, elevation had significant correlations (0.28 to 0.49) with all but one of the snowpack and stability variables. Both distance from ridge and radiation also had a number of significant correlations. When combining the effects of the terrain variables in multiple linear regression models, no valid models could predict the stability patterns observed on the first day. For the second sampling day, elevation,

radiation, distance from ridge, and east coordinate were all terms that appeared in at least one of four significant models for the various stability indices. None of these models explained more than 30% of the variance, indicating that many more complicating factors are involved. Birkeland (2001) also suggested incorporating wind parameters in future models and incorporating finer-scale variability into future analyses.

Previous studies in weak layer formation and spatial variability suggest that the influence of terrain is a very complex problem. The successful slope-scale studies of Birkeland et al. (1995), Shea and Jamieson (2010), and Lutz and Birkeland (2011) were in part because they focused on the influence of one or two parameters, or one type of weak layer on a simplified and specific slope. My goal is to incorporate all of the terrain parameters at our disposal that can be reasonably determined in the field or from a high resolution elevation map to model a more complete picture of snowpack evolution on complex slopes, including different weak layer types. This type of snowpack modeling has never been done before, but a number of studies have correlated avalanche activity with a collection of terrain parameters (e.g., McClung, 2003; Schaerer, 1977).

Of particular interest is the work of Gleason (1996), who characterized the terrain of avalanche paths on Lone Mountain and used several of the same slopes as the present study. He measured terrain parameters in the field and analyzed their influence on over 3500 recorded avalanche events. Gleason (1996) found that steeper slope angles up to 43^{o}, higher elevations, aspects receiving more solar radiation, and aspects clustered opposite the prevailing wind are positively correlated to natural avalanche frequency

using stepwise multiple linear regression. He also documented that avalanche frequency decreases for slopes above 43^{o} because of continuous sluffing.

Using Geographic Information Systems (GIS) to derive terrain attributes is a common practice in avalanche studies (Marienthal et al., 2010). For example, Maggioni and Gruber (2003) defined potential avalanche release areas using GIS by deriving slope angle, proximity to ridges, aspect, curvature, and elevation range from 10 m DEMs. They statistically identified mean slope, curvature, and distance to ridge as the most influential parameters in avalanche frequency. Studies that have used GIS to derive terrain parameters frequently cite poor DEM resolution as a source of inaccuracy, and the 10 m to 30 m DEMs commonly used are inadequate for describing some slope scale terrain parameters (Deems, 2002; Schmid and Sardemann, 2003; Schweizer and Kronholm, 2007). This current study is unique in that it uses a one meter DEM to derive terrain parameters, a resolution that has only recently been possible due to high-resolution airborne Light Detection and Ranging (LiDAR) technology. Presently, the best DEM source for the wide range of complex terrain features found in the alpine environment, especially gulleys, is LiDAR (Hopkinson et al., 2009).

The application of DEM-derived terrain parameters for modeling snow depth or snow water equivalent in hydrological studies has had documented successes. Although snow depth is not a measure of stability, stability test scores and snow strength have been empirically correlated to snow depth (e.g., Birkeland et al., 1995; Campbell and Jamieson, 2007; Kronholm and Schweizer, 2003). Thus, terrain parameters used to predict snow depth may be useful for predicting weak zones. Most hydrological research

has focused on the cirque or mountain range scale, and terrain predictors are commonly radiation or aspect, elevation, and slope or curvature (e.g., Blöschl et al., 1991; Elder et al., 1998). Winstral et al. (2002) designed two parameters that effectively predicted the effects of wind: an index of shelter/exposure from upwind terrain to characterize the wind scalar, and a drift delineator, which used upwind breaks in slope to indicate zones of lee deposition. Erickson et al. (2005) found that these two wind parameters, plus elevation, slope, and potential radiation were all significant predictors of snow depth using a complex mean geostatistical modeling approach when non-linear forms were employed. The wind shelter/exposure index had the greatest affect on predicted snow depth of these parameters.

The work of Wirz et al. (2011) is of interest because they characterized snow depth on a steep rock face at a similar scale and resolution as this study. Wirz et al. (2011) used a high-resolution terrestrial laser scanner to collect repeated snow depth measurements over two seasons. When comparing snow depths to slope angle, curvature, and roughness derived from a one meter DEM, only weak linear correlations were found (maximum=0.21). Based on comparisons of total snow depth observations and new snow distributions following snow/wind events and snow only events, they conclude that the wind-terrain interaction is the most dominant process for snow accumulation on steep faces. Wirz et al. (2011) also observed that overall snow depth distribution patterns were similar over two winters, but single snow loading events had varying patterns from storm to storm. Furthermore, spatial variability on the steep face was at least 30% more

variable and snow depth was always lower when compared to a similar site with gentler terrain.

Summary

In summary, persistent weak layers form under a complex regime of topographical and meteorological conditions. The spatial variability of these layers and their properties is well documented but predictive ability is very limited. Targeting weak layers is critical for slope stability assessment, and terrain is the most realistic tool for doing so. The successful use of terrain parameters to model weak layer properties on several simple slope-scale studies as well as snow depth distributions at larger scales provides optimism for our ability to predict weak zones in more complex, avalanche terrain.

3. METHODS

Study Sites

This study collected data from two mountain ranges with unique snow climates: the Teton Range in northwest Wyoming and the Madison Range in Southwest Montana (Fig. 1).

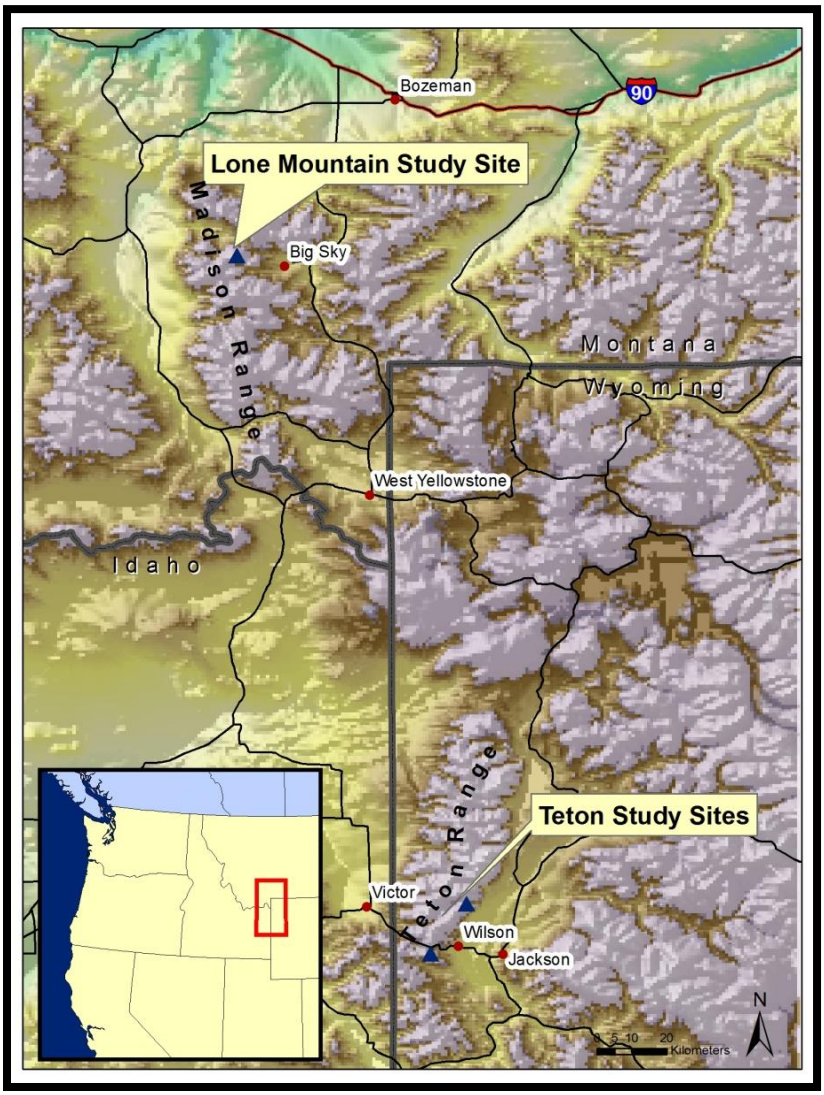

Fig. 1. Study sites in the Madison Range, Montana and Teton Range, Wyoming.

Big Sky Study Area

Seventeen couloirs were sampled from Lone Mountain in the Madison Range, near Big Sky, Montana (Fig. 2 and Table 1). Lone Mountain is located 50 km southwest of Bozeman. Big Sky Resort and Moonlight Basin operate lift-served ski areas on the mountain. Lone Mountain is a conical peak with several major ridgelines reaching its summit at 3403 m. The upper 670 m of the peak consist mostly of steep talus and scree above treeline (Savage, 2006). While Lone Mountain is situated in a region that is classified as an intermountain snow climate, its snowpack is usually characteristic of a continental climate due to its relatively colder and dryer winters (Mock and Birkeland, 2000). Few other peaks in the region approach the elevation of Lone Peak, so it receives exceptionally strong winds that are typically from the southwest to northwest. Winds are frequently in the 30-80 km/hr range, gusting in the 80-130 km/hr range several times each season. Prevailing winds are generally west to southwest (Table 1). Annual alpine snowfall averages 1100 cm at an average snow water equivalent (SWE) of 7% (Savage, 2006). The cold temperatures and low snowfall lend themselves to strong temperature gradients in the snowpack, and depth hoar or facets near early season crusts are commonly widespread and can be very problematic (e.g., Savage, 2010).

The Lone Mountain couloirs are on different headwalls and cirques above treeline (Fig. 2). The couloirs were chosen based on logistical accessibility (with cooperation from Big Sky Resort and Moonlight Basin), the existence of snowpacks relatively unaffected by skiers or explosives, and their wide range of aspects and snowpacks.

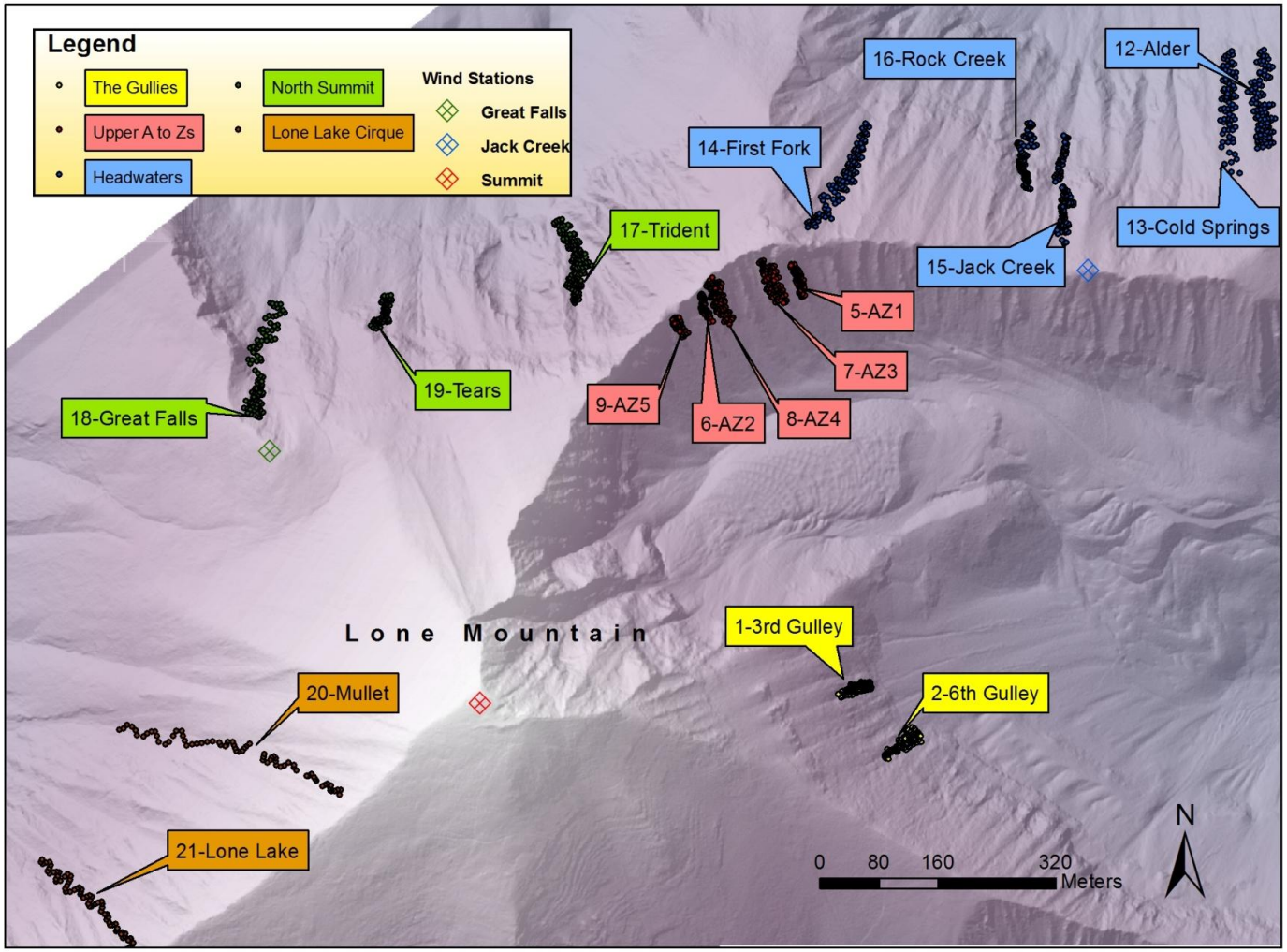

Fig. 2. Seventeen couloirs were sampled from five cirques or headwalls on Lone Mountain, encompassing a wide range of aspects and characteristics. Each dot represents a sample point.

Table 1. Characteristics of each couloir sampled.

Couloir	ID	Mountain, Range	Group/ Cirque	Date Sampled	Wind Station	Prevailing Wind Azimuth	# of Samples
3rd Gulley	1	Lone Mountain, Madisons	The Gullies	1/31/2010	Lone Summit	265°	119
6th Gulley	2	Lone Mountain, Madisons	The Gullies	2/9/2010	Lone Summit	260°	120
7 Dwarves	3	Rendezvous Mountain, Tetons	Granite Canyon	2/13/2010	Rendezvous Summit	250°	18
A-Chute	4	Rendezvous Mountain, Tetons	Granite Canyon	2/16/2010	Rendezvous Summit	250°	33
Upper AZ1	5	Lone Mountain, Madisons	Upper A to Z Chutes	2/11/2010	Lone Summit	265°	70
Upper AZ2	6	Lone Mountain, Madisons	Upper A to Z Chutes	2/28/2010	Lone Summit	270°	56
Upper AZ3	7	Lone Mountain, Madisons	Upper A to Z Chutes	3/9/2010	Lone Summit	265°	84
Upper AZ4	8	Lone Mountain, Madisons	Upper A to Z Chutes	3/11/2010	Lone Summit	265°	92
Upper AZ5	9	Lone Mountain, Madisons	Upper A to Z Chutes	3/11/2010	Lone Summit	265°	60
Unskiabowl	10	Mt. Glory, Tetons	Teton Pass	3/13/2010	Rendezvous Summit	250°	105
Claw	11	Mt. Elly, Tetons	Teton Pass	3/18/2010	Rendezvous Summit	250°	73
Alder	12	Lone Mountain, Madisons	Headwaters	12/9/2010	Jack Creek	270°	97
Cold Springs	13	Lone Mountain, Madisons	Headwaters	12/9/2010	Jack Creek	270°	74
First Fork	14	Lone Mountain, Madisons	Headwaters	12/10/2010	Jack Creek	270°	99
Jack Creek	15	Lone Mountain, Madisons	Headwaters	12/11/2010	Jack Creek	275°	104
Rock Creek	16	Lone Mountain, Madisons	Headwaters	12/11/2010	Jack Creek	275°	89
Trident	17	Lone Mountain, Madisons	North Summit	1/28/2011	Great Falls	240°	120
Great Falls	18	Lone Mountain, Madisons	North Summit	1/30/2011	Great Falls	240°	101
Tears	19	Lone Mountain, Madisons	North Summit	2/4/2011	Great Falls	240°	56
Mullet	20	Lone Mountain, Madisons	Lone Lake Cirque	2/27/2011	Great Falls	230°	72
Lone Lake	21	Lone Mountain, Madisons	Lone Lake Cirque	3/5/2011	Great Falls	230°	71

Field teams sampled two couloirs from the Gullies in January and February of 2010, a northeast-facing headwall within the boundaries of Big Sky Resort (Fig. 3). Prior to sampling, these couloirs were closed to skier traffic, but the snowpacks had been disturbed by daily explosive control on the faces above, shedding snow through the couloirs and onto their aprons.

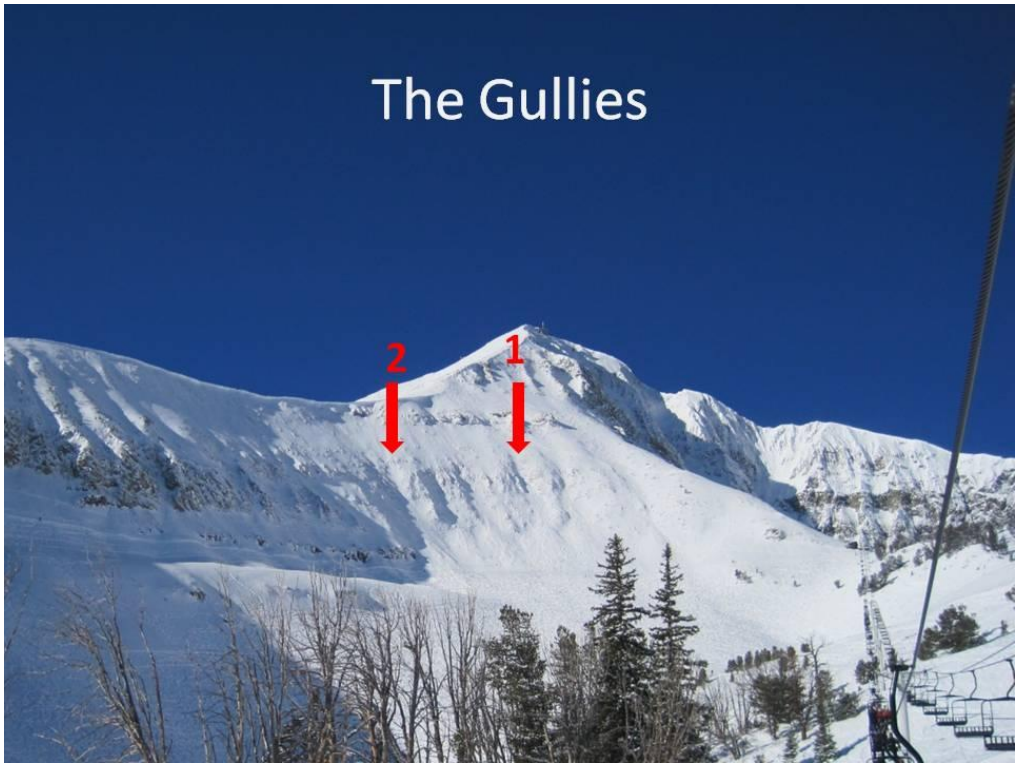

Fig. 3. 3rd Gulley (1) and 6th Gulley (2). Red arrows indicate approximate location of uppermost sampling point.

We sampled five couloirs from the Upper A to Z chutes, located on a south-facing headwall in Big Sky Resort, in February and March of 2010 (Fig. 4). During the sampling period, the Upper A to Z chutes were progressively opened to skier traffic, and we accessed these couloirs before any significant skier traffic. The layering in snowpack

was representative of a backcountry snowpack and undisturbed by explosives; Big Sky ski patrol does not apply explosive control until late season, when supportable sun crusts allow skiers to safely ski what is typically otherwise too shallow and rotten to ski. Prior to sampling, several large ANFO explosives were discharged at the base of the wall without any major results, although a large natural avalanche released earlier in the season from a different part of the headwall than our sampling locations. While the stability of the slopes may have been altered, the natural layering of the slopes, which is the focus of this study, remained intact.

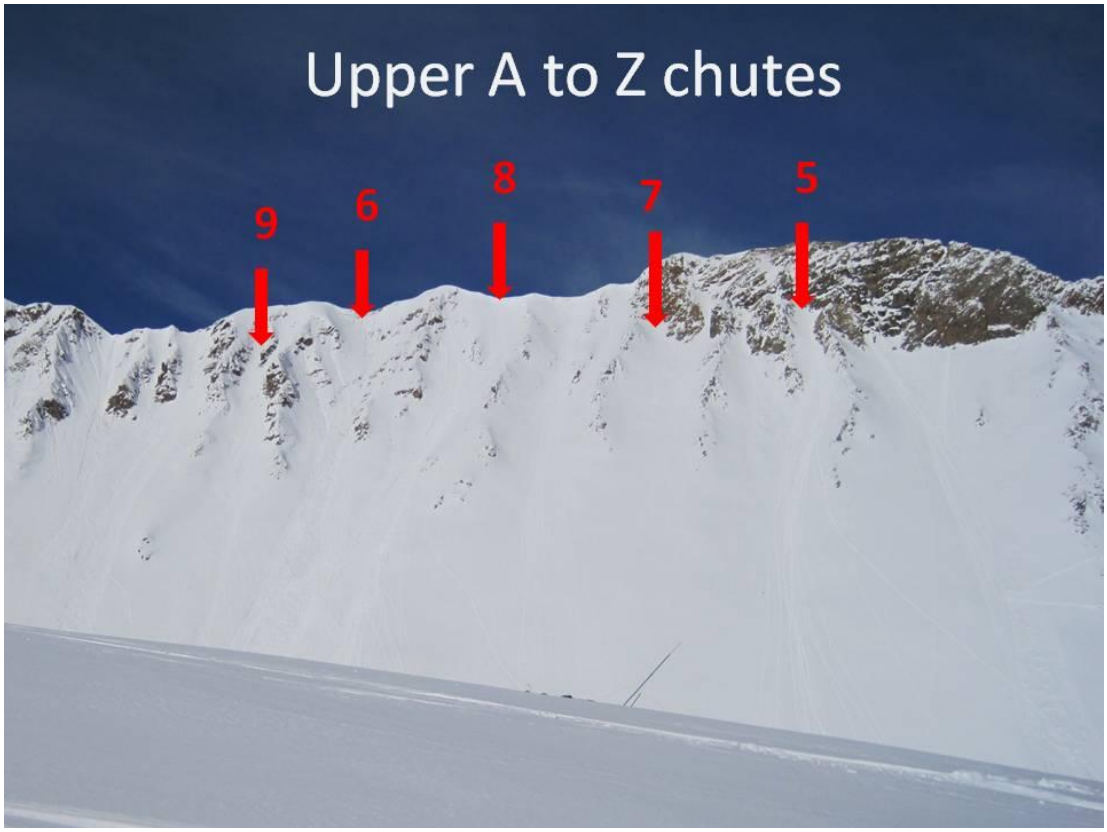

Fig. 4. Upper AZ1 (5), Upper AZ2 (6), Upper AZ3 (7), Upper AZ4 (8), and Upper AZ5 (9).

In December of 2010, teams sampled five couloirs from the Headwaters, a north to northeast-facing cirque in Moonlight Basin ski area (Fig. 5). These couloirs represented natural layering of backcountry conditions because we sampled them in the early season prior to any skier traffic. Moonlight Basin ski patrol applied one or two rounds of hand-charges prior to our sampling without any avalanche results, and the disturbance to layers was confined to small bomb holes which we avoided during sampling.

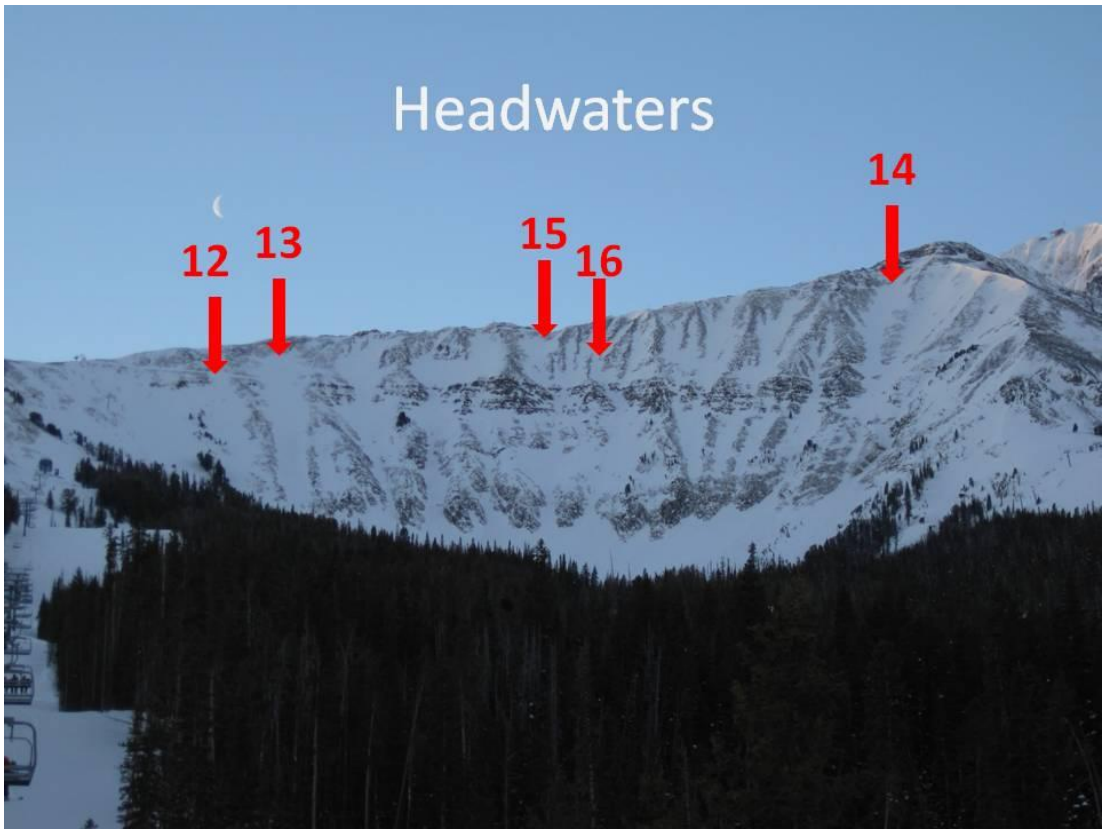

Fig. 5. Alderson (12), Cold Springs (13), First Fork (14), Jack Creek (15), and Rock Creek (16).

In January and February of 2011, we sampled three couloirs from the North Summit, a northeast to northwest-facing bowl in Moonlight Basin (Fig. 6). This area is closed to skier traffic early season, but saw a small amount of skier traffic before we sampled it, with the exception of Trident Couloir, which was closed prior to our sampling. By the time the North Summit was opened to skier traffic and our sampling teams, a well-developed wind slab prevented skiers from impacting deep weak layers. Moonlight Basin ski patrol runs routine control work in this zone after opening it, but again, the deep weak layers appeared to remain intact.

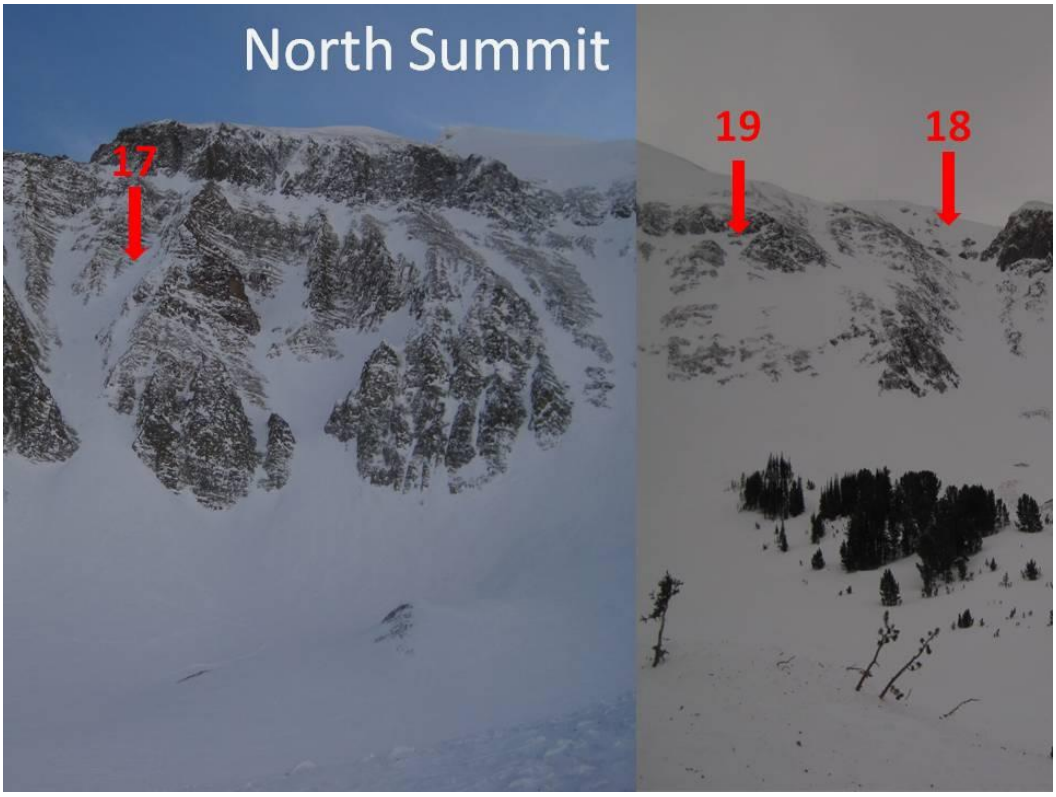

Fig. 6. Trident (17), Great Falls (18), and Tears (19).

Our last two samples from Lone Mountain were collected in February and March of 2011 from west and northwest couloirs in Lone Lake Cirque (Fig. 7). This area is out-of-bounds from the ski areas, but sees occasional backcountry skiers.

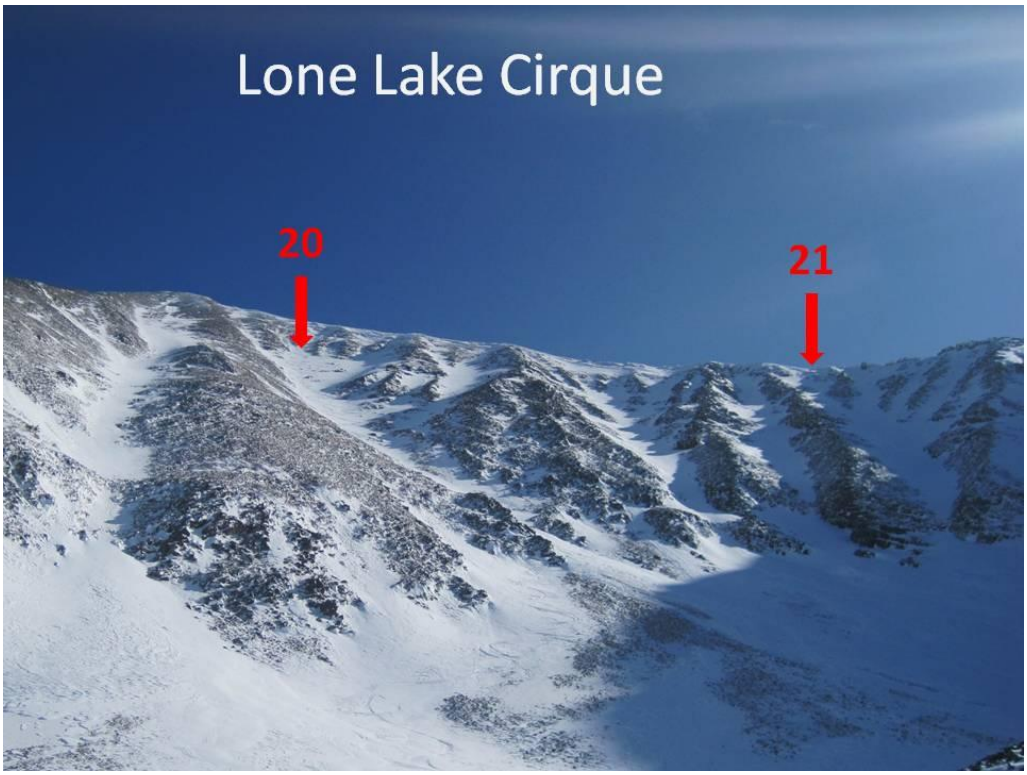

Fig. 7. Mullet (20) and Lone Lake (21).

Teton Study Area

Field assistants and I sampled four couloirs from the Southern Teton Range, near Jackson, Wyoming (Fig. 8 and Table 1). Two of the couloirs were sampled in backcountry areas near Jackson Hole Mountain Resort, located on Rendezvous Mountain with an elevation of 3185 m. We also sampled two couloirs near Teton Pass, where

Wyoming Highway 22 passes over the southern Tetons, 8 km west of Wilson, WY at an elevation of 2570 m.

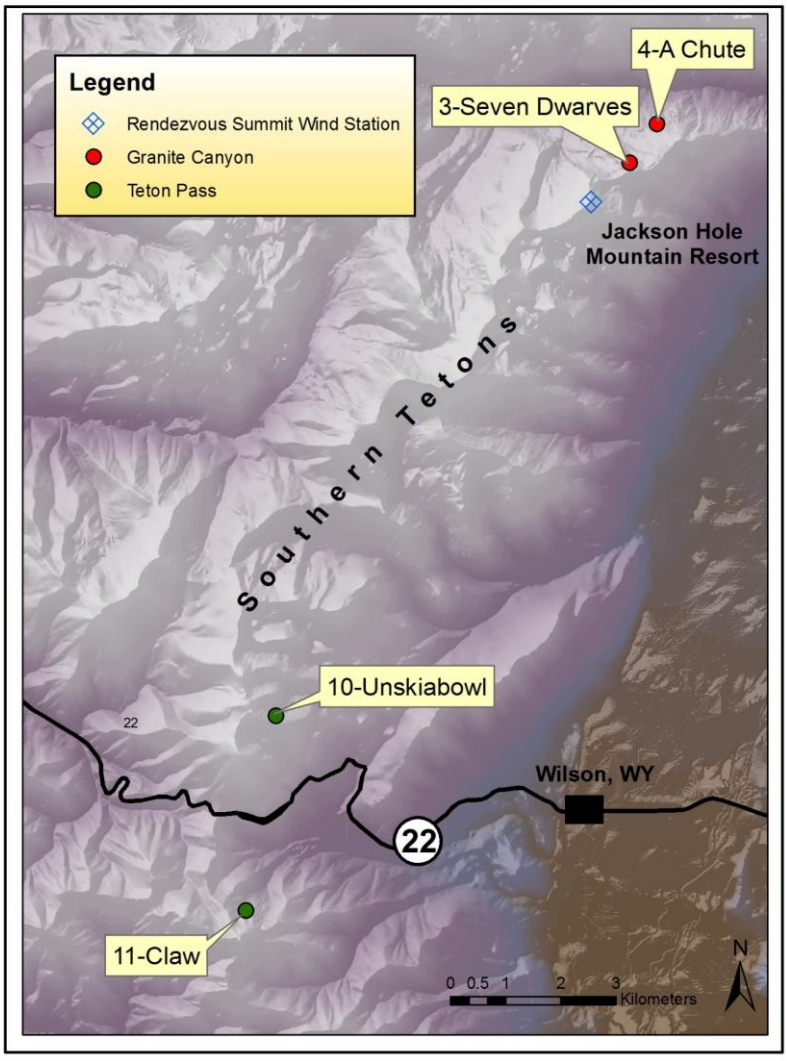

Fig. 8. Four couloirs were sampled from the Southern Tetons.

The Tetons generally receive more snowfall than Lone Mountain because Pacific moisture tracking along the Snake River Plain is intensified by orographic uplift as it encounters the Tetons. Average annual snowfall near the summit of Rendezvous Mountain is 1280 mm at an average SWE of 8.5% (Kozak, 2002). With more snowfall

and relatively warmer temperatures, the Tetons are classified as an intermountain snow climate (Mock and Birkeland, 2000). Winds generally prevail from the west to southwest (Table 1). All of the couloirs sampled from this region are below treeline and relatively more wind-sheltered than the terrain on Lone Mountain. The sites selected are all backcountry locations, devoid of avalanche control work. They are also in somewhat obscure locations and do not see much backcountry skier traffic.

In February of 2010, field assistants and I sampled two north-facing couloirs in Granite Canyon, which is out of ski area boundaries and on the back side of Jackson Hole Mountain Resort (Fig. 9). In March of 2010, we sampled two north-facing couloirs from Teton Pass (Fig. 10).

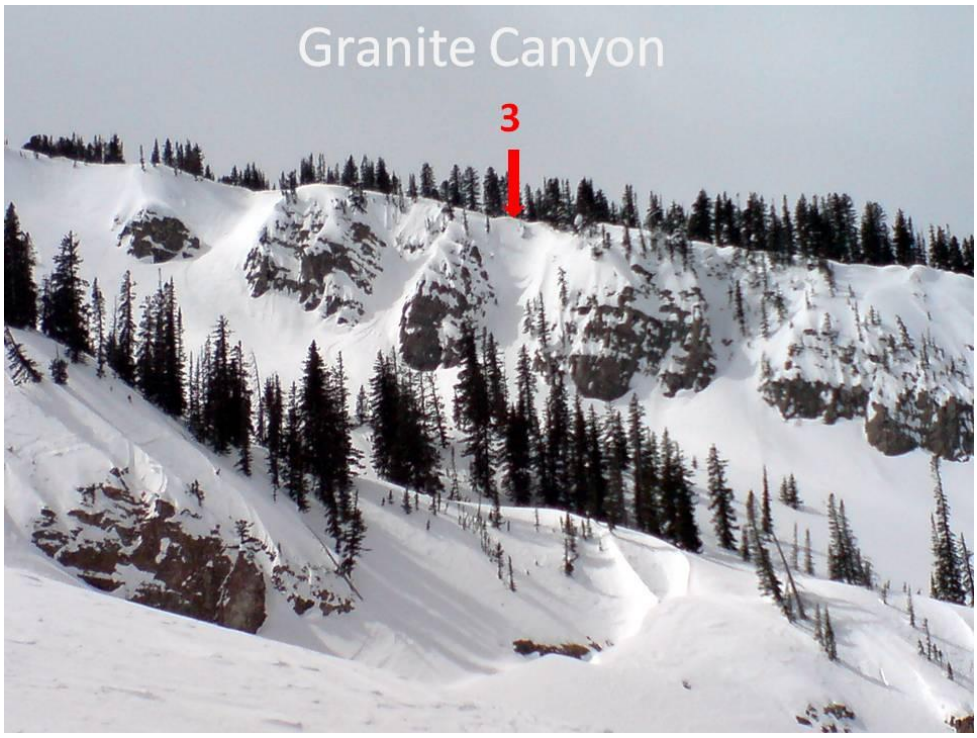

Fig. 9. Seven Dwarves (3).

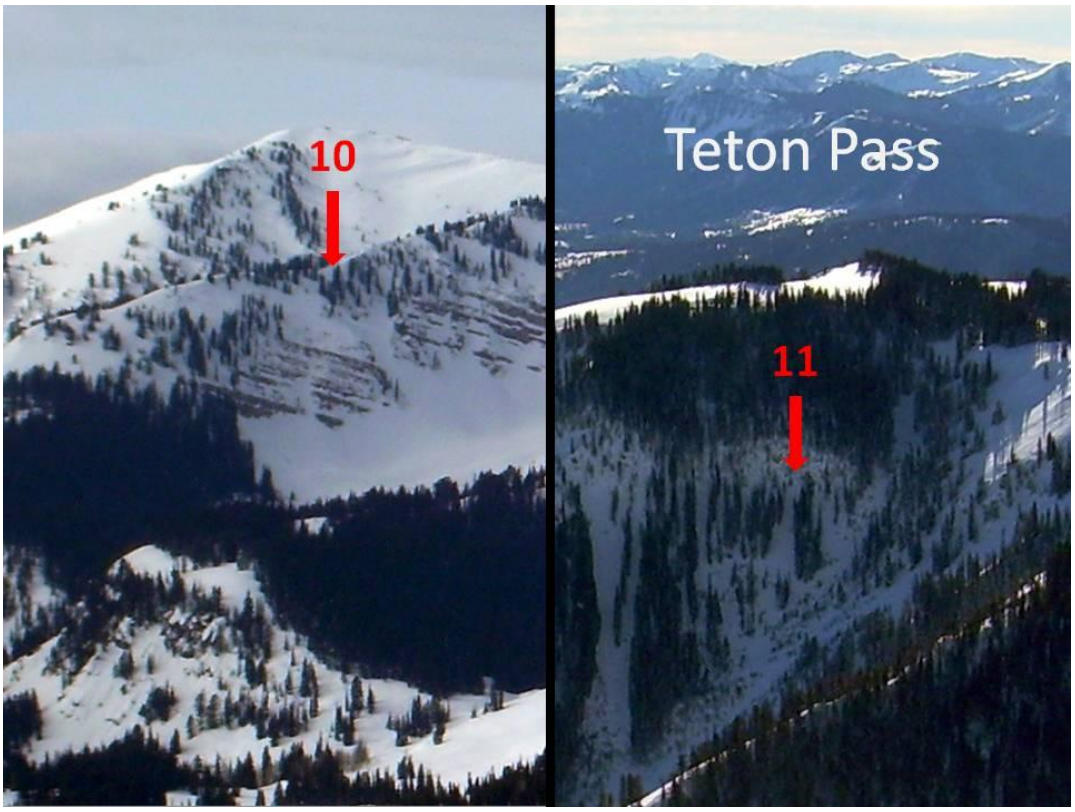

Fig. 10. Unskiabowl (10) and Claw (11).

Weather History

Weather patterns for the two winters sampled varied considerably. The winter of 2009-10 was an El Niño winter, with drier than usual conditions, and continental snowpacks developed in both study regions as the jet stream stayed south for most of the winter. A severe cold snap in December faceted most of the early season snows to depth hoar, and this layer plagued the Tetons through late January (Comey, 2010). The same layer plagued Southwest Montana for the entire season, causing the most active avalanche season in the Gallatin National Forest Avalanche Center's history (Staples, 2010).

The winter of 2010-11 was a La Niña winter, with unprecedented snowfall amounts in Montana's Madison Range. Copious early season snow fell with warm temperatures, creating one of the least reactive depth hoar seasons in southwest Montana in recent history (Staples, 2011). Despite these favorable conditions, depth hoar and basal faceting was still widespread on Lone Mountain, with avalanches occurring near the ground throughout the season in the Madison Range (e.g., Fig. 11).

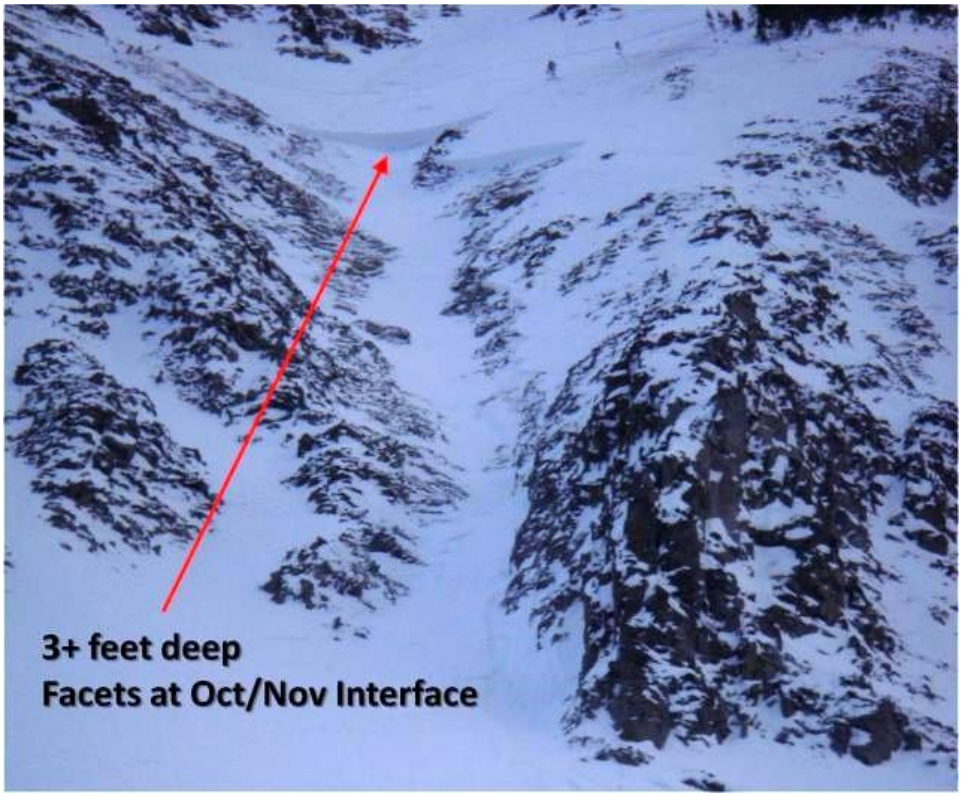

Fig. 11. A slab avalanche that was explosively triggered in the Headwaters on December 9, 2010, adjacent to Cold Springs. The avalanche failed on an early season weakness. Photo courtesy of B. Carpenter.

Field Methods

To sample each couloir, field assistants and I used an avalanche probe to track slabs and identifiable weak layers. In most cases, we tracked depth hoar or faceted snow near the base of the snowpack. For a number of couloirs, we were also able to track a weak layer that had recently formed near or at the surface of the snow (surface hoar or near-surface facets). These near-surface weak layers could be easily uncovered with a hand pit and viewed with a hand lens if necessary. At each location, we recorded total snow depth (*HS*), the thickness or presence of each identifiable weak layer (thickness of depth hoar or basal facets=*HDH*, thickness of near surface facets=*HFC*, presence of surface hoar= *SH*), the thickness of the snow slab overlying the weak layer which was typically composed of rounded grains and new snow (*HSlab*). In the absence of depth hoar, *HSlab* was given a null value. We also counted the number of and recorded the thickness of crust layers when applicable. We paid careful attention to keeping the probe vertical during field measurements. All vertical measurements were later converted to slope normal thicknesses or heights to account for variations in slope and to be consistent with crown profile protocols for avalanche observations (Greene, 2009). Slope angles for these conversions were derived from a one meter DEM (See page 39).

In each couloir, we conducted at least one full snow profile at what I judged to be a representative location (Greene, 2009). This also allowed for user calibration with the avalanche probe, making for easier and more reliable identification of weak layers of interest. To maintain consistency, I conducted all of the probing except in two couloirs (Alder Couloir and Rock Creek Couloir), where logistical constraints forced another

trained field assistant to conduct probing. When the snowpack was shallow or soft, field assistants or I dug hand pits to cross-verify probing results, and we would occasionally dig hasty shovel pits in areas of uncertainty. In general, weak layers were easily identified from probing as soft or hollow layers. Although user uncertainty exists with these techniques, the benefits of probing are quick data collection allowing a larger sample size and the ability to conduct research in steep terrain without burdensome equipment. Furthermore, Schweizer (1993), Schweizer and Lütschg (2001), and McCammon and Schweizer (2002) found that avalanche failure is most common at the transition from a hard to a soft layer; although grain identification was not always possible, sharp transitions in hardness were easily observed with a probe.

We collected 56 to 120 observations per couloir in a semi-systematic, stratified sampling scheme through repeated transects across the width of each couloir (Table 1). Though a random sampling design would have been optimal for geostatistical analysis (Kronholm and Birkeland, 2007), our sampling scheme was practical within the logistics of site accessibility, time constraints, preservation of snow, and safety in the challenging terrain. Snow observations were made with approximately equal spacing of several meters, and the design was stratified in that we made an effort to collect samples without bias from the top and bottom, sides and middle of the path (Fig. 12). Careful consideration was given to managing avalanche risk during sampling. We only sampled couloirs during extended dry periods with low avalanche danger or after a slope had been tested with explosives. Whenever possible, only one fieldworker was exposed on the

slope at a time. On several occasions, time constraints or increasing avalanche danger did not permit a completely stratified sampling pattern.

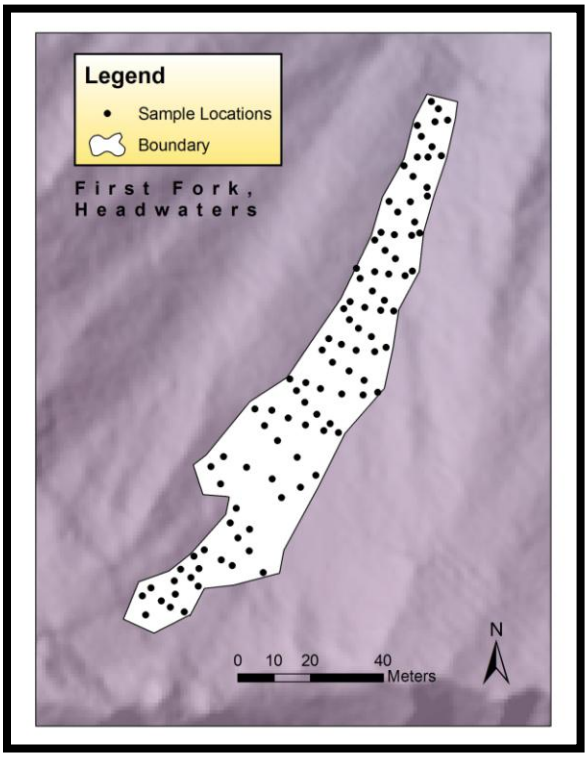

Fig. 12. Example of the sampling strategy in each couloir.

Two field days differed in sampling strategy due to heightened avalanche conditions. Several widespread and reactive surface hoar layers in A-Chute and Seven Dwarves prevented sampling teams from surveying the entire couloir. Instead, we gathered stability test data in the top of the starting zones while on roped belay. Our sampling strategy was to collect numerous sets of extended column tests (ECTs) across the width of the starting zone, with about five tests per set. The ECT is a relatively new stability test which has shown to be an effective indicator of slope stability, and it is more

aligned with our current understanding of avalanche mechanics (Simenhois and Birkeland, 2006; Simenhois and Birkeland, 2009). To perform the test, a 30 cm by 90 cm block of snow is isolated beyond the depth of the weak layer. On one end of the isolated column of snow, a series of calibrated loading taps (*n*) are performed until the weak layer fails or until *n*=30. If the failure propagates across the entire column in *n* or *n*+1 taps (recorded as "ECTP"), the test is interpreted as unstable. If the column fails and doesn't propagate or doesn't fail ("ECTN" or "ECTX"), the test is interpreted as stable (Simenhois and Birkeland, 2006).

We utilized a Trimble GeoXH 2008 handheld GPS to map sampling locations and spatially overlaid these observations on a one meter DEM, which is detailed in the next sections. Besides marking the location of snow observations, we also marked the boundaries of the couloirs, where the snow depth faded to zero and transitioned to talus or bedrock. These "zero" points are used for boundary reference and for terrain parameter analysis.

To assess the effectiveness of the sampling strategy for collecting unbiased snow observations throughout the entire couloir, I compared the distributions of several terrain parameters at the sampled locations with the distributions of these terrain parameters across the full length and width of the couloir. I used the Kolmogorov-Smirnov test (KS-test) to compare distributions of elevation, aspect, and slope angle values derived from the one meter DEM at each sample point with the respective distributions for all of the cells contained within the boundaries of the sampled couloir. The KS-test, which is described in more detail on page 55, tests whether two sets of data come from a

significantly different distribution (Massey, 1951). A p-value less than or equal to 0.05 rejects the null hypothesis that the two datasets come from the same distribution. By conducting a KS-test on the distribution of the sampled terrain parameters versus the terrain parameters from the entire couloir, I am testing whether the sampling strategy adequately characterizes the terrain of the complete couloir.

The results of the KS-test comparing the sampled locations to the each of the entire couloirs indicate that aspects and slope angles were fairly well represented by the sampling strategy, while elevation is moderately represented (Table 2). Without considering Seven Dwarves and A-Chute because only the starting zones were sampled, only one other couloir has a significantly different distribution of sampled aspects versus aspects from the entire couloir. Reasonably spaced transects across couloirs is an effective strategy for sampling changes in aspect without bias. Nine of the nineteen full-couloir samples have some form of bias in sampling with regards to elevation. In some cases, wider sections of the couloir, especially near the aprons, were not sampled at the same density as the rest of the couloir, and these elevation bands are underrepresented in the sampling design. In the example shown above for First Fork Couloir, the distributions of aspect and slope angle are adequately represented by the sampling pattern (KS-test p-values = 0.31, 0.69). The similarities between the sampled distributions and actual distributions are apparent in the probability distribution functions (Figs. 13a and 13b). However, the KS-test has a significant p-value of 0.05 when comparing the sampled elevations with the distribution of all elevation cells in First Fork. The probability distribution functions (PDFs) of these two datasets illustrate how a portion of

the upper elevation of First Fork Couloir is underrepresented by the sampling strategy (Fig. 13c), where the couloir is widest (Fig. 12) In summary, the sampling design was generally unbiased with regards to the terrain in each couloir, but it was not always completely stratified for elevation.

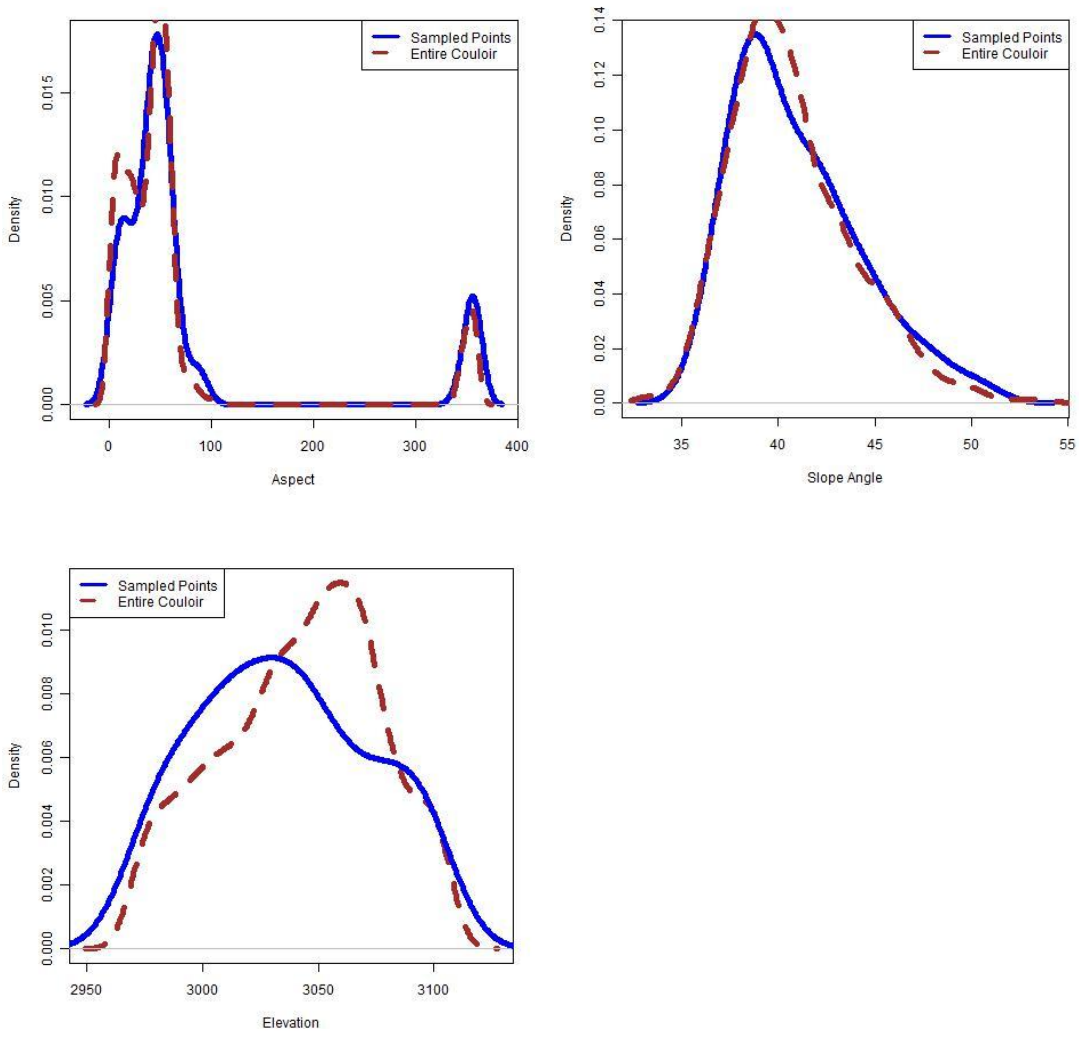

Fig. 13. Probability distribution functions for values of (a) aspect, (b) slope angle, and (c) elevation for sample locations and all of the one meter cells within the boundary of First Fork Couloir. Elevation is the only parameter with significantly different distributions, per the KS-test.

Table 2. PTL criteria for each couloir, uncertainty in field measurements and GPS readings, and KS-tests on whether the sample points are representative of the entire couloir's distribution of aspect, elevation, and slope (significantly different distributions are indicated by bold font).

Couloir	Couloir ID#	PTL Criteria	Estimated Sampling Confidence	Avg. Estimated Horizontal GPS accuracy (cm)	Estimated GPS st. dev (cm)	KS-test on aspect of couloir vs. sample	KS-test on elev of couloir vs. sample	KS-test on slope of couloir vs. sample
3rd Gulley	1	Presence of depth hoar & Slab > 15cm	90%	49	36	0.96	0.38	0.82
6th Gulley	2	Presence of depth hoar & Slab > 15 cm	90%	47	31	0.49	0.18	0.62
7 Dwarves	3	ECTP result or avalanche crown	100%	14	7	**0.01**	**0.00**	**0.00**
A-Chute	4a	ECTP result on top layer of surface hoar	100%	13	5	**0.00**	**0.00**	**0.00**
A-Chute	4b	ECTP result on lower layer of surface hoar	100%	13	5	**0.00**	**0.00**	**0.00**
Upper AZ1	5a	Presence of depth hoar & Slab > 15 cm	100%	51	23	0.06	**0.00**	**0.01**
Upper AZ1	5b	Presence of facets between two crusts	100%	51	23	0.06	**0.00**	**0.01**
Upper AZ2	6a	Presence of depth hoar & Slab > 15 cm	100%	45	28	0.63	**0.00**	0.30
Upper AZ2	6b	Presence of facets between two crusts	100%	45	28	0.63	**0.00**	0.30
Upper AZ3	7a	Presence of depth hoar & Slab > 15 cm	95%	97	181	0.69	0.96	0.85
Upper AZ3	7b	Presence of facets between two crusts	95%	97	181	0.69	0.96	0.85
Upper AZ4	8a	Presence of depth hoar & Slab > 15 cm	95%	43	20	0.85	0.61	0.57
Upper AZ4	8b	Presence of facets between two crusts	95%	43	20	0.85	0.61	0.57
Upper AZ5	9a	Presence of depth hoar & Slab > 15 cm	95%	118	74	0.45	0.12	0.75
Upper AZ5	9b	Presence of facets between two crusts	95%	118	74	0.45	0.12	0.75
Unskiabowl	10a	Presence of depth hoar & Slab > 15 cm	85%	240	237	0.77	0.61	0.46
Unskiabowl	10b	Presence of diurnal facets at the surface	95%	240	237	0.77	0.61	0.46
Claw	11a	Presence of depth hoar & Slab > 15 cm	85%	172	173	0.54	**0.00**	**0.01**
Claw	11b	Presence of diurnal facets at the surface	95%	172	173	0.54	**0.00**	**0.01**
Alder	12	Presence of depth hoar & Slab > 15 cm	95%	39	31	0.98	0.14	0.53
Cold Springs	13	Presence of depth hoar & Slab > 15 cm	95%	33	30	0.35	**0.02**	0.19

Table 2 Continued.

First Fork	14	Presence of depth hoar & Slab > 15 cm	95%	37	18	0.31	**0.05**	0.69
Jack Creek	15a	Presence of depth hoar & Slab > 15 cm	95%	42	37	0.44	**0.03**	0.59
Jack Creek	15b	Presence of surface hoar at the surface	100%	42	37	0.44	**0.03**	0.59
Rock Creek	16	Presence of depth hoar & Slab > 15 cm	95%	67	74	0.49	**0.00**	0.87
Trident	17a	Presence of depth hoar & Slab > 15 cm	90%	40	21	0.21	0.33	0.46
Trident	17b	Presence of diurnal facets at the surface	95%	40	21	0.21	0.33	0.46
Great Falls	18	Presence of depth hoar & Slab > 15 cm	90%	88	79	**0.03**	**0.00**	0.49
Tears	19a	Presence of depth hoar & Slab > 15 cm	95%	40	15	0.41	0.64	0.35
Tears	19b	Presence of diurnal facets buried under thin slab	100%	40	15	0.41	0.64	0.35
Mullet	20	Presence of depth hoar & Slab > 15 cm	95%	11	5	0.89	0.11	**0.05**
Lone Lake	21a	Presence of depth hoar & Slab > 15 cm	95%	43	24	0.97	**0.03**	0.12
Lone Lake	21b	Presence of diurnal facets buried under thin slab	100%	43	24	0.97	**0.03**	0.12

Mapping Points with GPS

All snow observation points and "zero" points were mapped using a Trimble GeoXH 2008 handheld GPS receiver. Post-processed differential corrections were used to improve the accuracy of the positions. In post-processed differential correction, a base station with a known location and ideally within 50km of the handheld unit tracks what errors the satellite data contains. Trimble's correction software processes this data to improve the accuracy of the data collected from the handheld unit (Trimble, 2008). For this study, positions were differentially corrected using the nearest base station with post-processing data available at the time of fieldwork. The Lone Mountain positions were

corrected from either the UNAVCO Big Sky, MT station (~30km), the UNAVCO Ennis, MT station (~27 km), or the CORS Bozeman (MTSU), MT station (~54km). While an effort was made to consistently process corrections from the closest station, UNAVCO Ennis base station data was not always readily available forcing the use of other nearby stations. The Teton positions were corrected from the CORS Driggs (IDDR), ID station or the UNAVCO Moose, WY station, depending on the study location. Distances to these stations varied but were all less than 35 km.

Under optimal conditions, the GeoXH 2008 is capable of 10 cm accuracy with differential correction. The GPS software reports an estimated root mean square (RMS) accuracies (68% confidence level) following post-processing based on the number of satellites, their elevation angle and signal strength, variances in correction type, and base station distance (Trimble, 2008). However, these estimates are unable to account for a number of sources of error: (1) Multipath signals, when a GPS signal reflects off of an object before reaching the handheld device; (2) measurement noise caused by electrical interference from external sources; (3) Poorly surveyed base station positions; (4) Correction source datum errors (Trimble, 2008). The latter source of error is negligible because all of the base stations use the ITRF 2000 geographic datum which is equivalent within several cm to the WGS 1984 datum that the GPS originally references (Janssen, 2009).

The positions were differentially corrected in the ITRF 2000 geographic datum. I imported the points into ArcMap and transformed the points to Universal Transverse Mercator (UTM) Zone 12 for analysis in the GIS using the *NAD_1983_To_WGS_1984_5*

transformation file (ESRI, 2009c). ITRF 2000 and WGS 1984 are essentially identical, with up to 2 cm shift (Janssen, 2009). After the points were correctly transformed to UTM Zone 12 and imported into ArcMap, they could be analyzed with the terrain parameters.

Given the one meter DEM available for terrain analysis, 50 cm accuracy from the GPS is ideal. Of the 21 couloirs, 14 have an average estimated RMS horizontal accuracy better than 50 cm, and all but three estimate sub-meter accuracy (Table 2). Standard deviations are also reported in Table 2, although the distribution of errors in each couloir is typically positively skewed, with several large values and most of the errors falling below the estimated mean. The average error is worst at Teton Pass where moderate tree cover inhibited satellite strength.

During most field days, at least one reference position was recorded to check for accuracy. These points were taken on ridgelines or obvious terrain features, and checked against the one meter DEM used for terrain analysis. With the exception of the two Teton Pass sites, the GPS control positions did not appear to be inaccurate given the resolution of the DEM. This leads to the conclusion that the GPS inaccuracies were minimal during fieldwork. For the Teton Pass sites, misalignment appeared to be on the order of 0-3 m, and this is considered in interpretation of statistical results.

Terrain Parameters

In the next stage of analysis, I derived suitable terrain parameters from a DEM in the GIS. LiDAR data provide a one meter resolution DEM of the study locations. Compared to the 30 m DEMs that are readily available for most locations in the U.S.,

McCollister and Comey (2009) demonstrated how one meter DEMs are far superior for calculating avalanche starting zone terrain characteristics. They also suggest that 30 m DEMs give inaccurate calculations for slope and aspect. The processed LiDAR datasets contain a bare-earth DEM with one meter resolution used for all parameters in this analysis. These raster grids are projected in UTM Zone 12, so all of the GIS analysis was standardized on UTM Zone 12.

I utilized ArcGIS (ESRI, 2009b) to derive twelve potential terrain parameters of snowpack structure (Table 3). All of the analyses utilized the Spatial Analyst extension in ArcGIS. In the following paragraphs, I explain why each terrain parameter is included as a potential parameter and how it was derived in the GIS when relevant. Supplementary three-dimensional maps of each of the parameters for Lone Lake Couloir are provided in Appendix C. Note that a number of the parameters described are likely to be correlated, but I accounted for this later in the modeling analysis.

Elevation, slope angle, and aspect are the most frequently used parameters for snow depth or snow strength modeling (e.g., Birkeland, 2001; Erickson et al., 2005). Elevation is a logical parameter because the snowpack can vary tremendously from the top of a couloir to the bottom due to varying wind or snow loading patterns, greater sluff accumulations near the bottom, and temperature lapses affecting precipitation and metamorphism differently (Birkeland, 2001; Dexter, 1986; Gleason, 1996; McClung and Schaerer, 2006). Slope angle affects the structure of the snowpack. Steeper slopes tend to shed snow accumulations while shallower slopes tend to accumulate avalanche debris and drifting snow (Gleason, 1996; McClung and Schaerer, 2006). Aspect affects

Table 3. Terrain parameters derived from a one meter DEM and used for analysis

Parameter name	Description	Example Value(s)
rel.elev	Relative elevation within the couloir (%) from an elevation grid (in meters)	0.892 (near the top); 0.128 (near the bottom)
slope	Slope angle (degrees)	49.2^{o}
EW.aspect	East-west component of aspect (Sine of aspect)	-0.299 (from 342.6^{o})
NS.aspect	North-south component of aspect (Cosine of aspect)	0.954 (from 342.6^{o})
prof	Profile curvature at 10 m resolution	-0.8(convex); 1.6 (concave)
plan	Plan curvature at one meter resolution	-8.5(concave); 2.3(convex)
rel.solar	Relative solar radiation within the couloir (%), calculated from cumulative direct and diffuse insolation (in WH/m^{2})	0.441
wind	Wind exposure index; the difference between the cell of interest and the mean elevations in a 10 m radius 120^{o} wedge into the seasonally averaged prevailing winds	0.42(exposed); -1.36 (sheltered)
rel.view	Relative viewshed within the couloir (%), based on visibility from the major windward ridgeline	0.70 (more visible); 0.2 (less visible)
expo	Exposure index; the difference between the cell of interest and the mean elevations within a 4 m donut-shaped search surrounding the cell.	0.32 (exposed); -0.46 (sheltered)
edge	Distance from the couloir's edge (meters)	8.1 m
wind.edge	Distance from the windward edge of the couloir (meters)	19.7 m

the snowpack through a number of mechanisms (McClung and Schaerer, 2006). For example, research has addressed the role of aspect on grain formation and metamorphism (e.g., Dexter, 1986; Jamieson and Langevin, 2004). The length and intensity of incoming solar radiation varies by aspect, which affects faceting and surface hoar growth (Cooperstein, 2008). Also the effects of wind, whether it is wind-loading or scouring, change with aspect (Gleason, 1996). Because of the circular nature of aspect data, I

created two parameters for analysis: an east-west contrast (*EW.aspect*) and a north-south contrast (*NS.aspect*) by taking the sine and cosine of aspect values in radians (Table 4).

Table 4. Reference table for the two aspect variables.

Quadrant	Azimuth	*EW.aspect*	*NS.aspect*
NE	45	0.71	0.71
E	90	1.00	0.00
SE	135	0.71	-0.71
S	180	0.00	-1.00
SW	225	-0.71	-0.71
W	270	-1.00	0.00
NW	315	-0.71	0.71
N	360	0.00	1.00

Curvature of the slope is another parameter that has been used in previous models (Blöschl et al., 1991; Wirz et al., 2011). I derived both plan (horizontal) and profile (vertical) curvature. Plan curvature delineates where down-slope gullies and ridges occur, and thus may be a good predictor of snow depth because in the alpine terrain, the gullies are usually loaded while the ridges get scoured (e.g., Fig. 5). Profile curvature allows identification of "rollovers" and aprons, where the snowpack structure is expected to differ significantly due to varying stresses in the snow and different loading/scouring patterns (McClung and Schaerer, 2006). To effectively identify these terrain features, I reduced the resolution of the DEM to 10 m before deriving profile curvature. This technique ignores subtle concavities or convexities to focus on major terrain features. Maggioni and Gruber (2003) also reduced the resolution of their DEM to 50 m relative to other terrain parameters (25 m) when calculating curvature. I chose 10 m resolution after

visually previewing a range of resolutions and found that for the scale of my study areas, 10 m profile curvature appears most suitable for identifying aprons and major rollovers.

Incoming solar radiation affects air temperature, snow temperature, and temperature gradients above and in the snow, which all have a profound effect on snow strength, grain formation, and metamorphism (Birkeland, 1998; Lutz and Birkeland, 2011; McClung and Schaerer, 2006; Slaughter et al., 2011). The solar radiation tool in ArcMap is used to sum direct and diffuse insolation (it does not calculate reflected solar radiation, which can be a significant contributor for snow covered surfaces). The calculation involves calculating an upward looking hemispherical viewshed based on topography, and overlaying the viewshed on a direct sunmap and a diffuse skymap (ESRI, 2009a). For each couloir, I calculated total insolation from November 1st, which roughly corresponds to the date that snow accumulation began, until the date that the couloir was sampled. Due to the complexity of such calculations and the number of unmeasured parameters involved (e.g., cloud cover and transmissivity), the solar radiation values, in watt hours per square meter (WH/m^2), should be viewed as relative to each other rather than absolute. I calculated cumulative totals as a way of determining average relative insolation values during the winter season prior to our sampling of each couloir.

Wind plays a critical role in snowpack development, especially in alpine terrain (Sturm and Benson, 2004) and steep faces (Wirz et al., 2011), and most studies on spatial variability have cited wind as a contributing factor (e.g., Conway and Abrahamson, 1984). I created a number of wind-related parameters which are dependent on seasonal

prevailing wind direction. Several weather stations record wind data near the study sites and are relatively unobstructed by terrain (Figs. 2 and 8). For each couloir, I selected the station that was closest or most representative with availability of wind data for that season. In the Big Sky area, I used wind data from the Lone Mountain summit station for the Upper A to Z chutes and the Gullies. I used the Jack Creek wind station for the Headwaters chutes, and I used the Great Falls wind station for the North Summit area and Lone Lake Cirque. In the Tetons, I used the Rendezvous Mountain Summit wind station for all of the couloirs (Table 1). For each couloir, I calculated the prevailing wind direction using hourly wind data from November 1st until the date that the couloir was sampled. The wind stations on Lone Mountain are operated by the ski areas, so they don't begin recording data until early to mid November. I calculated the prevailing wind direction by averaging the easterly and northerly components weighted by the wind velocity as follows:

$$Prevailing\ Wind\ Direction = \frac{180}{\pi} * \tan^{-1} \frac{\frac{\sum_{i=1}^{n} v_i * \sin d_i}{n}}{\frac{\sum_{i=1}^{n} v_i * \cos d_i}{n}} \qquad (1)$$

Where v_i is the hourly wind velocity reading, d_i is the hourly wind direction in radians, and *n* is the total number of hourly readings from November 1st until the sampling date. Prevailing wind direction calculations were rounded to the nearest 5 degrees. Wind speed data was unreliable for the Lone Peak summit station, so I used the same calculations without weighting the hourly wind directions with wind speed for those data. Also note that the Great Falls wind station on Lone Mountain only collected data starting January 5, 2011. The calculated prevailing winds are generally west to

southwest, with differences likely arising due to location relative to surrounding topography and seasonal trends (Table 1). The reason for using prevailing wind direction for the following terrain parameters is because it can be approximated in unfamiliar terrain where wind data is unavailable from flagging on trees, cornices, or seasonal snow-loading patterns.

A wind exposure index is a likely parameter for modeling snowpack. Schaerer (1977) found that an "Exposure to Wind" index was one of the most significant predictors of avalanches. In the Big Sky area, terrain that is exposed to the prevailing winds is typically scoured or shallow and subsequently faceted. However, we also observed that some areas that retain snow despite being exposed and battered by wind have stout, wind-packed grains without any weak layers. Deeper snowpacks are found in wind sheltered areas. Localized snow depth patterns are likely to be critically relevant to overall snow strength (Birkeland et al., 1995). To create a wind exposure index, I employed a similar GIS technique as Winstral et al. (2002). They found a "maximum upwind slope" parameter was significant for modeling spatial snow distribution, albeit at a much broader scale. Their parameter was determined using a 120^{o} pie-shaped area centered on the prevailing wind direction with search distances between 50 m and 2000 m. The slope between the steepest "sheltering" cell and the cell of interest was calculated as way to "quantify the extent of shelter or exposure provided by the terrain upwind of each pixel" (Winstral et al., 2002). For my wind exposure index, I used a 10 m search radius to calculate the average elevation of all of the cells within a 120^{o} pie shaped area centered on the prevailing wind direction (Fig. 14). The value of the parameter is the

difference between the cell of interest and the average elevation of these upwind cells, where values less than zero indicate a wind-sheltered cell. I selected a 10 m search pattern after visually previewing the outputs for several lengths. For the scale of this study and its terrain, a 10 m radius appeared to most effectively represent wind-loading and scouring patterns at a fine scale.

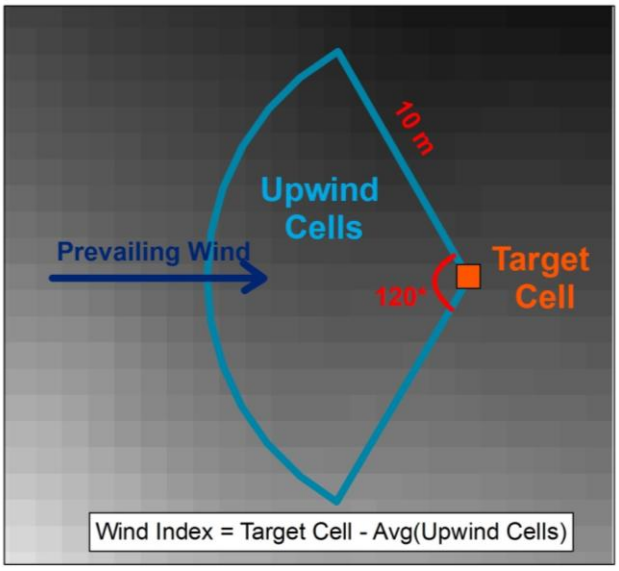

Fig. 14. Diagram of the technique used to calculate the wind exposure index. The wind exposure index equals the target cell minus the average of the upwind cells within a 120^{o} wedge with a 10 m radius.

I created another wind-related parameter called the viewshed index. This parameter quantifies how visible a cell is from its major windward ridgeline and is a measure of coarse scale wind exposure. As with the previous wind exposure index, the degree of exposure or sheltering strongly affects snowpack accumulation and metamorphism. I used a 30^{o} pie-shaped search into the prevailing wind direction from the boundaries of the couloir and digitized a line along the nearest major ridgeline

contained within the pie-shaped search. I then used the viewshed tool to count the frequency that each cell is visible from vertex points along the digitized ridge line (Fig. 15). A viewshed index of zero indicates a non-visible and highly sheltered location from prevailing winds.

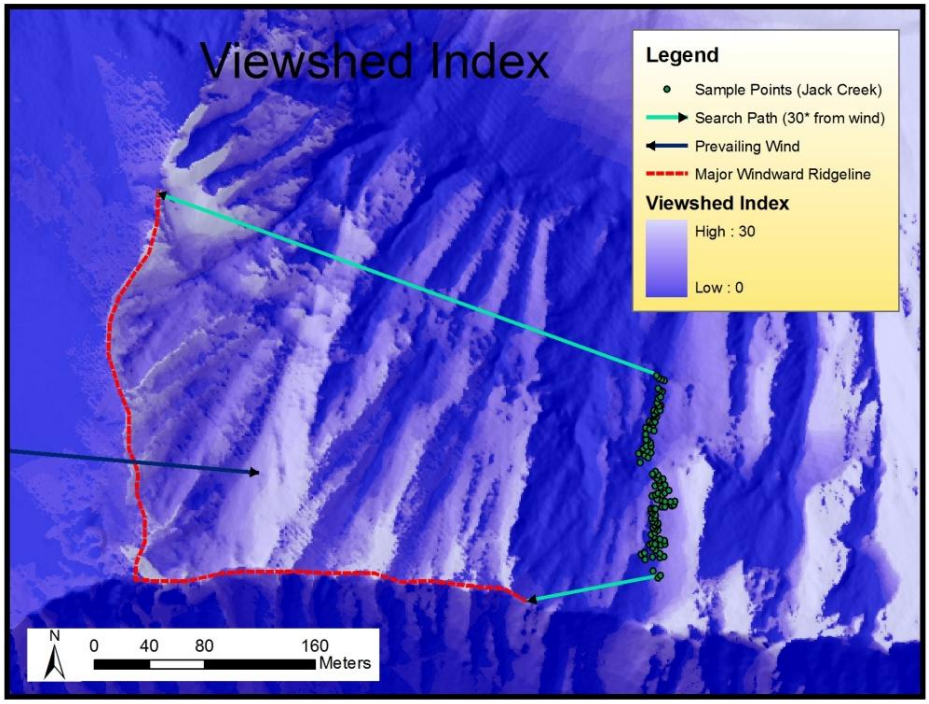

Fig. 15. Map illustrating how the viewshed index was calculated for Jack Creek couloir. A 30^{o} pie-shaped search from the couloir to the major windward ridgeline is used to define the endpoints of the viewing platform.

The exposure of the terrain also affects snowpack development. The degree of exposure not only affects how the wind interacts with the snow, but is also a measure of the skyview for each cell. Skyview affects the exchange of longwave and shortwave radiation, which in turn, affects temperature gradients and grain development such as surface hoar growth (Lutz and Birkeland, 2011; Shea and Jamieson, 2010). I created a

fine-scale exposure index as a potential parameter by conducting a 4 m annulus-shaped search around the cell of interest and calculating the average elevation of these cells. I subtracted this value from the elevation of the center cell; thus positive values are exposed cells (Fig. 16). This parameter is an indicator of whether, at a fine scale, the cell is on a protrusion or depression in the terrain, independent of wind direction. The calculation of this parameter is similar to a "roughness" parameter used by Hoechstetter et al. (2008).

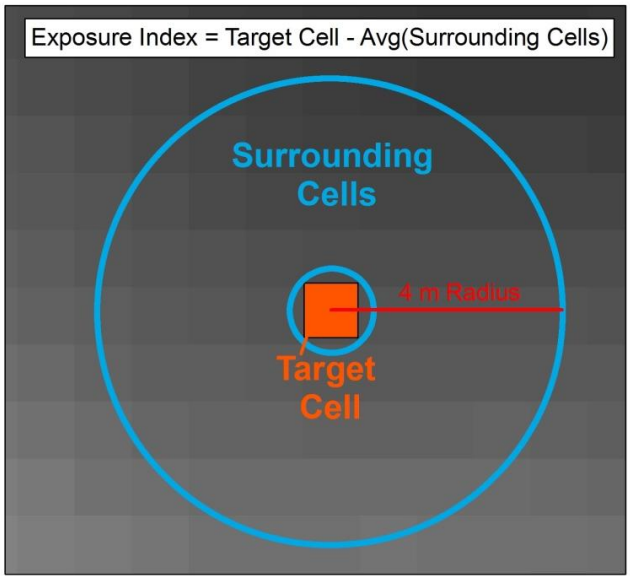

Fig. 16. Diagram of the technique used to determine the exposure index calculation. Exposure index equals the elevation of the target cell minus the average elevations of the surrounding cells within a 4 m radius.

The last two parameters are distance from the edge of the couloir and distance from the windward edge. The depth and structure of the snowpack significantly changes across the width of a couloir. Arons et al. (1998) and Birkeland (1995) showed that depth

hoar preferentially grows over rock outcrops, where snow depth is locally shallower, and it could be hypothesized that similar metamorphism occurs near the sides of couloirs. In alpine terrain, cross-loading winds are common, so distance from the windward edge is also a likely parameter. To create these terrain parameters, I digitized the couloir boundaries and calculated the distance of each cell from the boundaries. For the windward edge, I only digitized the windward boundary of the couloir based on field observations and prevailing wind calculations. To accurately digitize the couloir boundaries, I referred to the "zero" points collected in the field supplemented by a shaded relief layer created from the DEM. For the Teton area, I also used 15 cm orthorectified photographs for reference.

Note that the presence and influence of trees is an important parameter on the influence of spatial variability (e.g., Shea and Jamieson, 2010). All of the terrain sampled on Lone Mountain is above treeline and unaffected by trees. In the Tetons, three of the four sample sites, with the exception of A-Chute, have sparse or dense tree cover along the sides of the couloirs. This certainly affects snowpack development. Unfortunately, only the bare-earth LiDAR data was available from the Teton region, and no tree-related parameters were derived.

With the completion of the twelve terrain parameters, I spatially overlaid the mapped snow observations on each of the raster grids and prepared for statistical analysis. To allow for slope-to-slope modeling and cross-validation, elevation, solar radiation, and view were normalized for each slope. I am targeting the relative values rather than the absolute values of these parameters on each slope.

Exploratory Analysis

Designing the Response Variable

Designing a suitable response variable to be modeled by the terrain parameters presents a serious challenge. My objective is to create a model that predicts "weak zones," or locations where one would be more likely to trigger an avalanche, find instability in a snow pit, or have success with explosive control work. However, these trigger locations have to be modeled based on only crude snow profiles lacking stability test results. Using a subset of the current data, Guy and Birkeland (2010) modeled the response of a continuous variable using the percentage of the snowpack composed of weak layers. While this method is effective in identifying areas where faceting is most pronounced, it may be misleading for identifying trigger locations because such modeling targets areas where most or all of the snowpack is composed of weak layers while overlooking the importance of a mostly strong snowpack with a thin but dangerous weak layer. In practice, the latter scenario is typically more threatening, whereas the former could be a shallow, completely faceted, and relatively more benign location. Another continuous variable to model is simply weak layer thickness, such as the thickness of depth hoar (*HDH*). However, does a thicker layer of depth hoar necessarily mean a more dangerous situation? This presents a problem by highlighting locations where weak layers are thick, while again downplaying the importance of thin but extremely threatening weak layers. In practice, thicker weak layers aren't necessarily more dangerous (McCammon and Schweizer, 2002). For avalanches failing on depth hoar, the failure frequently occurs at the interface or in the top few centimeters of the layer, so

thicker layers of depth hoar aren't necessarily more threatening (Birkeland, pers. comm., 2011).

A solution to this dilemma is to model a binary response: the presence or absence of a Potential Trigger Location (PTL). The criteria for a PTL were defined on a case-by-case basis for each couloir based on the field observations and discussions with avalanche professionals. For most of the couloirs sampled, depth hoar is one of the layers of concern (e.g., Fig. 17). In these cases, the criteria for a PTL were defined as any location with the presence of the weak layer and an overlying slope normal slab thickness greater than 15 cm (Table 2). I required a minimum slab thickness because we frequently observed very shallow, faceted snow near the sides of the couloirs. However, with no slab in these locations, triggering an avalanche would not be possible. The minimum slab criterion filtered out these non-threatening locations from being identified as PTLs.

I chose the minimum slab depth with careful consideration. After discussions with several local avalanche experts and ski patrollers on Lone Mountain, I concluded that 15 cm was the most appropriate minimum slab depth for defining a PTL. Schwiezer and Lütschg (2001) found the lower quartile of fracture depths from a sample of 522 skier triggered avalanches was 30 cm (measured slope vertical). From a sample of 93 fatal avalanches in Canada, Jamieson and Johnston (1992) reported the lower quartile of slab thicknesses was 54 cm, and from 181 avalanche accidents from the Canadian Interior Ranges, the lower quartile was 30 cm (measured slope vertical). When corrected to slope normal thicknesses on a 45^{o} slope, these are 38 cm and 21 cm slab thicknesses, respectively. Patrollers at Moonlight Basin are concerned with fractures propagating to

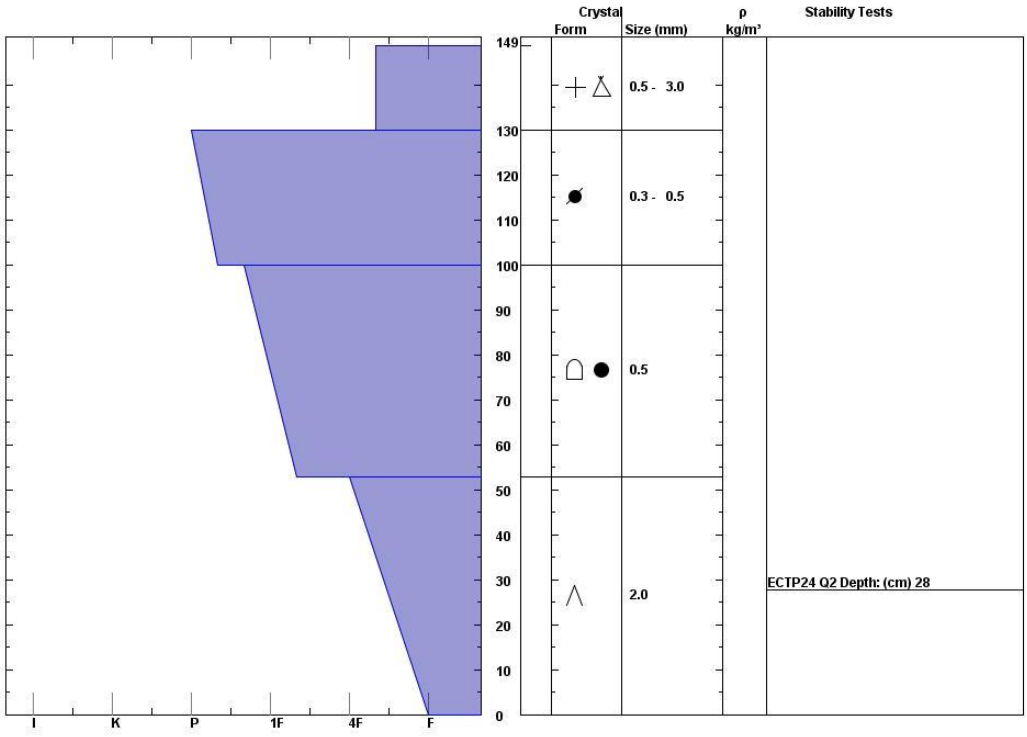

Fig. 17. Snow profile from First Fork showing the depth hoar layer that we tracked and the overlying slab.

full depth from around 15 cm or deeper (Carpenter, pers. comm., 2011). A number of techniques in this analysis deal with the uncertainty of defining the minimum slab depth.

In the Upper A to Z chutes, we frequently observed weak faceted layers between crusts. These were typically shallowly buried without a significant slab, but reactive in our stability tests (e.g., Fig. 18). In this case, I defined PTLs as any location with the layer of facets found between two crusts. In a few select couloirs, we observed near surface diurnal faceting or surface hoar formation at or near the surface of the snowpack. Because these layers had not been buried, I defined a PTL based simply on the weak

layer presence. In these last three cases, for those locations to be true PTLs, a slab of new or windblown snow would need to be added to the slope.

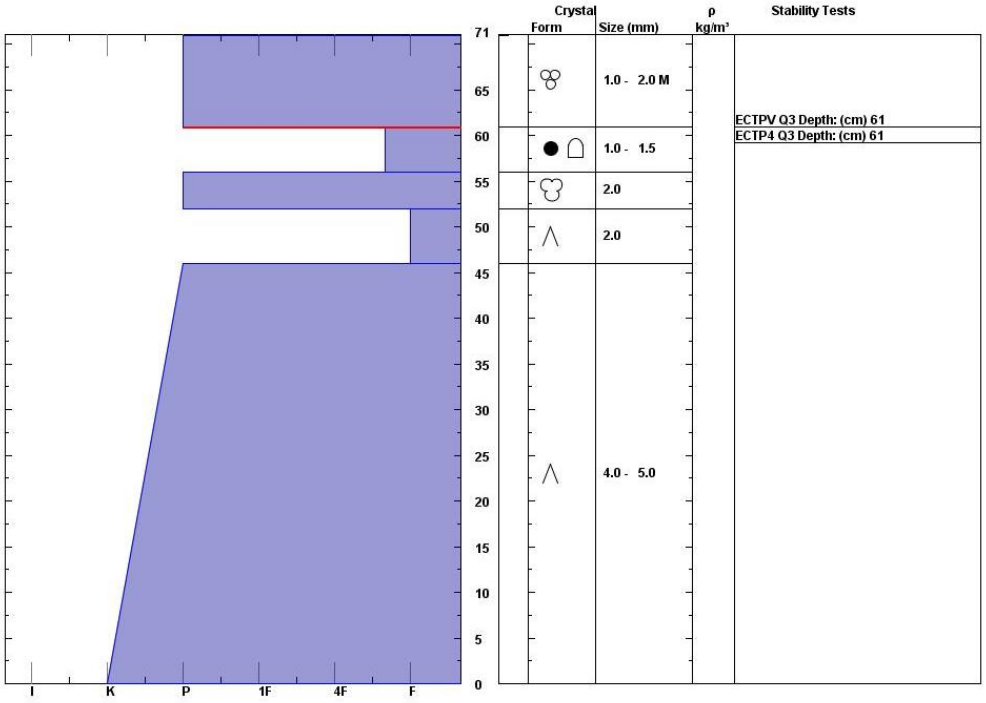

Fig. 18. Snow profile from Upper AZ1 showing the reactive faceted layer between two crusts that we tracked, as well as a depth hoar layer.

Lastly, I have two datasets where I collected ECT data on buried surface hoar layers (e.g., Fig. 19). For these days, I defined a PTL for a given surface hoar layer as any test site location where the extended column fully propagated across the layer. This is the suggested interpretation for the ECT (Simenhois and Birkeland, 2006). On one of the ECT sampling days, a portion of the slope avalanched, and I traced the crown line with the GPS. Points along the crown line are also classified as PTLs.

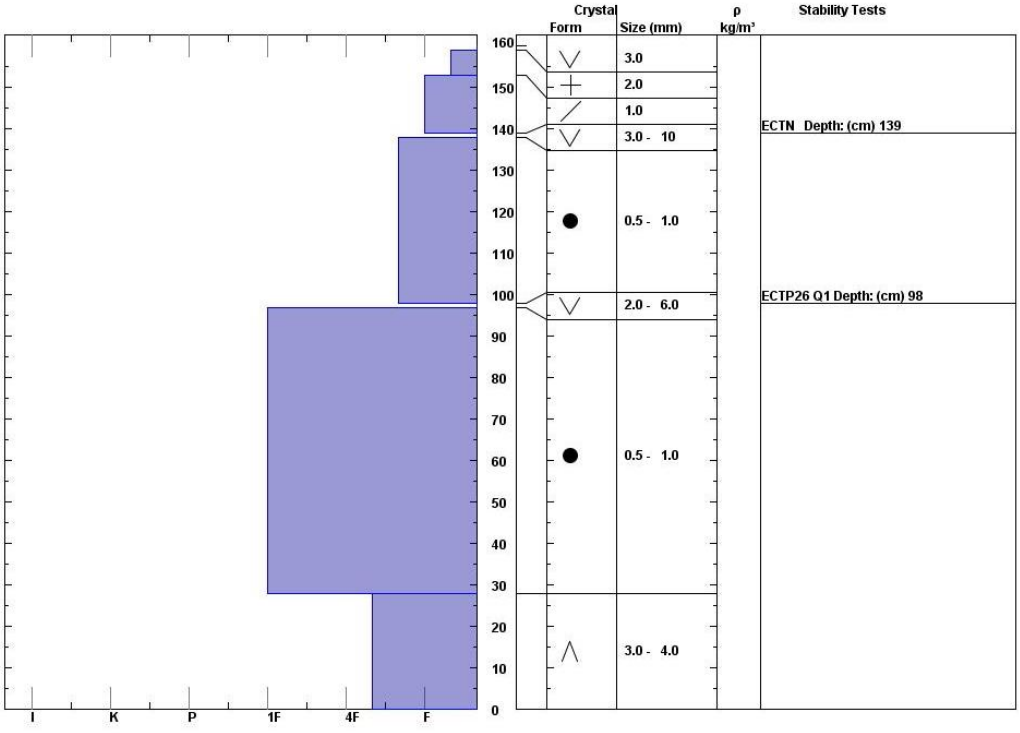

Fig. 19. Snow profile from A-Chute showing two reactive surface hoar layers that we repeatedly tested with ECTs.

Mapping PTLs

I visually represented the spatial patterns of PTLs on maps to complement my statistical analyses. In this section, I simply mapped the distribution of PTLs and non-PTLs over the twelve terrain parameter grids as well as a shaded relief map. The shaded relief maps for each couloir are included in Appendix A. Maps of PTLs over selected terrain parameters are integrated throughout the document to emphasize important relationships, and supplementary three-dimensional maps are included in Appendix C to aid in visualization.

Correlation Analysis

All statistical analyses are performed using R Software (2009) and are carried out for each of the identified weak layers in each of the 21 couloirs, for a total of 32 datasets (Table 2). For preliminary exploratory data analysis, I tabulated correlation coefficients for the snow observations (*HS*, *HSlab*, and *HDH*) and the terrain parameters described in previous sections. Testing the significance of linear correlations is a common practice in snow research when testing for the influence of terrain parameters (e.g., Birkeland, 2001; Gleason, 1996; Wirz et al., 2011). Because not all of the terrain parameters are normally distributed, I calculated the non-parametric Spearman's rank-order correlation coefficients. Significance of correlations are tested with the Student's t-test (Zar, 1972), and squaring the correlation coefficient gives the percentage of variance in the response that is explained by that variable in a linear regression. I output the correlations in a colored heat map using the gplots package in R (Warnes, 2009), which rearranges the rows of the parameters to form general clusters of positive and negative correlations, allowing a more visual display of the results.

Terrain Parameter distribution comparisons

Next, I compared the distribution of all the terrain parameters that are associated with the presence of a PTL against the distribution of all terrain parameters that are associated with the absence of a PTL. If a terrain parameter is strongly associated with the development of a PTL, we would expect to see a different distribution of values for locations where PTLs were observed, relative to non-PTL locations. The Kolmogorov-Smirnov goodness-of-fit test (KS-test) is a non-parametric method for testing the null

hypothesis that the difference between two distributions arises due to pure chance (Massey, 1951). A p-value less than 0.05 rejects the null hypothesis, indicating that the distributions are significantly different and that the terrain parameter in question is associated with the response of PTLs. This test assumes the data fit a continuous distribution function without numerous repeated values. All of the parameters meet this assumption, with the exception of *rel.view*, so I exclude *rel.view* from this section of analysis. This method was employed by Slaughter et al. (2011), where the most influential parameters in facet-forming days vs. non-facet-forming days were determined using the KS-test. Additionally, I plotted estimated probability distributions functions (PDFs) of terrain parameters for PTL and non-PTL locations to show how the distributions vary. The KS-test identifies whether distributions are significantly different, but it does not identify where. Qualitatively identifying where the distributions differ from the PDFs is not statistically supported.

Modeling Potential Trigger Locations

The previous two tests have clear and simple results, but are limited in that they isolate the effects of each parameter. Because the formation of PTLs is a complex process, modeling the influences of terrain parameters together is necessary for both prediction and interpretation. Although the quest for a single, optimal model is frequently the objective of environmental research, mathematical models of environmental systems can't entirely capture the complexity of processes, parameters, and scales involved. The concept of equifinality suggests that there are several acceptable model structures or many acceptable parameter sets with similar levels of

model performance (Beven and Freer, 2001). I approached the complex problem of modeling PTLs from terrain parameters with two different model structures, each attempting to characterize the process using a different approach. In the following sections, I describe the background and application of classification trees and logistic regression modeling.

Classification Tree Modeling

Classification trees are an excellent tool for modeling binary responses with non-parametric parameters, especially for data with unknown relationships. One of the primary strengths of classification tree modeling, when compared to common linear approaches, is the ability to capture hierarchal and non-linear relationships. Classification trees are more effective in modeling thresholds and complex interactions between parameters. Also, outliers and correlated parameters aren't problematic for modeling with classification trees (Breiman et al., 1993). Furthermore, the simplicity of the modeling results and accuracy scores allow for understanding from a wide range of audiences, which is a key component of avalanche science. Several studies have employed classification trees or regression trees to relate meteorological parameters with avalanche activity (Davis et al., 1999; Hendrikx et al., 2005) or to predict snow depth (Winstral et al., 2002).

In classification tree modeling, an algorithm conducts an exhaustive search of all possible threshold values within the parameter set and splits the data into increasingly homogenous nodes in order to minimize the predictive error of the model. This process of recursive partitioning of the data continues to a given endpoint depending on the data

size; the result is a tree with nodes and branches (Breiman et al., 1993). I implemented the initial classification tree modeling using the mvpart package in R (Therneau and Atkinson, 2010), and I used the complete set of twelve parameters described previously. The algorithm splits data at nodes using the Gini index, which is a measure of how diverse subsets become once a particular variable is used to split at a node. The tree is initially overfit, but I used a cross-validation process to prune the tree branches to the optimal tree size that minimizes cross-validation error (Breiman et al., 1993).

A more robust method for improved prediction accuracy for classification tree modeling is a boot-strapping based technique called Random Forest (Breiman, 2001). This method, implemented through the randomForest package in R (Liaw and Wiener, 2002) builds a diverse forest of classification trees by using a bootstrap sample of data and modeling from a random subset of variables at each split. The data withheld during each bootstrap iteration, known as the "out-of-bag" (OOB) data, are used to calculate prediction error at each step. The OOB estimated error rate, which depends on individual tree strength and correlations between trees, converges as the number of trees approaches 500. The estimated error rate from the OOB data is used to calculate the success rate of the model. At the cost of interpretability, the trees are averaged to create an effective tool for prediction. The randomness of the variable subsets makes the method more robust to noise in the data, and the large number of trees prevents overfitting. While there is no "average tree" that can be plotted or easily reported, this technique allows for quantification of parameter importance. For each tree, the OOB prediction error is calculated, and then the OOB prediction error is recalculated by withholding each of the

terrain parameters iteratively. The differences between these two values for each parameter are averaged and normalized over the entire forest. The resulting "mean decrease in accuracy" for each parameter gives a measure of how much the full forest's OOB estimated error rate would decrease without each term in the model.

For the relatively large sample of depth hoar PTLs and near-surface facet PTLs, I cross validated the Random Forest predictive model by applying it to each of the other couloirs. This allows interpretation of how well the modeled effects in a given couloir can be extrapolated to other couloirs. The results of a prediction model can be classified into a 2x2 confusion matrix (Table 5). H denotes "hits", where the presence of PTLs are correctly predicted. F is the "false alarms", where a PTL is predicted but not observed. M is the "false stable" group, where PTL predictions are missed. Z is all of the correct predictions of strong snowpacks.

Table 5. Confusion matrix for a binary response.

		Observed	
		PTL	no PTL
Predicted	PTL	**H**	**F**
	no PTL	**M**	**Z**

For cross-validation, I calculated the success rate, which is simply the number of successful predictions over the sample size (Allouche et al., 2006):

$$Success\ Rate = \frac{H+Z}{H+F+Z+M} \quad (2)$$

This statistic can be misleading, depending on the prevalence of the response. For example, if you had a horribly inaccurate model that always predicted "no PTL", and an observed dataset with 1 PTL and 99 non-PTLs, you would get a success rate of 99%, even though the model has no ability to separate PTLs and non-PTLs. A measure of this ability is the True Skill Statistic (Allouche et al., 2006):

$$TSS = \frac{H}{H+M} - \frac{F}{Z+F} \quad (3)$$

The first fraction measures the probability of detection, or the "hit rate", and the second fraction measures the probability of false detection, or the "false alarm rate". True skill statistics range from +1 to -1, where a score of +1 means the model perfectly discriminates all PTLs and non-PTLs, a score of 0 means the model has no ability to discriminate, and -1 means the model perfectly discriminates all of the observations incorrectly.

As described previously, the minimum slab thickness criterion, though carefully selected, is subject to uncertainty. I investigated the robustness of parameter importance findings with a Monte Carlo approach. I iteratively redefined the minimum slab thickness for PTLs, in 1 cm increments from 1 cm to 60 cm and refit the Random Forest model for each unique slab thickness. At each iteration, I plotted how the mean decrease in accuracy (i.e., importance) for each parameter changed across the range of minimum slab thicknesses. I also calculated the averaged mean decrease in accuracy over all slab

thicknesses, which shows how important the parameter is over the entire range of slab thicknesses. Because a number of couloirs have a shallower snowpack with thinner slabs, I adjusted the range of slab thicknesses to 40 cm or 50 cm for these couloirs.

Logistic Regression Modeling

Logistic regression is widely accepted as the most appropriate tool for binary data because of its flexibility, ease of modeling, and meaningful interpretations derived from the model coefficients (Hosmer and Lemeshow, 2000). Schweizer and Kronholm (2007) used logistic regression to model the presence/absence of surface hoar. Logistic regression uses a generalized linear model in which the PTLs can be related to the terrain parameters through a linear regression of the form:

$$logit(p) = \beta_0 + \beta_1 X_1 + \ldots + \beta_n X_n = \log\left(\frac{p}{1-p}\right) \quad (4)$$

where β_1 is the coefficient of the terrain parameter X_1, and $logit(p)$ specifies the link function for the probability of a PTL, p. Because the logit is the log odds function, exponentiating the logit yields the odds. The odds that PTL=1 is $e^{\beta_0 + \beta_1 X_1 + \ldots + \beta_n X_n}$ (Hosmer and Lemeshow, 2000). The odds are the probability that an event will occur, divided by probability that it won't. For a probability of 0.8, the odds=4, which is commonly phrased as "four to one odds."

Logistic regression is essentially a linear regression on the probability of a PTL, and thus, it shares many of the same benefits of multiple linear regression but without the burden of many of the assumptions. Analysis of logistic regression is guided by the same principles used in linear regression, except that it is based on the binomial distribution rather than the normal distribution, and the method of maximum likelihood is used to fit a

logistic regression model (Hosmer and Lemeshow, 2000). An advantage of logistic regression is that no assumptions are made about the distributions of the explanatory variables, which can often be problematic for ordered or non-normal data frequently used in snow science (e.g., Birkeland, 2001). Observations assume independence, and an absence of multicollinearity among parameters is necessary for accurate estimations (Hosmer and Lemeshow, 2000).

Logistic model selection techniques are guided by methods described in Hosmer and Lemeshow (2000) and Dalgaard (2008). I fit a full model with all of the terrain parameters. I also included the following quadratic forms: $rel.elev^2$, $slope^2$, $prof^2$, $wind^2$, $edge^2$, and $wind.edge^2$. I exclusively chose to include these for several reasons. First, I considered the effect that I am attempting to model with each term and how that effect may have been exhibited in the snowpack. I hypothesize the selected terms may have quadratic effects on the presence of PTLs, but including the quadratic forms of all of the terrain parameters could have resulted in overfitting or finding a significant but meaningless relationship during model selection. For example, the probability of finding a PTL may be high at mid-elevations but low at high elevations and low elevations where ridgetop winds or avalanche debris strengthen the snowpack, respectively. Another example is distance from windward edge, where faceting may be prevalent near the edge, nonexistent in the middle, and prevalent again further from the middle, which is modeled by a quadratic form. Furthermore, previous research found the quadratic forms of slope and wind index to be significant parameters of snow depth, while the linear counterpart of slope was not (Erickson et al., 2005).

Using the terrain parameters and the quadratic terms described above, I reduced the full model to a list of reduced models by using an automated model selection technique that finds the "best" models from a semi-exhaustive search of all possible models. With just the main effects considered, there are over 40,000 candidate models. Glmulti is a powerful tool that uses a genetic algorithm to explore a random subset of all possible models, but with a bias towards better models defined by an information criterion (Calcagno and de Mazancourt, 2010). Repeated simulations have shown that the genetic algorithm effectively converges on the best models when compared to an exhaustive search (Calcagno and de Mazancourt, 2010). In my analysis, I found models that minimize the corrected Akaike's Information Criterion (AICc), which is a widely used statistical tool for comparing models and is preferred over the Akaike's Information Criterion (AIC) for smaller sample sizes (Burnham and Anderson, 2002). AICc is calculated as follows:

$$AICc = 2k - 2\ln(L) + \frac{2k(k+1)}{n-k-1} \quad (5)$$

where k is the number of parameters, L is the maximized value of the likelihood function, and n is the sample size.

Automated stepwise methods are commonly used for model parameterization by sequentially subtracting or adding previously removed parameters until a best fit is reached. Stepwise reduction is based on significance testing (e.g., Birkeland, 2001) or a criterion such as AIC (e.g., Guy and Birkeland, 2010). Though extremely popular in model building, stepwise procedures are frequently criticized for having "no theoretical basis" (Davison, 2003). These stepwise methods attempt to choose an optimal model, but

depending on starting points and stopping rules, forward and backwards approaches rarely converge (Fig. 20).

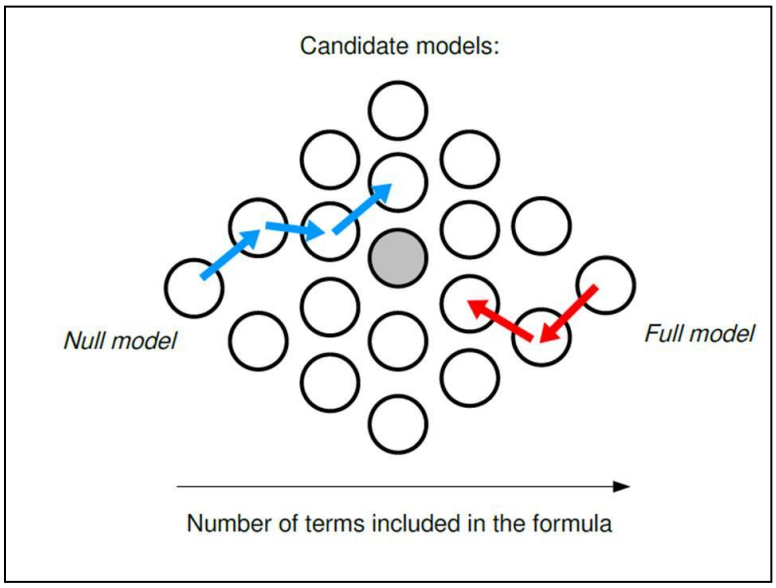

Fig. 20. Diagram showing how stepwise models rarely converge on the model with the lowest AIC, indicated by the grey circle (Calcagno and de Mazancourt, 2010).

The glmulti approach, implemented with the glmulti package in R (Calcagno, 2011) compares all candidate models and ranks them based on their AICc value. One advantage of glmulti over stepwise selection is that it ensures the best model according to AICc is selected. AICc is a measure of goodness of fit, but it penalizes each additional term added to a model in order to minimize overfitting and multicollinearity between terms. The key advantage of glmulti is that, by ranking the models with the lowest AICc, it allows multi-model inferences. With a relatively small number of carefully chosen parameters and a robust automated selection technique, my model selection technique is not a 'fishing expedition.' Furthermore, Hosmer and Lemeshow (2000) suggest that

automated techniques are effective when "the outcome being studied is relatively new and the important covariates may not be known and associations with the outcome not well understood."

I intentionally excluded interactions from the logistic regression model for several reasons: (1) There are 18 main effects fit to the full model with quadratic terms included, and the number of possible pairwise interactions exceeds 150. Including all of these terms in the full model increases the chances of finding significant but meaningless parameters using automated model selection. (2) The number of potential models explodes exponentially if interactions are included and is beyond the computing power of the glmulti package. (3) The classification trees are superior at modeling interactions and will capture important relationships. (4) My primary objective is a cognitive understanding of the interactions between terrain parameters and snowpack weaknesses, not a predictive model. Including numerous interactions will yield undesirable complexity and challenging interpretations. (5) Given the amount of uncertainty with this study, including more complex interactions compounds error and produces more uncertainty.

Following the glmulti model reduction, I defined the number of models to be averaged in the final model by previewing a plot of the top thirty models with the lowest AICc values. A general rule of thumb is that all models that fall within two values of the minimum AICc should be considered for multi-model inferences (Burnham and Anderson, 2002). I selected all of the models that fell below this threshold and weighted them according to their AICc values with a relative evidence weight of $e^{-\Delta AICc/2}$. A

Student-based method proposed by Burnham and Anderson (2002) calculated coefficients and their 95% confidence levels. Confidence intervals that include zero are generally not highly significant, but are still important if selected by AICc. Note that significance testing of parameters is invalid for models chosen with an information criterion, but rather, confidence intervals should be examined (Greenwood, pers. comm., 2011). I also calculated the odds ratios for each of the parameters in the model and their 95% confidence limits. The odds ratios are simply the exponential of the coefficient of a given parameter, but they provide a logical interpretation for the coefficients. If the parameter increases by one unit, the odds ratio is the multiplicative effect on the probability of a PTL occurring, given all other parameters are held constant. For example, when all other parameters are constant, an odds ratio of 1.04 for *slope* can be interpreted as: "A one degree increase in slope will be 1.04 times more likely to be a PTL" (Ramsey and Schafer, 1997).

I also calculated a measure of parameter importance for the averaged logistic models. This is the sum of relative evidence weights for each of the top models that the parameter appears in. Note that this measure of importance is interpreted differently than importance of terms in the classification trees. In classification trees, the loss of predictive power was calculated with the term removed from the model, whereas the logistic model importance is a measure of how frequently each term appears in the best models, weighted by how good each model fits. In logistic regression, the importance of a parameter highly depends on what other parameters are in the model. In an AICc reduced model, a parameter with strong predictive power may not show up as important

if a highly correlated term is a better parameter. For example, *wind.edge* and *edge* are expected to model similar behavior, and though they both may have strong associations with PTLs, it is unlikely that both parameters will be fit into the lowest AICc models. The parameter with the strongest relationship will have a high importance, while the other will show little or no importance. This is consistent with the assumption of absence of multicollinearity for logistic models.

A number of diagnostic tests have been developed to assess goodness of fit for logistic models, described in Hosmer et al. (1997) and Hosmer and Lemeshow (2000). However, most of these tests apply to single model structures. Many of these tests are not entirely robust, and the process of reducing a full model is the best check on overall fit, especially considering the robust reduction technique (Ramsey and Schafer, 1997). Note that I did implement several of these tests (the Pearson chi-square/unweighted sum-of-squares test, drop-in-deviance chi-square test, and the area under the ROC curve) using the single "best" models from approximately one quarter of the modeled couloirs and found that the lowest AICc models are statistically significant and generally fit the data well. The details and results of these tests are superfluous because model averaging is more robust and better than relying on a single model form (Burnham and Anderson, 2002). Checking for outliers is unnecessary because only two distinct values for the response are possible (Ramsey and Schafer, 1997).

A coarse method for assessing the overall fit and predictive ability of the final logistic model is a 2x2 confusion matrix to compare the percentage of predicted outputs that match the observations (Table 5). Because the predicted values for the logistic

regression model are a range of probabilities from 0 to 1, it is necessary to define a cutoff point, $\boldsymbol{c}$. The value of the cutoff point can be changed to optimize the discrimination power of the model, but for simplicity I used the most intuitive value of **c**= 0.5 for all of the individual couloirs. I transformed the predicted probabilities from the averaged final model into binary data by rounding all values greater than 0.5 up to 1 and all values less than 0.5 down to 0 and calculated the success rate (Equation 2). Unfortunately, this approach can give misleading results because it depends heavily on the distribution of the probabilities in the sample (Hosmer and Lemeshow, 2000). For example, if the weatherman predicts a 95% chance of rain, and it rains, he is classified as right. If the weatherman predicts a 55% chance of rain, and it rains, he is also classified as right. Clearly, the first weather model is a better predictor. Therefore, I also calculated the mean absolute error, which is the absolute difference between the predicted probabilities and the true observations averaged over the entire couloir. In the weatherman example, the first model would have an absolute error of 0.05 while the second model would be 0.45. Thus, smaller mean absolute error values indicate the logistic regression model performs better. For each couloir, I also calculated the true skill statistic of the logistic regression model like I did with the classification tree models (Equation 3).

The structure of the data needs to be considered for logistic regression to meet the assumption of independence. This logistic regression assumes a binomial distribution, with mean $n * p$ and variance $n * p(1 - p)$. If the parameters are clustered, that is, if we observe numerous repeated values for the terrain parameters, then the response may not fit a binomial distribution (Ramsey and Schafer, 1997). This results in the variance of the

observed response being greater than expected, termed overdispersion. Overdispersion causes confidence intervals to be underestimated, but can be accounted for with an inflation factor or dispersion parameter:

$$\hat{\Psi} = \frac{\Sigma \chi^2}{n-k} \tag{6}$$

where the sum of squared Pearson residuals is divided by the degrees of freedom (Ramsey and Schafer, 1997). For each single couloir, overdispersion is not an issue because we have mostly unique response values. The sample sizes are relatively small and most of the sampling points are spaced wider than the highly variable one meter DEM grids. Thus, the data are unique and continuous with the exception of the *view* parameter, which should have minimal overdispersion on the entire model.

When fitting a multi-couloir model, as described in the following section, overdispersion may be problematic. When overdispersion was suspect, I modeled the logistic regression using a quasibinomial distribution. I fit a full model as before, but rather than reduce the model using AICc, I reduced it using the quasi-AICc (QAICc). The QAICc adjusts for the dispersion parameter ($\hat{\Psi}$), as follows:

$$QAICc = 2k - \frac{2\ln(L)}{\hat{\Psi}} + \frac{2k(k+1)}{n-k-1} \tag{7}$$

The remainder of the analysis is the same as for non-dispersed data, except that I adjusted the confidence intervals for the increased variance.

As with the classification tree modeling, I explored the uncertainty in the minimum slab criterion for a PTL for the logistic regression modeling. I refit an

averaged final model and calculated parameter importance at different intervals of minimum slab thickness. Because of the extensive computation time needed to reduce and fit a final model, I refit at only two other intervals. For couloirs where deeper slabs were found, I redefined the minimum slab criterion at 30 cm and 45 cm, and for shallower snowpacks, I refit for slabs at 5 cm and 25 cm.

Finally, I used the averaged AICc (or QAICc) reduced models for the fixed definition of PTLs for cross validation as I did with the classification trees. I calculated two measures to compare the predictive power of the model: the success rate using a 2x2 confusion matrix (Equation 2), and the mean absolute error. As described earlier, the success rate is a crude estimate because it doesn't account for the distributions of predicted probabilities and it depends on the prevalence of the response. Mean absolute error quantifies the difference between each observation and the predicted probability at the same location and it is a better measure for reporting relative logistic model performance across couloirs.

Groupwise Modeling

I repeated the classification tree and logistic regression modeling processes described above for several groups of couloirs identified as having similarities while taking into consideration the effects of overdispersion. I designed four groups based on weak layer type: depth hoar, surface hoar, diurnal facets, and facets on crusts (Table 2). I reduced these groups further into geographic groups based on proximity in space and date of sampling (Table 1). These geographic groups incorporate two different scales of analysis: mountain and cirque scales (Fig. 21). Each of the cirque groups contains all of

the couloirs that share the same headwall, cirque, or alpine basin. We sampled the couloirs in each of these cirques during roughly the same time period to minimize temporal variability. The mountain scale analysis includes all of the couloirs on Lone Mountain collected over two winter seasons from nearly all aspects and five different headwalls or cirques on the mountain.

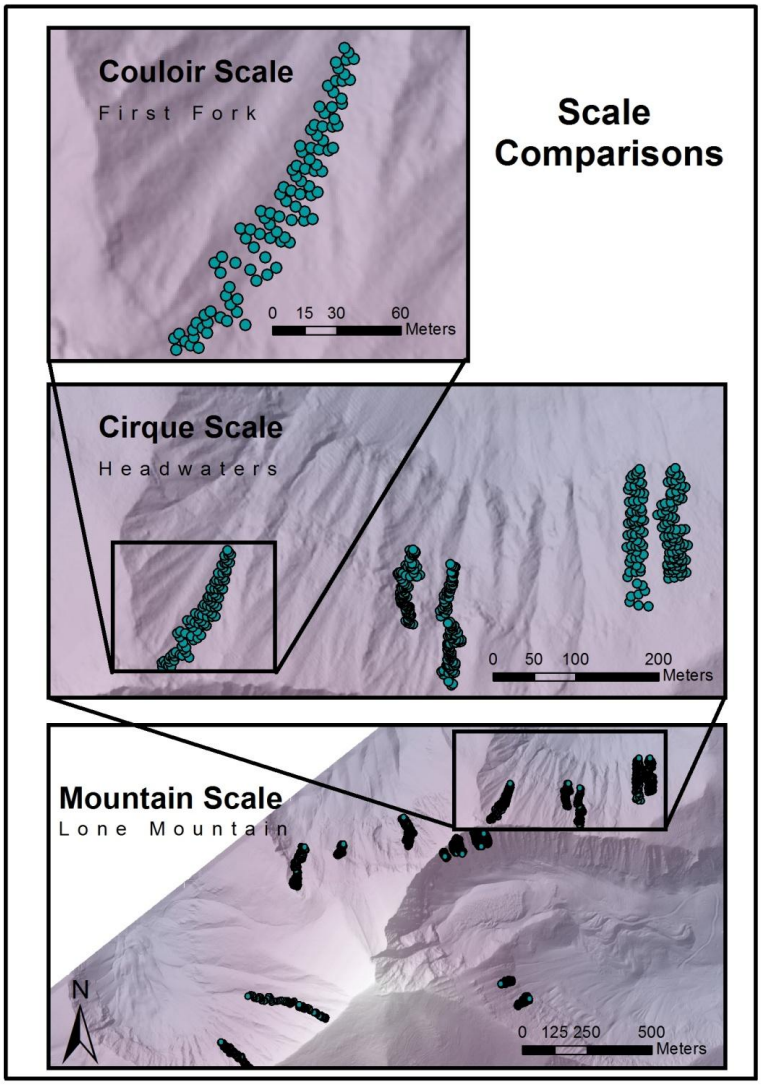

Fig. 21. An illustration of the three different geographic scales used for modeling PTLs: couloir (or slope) scale, cirque (or headwall) scale, and mountain scale.

To better assess the fit of the logistic model for the group modeling, I found an optimal cutoff value for calculating the success rate. Because these sample sizes are considerably larger, more predicted probabilities fall near 0.5, so it becomes increasingly important to define a cutoff value that optimizes the model's ability to discriminate between PTLs and non-PTLs in the "grey" area around 0.5. To estimate the optimal cutoff value, I extracted the lowest AICc model from the glmulti reduction and fit it to a Receiver Operating Characteristic (ROC) curve using the Epi package in R (Carstensen et al., 2010). The ROC curve plots the "hit rate" versus the "miss rate" for different cutoff values and estimates the value that optimizes the skill of the model for binary prediction. For example, a logistic model might return a long list of predicted probabilities in a grey area ranging between 0.4 and 0.5. Rather than selecting all values above a cutoff value of 0.5 as PTLs, the model may have a better ability at discriminating if it selects all values above 0.46 as PTLs. I reported the true skill statistics and the associated success rates with the optimal cutoff value for these larger datasets.

4. RESULTS AND DISCUSSION

Case Study: Upper AZ1 Depth Hoar Layer

This section provides a detailed, step-by-step illustration of the previously described statistical methods using the depth hoar layer in Upper AZ1 couloir. I demonstrate how the analysis was conducted and how the various outputs can be interpreted. The details of the intermediate analysis steps are omitted for the remainder of the couloirs, but the important figures are included in Appendix B and summarized in tables within the body of this document. Important findings from the results are summarized and discussed in the following sections.

A moderately developed, fist-hard layer of depth hoar pervaded most of the upper section of Upper AZ1 and was overlain with various crusts, mixed and faceted forms, and new snow (e.g., Fig. 15). In the lower sections of the couloir and near the sides of the upper part, the hollow depth hoar layer transitions to a pencil-hard crust. Though still composed of cupped grains, it is well sintered and considered non-threatening. Potential Trigger Locations (PTLs) for the depth hoar layer in Upper AZ1 are defined as any location with the presence of the weak, hollow depth hoar layer and an overlying slab of at least 15 cm (Table 2).

I mapped the spatial distribution of PTLs over grids of the terrain parameters for previewing (Fig. 22). Some relationships between PTLs and terrain, such as a strong relationship with the exposure of terrain and elevation, are immediately apparent. Snow depths for Upper AZ1 average 50 to 60 cm, and most of the overlying slabs range between 20 and 30 cm (Fig. 23). Upper AZ1's terrain parameters are continuous but not

normally distributed; thus the non-parametric modeling techniques of classification trees and logistic regression are ideal for modeling this data (Fig. 23).

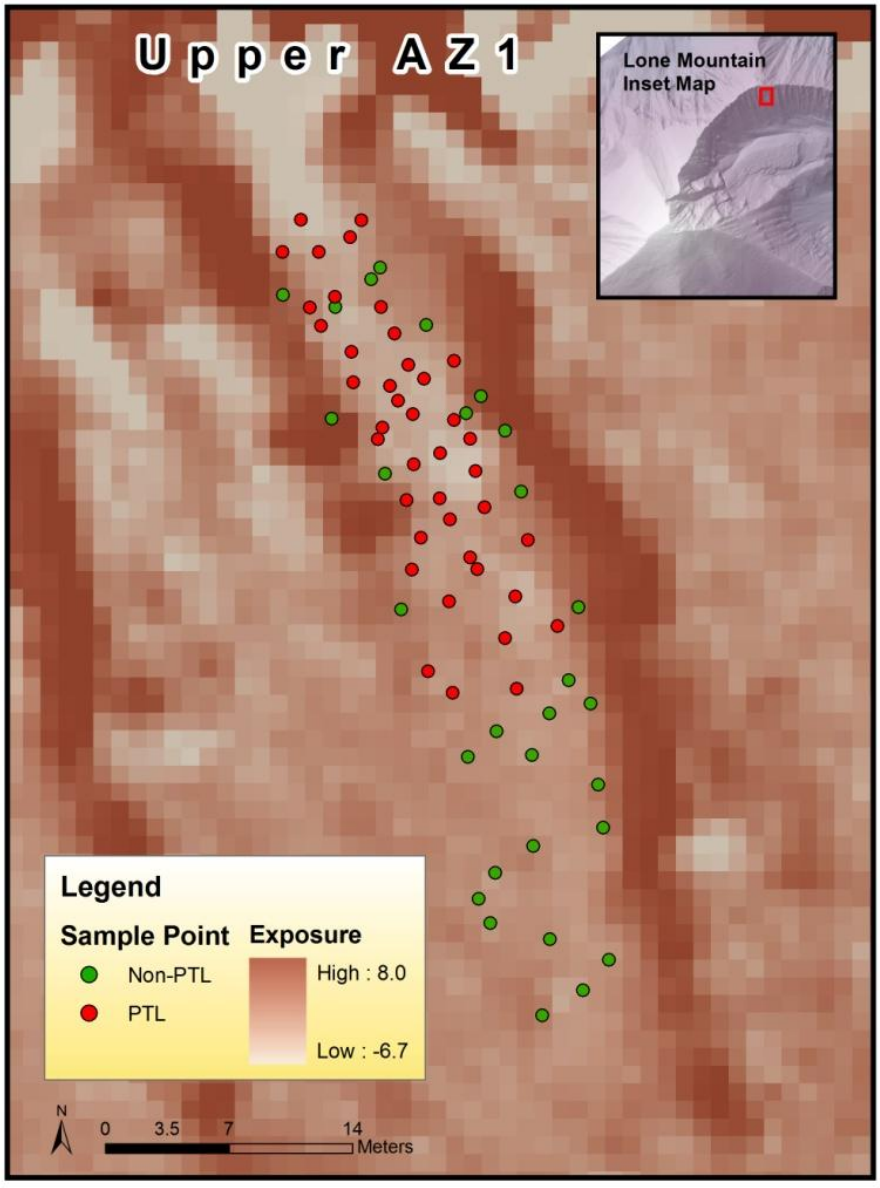

Fig. 22. Spatial distribution of PTLs and non-PTLs for Upper AZ1 over the grid of terrain exposure. A strong association between PTLs and low exposure is apparent, as well as an obvious trend of more PTLs at higher elevations, which are at the top of the figure.

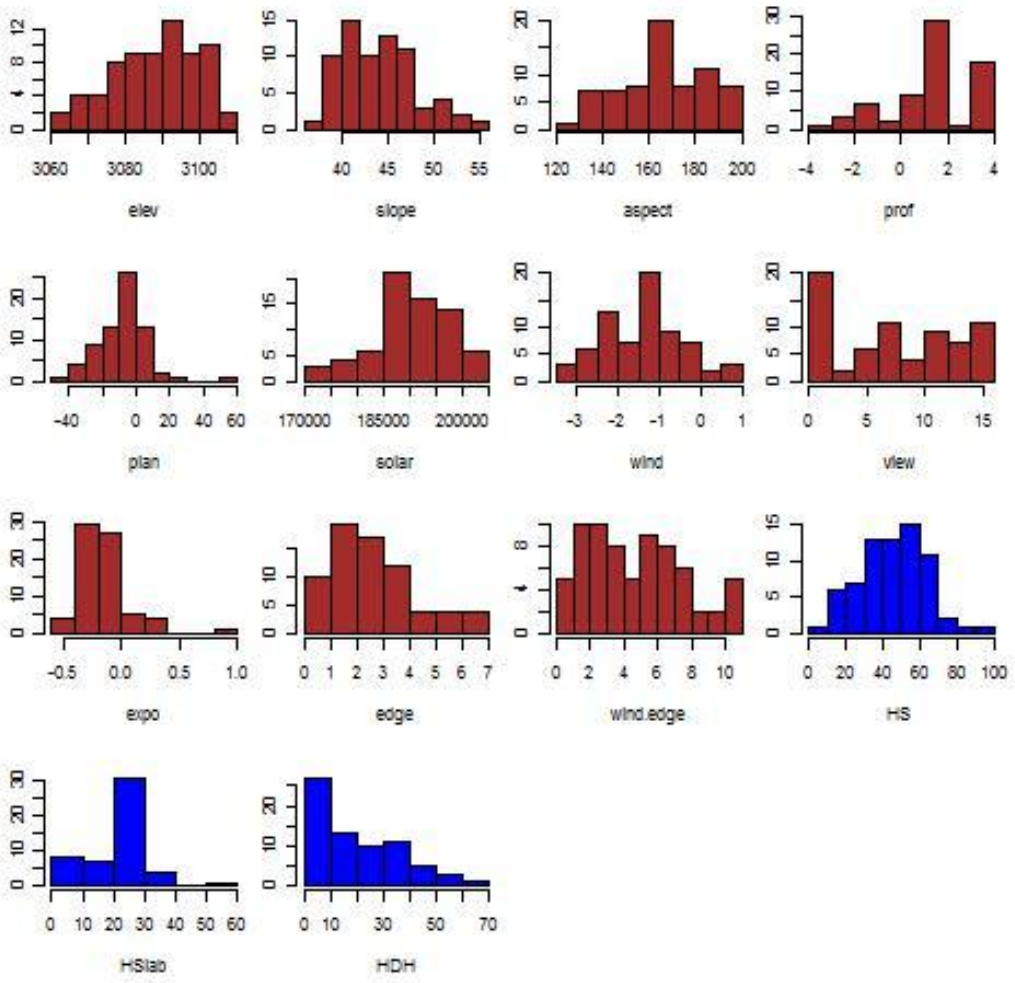

Fig. 23. Histograms of terrain parameters and snow observations for Upper AZ1, showing a shallow snowpack and high density of fairly shallow slabs. Terrain parameters are shown in brown and snowpack parameters are shown in blue.

With a sample size of 70, Spearman's rank-order correlation coefficients are significant for values greater than 0.235 from a two-tailed distribution at the α=0.05 level (Zar, 1972). A number of terrain parameters are significantly correlated with *HS*, *HSlab*, and *HDH* (Fig. 24). The linear and quadratic forms of *edge*, *slope*, and *elev* have particularly strong correlations, as do the linear affects of *plan* and *expo*.

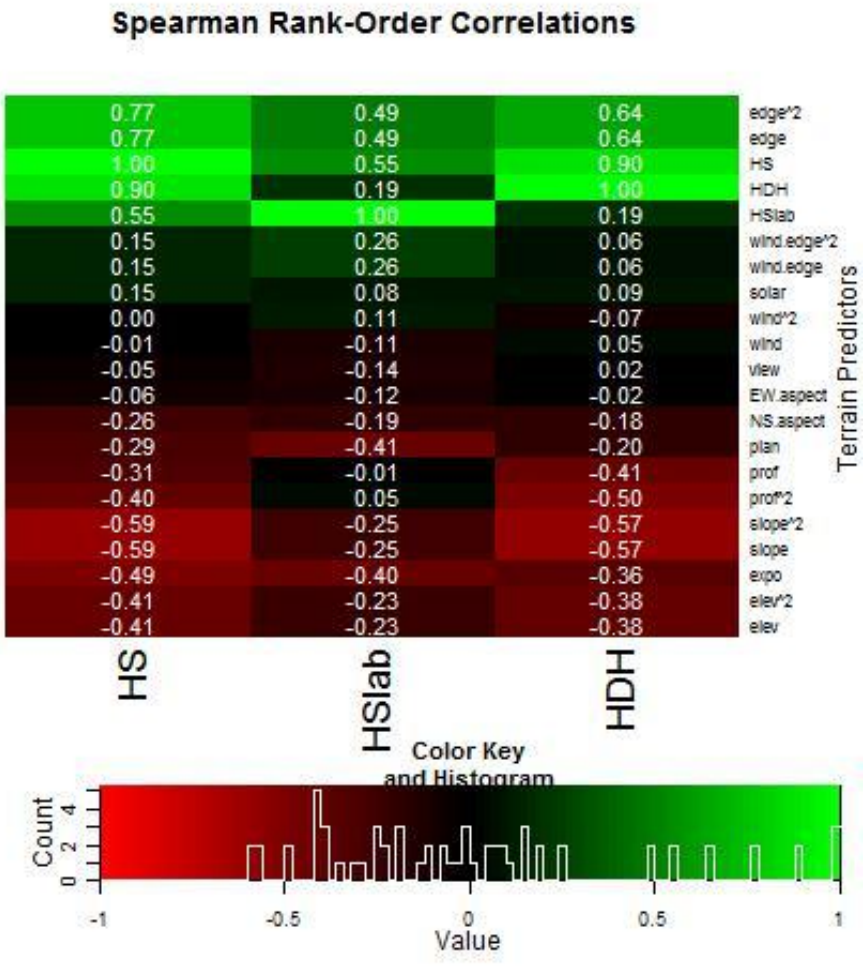

Fig. 24. Heat map of Spearman's rank-order correlation coefficients for snow depth (*HS*), slab thickness (*HSlab*), and depth hoar thickness (*HDH*). Correlations greater than 0.235 or less than -0.235 are significant (shown in lighter color values).

With the exception of *edge*, all of the parameters reject the null hypothesis of the KS-test that the PTL and non-PTL samples are from the same distribution (Table 7). In other words, the distribution of these terrain parameter values at PTLs differ significantly from non-PTLs, and this suggests that, when considered independently, each of these terrain parameters has the potential to help discriminate between PTLs and non-

PTLs. A comparison of the estimated probability distribution functions (PDFs) shows general patterns of how differences between the presence or absence of PTLs are conveyed in the terrain. For example, PTLs appear to have a higher density at higher elevations and less exposed terrain (Fig. 25), suggesting that for this couloir we are more likely to find a PTL in those areas. Furthermore, this suggests that a snow pit dug at lower elevations or more exposed terrain is likely to give misleading results about instabilities higher on the slope or in more sheltered terrain. These plots are consistent with the results of the KS-test (Table 6) and the patterns identified from the map (Fig. 22).

Table 6. Results from the KS-test on whether the terrain parameters come from the same distributions for PTL and non-PTL occurrences. The parameters that reject the KS-test have the potential to independently discriminate between PTLs and non PTLs.

Parameter	P-Value	H_0 result
elev	**0.0002**	reject
slope	**0.0412**	reject
EW.aspect	**0.0172**	reject
NS.aspect	**0.0172**	reject
prof	**0.0075**	reject
plan	**0.0090**	reject
solar	**0.0048**	reject
wind	**0.0002**	reject
expo	**0.0001**	reject
edge	0.5543	fail to reject
wind.edge	**0.0028**	reject

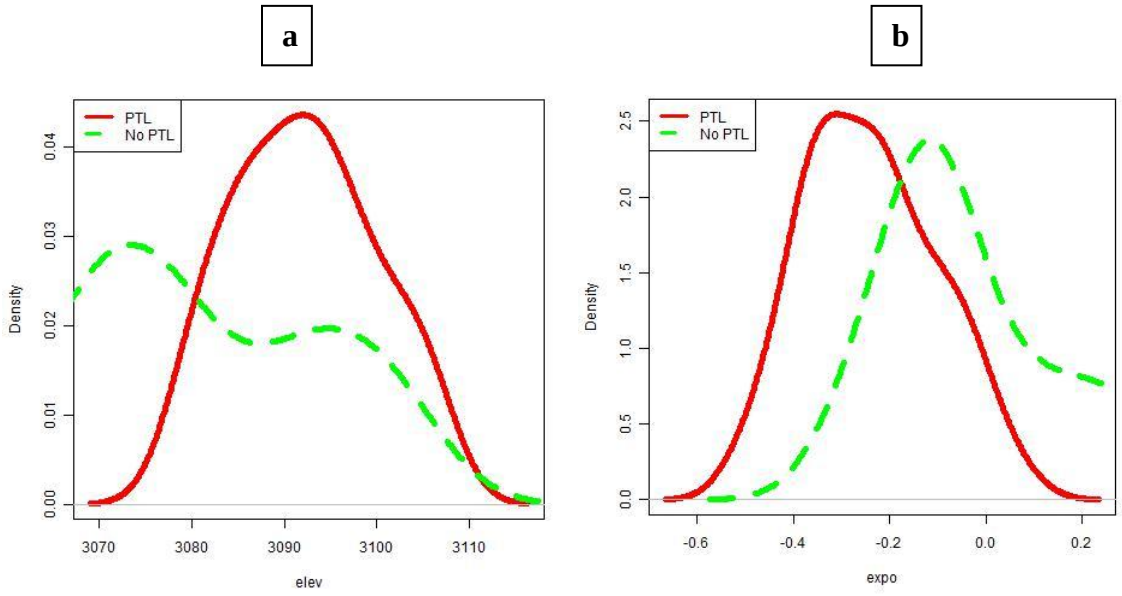

Fig. 25. The distributions of *elev* and *expo* (b) for PTL and non-PTL observations. For Upper AZ1, PTLs are associated with higher elevations and less exposed terrain than non-PTLs.

To explore hierarchal relationships between PTLs and terrain parameters, I fit a full model of all twelve parameters in the classification tree model of the form:

$$\text{PTL} \sim edge + prof + expo + rel.view + slope + rel.elev + rel.solar + plan + wind.edge + wind + EW.aspect + NS.\text{aspect} \quad (8)$$

Cross validation error of the overfit tree is minimized at a complexity parameter of 0.13, corresponding to a pruned tree size with three nodes (Fig. 26).

The pruned tree recursively partitions 29 non-PTL locations with threshold values for *rel.elev*, *plan*, and *edge*. The final model correctly classifies all but five of the observations (Fig. 27). Note that independently, *edge* is not found to have differing distributions for PTL or non PTL locations, but its interactions with *rel.elev* and *plan* lead to its inclusion in the tree model. The interaction is as follows: at relatively higher

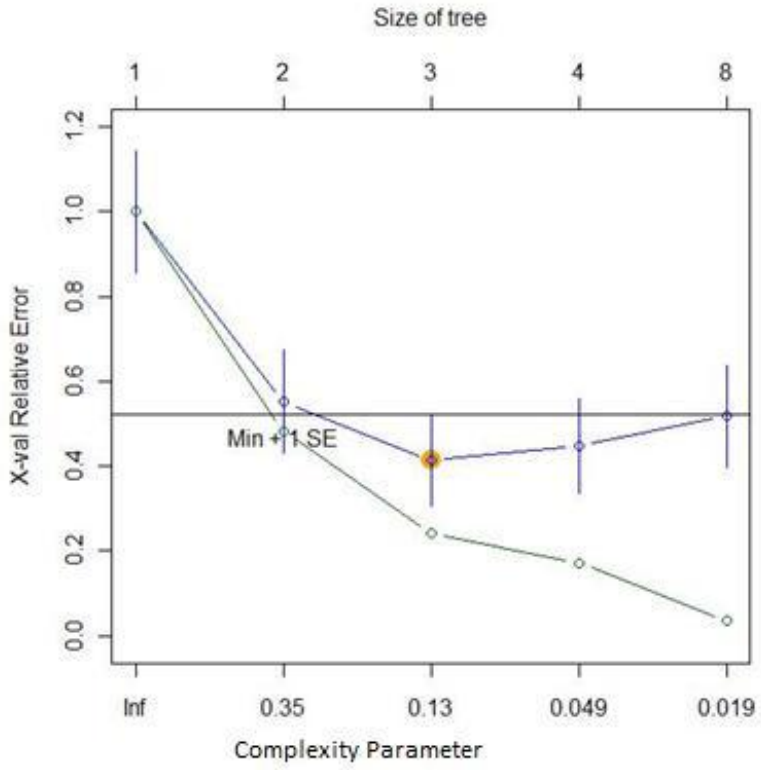

Fig. 26. Cross-validation results for tree pruning. The yellow dot indicates the complexity parameter that minimizes cross-validation error. The classification tree was pruned back to this complexity. The upper blue line shows relative cross validation error and the lower green line shows relative error.

locations in the couloir (*rel.elev* >= 0.36), where the plan curvature of the slope is relatively more concave (*plan* < 3.6), PTLs are unlikely within 0.65 m of the edge of the couloir (*edge* >= 0.65). This relationship makes sense. In the upper part of the couloir (high *rel.elev*) there is an absence of PTLs near the fall-line ridges (high *plan*) where wind prevented significant snow or slab accumulation and subsequent melting from exposed rocks strengthened the surrounding snowpack. Other locations near the sides of the couloir that are not near the fall-line ridges are also typically too shallow for significant slabs, thus the inclusion of *edge*. This example highlights the importance of

considering the how terrain parameters interact in full models rather than just their independent influences (as identified with the KS-test).

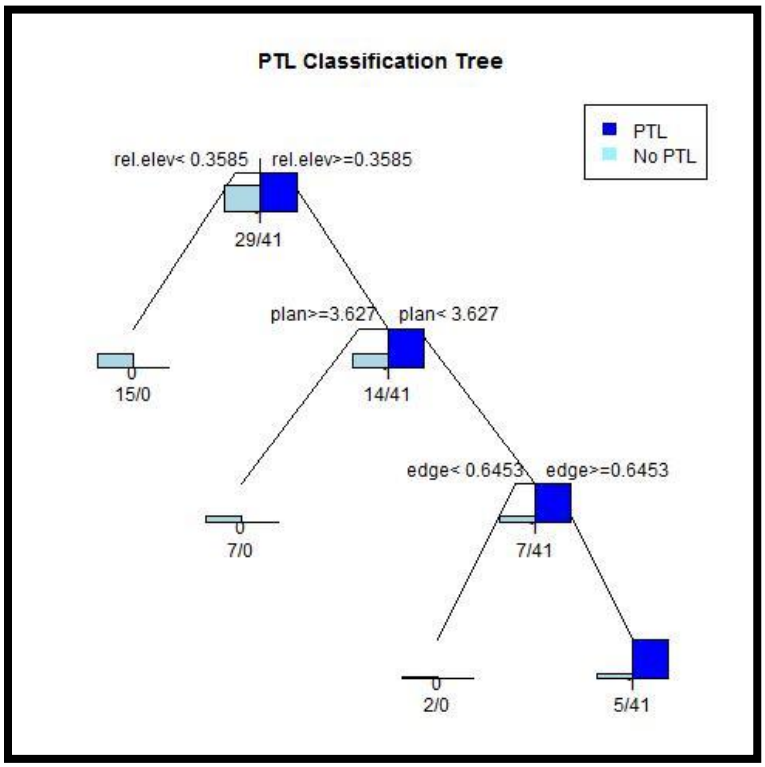

Fig. 27. The pruned classification tree for Upper AZ1 (with 3 nodes) showing that most of the discriminating power for PTLs comes from relative elevation in the first node.

Using the same structure and fitting principals as the classification tree, the Random Forest boot-strapping technique creates a more robust predictive model for comparison with other couloirs by averaging the most important trends in the data (Breiman, 2001). The pruned tree described above is likely the "best" classification tree for the data but, by repeatedly withholding "out-of-bag" (OOB) samples of data, refitting the model, and cross-validating the accuracy using these OOB samples to hone in on a group of "good" trees, I create a classification model that does not rely on intricate

relationships that may be spurious or too specific for comparing to other couloirs. The parameter importance from this robust Random Forest model, quantified by the mean decrease in accuracy, is plotted for two scenarios: Fixed PTLs and Uncertain PTLs. For Fixed PTLs I maintain the minimum slab criterion for a PTL at 15 cm and plot the parameter importance from the Random Forest model. For the Uncertain PTLs I iteratively refit the Random Forest model with increasing minimum slab criteria from 1 cm to 40 cm and average the importance values at each step.

Rel.elev has the most predictive power for both Fixed PTL and Uncertain PTL scenarios (Fig. 28). This suggests that, regardless of the uncertainty in defining the minimum slab required for a PTL, *rel.elev* is still a strong parameter. Again, this agrees with our observations because in the lower portion of the couloir, we found no depth hoar, but at the higher elevations, depth hoar was fairly widespread, so regardless of the minimum slab criteria for PTLs, the lower elevations are still considered non-PTLs without the presence of a weak layer. The Random Forest model for the Fixed PTL has an OOB estimated success rate of 80% for this data. The mean decrease in accuracy for *rel.elev* is 0.08, suggesting that in the absence of *rel.elev*, the model is only capable of a 72% success rate. None of the other parameters are particularly robust to changes in PTL slab criteria, but *plan*, *expo*, and *rel.view* are noticeably more important for the fixed definition of PTLs. The model shows good discrimination ability for PTL and non-PTLs with a true skills score of 0.59 (Table 7).

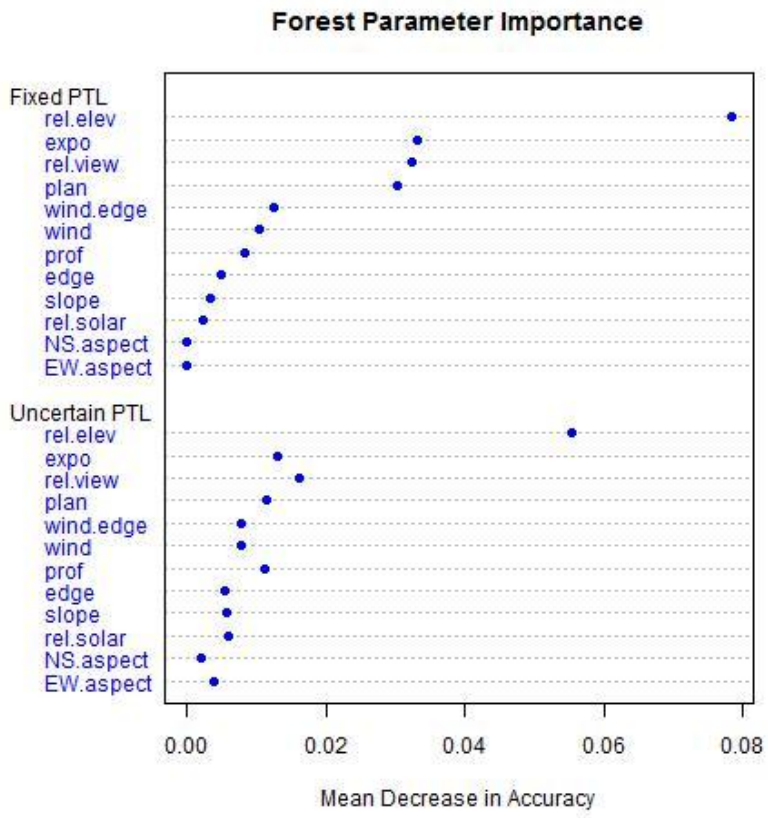

Fig. 28. Terrain parameter importance for the Random Forest model for Upper AZ1. Fixed PTL points show the importance when the minimum slab criterion is 15 cm. Uncertain PTL points show the importance when the minimum slab criterion varies from 1 cm to 40 cm.

I also fit a smoothed regression line to a plot of the mean decrease in accuracy values for selected strong parameters versus the minimum slab criteria for a PTL (Fig. 29). In the absence of any slab, *rel.elev* is the only strong parameter, with a small effect from *rel.view*. This implies that *rel.elev* is strongly associated with depth hoar presence, while the other parameters are more closely associated with slab thickness. Note that all of the parameters converge on zero near a 30 cm slab. This is a by-product of the data and boot-strapping technique, rather than a meaningful relationship, which consistently

appears in many of the individual couloir datasets. Because there are only several locations observed with slabs thicker than 30 cm (Fig. 23), it is difficult to model their presence. The boot-strapping technique makes it nearly impossible to find a parameter that consistently predicts the location of those few points.

Table 7. Confusion matrix for the prediction of Upper AZ1 observations using the Random Forest model.

		Observed	
		PTL	no PTL
Predicted	PTL	**35**	**7**
	no PTL	**7**	**22**

In order to test how effective the specific PTL/terrain relationships are for this couloir when used to predict PTLs for other couloirs, I cross-validated this Random Forest model to the entire dataset of twenty other couloirs. I applied the same nodes and branches from the averaged classification trees to the terrain values associated with the other couloirs, and compared the predicted results versus the results that we observed from the field. I averaged the mean success rates and true skill statistics for the entire dataset of all weak layer types, for each unique weak layer type, for each group that contains depth hoar as a weak layer, and for each winter season (Fig. 30). The predictive success rate for the

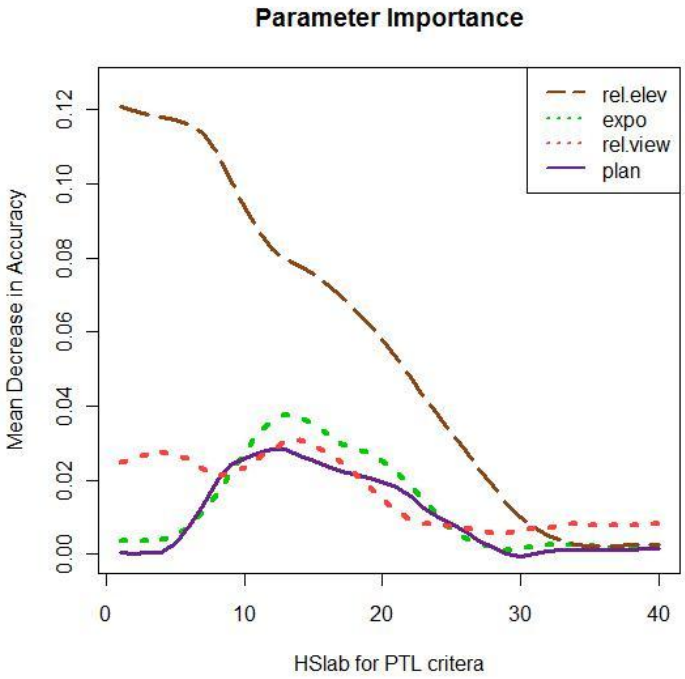

Fig. 29. Smoothed regression lines for the importance of selected parameters plotted against changing minimum slab criteria.

entire dataset is 51%, which is essentially the same as flipping a coin. In other words, the specific hierarchal relationships defining the presence/absence of PTLs in this one couloir only correctly predicted 51% of all of our snowpack observations through the course of two seasons. There is little improvement in the predictive ability for groups that might be expected to have similarities, such as the other Upper A to Z chutes, other depth hoar layers, or other samples collected during the same season. The cross-validated true skill statistics show the same pattern of poor model discrimination ability. These results imply that the relationships between PTLs and terrain identified by the Random Forest model are specific to Upper AZ1; thus, predicting locations of PTLs in other couloirs based on these specific relationships would be unsuccessful.

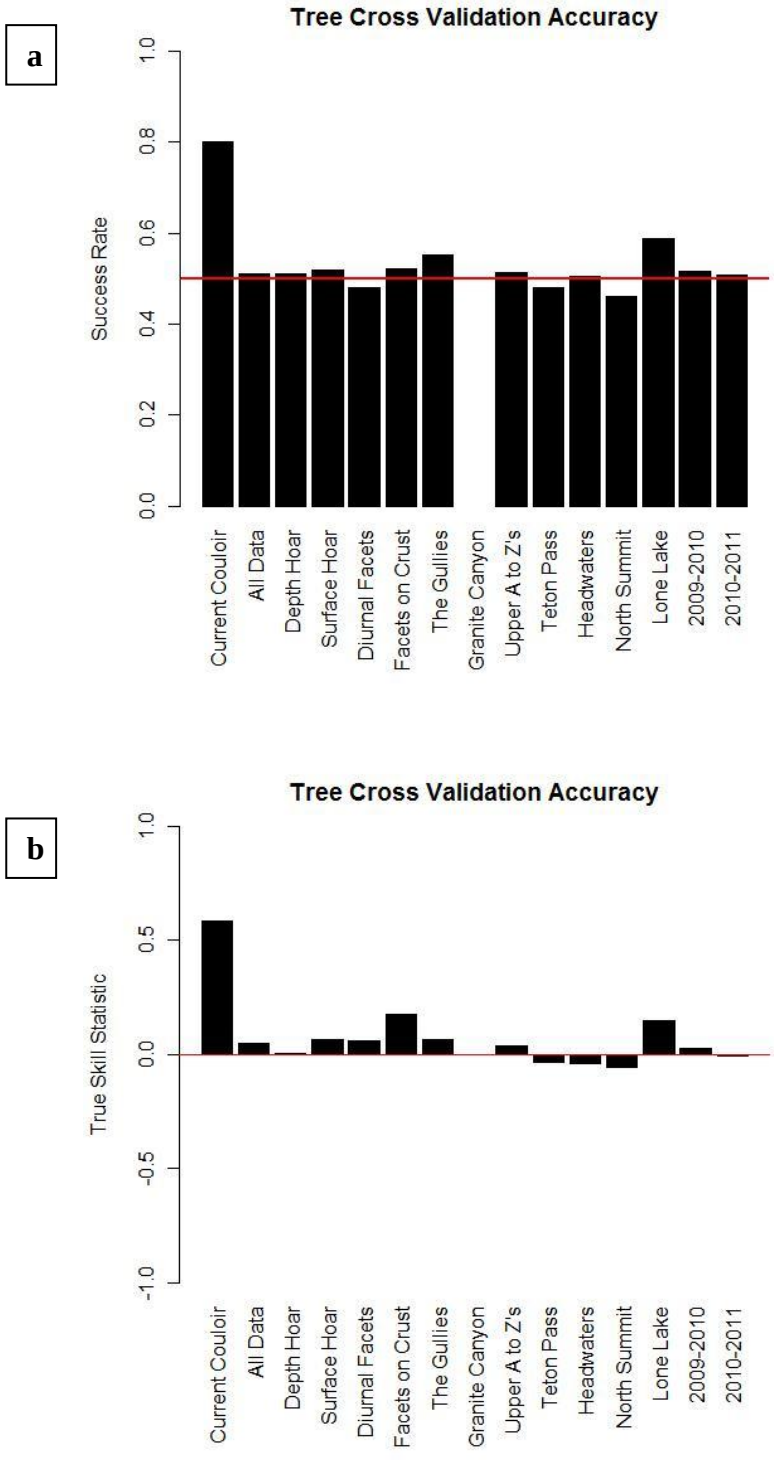

Fig. 30. Success rate (a) and true skill score (b) cross-validation results for Upper AZ1 Random Forest model against different weak layer types, different groups with depth hoar, and different winter seasons.

Random Forest classification model predictions utilize specific hierarchal and threshold relationships within the data. To explore the possibility of highlighting different linear relationships, and to test their predictive success when cross-validated against other couloirs, I apply an entirely different model structure to the same data from Upper AZ1. I fit a logistic model of all of the linear main effects and the pre-selected quadratic terms, with the form:

$$\begin{aligned} PTL \sim\ & edge + edge^2 + prof + prof^2 + expo + rel.view + slope + \\ & slope^2 + rel.elev + rel.elev^2 + rel.solar + plan + wind.edge + \\ & wind.edge^2 + wind + wind^2 \end{aligned} \quad (9)$$

The glmulti genetic algorithm finds the top 30 models with the lowest AICc (Calcagno and de Mazancourt, 2010). I select all of the models that fall within the threshold of two AICc values of the minimum AICc model as the final logistic model (Fig. 31).

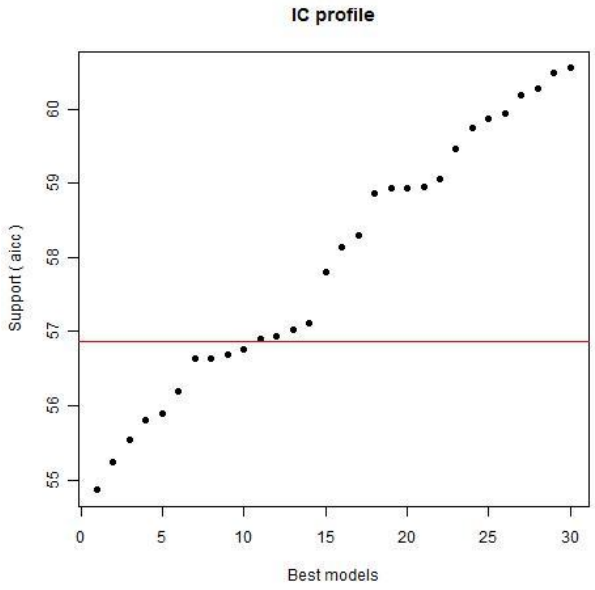

Fig. 31. Profile of AICc values for the top 30 models in the glmulti reduction of the full logistic regression model for Upper AZ1. The red line indicates the threshold value at which all models below it are selected for the final logistic model.

Table 8. All of the models averaged for the final logistic model of Upper AZ1.

AICc	Lowest AICc Model
54.87	$PTL \sim 1 + expo + rel.elev + rel.elev^2$
55.25	$PTL \sim 1 + expo + rel.elev + rel.elev^2 + wind.edge$
55.54	$PTL \sim 1 + expo + rel.view + rel.elev + rel.elev^2$
55.81	$PTL \sim 1 + edge + expo + rel.elev + rel.elev^2 + wind.edge$
55.89	$PTL \sim 1 + prof + expo + rel.elev + rel.elev^2$
56.20	$PTL \sim 1 + edge + expo + rel.elev + rel.elev^2$
56.63	$PTL \sim 1 + edge^2 + expo + rel.elev + rel.elev^2 + wind.edge$
56.64	$PTL \sim 1 + expo + rel.elev + rel.elev^2 + rel.solar + wind.edge$
56.68	$PTL \sim 1 + edge^2 + expo + rel.elev + rel.elev^2$
56.77	$PTL \sim 1 + expo + rel.elev + rel.elev^2 + rel.solar$

In this case, ten models are selected and weighted according to their AICc (Table 8). Again, *rel.elev*, and additionally, *rel. elev*^{2} are in every model and have the highest parameter importance, along with *expo* (Fig. 32). Because *expo* and *plan* are highly correlated parameters, it is not surprising to see only one of them in the most important terms, unlike in the Random Forest model. Here it seems that a linear relationship with *expo* better describes the ridge scouring than *plan* without correlating with other terms. The logistic model shows an improved success rate over the Random Forest model, predicting 87% of the observations correctly based on the terrain.

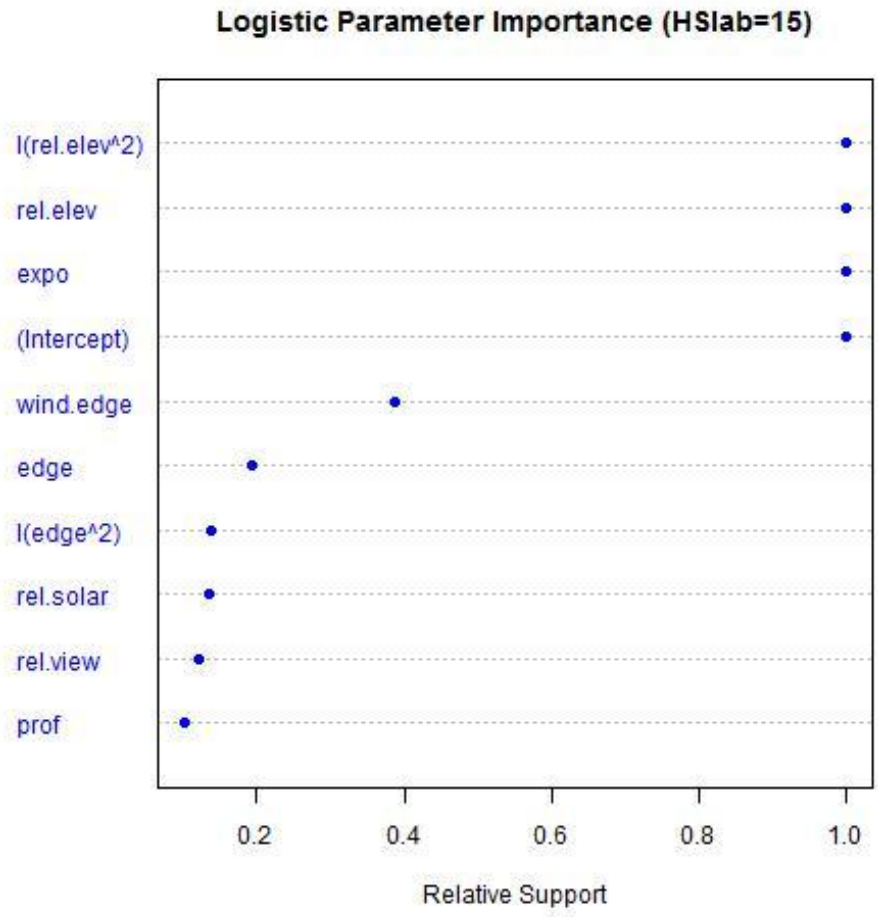

Fig. 32. Importance of parameters in the logistic regression of Upper AZ1 for a minimum slab criterion of 15 cm.

Parameter importance varies for changes in slab criteria for PTLs (Fig. 33). Again, *rel.elev* and *expo* both appear important for changing minimum slab criteria, suggesting that these are robust predictors of PTLs for Upper AZ1.

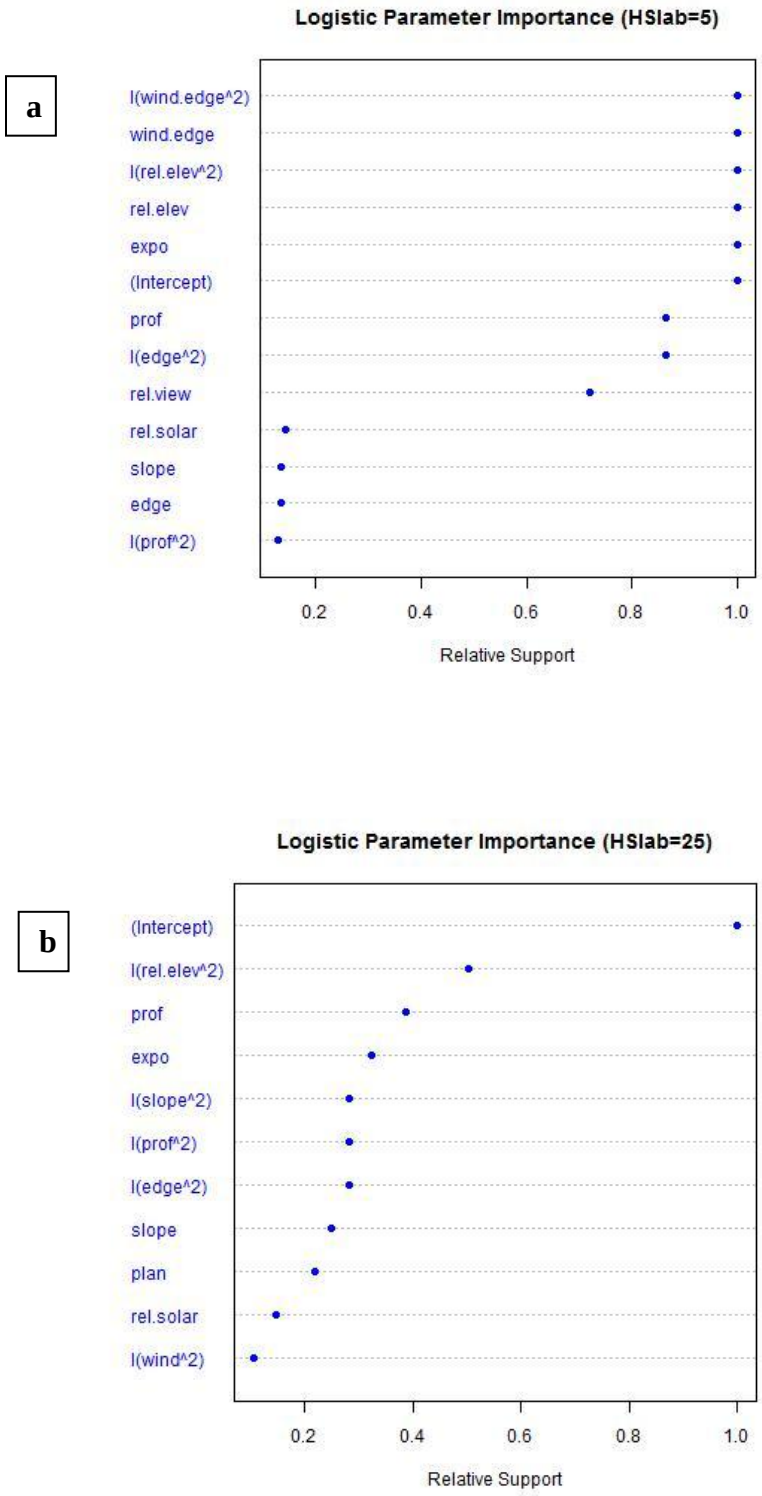

Fig. 33. Importance of parameters in the logistic regression of Upper AZ1 for a minimum slab criterion of 5 cm (a) and 25 cm (b).

A computational problem arises in logistic regression if a model is too "perfect" in that it is able to correctly separate all of the successes and failures. This leads to probabilities of 100% or 0%, and yields very large estimates because the model attempts to transition rapidly at the threshold point, rather than linearly (Greenwood, pers. comm., 2011). These terms are highly important, even though they have large standard errors and massive confidence intervals. However, their coefficients, log-odds ratios, and confidence intervals are difficult to interpret. Upper AZ1 is one of the few couloirs in this study with the problem of perfect separation (Table 9). *Rel.elev*, $rel.elev^2$, *expo*, and the intercept combine to create one of several models with perfect separation, which is readily apparent because of their large confidence intervals. These terms are highly important in the model, and the signs of their coefficients are still meaningful for interpretation. The negative coefficient of *expo* implies that for increasing exposure values, the probability of a PTL decreases (has a negative linear relationship) when all other parameters are held constant. The inclusion of *rel.elev* and $rel.elev^2$ in the same model may seem unusual, but they combine to explain a non-linear probability of PTLs. The positive coefficient for *rel.elev* and negative coefficient for $rel.elev^2$ implies that at lower elevations (small *rel.elev* values) the probability of a PTL increases. However, with increasing *rel.elev*, the negative coefficient on $rel.elev^2$ gains power, and thus, the probability of PTLs at higher elevations decreases again. This highlights a relative clustering of PTLs in the middle of the couloir, which is evident from the PDF of *rel.elev* (Fig. 25a) and the map of PTLs (Fig. 22). This example demonstrates how both

modeling techniques are capable of explaining the strong relationship between *rel.elev* and PTLs despite differences in model structure.

The other estimates included in the final averaged model have standard interpretations from their odds ratios. For example, *edge* has an odds ratio of 1.10, meaning that if all other terms are held constant, moving one meter further from the edge of the couloir yields a 10% increase in the probability of finding a PTL (Table 10). This agrees with our observations: as we sampled closer to the edge of the couloir, we were more likely to find an insignificant slab above the depth hoar or no depth hoar at all.

Table 9. Coefficients, odds ratios, 95% confidence limits, and importance values for the averaged final logistic model of Upper AZ1. Parameters that are considered highly significant, based on their exclusion of zero in their confidence interval, are highlighted in green.

	Estimates	Lower CL	Upper CL	Odds Ratio	Upper CL Odds Ratio	Lower CL Odds Ratio	Importance
Intercept	-9.931	-17.793	-2.070	5.00E-05	1.26E-01	0	1
expo	-9.193	-15.710	-2.676	1.00E-04	6.88E-02	0	1
rel.elev	34.218	9.790	58.649	7.26E+14	2.96E+25	17817.93	1
rel.elev^2	-26.336	-45.512	-7.160	0.00E+00	8.00E-04	0	1
wind.edge	-0.092	-0.368	0.184	9.12E-01	1.20E+00	0.6922	0.386
edge	0.092	-0.270	0.454	1.10E+00	1.57E+00	0.7637	0.193
edge^2	0.007	-0.024	0.038	1.01E+00	1.04E+00	0.9759	0.139
rel.solar	-0.201	-1.148	0.746	8.18E-01	2.11E+00	0.3173	0.136
rel.view	-0.280	-1.422	0.863	7.56E-01	2.37E+00	0.2412	0.121
prof	0.032	-0.102	0.165	1.03E+00	1.18E+00	0.9025	0.102

The cross-validation results from the logistic regression model show equally poor predictive power as the Random Forest model, with success rates hovering around 50% and mean absolute error around 0.5 (Fig. 34). This reinforces the conclusion that this

couloir's characteristics are relatively unique, and that predicting PTLs in other couloirs based on the specific relationships from this couloir is challenging at best.

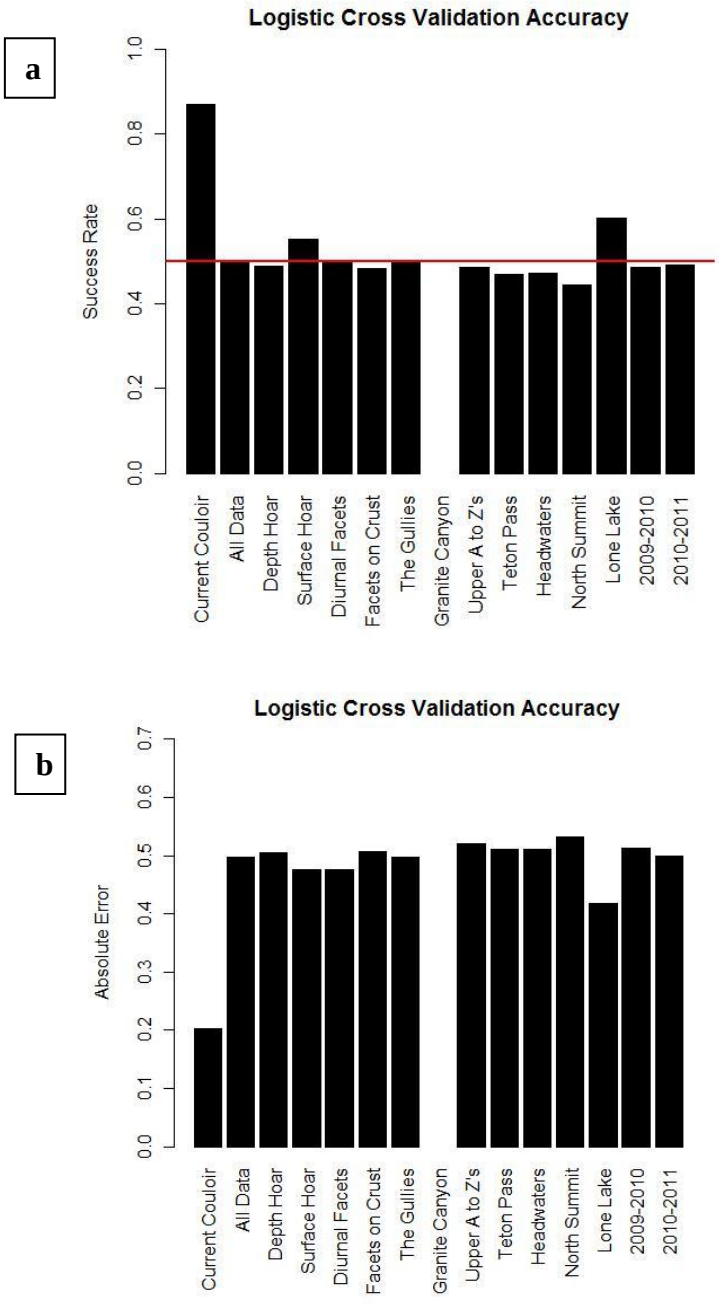

Fig. 34. Success rate (a) and absolute error (b) cross-validation results for the final logistic model of Upper AZ1.

In summary, classification techniques or logistic regression models are both capable of successfully modeling the observed patterns of PTLs in Upper AZ1, with success rates above 80%. While some of the secondary parameters vary in the models, both model structures agree on a very strong association between relative elevation and PTLs that is robust to changing minimum slab criteria. Exposure is also important in both models and robust to different slab criteria, but with a somewhat weaker contribution. Although the models suggest that specific relationships exist between PTLs and the terrain for this couloir, these relationships carry poorly to other couloirs. For example, the classification models for this couloir draw a considerable amount of success from the strong relationship with *rel.elev* by partitioning a high proportion of observations towards PTLs above a relative elevation threshold of 35%. This specific relationship does not successfully apply to the other couloirs in this study, thus the poor cross-validation results. However, this case study illustrates how for a specific couloir, certain terrain parameters are strongly associated and able to reasonably predict the presence of PTLs in that couloir.

Depth Hoar Results and Discussion

Individual Couloirs

The results and discussion in this section are for all of the couloirs in which a layer of depth hoar (or developed facets at the base of the snowpack) was tracked. This includes all of the couloirs on Lone Mountain and the two couloirs on Teton Pass. PTLs for these data are defined as any location with the presence of a basal weakness and an overlying slab of at least 15 cm (Table 2). Here I examine whether our observations of

depth hoar PTLs can be successfully modeled for each individual slope and, if so, which parameters are most important for these models and how well these models apply to other couloirs. The results of the KS-tests and individual modeling are summarized in Tables 10 and 11 and Fig. 35.

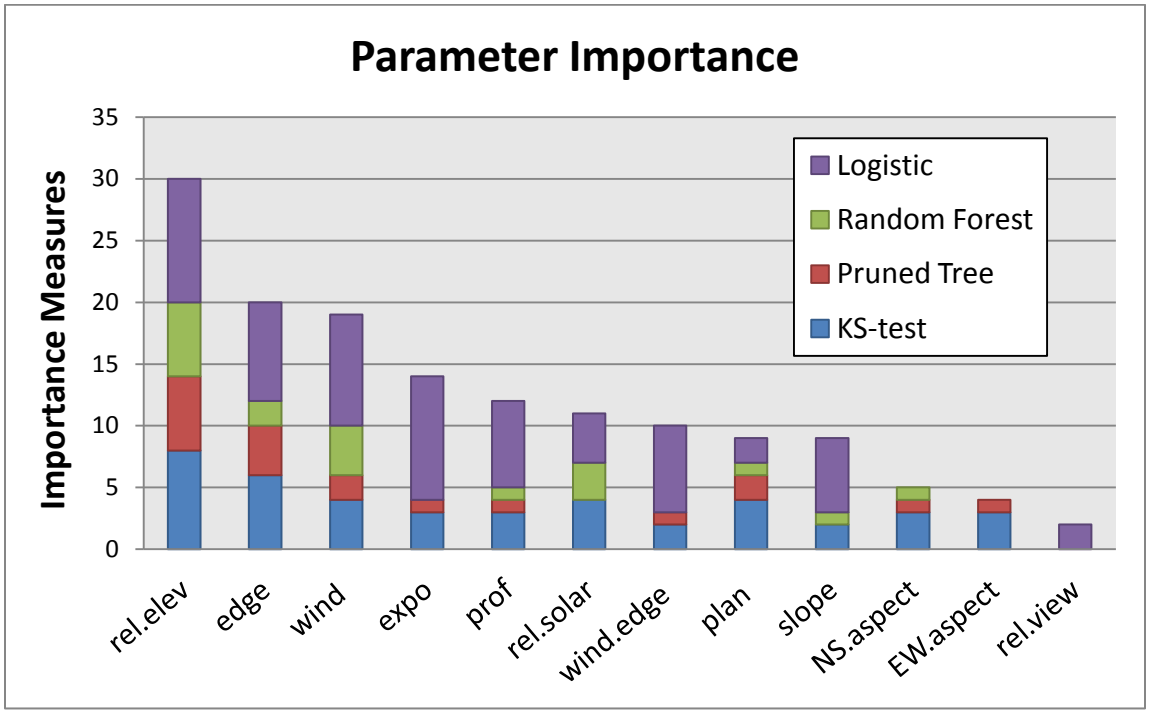

Fig. 35. Cumulative measures of importance for each parameter for depth hoar PTLs from four tests: significance from the KS-test, first node in the pruned classification tree, most important parameter in the Random Forest model, and appearance in the lowest AICc logistic regression model.

Table 10. KS-test results testing whether the distributions of individual couloir depth hoar PTLs and non-PTLs are different for each parameter. Significant results, indicated by bold text and green cells, suggest that the parameter may be useful in independently discriminating locations of PTLs.

Kolmogorov-Smirnov goodness-of-fit test results: P-values																			
Couloir ID#	**1**	**2**	**5a**	**6a**	**7a**	**8a**	**9a**	**10a**	**11**	**12**	**13**	**14**	**15a**	**16**	**17a**	**18**	**19a**	**20**	**21a**
rel.elev	**0.03**	**0.00**	**0.00**	0.46	**0.00**	**0.02**	0.38	0.11	0.90	0.08	0.71	**0.01**	0.26	0.19	0.08	**0.01**	0.63	0.83	**0.00**
slope	0.41	0.09	**0.04**	0.59	**0.00**	0.40	0.07	0.06	0.77	0.37	0.98	0.12	0.15	0.89	0.70	0.05	0.21	0.50	0.16
EW. aspect	0.30	**0.01**	**0.02**	0.82	0.26	0.92	0.42	0.64	0.77	0.30	0.69	0.96	0.28	0.57	0.63	0.55	0.10	**0.04**	0.77
NS. aspect	0.25	**0.01**	**0.02**	0.82	0.65	0.98	0.42	0.97	0.63	0.24	0.30	0.96	0.40	0.65	0.07	0.89	0.16	**0.04**	0.77
prof	0.26	0.26	**0.01**	0.83	0.33	0.99	0.93	**0.04**	0.82	0.51	0.97	0.48	0.52	0.35	0.46	0.18	0.73	0.67	**0.02**
plan	0.10	0.97	**0.01**	**0.04**	0.10	0.60	0.98	0.48	0.27	0.34	**0.03**	0.64	0.66	0.11	0.61	0.39	**0.00**	0.58	0.68
solar	0.27	**0.03**	**0.00**	0.70	**0.03**	0.31	0.27	0.23	0.55	0.85	0.34	0.12	0.47	0.54	0.74	**0.02**	0.29	0.21	0.24
wind	0.59	**0.00**	**0.00**	**0.00**	0.09	0.91	0.67	0.22	0.94	**0.04**	0.23	0.23	0.91	0.55	0.53	0.45	0.59	0.66	0.80
expo	0.18	0.31	**0.00**	**0.00**	0.08	0.07	0.32	0.17	0.06	0.22	0.06	0.92	0.51	0.42	0.94	0.66	**0.01**	0.83	0.59
edge	0.30	**0.01**	0.55	0.26	**0.00**	0.38	**0.03**	0.15	0.10	0.14	0.99	**0.02**	**0.00**	0.21	0.10	0.26	0.34	0.41	**0.01**
wind. edge	0.38	**0.01**	**0.00**	0.60	0.10	0.47	0.12	0.11	0.47	0.88	0.58	0.71	0.07	1.00	0.25	0.14	0.15	0.53	0.11

Table 11. A summary of predictive success and skill for both model structures, as well as most important parameters associated with these models for the individual couloir modeling of depth hoar PTLs.

Couloir ID#	First node	RF most important (Fixed PTL)	RF True Skill Stat	RF Success Rate	RF most important (Uncertain PTL)	Lowest AICc logistic model	Logistic Mean Absolute Error	Logistic Success Rate	Logistic True Skill Stat
1	*rel.elev*	*rel.elev*	0.11	61%	*rel.elev*	*PTL ~ 1 + prof^2 + expo + rel.elev + rel.solar + wind.edge + wind*	0.37	73%	0.35
2	*rel.elev*	*rel.elev*	0.36	69%	*rel.elev*	*PTL ~ 1 + prof + rel.elev + rel.elev^2 + wind + wind^2*	0.35	75%	0.46
5a	*rel.elev*	*rel.elev*	0.55	80%	*rel.elev*	*PTL ~ 1 + expo + rel.elev + rel.elev^2*	0.20	87%	0.72
6a	*wind*	*wind*	0.43	71%	*wind*	*PTL ~ 1 + rel.elev + wind*	0.33	79%	0.57
7a	*edge*	*slope*	0.37	74%	*slope*	*PTL ~ 1 + expo + rel.view + slope^2+ rel.elev^2 + wind^2*	0.26	79%	0.42
8a	*rel.elev*	*rel.elev*	0.18	62%	*rel.elev*	*PTL ~ 1 + prof + prof^2 + expo + rel.elev + rel.elev^2 + plan + wind.edge + wind.edge^2*	0.29	79%	0.57
9a	*edge*	*rel.solar*	0.12	57%	*wind*	*PTL ~ 1 + edge + prof + prof^2 + slope + slope^2*	0.32	78%	0.52
10a	*prof*	*prof*	-0.05	49%	*rel.elev*	*PTL ~ 1 + edge^2 + rel.view + rel.elev + rel.elev^2 + rel.solar*	0.43	70%	0.31
11	*expo*	*rel.solar*	-0.15	42%	*rel.solar*	*PTL ~ 1 + edge^2 + expo + slope^2 + wind.edge^2 + wind + wind^2*	0.40	71%	0.42
12	*wind*	*wind*	0.22	65%	*wind*	*PTL ~ 1 + edge + expo + slope + slope^2 + rel.elev^2 + rel.solar + wind + wind^2*	0.37	72%	0.39
13	*plan*	*wind*	-0.15	51%	*wind*	*PTL ~ 1 + prof^2 + expo + wind^2*	0.40	69%	0.08

Table 11 Continued

Couloir ID#	First node	RF most important (Fixed PTL)	RF True Skill Stat	RF Success Rate	RF most important (Uncertain PTL)	Lowest AICc logistic model	Logistic Mean Absolute Error	Logistic Success Rate	Logistic True Skill Stat
14	*edge*	*edge*	0.31	66%	*edge*	*PTL ~ 1 + prof + prof^2 + slope + wind.edge^2*	0.40	72%	0.40
15a	*edge*	*edge*	0.13	58%	*edge*	*PTL ~ 1 + edge + expo + wind.edge*	0.42	68%	0.34
16	*rel.elev*	*rel.elev*	0.00	75%	*rel.elev*	*PTL ~ 1 + rel.elev^2 + plan*	0.31	80%	0.16
17a	*NS.aspect*	*wind*	-0.02	60%	*wind.edge*	*PTL ~ 1 + edge^2 + rel.elev + wind.edge^2 + wind*	0.35	71%	0.22
18	*wind.edge*	*rel.solar*	0.10	60%	*rel.solar*	*PTL ~ 1 + edge + edge^2 + rel.solar + wind^2*	0.37	73%	0.31
19a	*plan*	*plan*	0.06	57%	*plan*	*PTL ~ 1 + prof + expo + slope^2 + rel.elev^2*	0.36	75%	0.49
20	*EW.aspect*	*NS.aspect*	0.13	58%	*NS.aspect*	*PTL ~ 1 + expo + wind.edge^2*	0.46	64%	0.18
21a	*rel.elev*	*rel.elev*	0.31	72%	*rel.elev*	*PTL ~ 1 + edge + prof + rel.elev + rel.elev^2*	0.28	82%	0.62
Mean			**0.16**	**62%**			**0.35**	**75%**	**0.40**

The modeling of individual couloirs shows a wide range of different parameters are influential in PTL modeling. Sixteen of the nineteen samples have at least one parameter that has a significantly different distribution for PTLs and non-PTLs (Table 10). *Rel.elev* and *edge* are most frequently associated with these differences, per the KS-test. The first node used in the pruned classification tree, which indicates which parameter best differentiates the PTLs observations from non-PTLs, is also most consistently *rel.elev* and *edge* (Table 11). In the Random Forest models, *rel.elev* is most frequently the most important as well. *Wind* appears second most frequently. Both of these parameters are robust to changes in the PTL slab criteria, implying that they are important no matter the slab depth considered. The important parameters in the final logistic models are more variable between couloirs and include some parameters that are not important in the classification models. However, *rel.elev* and/or its quadratic term are again in the majority of the "best" logistic models, followed by *expo* in importance (Table 11). In the cases where the most important term from the Random Forest model is not used in the logistic model, it is usually because the logistic model selects a correlated parameter that describes a similar physical process but is more effective in doing so linearly. When all of these measures of importance from each model or statistical test are considered, *rel.elev* has the most discriminating power of all of the parameters (Fig. 35).

Random Forest model success rates range from 42% for the Claw on Teton Pass to 80% for Upper AZ1, averaging 62% (Table 11). Logistic model success rates are consistently higher, predicting on average 75% of the observations correctly with over twice the model skill. The mean absolute error is 0.35, so that on average for each sample

point the predicted probability from the model is 35% off of the true observation. Given the highly complex and variable nature of these couloirs, this is an encouraging result.

Table 12. Averaged cross validation results for depth hoar PTL models of each of the individual couloirs used to predict PTLs for each of the remaining couloirs.

	RF success rate	RF True Skill Stat	Logistic success rate	Logistic absolute mean error
Average Xval Results	52.1%	0.017	51.6%	0.489

Similar to the AZ1 case study, cross validation results between couloirs or within common geographic groups or common weak layers are generally poor, averaging 52% for the entire dataset (Table 12). Although the two models differ in structure and frequency in the parameters used, their prediction success rates are comparably poor across couloirs. True skill scores and absolute mean errors fluctuate over the entire cross-validated dataset, but generally show an inability to discriminate (Table 12). Several exceptions exist where cross-validation results are more promising, particularly within the Upper A to Zs and the Headwaters. For example, Upper AZ3 averages a 59% success rate and a true skill score of 0.19 across the other Upper A to Zs in the Random Forest model (Table 13). This is only an 11% decrease in success from the estimated success rate for the data used to calibrate the model. These successes are usually limited to only the geographic group that the couloir belongs to and not the depth hoar group as a whole.

Table 13. Cross validation results for the Random Forest model for Upper AZ3 compared to other couloirs on the same headwall.

Cross-validation statistic	**Current: AZ3**	AZ1	AZ2	AZ4	AZ5
True Skill Stat	**0.27**	0.20	0.20	0.16	0.20
Success Rate	**70%**	61%	59%	55%	62%

A more typical example of cross-validation results is Great Falls where success rates fluctuate above or below 50% and are only slightly above 50% for couloirs of the same geographic group, the North Summit in this case (Fig. 36a). The worst-case scenario is exemplified by Upper AZ2, where the Random Forest model predicts nearly all of the other couloirs worse than the flip of a coin (Fig. 36b). These results show how specific rules of thumb for the terrain in one couloir would be troublesome if applied to others.

Results from the individual couloir models have numerous implications. First, it appears that several parameters are more frequently associated with the presence or absence of PTLs, namely *rel.elev*, *edge*, *expo* and *wind*. This implies that differences in PTLs are most frequently associated with different elevations along the couloir, different distances from the edge of the couloir, or different levels of wind or terrain exposure (e.g., Fig. 37). These parameters are all closely related to the effects of wind loading, wind scouring, and wind protection, a point which I explore in the following sections. Relative elevation is the most important parameter in nearly half of the couloirs. These results have important implications: a snow pit showing the presence or absence of a weakness at the bottom of a couloir is unlikely to be representative of the top, and vice versa. The same concept applies to these other important parameters.

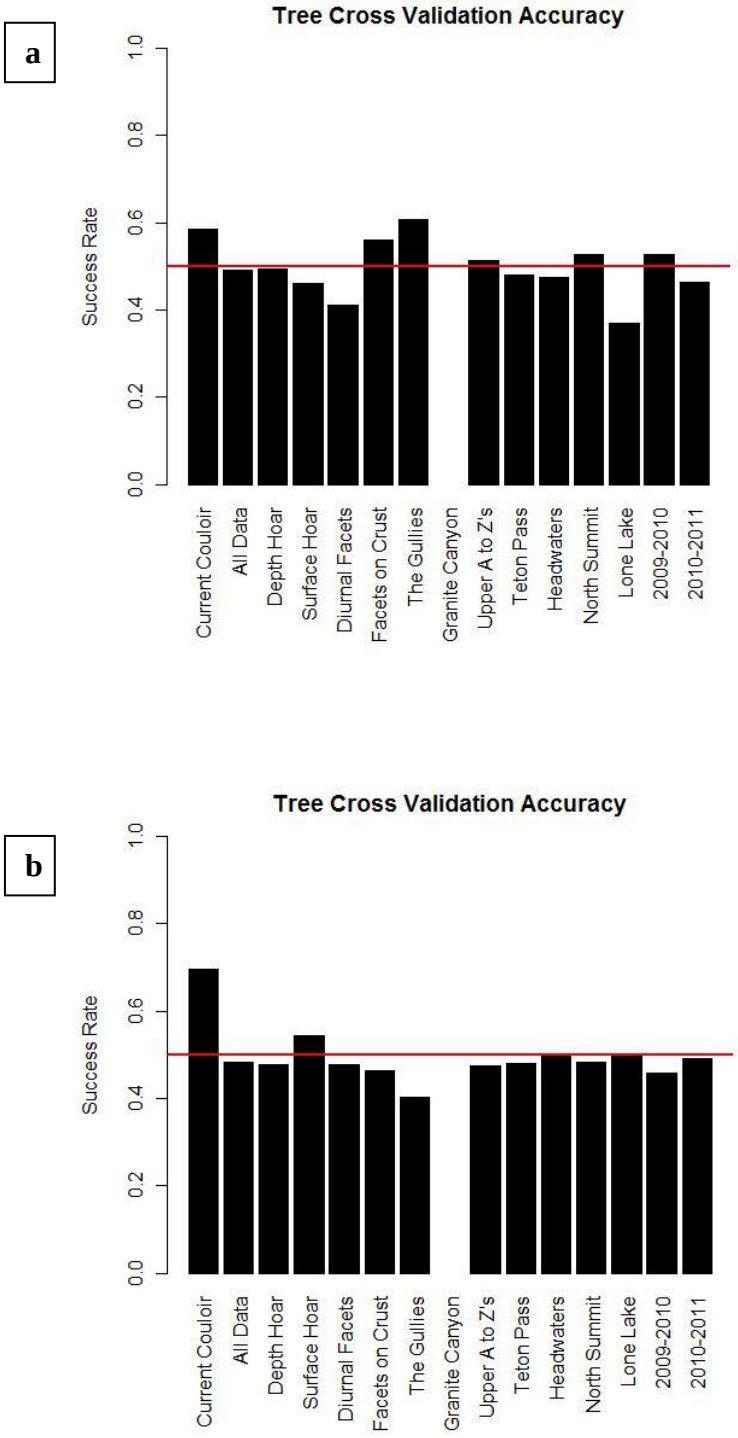

Fig. 36. (a) Cross-validation results for Great Falls, exemplifying typical cross-validation results from the set of 21 couloirs. (b) Upper AZ2 showing worst-case scenario cross-validation results, where applying the model to other couloirs causes worse predictive success than flipping a coin

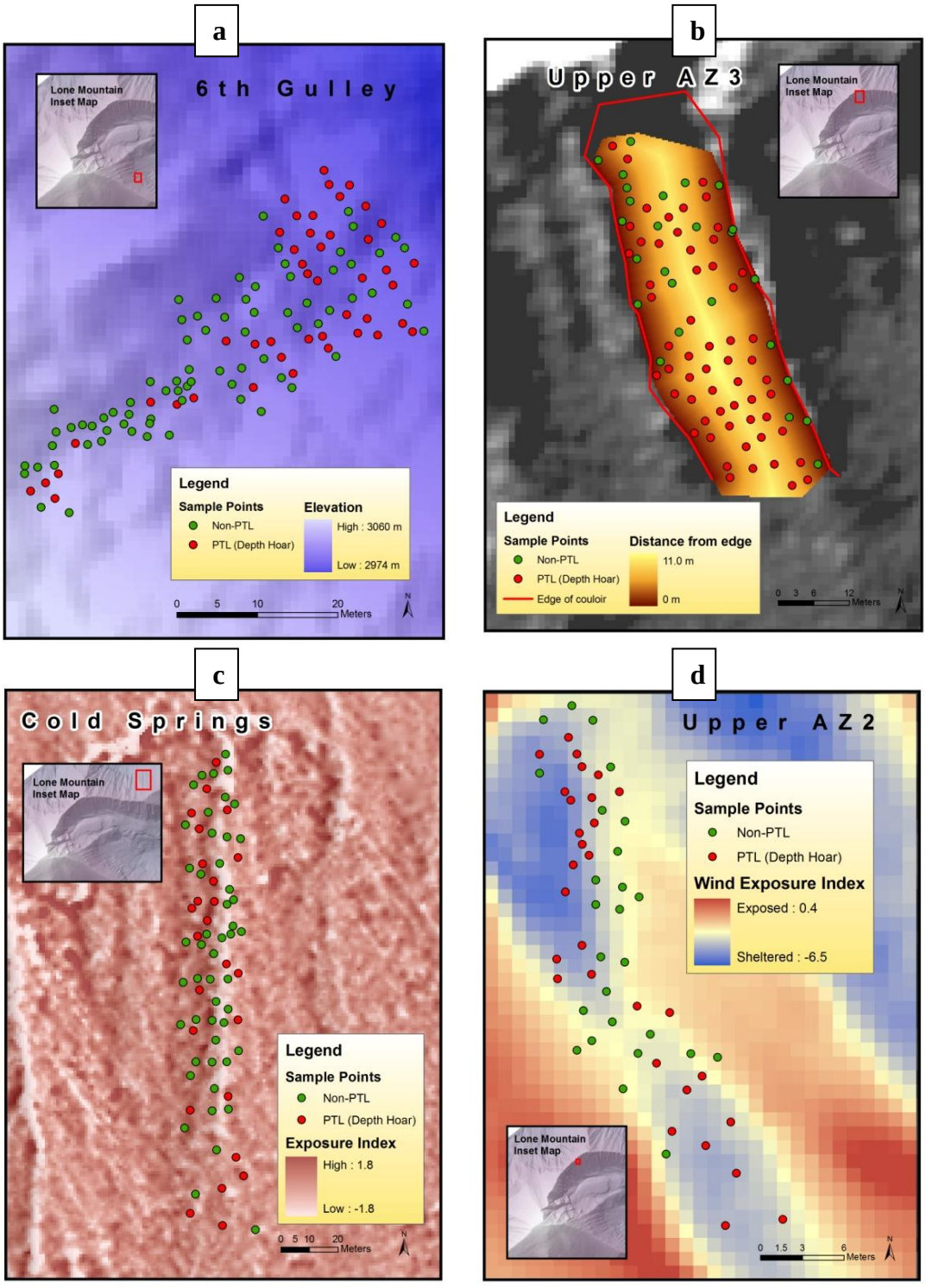

Fig. 37. Examples of four parameters that are most commonly associated with presence/absence of PTLs for individual couloirs. (a) Relative elevation (b) Distance from the edge of the couloir. (c) Exposure index. (d) Wind exposure index.

Although results suggest that some parameters are more frequently associated with PTLs, the cross-validation results suggest that their slope-scale influences vary significantly and are generally unpredictable from couloir to couloir. For a given parameter that appears important in several couloirs, unique thresholds are used in the classification trees and different coefficients are used in the logistic regression models, and these modeled effects do not appear to carry over well from one couloir to the next. In several cases, a given terrain parameter actually has an entirely opposite effect on the presence of a PTL. For example, higher relative elevations are strongly associated with PTLs on Lone Lake Couloir, while more PTLs are found at the lower elevations on Upper AZ4.

The marginally successful cross-validation results for several couloirs such as Upper AZ3 suggest that in some cases, specific terrain influences from one couloir may be somewhat useful for predicting weak zones for other couloirs in the same cirque. The best predictive success rates are for couloirs where I was most capable of predicting PTLs as we moved across the slope during field sampling. This is exciting because it suggests the models incorporate some of the physical processes that I intuitively draw from as an experienced practitioner.

Geographic Groups

The following results and discussions are for all geographically similar groups in which we tracked depth hoar (Table 2). This analysis changes scale from individual couloirs to groups of closely spaced couloir or couloirs at the mountain scale (Fig. 21). I also consider the multi-mountain range scale by combining the Teton Pass couloirs with

the Lone Mountain couloirs. Data for each group are analyzed as a whole and summarized in Tables 14 – 18, with statistical outputs in Appendix B. I then attempt to explain slope-scale terrain/PTL relationships that exist at the cirque or headwall scale, mountain scale, or multi-mountain range scale.

Table 14. Model success rates and true skill scores (TSS) for depth hoar group modeling.

Cirque Groups	Pruned Tree nodes	Pruned Tree Success	Pruned Tree TSS	Random Forest success	Random Forest TSS	Logistic Success	Logistic TSS
The Gullies	8	79%	0.60	67%	0.27	68%	0.21
Upper A to Zs	7	75%	0.49	68%	0.34	68%	0.34
Teton Pass	10	80%	0.61	42%	-0.17	53%	0.01
Headwaters	6	69%	0.45	62%	0.12	56%	0.18
North Summit	8	78%	0.53	60%	0.03	61%	0.22
Lone Lake Cirque	8	85%	0.71	59%	0.09	54%	0.22
Cirque Means	**7.8**	**78%**	**0.57**	**60%**	**0.11**	**60%**	**0.20**
Lone Mountain	2	63%	0.28	62%	0.18	52%	0.10
All Depth Hoar Samples	2	63%	0.28	63%	0.18	52%	0.10

Table 15. KS-test results for depth hoar couloir groups, testing whether each parameter has a significantly different distribution for PTLs in comparison to non PTLs when considering all of the couloirs in a single geographic group. Significant results, identified by bold font and green cells, suggest that these parameters may be independently used to indentify PTLs across an entire cirque or mountain.

Kolmogorov-Smirnov goodness-of-fit test results: P-values								
Group	Gullies	Upper AZs	Teton Pass	Headwaters	N. Summit	Lone Lake	Lone Mtn	All Depth Hoar Samples
rel.elev	0.22	0.10	0.36	0.32	0.91	**0.00**	0.64	0.64
slope	0.14	**0.00**	0.54	**0.01**	**0.02**	0.49	0.31	0.31
EW.aspect	0.07	0.17	0.28	0.67	0.42	0.24	**0.04**	**0.04**
NS.aspect	0.07	0.29	0.96	0.53	0.06	0.24	**0.00**	**0.00**
prof	0.49	0.12	0.05	0.21	0.40	0.14	0.09	0.09
plan	0.41	**0.00**	0.83	**0.03**	0.14	0.92	0.60	0.60
rel.solar	**0.04**	**0.03**	0.87	0.60	0.06	0.87	0.54	0.54
wind	**0.03**	0.28	0.65	0.35	0.73	0.73	0.13	0.13
expo	0.44	**0.00**	0.20	0.05	0.11	0.53	0.19	0.19
edge	0.50	**0.00**	0.80	**0.00**	0.07	0.18	**0.00**	**0.00**
wind.edge	0.28	0.47	0.31	0.21	0.13	0.24	0.22	0.22

Table 16. The top logistic model for each depth hoar group with the lowest QAICc.

Group	**Lowest QAICc Model**
Gullies	$PTL \sim 1 + prof + expo + rel.view + wind^2$
Upper AZ's	$PTL \sim 1 + expo + rel.view + slope^2 + wind^2$
Teton Pass	$PTL \sim 1$
Headwaters	$PTL \sim 1 + edge$
N. Summit	$PTL \sim 1 + edge^2 + wind.edge^2$
Lone Lake	$PTL \sim 1 + prof$
Lone Mountain	$PTL \sim 1 + edge + edge^2$
All Depth Hoar	$PTL \sim 1 + edge + edge^2$

Table 17. The most important parameters for each depth hoar group, their general association with PTLs, and under what minimum slab criteria they perform best.

	Parameter	PTL distribution pattern	Robustness to Uncertain PTLs
The Gullies	*rel.elev*	more at lower elevations below 45%	all slabs
	Prof	more on moderate concave slopes	all slabs
	Wind	more in moderate wind shelter	thick slabs
	Aspect	more on aspects 25° to 45°, less on 65° to 95°	thin slabs
	wind.edge	more 12 to 23 m from windward edge	thick slabs
Upper A to Zs	*Expo*	more on unexposed terrain	thin slabs
	rel.view	less at more visible points from ridge	all slabs
	Wind	more in moderate wind shelter	all slabs
	Edge	more further than 2.5 m from edge	thick slabs
	Slope	more below 46°	thick slabs
	rel.elev	more at lower elevations below 25%	thick slabs
	rel.solar	more between 50% and 95%	all slabs
Teton Pass	*Prof*	more on convex slopes	all slabs
	rel.solar	more above 50%	thick slabs
Headwaters	*Edge*	more further than 3 m from edge, less at the furthest from edge	all slabs
	Wind	more at higher wind exposure	thin slabs
	Expo	less at highly unexposed	thin slabs
	Plan	less at highly concave	all slabs
	Slope	more below 43°	all slabs
North Summit	*Edge*	less further than 7 m from edge	thin slabs
	wind.edge	more 15 m from windward edge	all slabs
Lone Lake Cirque	*rel.elev*	more at upper elevations above 50%	thin slabs
	Prof	more on concave slopes	all slabs
	wind.edge	more closer than 8 m from the edge	thick slabs
	Aspect	more on aspects 295° to 320°	thick slabs
All Depth Hoar & Lone Mountain	*Aspect*	more on aspects 115° to 180°	thin slabs
	Edge	more between 3 m and 6 m from edge	moderate slabs
	wind.edge	more between 3 m and 7 m from windward edge	thick slabs
	Wind	more in moderate wind shelter	thick slabs
	rel.view	more on less visible slopes from ridgeline	thick slabs

Table 18. The most important parameters in each depth hoar group and the measures used to identify their importance.

	Parameter	Pruned Tree **Level of Node Appearances**	Random Forest **Mean Decrease in Accuracy**	Logistic **Relative Support**	Logistic **Significant confidence intervals?**	Logistic **Odds Ratio**
The Gullies	*rel.elev*	None	0.024	*rel.elev*^{2}=0 .10	no	
	prof	4th	0.008	*prof*=1.00	yes	1.074
	wind	None	0.010	*wind*^{2}=0.90	no	
	aspect	*NS*=2nd	*NS*=0.022	*NS*=0.00	no	
			EW= 0.014	*EW*=0.00		
	wind.edge	None	0.009	0.00	no	
Upper A to Zs	*expo*	1st	0.024	*expo*=1.00	yes	0.920
	rel.view	None	0.013	*rel.view*=0.96	yes	0.751
	wind	None	0.018	*wind*^{2}=0.77	no	
	edge	4th	0.016	*edge*^{2}=0.10	no	
	slope	6th	0.011	*slope*^{2}=0.84	no	
				slope=0.16		
	rel.elev	3rd	0.013	*rel.elev*=0.28	no	
	rel.solar	2nd, 5th	0.010	*rel.solar*=0.34	no	
Teton Pass	*prof*	1st, 2nd	0.010	0.00	no	
Headwaters	*edge*	1st, 4th	0.007	*edge*=0.84	no	
				edge^2=0.07		
	wind	5th	0.009	*wind*^{2}=0.09	no	
				wind=0.06		
	expo	2nd	0.004	*expo*=0.14	no	
	plan	None	0.004	*plan*=0.07	no	
	slope	3rd	0.008	*slope*=0.07	no	
North Summit	*edge*	1st, 4th, 5th	0.008	*edge*^{2}=0.96	yes	0.998
	wind.edge	2nd	0.010	*wind.edge*^{2}=0.59		
				wind.edge=0.08		
Lone Lake Cirque	*rel.elev*	1st, 3rd	0.015	*rel.elev*=0.09	no	
				rel.elev^2=0.08		
	prof	3rd	0.008	*prof*=0.81	no	
	wind.edge	None	0.004	*wind.edge*^{2}=0.14	no	
				wind.edge=0.12		
	aspect	2nd	*NS*=0.009	0.00	no	
			EW=0.008			
All Depth Hoar & Lone Mountain	*aspect*	1st	0.025	0.00	no	
	edge	None	0.010	*edge*=1.00	*edge*=yes	*edge*=1.050
				edge^2=1.00	*edge*^{2}=yes	*edge*^{2}=0.996
	wind.edge	None	0.008	*wind.edge*=0.07	no	
				wind.edge^2=0.07		
	wind	None	0.008	*wind*^{2}=0.14	no	
				wind=0.07		
	rel.view	None	0.007	*rel.view*=0.10	no	

In comparison to individual couloirs, the cirque-scale groups of couloirs have decreased success rates and model skill, with a loss of roughly 10% in predictive success (Figs. 38 and 39). Despite this loss in modeling ability from individual couloirs, Random Forest and logistic regression models have promising results considering the complexity of the environment: predictive success rates average around 60% (Table 14). These results have important implications. First, slope-scale terrain parameters can still be used to describe the presence of PTLs across cirques or headwalls, but these relationships are not as strong: predictive ability suffers as a consequence. The complex terrain/PTL relationships in a couloir are best described at the single slope scale, but broader patterns still exist for larger geographic regions.

When modeling the effects of terrain on PTLs at an even larger scale (all of Lone Mountain), the success rates average below 60% (Fig. 40 and Table 14), indicating that relationships with slope-scale parameters have reduced applicability beyond their respective cirque or headwall. Including the Teton Pass couloirs to expand to a multi-mountain range scale has nearly the same results as the Lone Mountain group with the same interpretation.

For the cirque scale groups, there are a number of parameters that have strong relationships with PTLs for each of the couloirs in the group. Although the influences of the parameters change for each cirque, they are related to similar physical processes. These parameters are described below using examples from the cirques and headwalls on Lone Mountain.

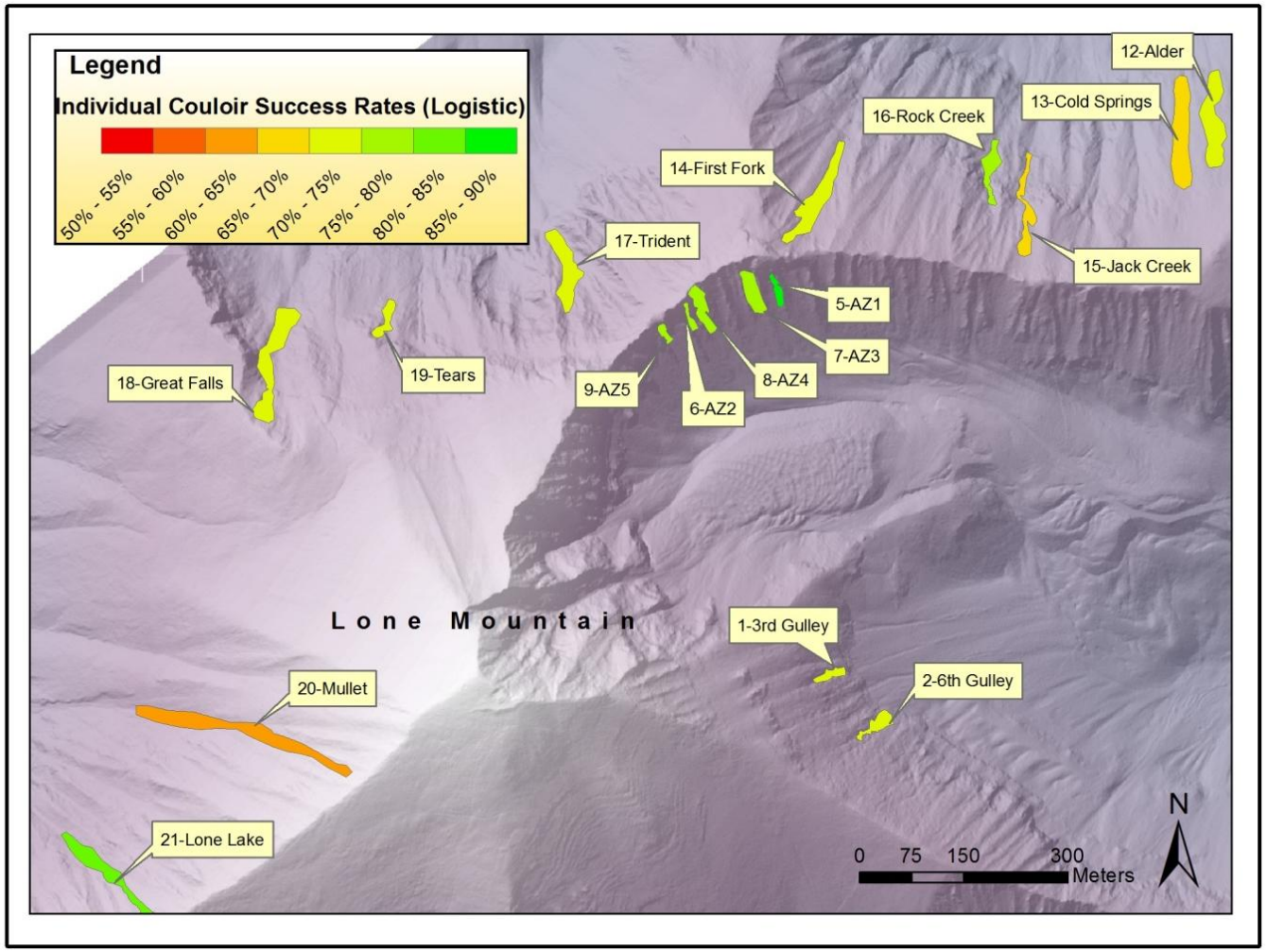

Fig. 38. Logistic model success rates for individual couloir modeling, showing relatively high success rates for slope scale predictions.

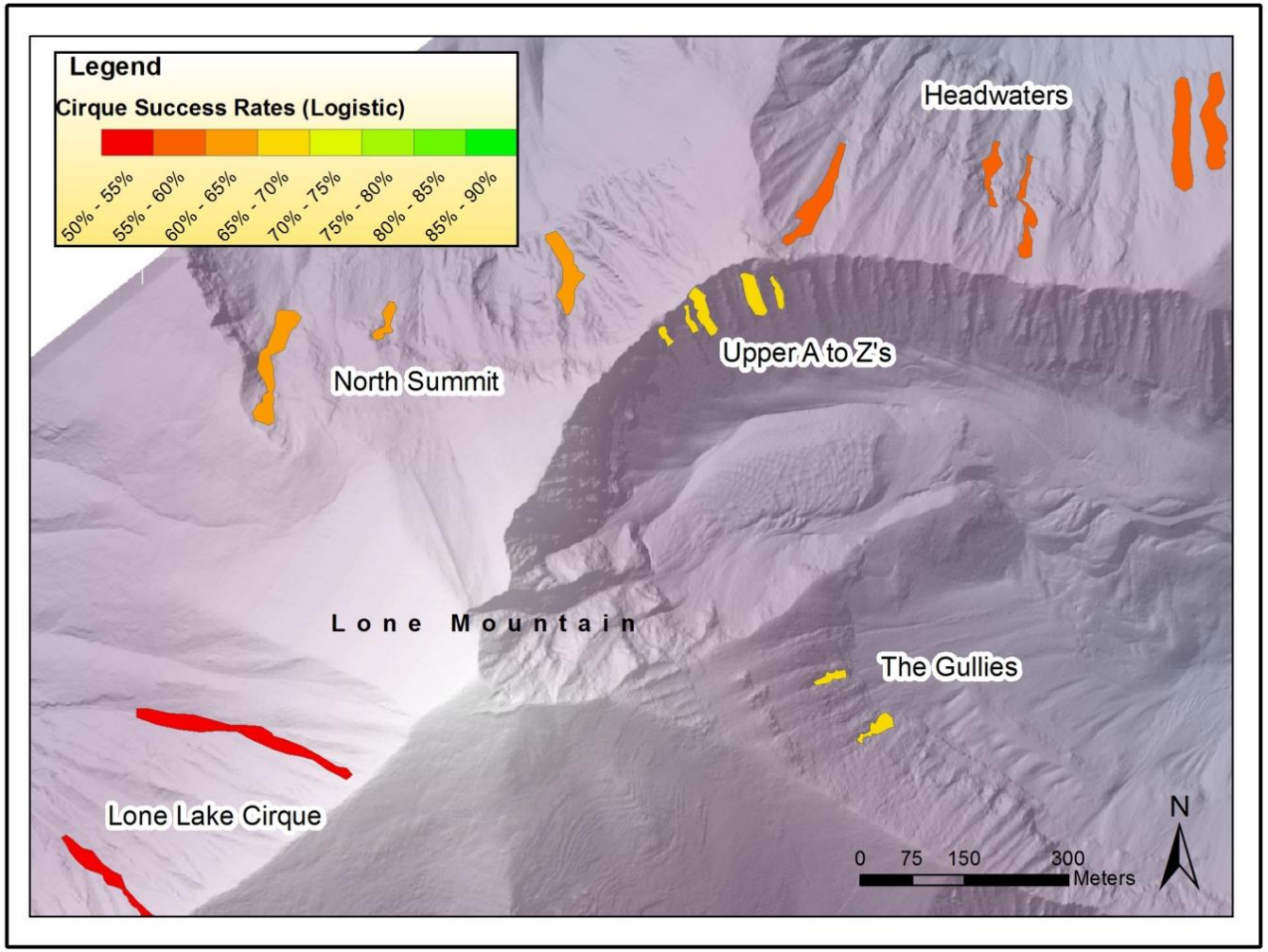

Fig. 39. Logistic model success rates for couloirs in the same cirque, showing relatively moderate success rates for cirque scale predictions.

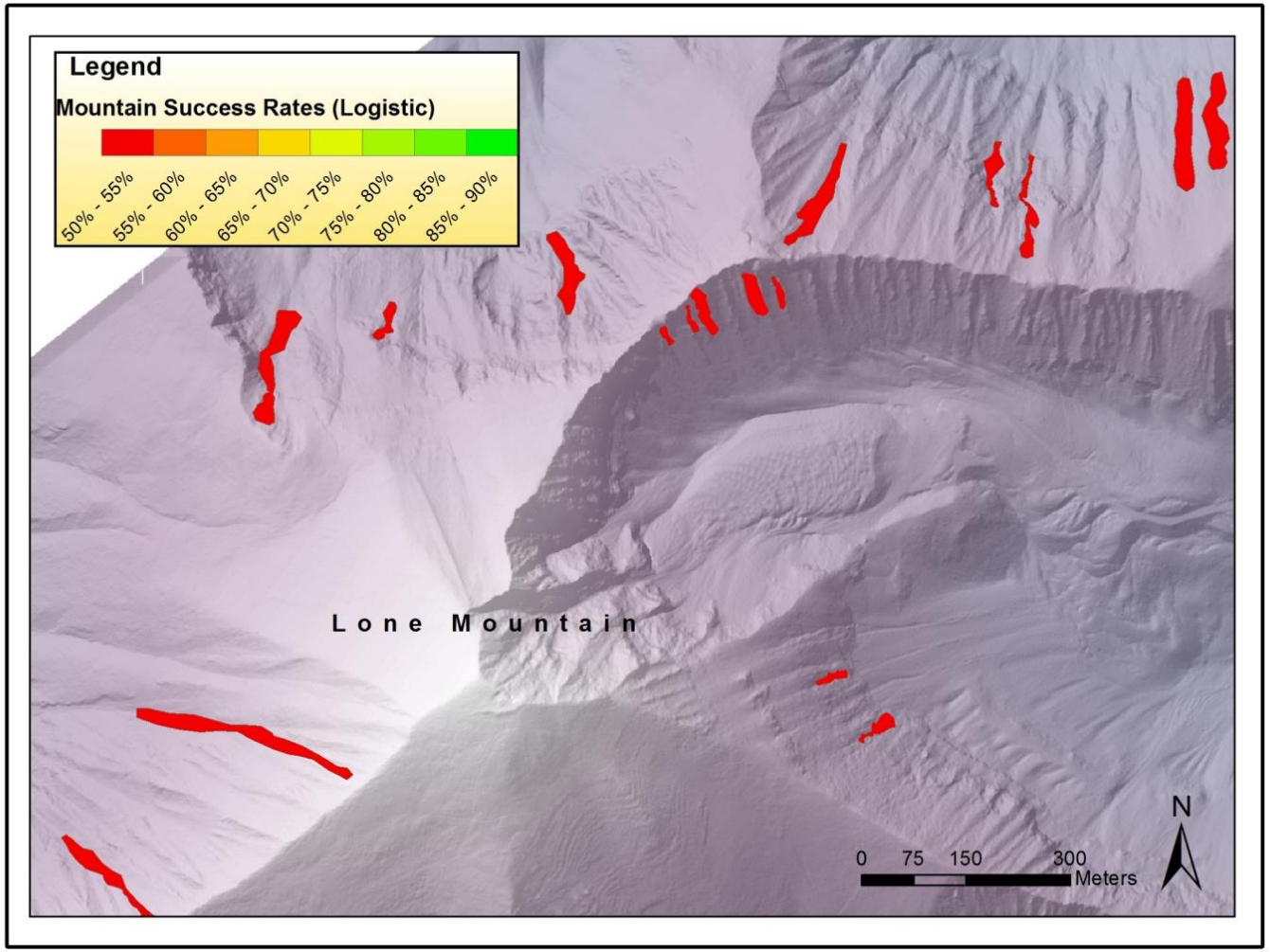

Fig. 40. Logistic model success rates for all of the couloirs on Lone Mountain, showing relatively poor success rates for mountain scale predictions.

One of the key physical processes in depth hoar formation and the presence of PTLs is a strong temperature gradient driven by a shallow snowpack. This is conveyed through the terrain differently depending on the season, the time of year, the depositional patterns in a cirque, and finally the slope-scale patterns within a couloir. The influence of cirque-scale terrain on the slope-scale relationship with PTLs is best illustrated by the Lone Lake Cirque group.

The couloirs sampled in Lone Lake Cirque are unique because they are more west-facing than any of the other couloirs on Lone Mountain. With a more windward aspect, wind erosion prevented deep, stable snowpacks from developing, despite the late timing of sampling for these two couloirs. For the two couloirs sampled in this cirque, *rel.elev* and *prof* are highly important; both are independently capable of describing a noticeable decrease in PTLs at lower elevations (Tables 17 and 18). Without considering larger scale effects, the physical process explaining why lower elevations have fewer PTLs is not obvious. The classification tree's first node is at *rel.elev* = 0.51, with fewer PTLs at lower elevations. This elevation roughly corresponds with the height of the west wall of the cirque, which offers protection from the prevailing southwest winds and promotes deep and stable snow at most lower elevations, especially for couloirs closer to the wall. The upper elevations, however, are blasted by some of the strongest winds on the mountain, scouring the snowpack to depths that allow strong temperature gradients and depth hoar formation (Fig. 41).

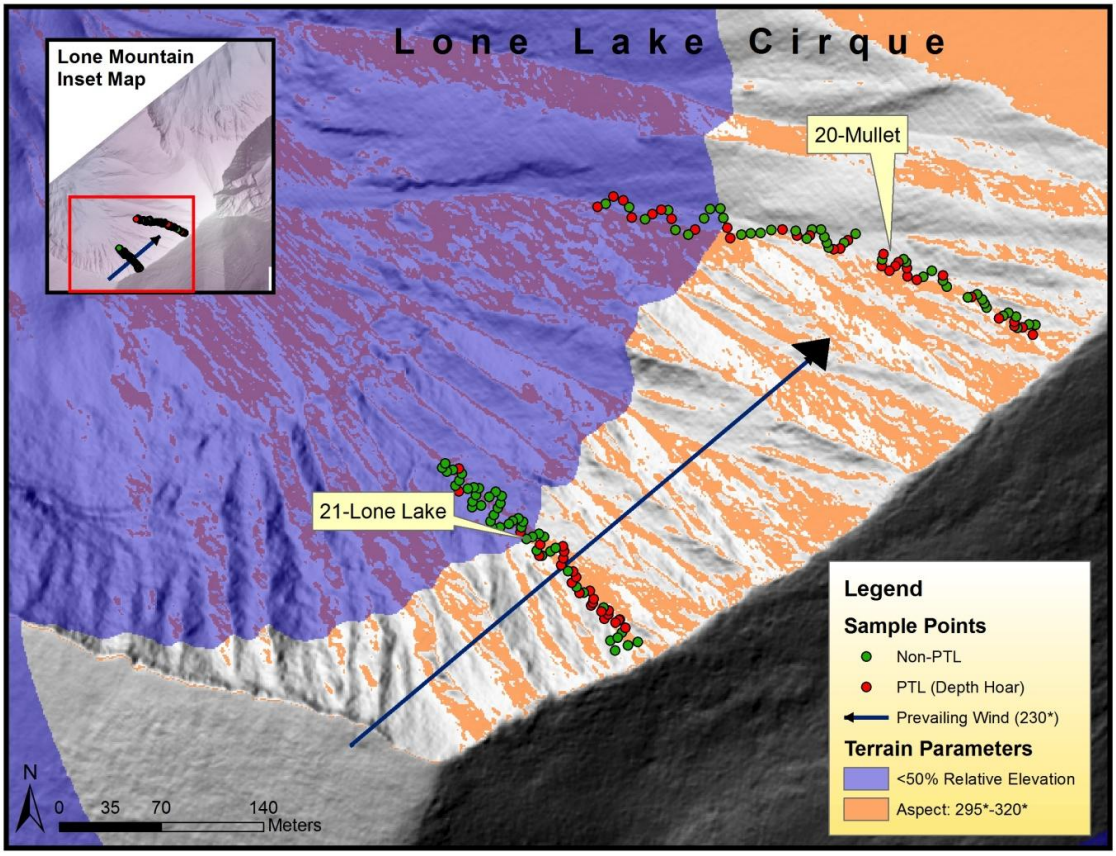

Fig. 41. Map of Lone Lake Cirque, which shows how the west wall of the cirque provides protection from the prevailing winds at lower elevations, which fosters a deep and stable snowpack late in the season. At upper elevations where the snowpack is generally shallow and faceted, the leeward aspects provide enough shelter from winds to preserve depth hoar from wind erosion and develop significant slabs, especially on Mullet Couloir.

The second process relating to PTLs in Lone Lake Cirque is fierce wind erosion on the leeward sides of the couloirs at the most exposed upper elevations which prevents PTLs. The very shallowest portions of the slope are comprised of stout, pencil to knife-hard wind-packed grains without depth hoar. It appears that the snowpack here gets overturned and beat by the wind with such force that it becomes a solid wind slab without adequate pore space to allow depth hoar growth, despite its shallow depth. Another

possible explanation is that all of the snow grains, including any depth hoar, are swept away during high winds leaving only a stout early season crust. Both models explain this relationship differently; the logistic regression model uses *wind.edge,* while the Random Forest uses a threshold aspect of roughly 295^{o} to differentiate PTLs. On the windward edges (or aspects greater than 295^{o}), the snow is protected enough to preserve depth hoar and grow significant slabs (Fig. 41), especially on Mullet Couloir which is more exposed to prevailing winds at all of its elevations.

Lone Lake illustrates how slope-scale terrain influences are highly dependent on the characteristics of the cirque or larger scale processes. For example, the threshold value of *rel.elev*=0.51 is due to the west wall of the cirque which is specific to the Lone Lake Cirque samples only.

Another key process relating to the presence of PTLs is accumulation of a sizeable enough slab over depth hoar to be threatening. This process is influenced by parameters associated with wind deposition, wind protection, and sluffing. Although the parameters influencing these processes are consistent (*wind.edge*, *wind*, *expo*, *plan*, *edge*, *rel.view*, *rel.elev*, *aspect*, *prof*, and *slope*), their importance and influence vary depending on larger terrain characteristics, time of year, and seasonal trends. A comparison of the Upper A to Zs and Headwaters groups demonstrates how the influences of terrain as it relates to slab formation for PTLs can be entirely opposite depending on mountain-scale effects .

The snowpack on the Upper A to Z Headwall is notoriously shallow with widespread depth hoar (Babinou-Z, pers. comm., 2010). In the season that we sampled

the Upper AZ's, a fairly thin but uneven slab covered a widespread layer of depth hoar (Fig. 42). Thus, the most important parameters for PTLs on Upper AZ's those that predict deep enough slabs to be threatening. These are *edge, expo, rel.view, wind, slope,* and *rel.elev* (Tables 17 and 18). The latter two parameters associate with frequent sluffing which generally prevents slabs from forming on the upper parts of the couloirs (Fig. 43). These effects are enhanced with frequent near-ridge wind scouring. However, *edge, expo, rel.view*, and *wind* are all important in one or both of the model structures for characterizing locations where slabs of critical size form over the pervasive depth hoar (Tables 17 and 18). PTLs have a positive association with distance from edge, decreasing terrain exposure, low visibility from the major windward ridgeline, and high wind sheltering, as these are all related increased windloading (Fig. 43 and Table 17).

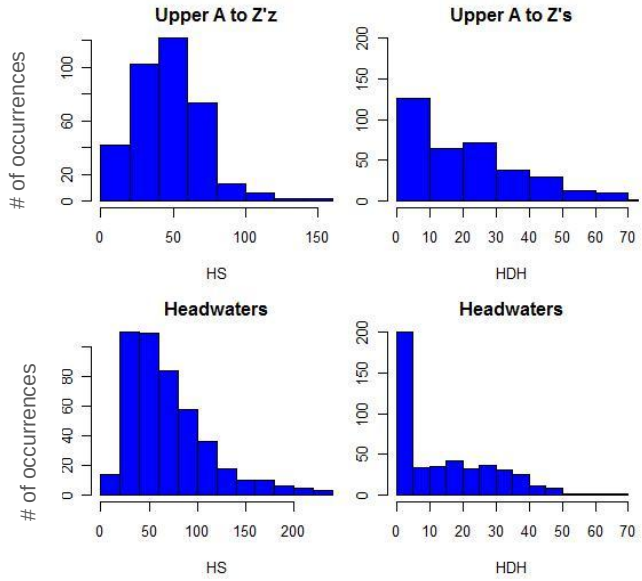

Fig. 42. Histograms of snow depth (*HS*) and thickness of depth hoar (*HDH*) for the Upper A to Zs and the Headwaters, showing a different snowpack structure between the two locations with much shallower snow depths and more depth hoar growth in the Upper A to Zs.

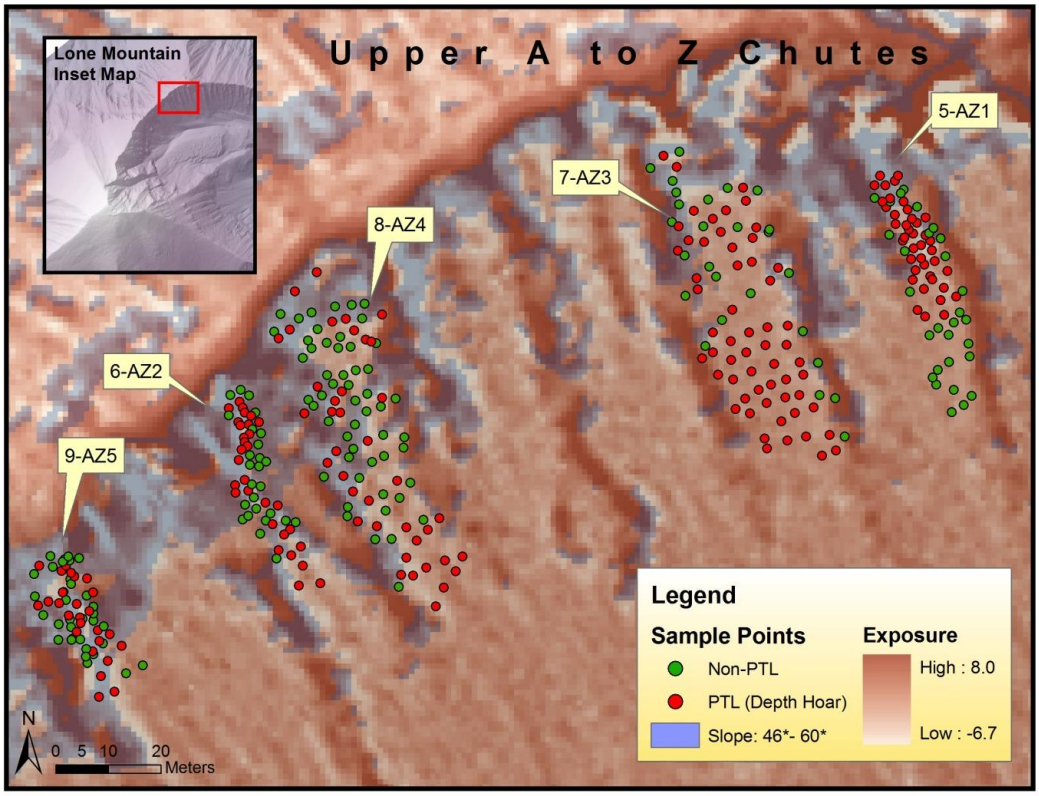

Fig. 43. Map of the Upper A to Z chutes, showing how PTLs are associated with lower exposure and lower slope angles in general due to their influence on slabs of threatening depth. The influence of distance from the edge is also apparent.

In contrast, the Headwaters couloirs, which are on opposite side of the ridge from the Upper A to Zs, have a much deeper snowpack (Fig. 42). These couloirs characteristically have a deep slab in the middle (>200 cm) tapering in thickness towards the sides and prevalent depth hoar near the sides tapering and strengthening towards the middle, where depth hoar typically is not present because the snow is too deep to facilitate strong temperature gradients and depth hoar growth.

Thus, the effects of some of the terrain parameters predicting PTLs are opposite for the Headwaters compared to the Upper A to Zs (Tables 17 and 18). Unlike the Upper A to Zs, in the Headwaters *wind*, *plan*, and *expo* are all important parameters in relating

to sheltered zones where the shape and exposure of the couloir promote development of deep and/or dense snowpacks without PTLs (Fig. 44). The effect of *edge* is different too. For the furthest distances from the edge of the couloir, the snow is deep and strong, so few PTLs are present. Nearest the couloir, depth hoar typically prevails but lacks a threatening slab (Fig. 44). Thus, more PTLs are concentrated between 3 m and 6 m from the edge. This is a fairly weak relationship compared to the others, but it is successfully modeled with two *edge* nodes in the classification models and an extra $edge^2$ term in the logistic regression model.

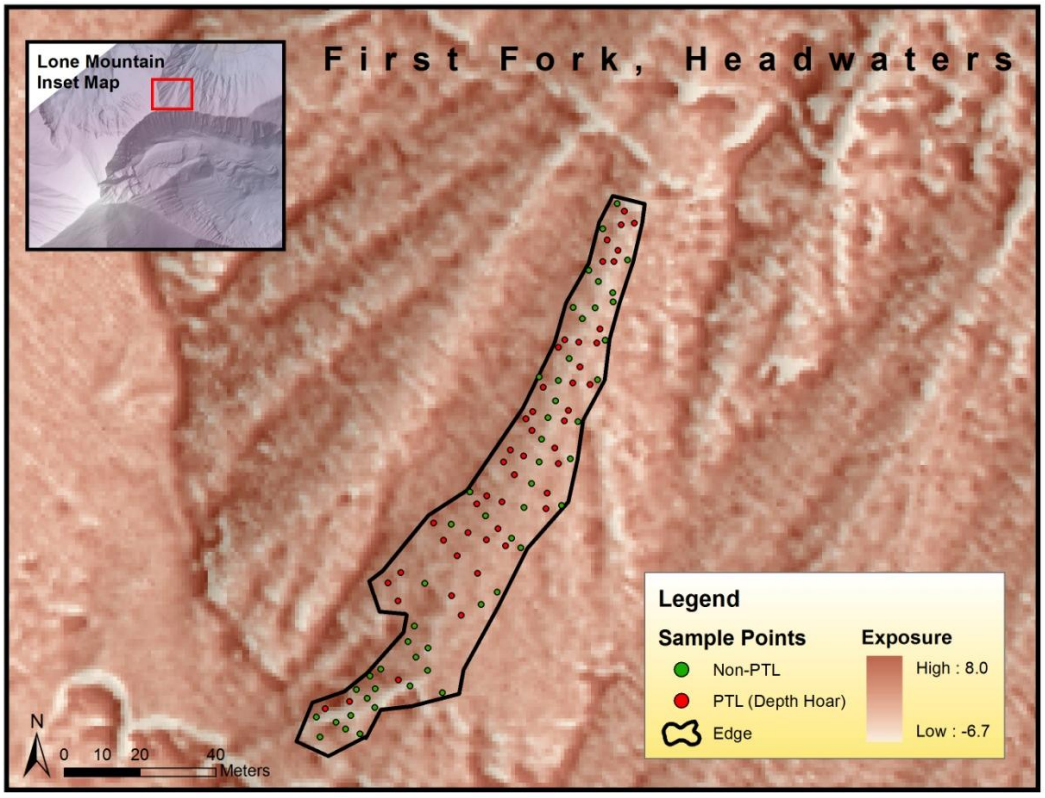

Fig. 44. Map of PTLs on First Fork in the Headwaters, illustrating how the effect of terrain exposure is opposite for the Headwaters than for the Upper A to Z chutes (Fig. 43). Also, the effect of distance from the edge of the couloir is apparent, especially with Cold Springs (Fig. 45) and First Fork, where PTLs are concentrated several meters from the edge.

The three couloirs on the North Summit are fairly diverse despite being located in the same alpine cirque (Fig. 6). Trident is a more west-facing couloir and can be stripped of snow with strong northwest winds, whereas Great Falls is on the leeward side of the cirque. It has a much deeper snowpack that can get loaded while Trident gets scoured. Tears Couloir is located between the two and shares characteristics of both. Despite this diversity, a decrease in PTLs with increasing distance from the edge of the couloir is a consistent relationship for this cirque. This effect is similar to the relationship observed in the Headwaters, which is reasonable because these two cirques have similar characteristics. However, the presence of more PTLs closer to the edges on North Summit differs from the relationship in the Headwaters. This may be due to a sampling date of nearly two months later for the North Summit couloirs. For the relatively early season sampling of the Headwaters, the points nearest the edge were faceted but lacking a slab, whereas similar faceted locations in the North Summit were buried beneath a threatening slab later in the season. This exemplifies how the influences of terrain also depend on the progression of the winter season.

There are several other physical processes explained by parameters on the south-facing slopes of the Upper A to Zs that are associated with PTLs. Despite extensive depth hoar on these slopes, there are two general terrain areas where depth hoar is most noticeably absent: deeper pillows which are in the most shaded slopes and the slopes that are shallow enough to allow solar radiation to strengthen the entire snowpack (Tables 17 and 18). Solar radiation only penetrates the upper 20 to 40 cm of old snow (McClung and Schaerer, 2006). The strengthening of buried depth hoar through melt freeze

processes or insolation is related to a shallow snowpack, where free water or solar radiation is able to contact existing depth hoar in areas that receive abundant solar radiation. Terrain exposure and slope angle associate with fewer PTLs based on both their lack of significant slabs and strengthening of weaknesses from solar radiation (Fig. 43 and Table 18). The areas that receive the least amount of radiation are also associated with an absence of depth hoar and no crust formation. I hypothesize that the widespread melt-freeze crusts on the Upper A to Zs enhance faceting (Colbeck, 1991), so the absence of crusts, along with deeper snow depths, cause these areas to lack depth hoar.

The models for Teton Pass have inferior predictive abilities compared to all of the other locations. There are several reasons for the poor results from these couloirs. First, both of these couloirs are on moderately treed slopes. During field observations I noted that the presence of weak depth hoar was most noticeable near trees, where temperature gradients are likely amplified by warmer tree trunks. My analysis does not include any parameters such as proximity to trees, and furthermore, a number of the parameters, such as *rel.solar*, *wind*, and *expo*, are simply wrong without including the effect of trees in these areas. Second, the GPS accuracy was far worse on Teton Pass than in any other location, with average estimated horizontal RMS accuracies of 240 cm and 172 cm (Table 2). I treated these two couloirs as outliers for modeling the entire depth hoar dataset by comparing results before and after their exclusion. The results are very similar between the entire depth hoar dataset and just the Lone Mountain couloirs, so I kept them in the analysis.

By grouping together all of the couloirs with depth hoar and all of the couloirs on Lone Mountain, I introduce significant temporal and geographic variability that doesn't exist for individual couloir modeling and is not as complex as the cirque group modeling. Not surprisingly, the predictive abilities of the models are poor (Fig. 40 and Table 14). All of the unique interactions between terrain and PTLs at the slope scale and cirque scale are "averaged out." Not only does this analysis group together couloirs from different headwalls and different months of the year, but also completely contrasting winter seasons. The classification trees, which have success rates just above 60% for these two larger groups (Table 14), draw most of their success from a non-slope-scale relationship, segregating PTL-dense Upper A to Zs from the rest of the data with the *NS.aspect* parameter (Table 18). If this parameter was normalized for each slope to be a more adequate slope-scale parameter, the success rates of the Random Forest models and pruned tree models for the Lone Mountain group and "All Depth Hoar" group would be considerably lower. This simply re-emphasizes the point that the influences of slope-scale terrain parameters depend on larger terrain characteristics and meteorological conditions.

Although the predictive strengths of these all-encompassing models are weak, they do identify *edge* as an important parameter. The dueling affect of *edge*, with fewer PTLs at short distances and fewer at long distances is modeled by the use of $edge^2$ in the logistic regression model (Table 16 and Table 18). The odds ratio estimates for *edge* suggest that for every meter away from the edge of the couloir, the odds of observing a PTL increase linearly by 5% with all other terms held constant. However, the odds ratio

estimates for $edge^2$ suggest that for every meter away from the edge of the couloir, the odds of finding a PTL decrease by 4% multiplied by the squared distance from the edge. Together these terms describe how within the first meter away from the edge, PTLs increase in probability as distance from the edge increases up to one meter. After one meter, the probability of finding a PTL decreases at an increasingly greater rate. While this describes an average relationship for all of the data, it suggests that a general "sweet spot" for these depth hoar weaknesses is somewhere between 0.5 m and 1.5 m from the edge of the couloir (Fig. 45). Although both of these terms have significant confidence limits (Table 18), the final logistic model has a success rate of only 52.4%, so relationships described by it are far from a gold standard, but rather, relationships that we should be attentive to in avalanche terrain.

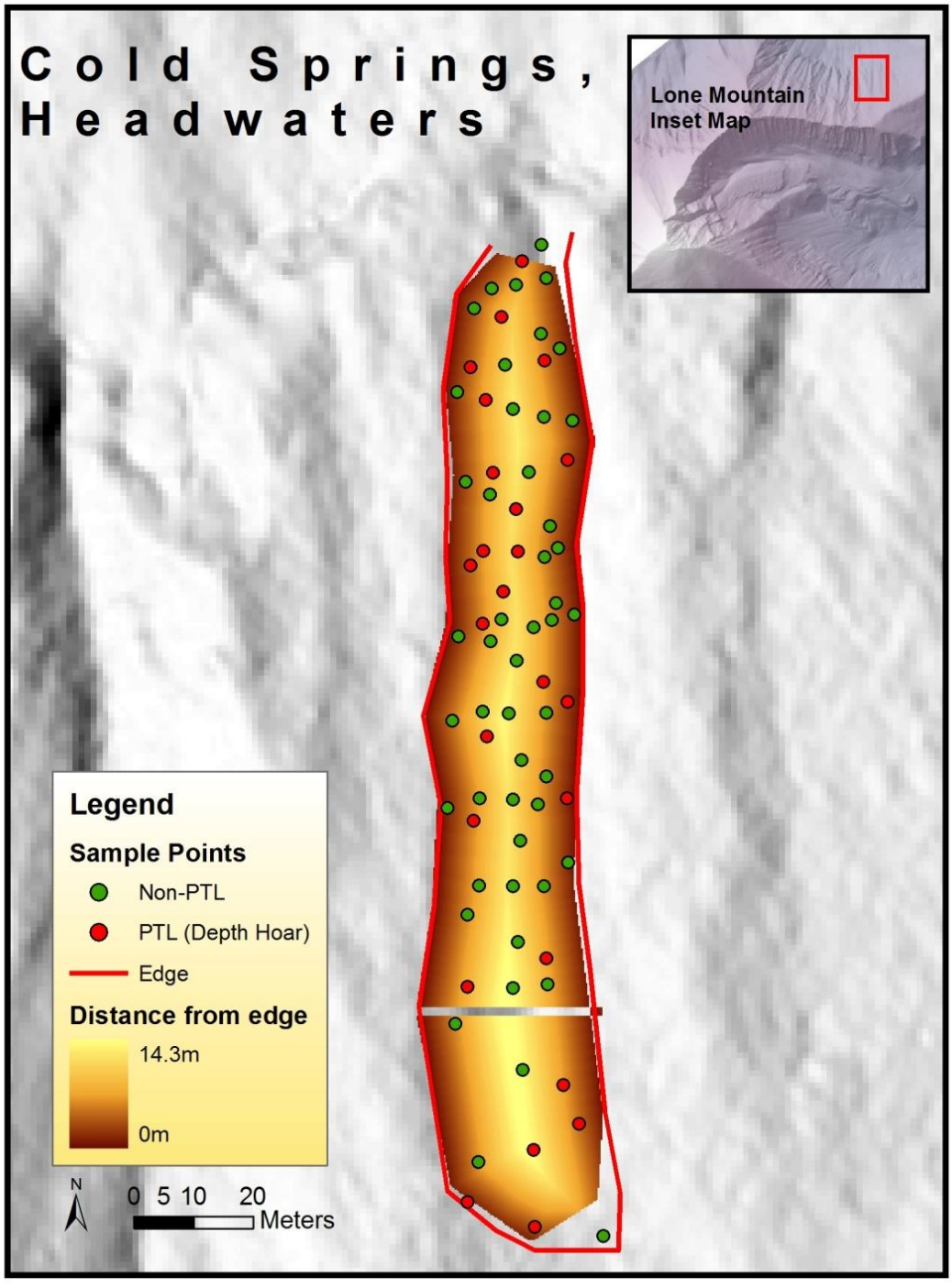

Fig. 45. Map of Cold Springs, which exemplifies the "sweet spot" relationship between depth hoar PTLs and distance from edge. More PTLs are clustered between 0.5 m and the first several meters from the edge of the couloir.

Facet Results and Discussion

The following results and discussions are for all of the couloirs in which we tracked a near-surface faceted layer. The faceted layers from the Claw and Unskiabowl on Teton Pass are not included in this analysis because the weak layers were too widespread for modeling presence/absences, and the GPS and terrain parameters for that location are poor quality.

Individual Couloirs

The results and discussion in this section are for all of the couloirs in which a layer of facets that formed near the surface were tracked. This includes all five couloirs from the Upper AZs where we observed a layer of facets preserved between crusts and three couloirs on the northern aspects of Lone Mountain with diurnal facets. Note that both couloirs on Teton Pass exhibited diurnal facets that were nearly entirely widespread so modeling their presence as a binary response was not practical, especially considering the poor GPS accuracy for these locations. PTLs for these data are defined as any location with the presence of the weak layer (Table 2). Here I model each individual slope, examine the most important parameters from these models, and compare the results to depth hoar PTLs. The results of KS-tests and individual modeling are summarized in Tables 19 and 20 and Fig. 46.

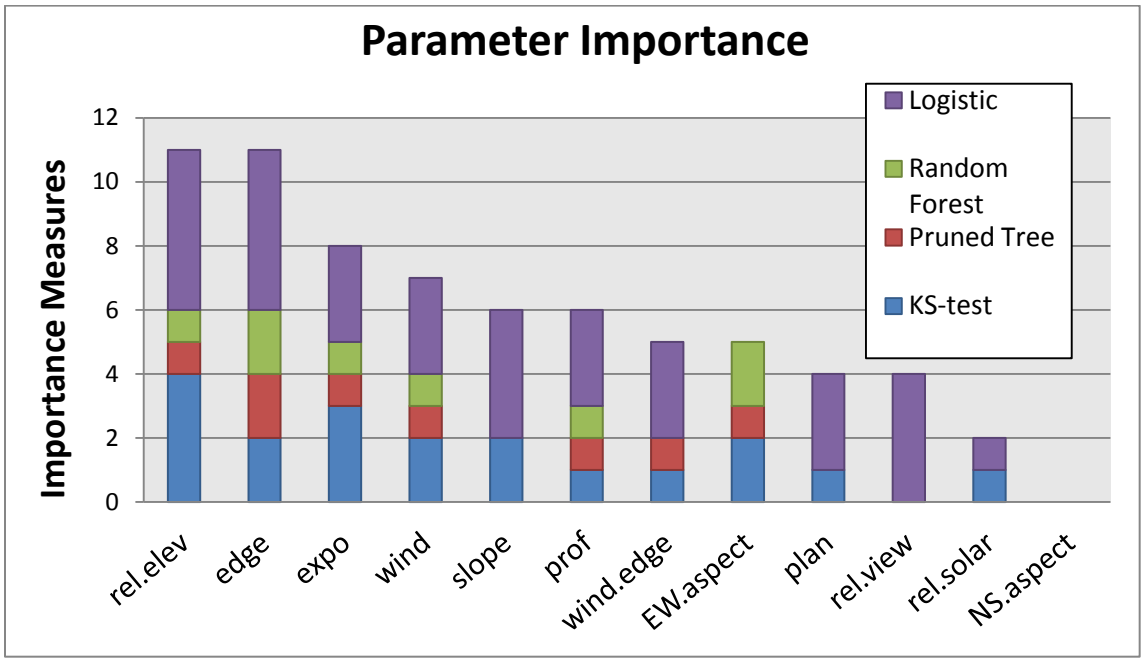

Fig. 46. Cumulative measures of importance for each parameter for near-surface facet PTLs from four tests: significance from the KS-test, first node in the pruned classification tree, most important parameter in the Random Forest model, and appearance in the lowest AICc logistic regression model.

Table 19. KS-test of whether each parameter has a significantly different distribution for facet layer PTLs in comparison to non-PTLs. Significant results, identified by bold font and green cells, suggest that these parameters may be used independently to discriminate between PTLs and non-PTLs in each couloir.

Kolmogorov-Smirnov goodness-of-fit test results: P-values								
Couloir ID#	**5a**	**6a**	**7a**	**8a**	**9a**	**17a**	**19a**	**21a**
rel.elev	0.14	0.08	**0.00**	**0.02**	**0.01**	0.25	0.46	**0.00**
Slope	0.15	0.86	**0.00**	0.76	0.90	0.81	0.96	**0.00**
EW.aspect	0.55	0.19	0.31	0.75	0.07	**0.01**	**0.01**	0.93
NS.aspect	0.55	0.19	0.49	0.75	0.07	0.20	0.04	0.93
Prof	0.63	0.98	0.18	0.30	0.26	0.94	0.48	**0.02**
Plan	**0.00**	0.44	0.14	0.14	0.23	0.85	0.69	0.08
Solar	0.96	0.15	**0.02**	0.17	0.28	0.95	0.16	0.23
Wind	0.22	**0.00**	**0.03**	0.29	0.17	0.07	0.11	0.39
Expo	**0.00**	0.05	**0.03**	**0.00**	0.42	0.56	0.71	0.06
Edge	**0.00**	0.72	**0.00**	0.62	0.33	0.22	0.72	0.93
wind.edge	0.04	0.86	0.12	0.41	0.24	0.67	**0.00**	0.95

Table 20. A summary of predictive success and skill for both model structures, as well as most important parameters associated with these models for the individual couloir modeling of facet layer PTLs.

Couloir ID#	First Node	RF most important	RF True Skill Stat	RF Success Rate	Lowest AICc logistic model	Logistic Mean Absolute Error	Logistic Success Rate	Logistic True Skill Stat
5a	*Edge*	*edge*	0.53	91%	*PTL ~ 1 + edge + prof^2 + rel.elev + plan*	0.03	97%	0.89
6a	*wind*	*wind*	0.13	88%	*PTL ~ 1 + edge + edge^2 + expo + wind*	0.04	96%	0.81
7a	*edge*	*edge*	0.47	77%	*PTL ~ 1 + expo + rel.view + slope^2 + rel.elev^2 + wind^2*	0.23	80%	0.51
8a	*expo*	*expo*	0.32	66%	*PTL ~ 1 + prof^2 + expo + rel.view + rel.elev + rel.elev^2 + plan + wind.edge +wind.edge^2*	0.39	66%	0.48
9a	*rel.elev*	*rel.elev*	-0.06	73%	*PTL ~ 1 + edge + rel.view + slope + slope^2+ rel.elev^2 + wind.edge + wind.edge^2*	0.13	90%	0.71
17a	*EW.aspect*	*EW.aspect*	-0.01	90%	*PTL ~ 1 + edge + wind + wind^2*	0.15	91%	0.00
19a	*wind.edge*	*EW.aspect*	0.37	70%	*PTL ~ 1 + edge + edge^2 + slope + slope^2 + rel.elev + rel.elev^2 + wind.edge*	0.24	84%	0.69
21a	*prof*	*prof*	0.45	80%	*PTL ~ prof + prof^2 + rel.view + slope + slope^2 + rel.solar + plan*	0.07	97%	0.88
Mean			**0.27**	**79%**		**0.16**	**88%**	**0.62**

Similar to the results from the depth hoar layers in individual couloirs, the most important terrain parameters associated with near-surface faceting vary in each couloir. Again, relative elevation is most frequently different for facet PTLs and non-PTLs (Table 19). Four couloirs are identified with statistically different distributions for *rel.elev* and three for *expo*. *Edge* is the only parameter that is in the first node (i.e., the highest discriminating power) of the pruned classification trees more than once (Table 20). It is also the most important parameter in the Random Forest models twice. In comparison to the depth hoar layers, the near-surface faceted layers have a slightly wider variety of important parameters, although the sample size is smaller and describes two different types of faceting: diurnal facets and facets between crusts. However, *rel.elev* and *edge* have the highest cumulative parameter importance, and the top four most important parameters are the same for near-surface facet PTLs as for depth hoar PTLs (Fig. 46). These near-surface layers are generally more predictable than depth hoar layers, improving upon depth hoar success rates by 15%, on average (Table 20). There is also a general pattern where couloirs that have more success in modeling depth hoar also have more success in modeling facets (Fig. 47).

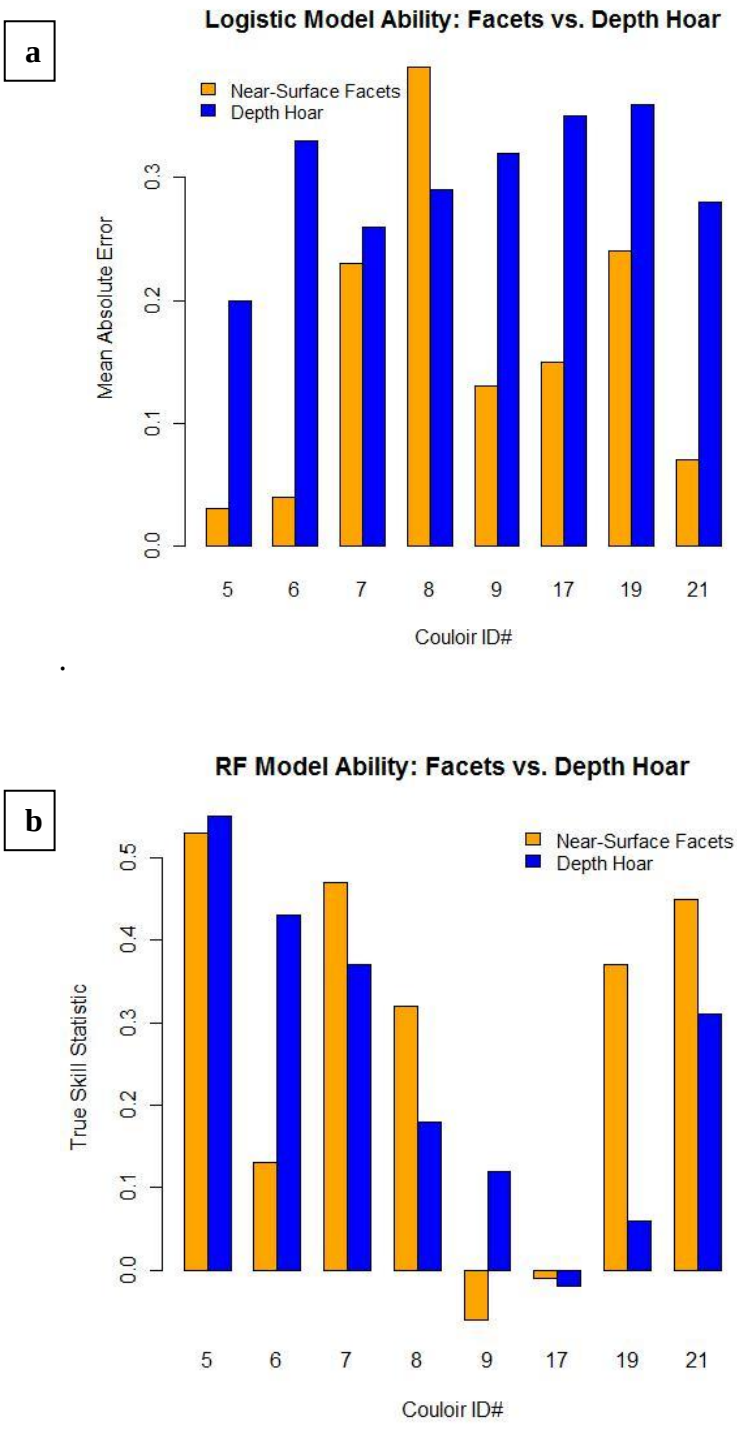

Fig. 47. Comparisons of logistic (a) and Random Forest (b) model ability for couloirs with both depth hoar and near surface facets, showing that in general, models predict near-surface facet layers better.

Table 21. Averaged cross validation results for facet PTL models of each of the individual couloirs used to predict PTLs for each of the remaining couloirs.

	RF success rate	RF True Skill Stat	Logistic success rate	Logistic absolute mean error
Average Xval Results	49.3%	0.044	52.8%	0.478

Despite higher modeling success at the individual couloir level for facets, average cross-validation results are also weak as with depth hoar (Table 21); this again emphasizes the unique nature of each couloir for this weak layer. However, there are several cases with higher success rates and noticeably better results than any cross-validation from the depth hoar layers. From the earlier example with Upper AZ3, the true skill statistics are nearly double the cross-validated results on Upper AZ1 and Upper AZ2 compared to depth hoar results (Table 22).

Table 22. Comparison of Random Forest cross-validation results for the Upper AZ3 depth hoar layer and facet layer with other couloirs in the same headwall. This shows considerable improvement in model skill for predicting facets in other couloirs based on facet observations in Upper AZ3.

Cross-Validation Statistic	**Current (AZ3)**	AZ1	AZ2	AZ4	AZ5
True Skill Stat (Depth Hoar)	**0.27**	0.20	0.20	0.16	0.20
True Skill Stat (Facets)	**0.47**	0.48	0.17	0.01	0.42
Success Rate (Depth Hoar)	**70%**	61%	59%	55%	62%
Success Rate (Facets)	**77%**	69%	39%	51%	77%

The results from all of the couloirs with near-surface facets carry the same message as the individual couloirs analyzed for depth hoar: the influence of parameters vary from slope to slope; therefore, between-couloir predictability is poor. Compared to depth hoar, modeled success rates of the near-surface facets are significantly improved, as are several cross-validation results. This suggests that these near-surface processes are easier to predict based on terrain. This makes sense because the layers we tracked were recently formed, thus they have been less exposed to dynamic meteorological and metamorphic processes after formation that alter their variability and create unpredictable spatial patterns.

Although this is a smaller sample size with a wider variety of influential parameters in both models, relative elevation, distance from edge, wind exposure, and terrain exposure are most frequently important. Again, these all relate to wind influences. As with the depth hoar layers, the influence of these parameters depend on larger scale terrain and weather history prior to sampling. When compared to depth hoar PTLs, there are generally a greater number of important parameters in these models. This indicates that more parameters are associated with the presence of near-surface facets at the slope scale, which accounts for the improved predictability. This is probably because formation and preservation of recent near-surface layers is controlled by a variety of physical processes that interact in a distinct pattern with terrain over a short period of time, including wind erosion, solar radiation, and sluffing. In contrast, depth hoar is a slower-forming weak layer influenced by dynamic processes over a longer period of

time; thus, the associations between depth hoar PTLs and terrain are limited to the most dominant processes.

There is a pattern in modeled PTLs where couloirs with higher success rates for depth hoar PTLs also have higher success rates facet PTLs in the same couloir (Fig. 47). This has several possible explanations. It could suggest that certain terrain features affect different types of weak layers in the same manner. The more successful predictions for both layer types are from couloirs in which these types of features and their influences are most pronounced and can be modeled successfully. The couloirs with less successful predictions for both depth hoar PTLs and facet PTLs are because the current terrain parameters have relatively weaker relationships, and weak layer presence may be controlled by other processes of which we can't characterize with the current set of parameters. Another possible explanation is that this pattern of similar relative predictability is a byproduct of sampling design. Depth hoar and facet observations were collected at the same points in the couloir and are not spatially independent of each other.

Geographic Groups

These results are for the geographically similar groups in which we tracked near-surface facets. These include faceted layer between two crusts that was fairly widespread across the Upper A to Zs and diurnal facets that were shallowly buried in the North Summit/Lone Lake Cirque area. Data for each group are analyzed as a whole and summarized in Tables 23 – 27, with statistical outputs in Appendix B. In this section I summarize and discuss important relationships between PTLs and terrain.

Table 23. KS-test of whether each parameter has a significantly different distribution for facet layer PTLs in comparison to non-PTLs when considering all of the couloirs in the same geographic group. Significant results, identified by bold font and green cells, suggest that these parameters may be independently used to indentify PTLs across an entire cirque or mountain.

Kolmogorov-Smirnov goodness-of-fit test results: P-Values		
Group	Upper AZs	North Summit/ Lone Lake
rel.elev	0.03	0.23
slope	0.00	0.04
EW.aspect	0.00	0.01
NS.aspect	0.00	0.09
prof	0.00	0.22
plan	0.00	0.17
rel.solar	0.28	0.80
wind	0.05	0.01
expo	0.00	0.01
edge	0.00	0.15
wind.edge	0.28	0.01

Table 24. Model success rates and true skill scores (TSS) for facet layer group modeling.

	Pruned Tree nodes	Pruned Tree Success	Pruned Tree TSS	Random Forest success	Random Forest TSS	Logistic Success	Logistic TSS
Upper A to Zs	10	84%	0.68	77%	0.46	65%	0.31
North Summit/ Lone Lake	1	78%	0.63	79%	0.29	57%	0.13
Group Means	**5.50**	**81%**	**0.66**	**78%**	**0.38**	**61%**	**0.22**

Table 25. Top logistic regression model for each facet layer geographic group with the lowest QAICc.

Group	**Lowest QAICc Model**
Upper AZs	*PTL ~ 1 + expo + rel.elev + plan + wind.edge^2 + wind^2*
N. Summit/ Lone Lake	*PTL ~ 1 + wind.edge*

Table 26. The most important parameters for each facet layer group and their general association with PTLs.

	Parameter	**PTL distribution pattern**
Upper A to Zs	*Expo*	more on unexposed terrain
	Plan	more at concavities
	Wind	more in moderate wind shelter
	Edge	more further than 2.5 m from edge, less at 5-7 m from edge
	Slope	more below 44^{o}
	Prof	more at moderate concavities and convexities
	rel.elev	more at lower elevations below 50%
North Summit & Lone Lake	*Wind*	more in high wind shelter
	EW.aspect	more on aspects 0^{o} to 180^{o}
	wind.edge	more closer than 8 m from the edge

Table 27. The most important parameters in each facet layer group and the measures used to identify their importance.

		Pruned Tree	Random Forest	Logistic	Logistic	Logistic
	Parameter	**Level of Node Appearances**	**Mean Decrease in Accuracy**	**Relative Support**	**Significant confidence intervals?**	**Odds Ratio**
Granite Canyon	*rel.elev*	None	0.001	*rel.elev*=0.79	no	
	EW.aspect	None	0.006	0.00	no	
	wind.edge	1st	0.000	*wind.edge*=0.18 *wind.edge*^{2}=0.17	no	
	Edge	None	-0.013	*edge*=0.77 *edge*^{2}=0.14	no	
Jack Creek	*rel.elev*	None	0.050	*rel.elev*=1.00 *rel.elev*^{2}=1.00	*rel.elev*=yes *rel.elev*^{2}=yes	perfect separation
	Prof	1st	0.061	*Prof* ^{2}=0.57, *prof*=0.43	no	
	Slope	3rd	0.021	*slope*^{2}=0.81 *slope*=0.37	no	
	wind.edge	None	0.020	*wind.edge*=1.00	yes	perfect separation
	Edge	3rd	0.031	*edge*=1.00	yes	perfect separation
	Wind	2nd	0.021	*wind*=0.08	no	

The initial faceting of the layer in the Upper A to Zs may be attributed to melt-layer recrystallization or radiation recrystallization, but I am hesitant to apply these labels. The faceted layer was fairly thick (~5 cm), and I believe the majority of the faceting was enhanced by the location of the layer between the two crusts and a generally high temperature gradient in the shallow snowpack. This layer was only absent in areas where no crusts had formed or in areas where the top-most melt-freeze crust was so pronounced that it had agglomerated with the crust below it and destroyed the facets between the two layers. This facet layer produced easy stability test results and frequently failed in compression tests or extended column tests (e.g., Fig. 18).

This widespread layer of facets in the Upper A to Zs had a very recognizable pattern (Fig. 48). A majority of the observations are PTLs, with the few non-PTLs located along the peripheries of the couloirs where thinner snowpacks resulted in the merging of the two crusts into one without preserving the facets between them. Any number of parameter combinations can accurately predict this spatial pattern; we need to identify all of the parameters that are associated with shallow snowpacks for the Upper A to Z terrain (Tables 26 and 27). These are high exposure or wind exposures, steep slopes, higher elevations, proximity to the edge, and most prominent convexities. The models simply look to exclude points with the most extreme collection of these values as non-PTLs. Accordingly, numerous parameters are important and the models are larger than most of the previous depth hoar models (Table 27). The greatest success in the entire dataset for couloir to couloir cross-validation is on this layer in the Upper A to Zs, demonstrating how some layers are more predictable across numerous couloirs.

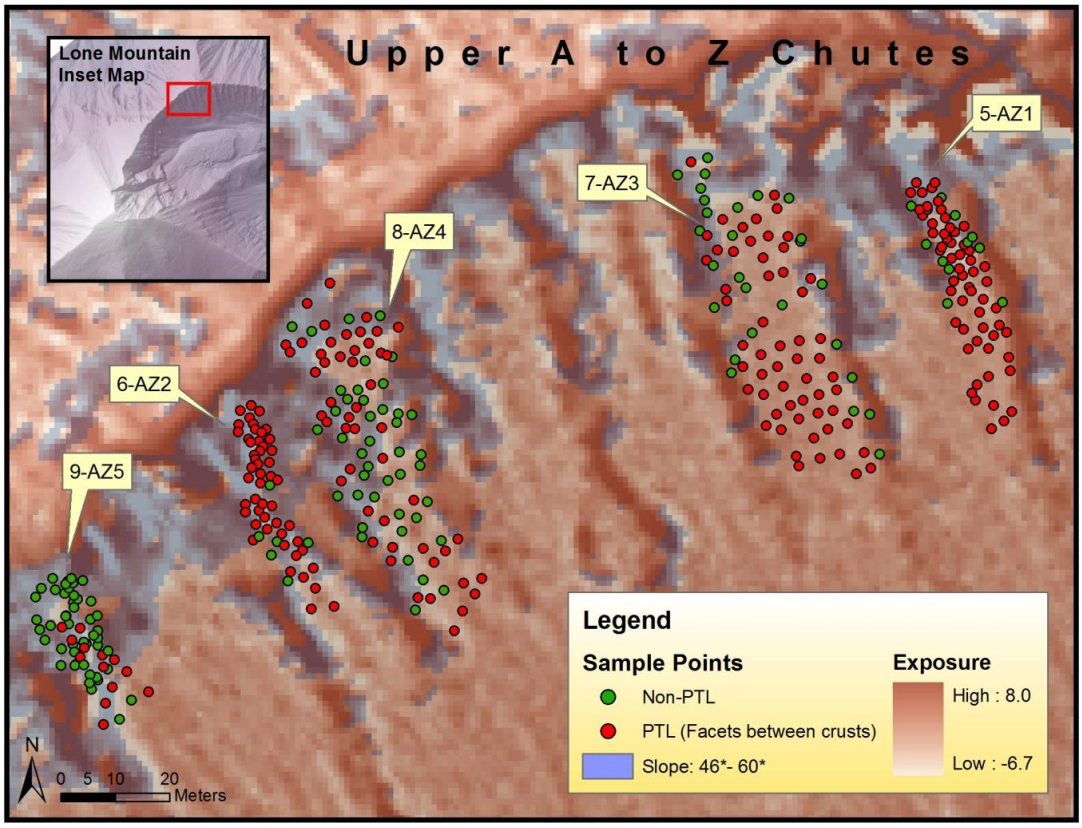

Fig. 48. Map of the facet layer between two crusts that was observed in the Upper A to Zs. The map shows how non-PTLs are associated with steeper slopes, higher exposure, proximity to the edge of couloirs, and higher elevations.

There are three couloirs from north-facing aspects on Lone Mountain where we found diurnal facets that had been recently buried by thin wind slabs. These layers are likely the result of two different faceting events, but both formed under similar meteorological conditions.

There are two physical processes that either combine or uniquely contributed the presence of these diurnal facets. The first process relates to the formation of this layer and the second to its preservation. The facets formed following a new snowfall of low density powder. Although temperature gradients associated with the incoming and

outgoing radiation balance are what ultimately drive diurnal faceting, I suspect that radiation balance conditions were suitable for faceting across the entire couloir, or that any differences were challenging to model at this scale. However, with everything else being equal, faceting is enhanced in high porosity snow (McClung and Schaerer, 2006). The diurnal facets likely only formed in low density, high porosity snow and not in hard wind slabs that are typical of the alpine terrain on Lone Mountain. Therefore, the facets are most prevalent where new, low density snow is preserved during or following a storm. The terrain parameters that relate to low density snow are those that are associated with protection from the prevailing winds: *wind, wind.edge,* and *EW.aspect* for this group (Fig. 49, and Tables 26 and 27).

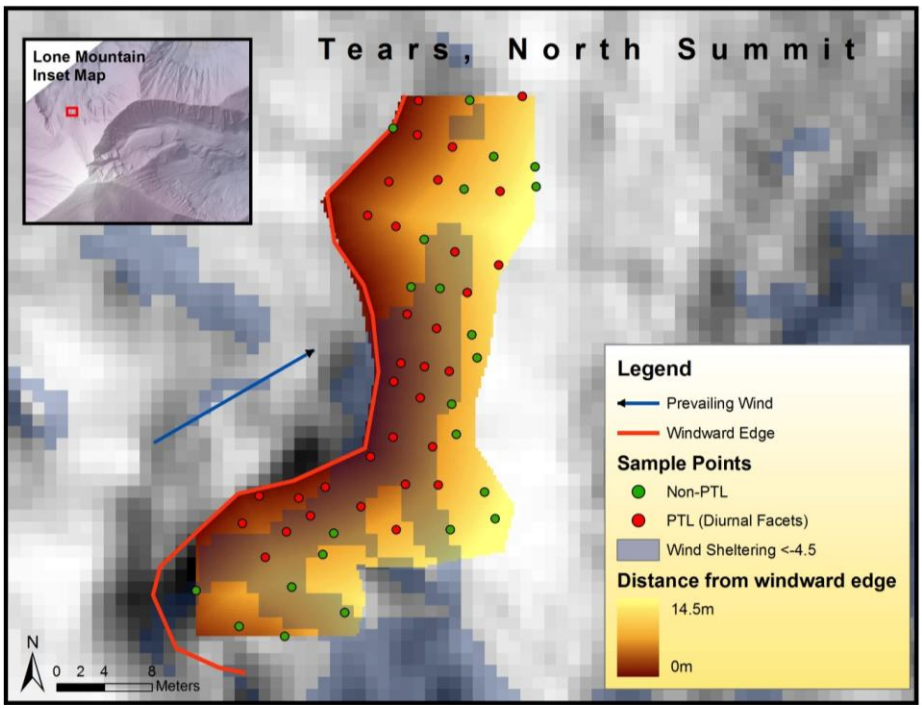

Fig. 49. Map of Tears Couloir showing how presence of near-surface diurnal facets are strongly associated with protection from the wind, which can be explained with the wind sheltering parameter or distance from the windward edge.

The second physical process that likely affected the presence of PTLs is their preservation following formation and prior to our sampling. Weak surface layers are easily destroyed and swept away in alpine terrain, but the layers are preserved if they are protected from wind prior to burial from new snowfall or wind-blown snow. Again, these locations are modeled by the same parameters for the first physical process: parameters that associate with wind protection (Fig. 49).

The results from these samples suggest that diurnal facets in complex alpine terrain are favored in wind protected zones, which are associated with *wind, wind.edge*, and a leeward aspect parameter. It is obvious from both the Upper A to Zs and the North Summit/Lone Lake groups that the parameters associated with near-surface faceting highly depend on the physical processes that are either forming or destroying the weak layer.

Surface Hoar Results and Discussion

This analysis and discussion includes several surface hoar layers that were tested with ECTs in Granite Canyon and the presence of a shallowly buried surface layer in Jack Creek Couloir. PTLs are defined differently for the two groups. In Granite Canyon, PTLs are where any extended column tests (ECT) failed with full propagation or any points along the avalanche crown line that occurred during sampling. For Jack Creek Couloir, a PTL is defined as the presences of preserved surface hoar. It is important to note that the Granite Canyon PTLs are a different type of classification of PTLs from the rest of this study: not the presence of a weak layer but the propagation propensity of a weak layer. Thus, the results have different implications than the rest of the dataset.

Modeling and KS-test results for each surface hoar group are presented in Tables 28 – 32, with statistical outputs in Appendix B. In this section I highlight and discuss important relationships between surface hoar PTLs and terrain.

Table 28. KS-test of whether each parameter has a significantly different distribution for surface hoar PTLs in comparison to non-PTLs when considering all of samples in the same geographic group. Significant results, identified by bold font and green cells, suggest that these parameters may be independently used to indentify PTLs for these groups.

Kolmogorov-Smirnov goodness-of-fit test results: P-Values		
	Granite Canyon	Jack Creek
rel.elev	0.014	0.004
slope	0.500	0.011
EW.aspect	0.015	0.024
NS.aspect	0.015	0.122
prof	0.135	0.000
plan	0.807	0.916
rel.solar	0.879	0.291
wind	0.794	0.002
expo	0.794	0.688
edge	0.027	0.003
wind.edge	0.026	0.014

Table 29. Model success rates and true skill scores (TSS) for modeling of surface hoar layers.

	Pruned Tree nodes	Pruned Tree Success	Pruned Tree TSS	Random Forest success	Random Forest TSS	Logistic Success	Logistic TSS
Granite Canyon	3	73%	0.46	44%	-0.12	66%	0.27
Jack Creek	7	96%	0.92	88%	0.59	92%	0.85
Group Means	**5**	**85%**	**0.69**	**66%**	**0.24**	**79%**	**0.56**

Table 30. Top logistic regression model for each surface hoar geographic group with the lowest AICc (for Jack Creek) or QAICc (for Granite Canyon).

Group	Lowest (Q)AICc Model
Granite Canyon	PTL ~ 1 + edge + rel.elev
Jack Creek	PTL ~ 1 + edge + prof^2 + rel.view + slope^2 + rel.elev + rel.elev^2 + wind.edge

Table 31. Important parameters for each surface hoar group and their general association with PTLs.

	Parameter	PTL distribution pattern
Granite Canyon	*rel.elev*	more at lower elevations below 40%
	EW.aspect	more at aspects from 35^{o} to 180^{o}
	wind.edge	more closer than 5 m from windward edge
	edge	more closer than 5 m from edge
Jack Creek	*rel.elev*	more at mid elevations between 35% and 75%
	prof	more on concavities
	slope	more below 43^{o}
	wind.edge	more further than 6 m from windward edge
	edge	more further than 4 m from edge
	wind	more on wind exposed

Table 32. The most important parameters for each surface hoar group and the measures used to identify their importance.

		Pruned Tree	Random Forest	Logistic	Logistic	Logistic
	Parameter	**Level of Node Appearances**	**Mean Decrease in Accuracy**	**Relative Support**	**Significant confidence intervals?**	**Odds Ratio**
Granite Canyon	*rel.elev*	none	0.001	*rel.elev*=0.79	no	
	EW.aspect	none	0.006	0.00	no	
	wind.edge	1st	0.000	*wind.edge*=0.18 *wind.edge*^{2}=0.17	no	
	edge	none	-0.013	*edge*=0.77 *edge*^{2}=0.14	no	
Jack Creek	*rel.elev*	none	0.050	*rel.elev*=1.00 *rel.elev*^{2}=1.00	*rel.elev*=yes *rel.elev*^{2}=yes	perfect separation
	prof	1st	0.061	*prof*^{2}=0.57, *prof*=0.43	no	
	slope	3rd	0.021	*slope*^{2}=0.81 *slope*=0.37	no	
	wind.edge	none	0.020	*wind.edge*=1.00	yes	perfect separation
	edge	3rd	0.031	*edge*=1.00	yes	perfect separation
	wind	2nd	0.021	*wind*=0.08	no	

The surface hoar layers in Granite Canyon were very reactive (Fig. 19). Numerous avalanches failed on these layers in the surrounding backcountry during the time frame of our sampling, including one in our study site on the Seven Dwarves. From the poor modeling results for Granite Canyon, it is evident that both robust models have difficulty predicting surface hoar weak layer propagation locations based on terrain for the entire group analyzed as a whole (Table 29). It is unclear to me what key physical processes are related to PTLs for Granite Canyon, but I suggest PTLs are most strongly associated with the slab properties rather than the properties of the buried surface hoar. In general, the top layer of surface hoar in A-Chute (SH 4a) and the layer of surface hoar in Seven Dwarves (SH 3) are more reactive under thicker slabs. The areas where ECTs

do not propagate are where the load on the layer is not large enough to drive propagation. However, the lower layer on A-Chute (SH 4b) has an inverse relationship to slabs, where lighter loads are associated with propagation in the ECTs. This layer is older; propagation may be more likely in areas where it has had less overburden and less induced strengthening since being buried.

These opposing physical processes are challenging to model with terrain. Modeling couloirs separately results in stronger relationships and explainable patterns. PTLs are strongly associated with proximity to windward edge and leeward aspects for SH3, where the slab was considerably larger and surface hoar had been protected from destructive winds (Fig. 50). This is where a 20 – 30 cm avalanche released during sampling (Fig. 51). Greater wind-loading occurred further from the windward edge and further down-slope for SH 4a and SH 4b. These differences from SH 3 may not be due to different processes; SH 3 was collected over a much wider portion of the starting zone, while SH 4a and SH 4b are in a smaller zone, so the scales sampling extent are different. Distances further down-slope and from the windward edge are associated with PTLs for SH 4a, and non-PTLs for SH 4b (Fig. 50). When SH 3, SH 4a, and SH 4b are analyzed as a group, all of the relationships are fairly weak, but locations further down-slope in the starting zones and closer to the edge or windward edge are more frequently associated with PTLs (Tables 31 and 32).

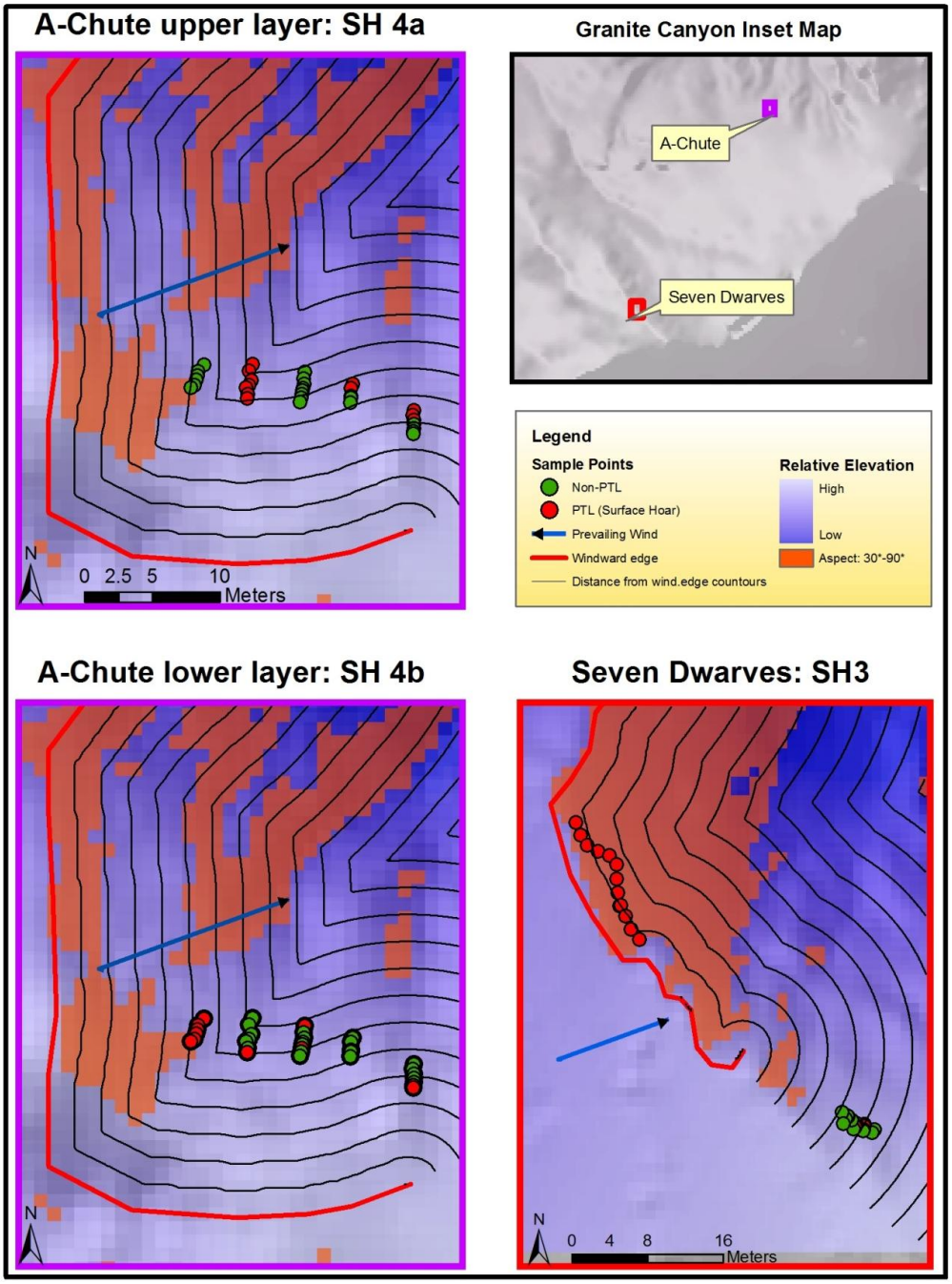

Fig. 50. Map of important terrain parameters and PTLs for the two couloirs in Granite Canyon. The map shows the convoluted relationship between distance from windward edge and PTLs, where SH 4a and SH 4b have opposing relationships. The same is true for relative elevation. PTLs for SH3 are strongly related to proximity to windward edge and more leeward aspects, where slab development was greater, as well as lower elevations, where winds were likely less destructive prior to burial.

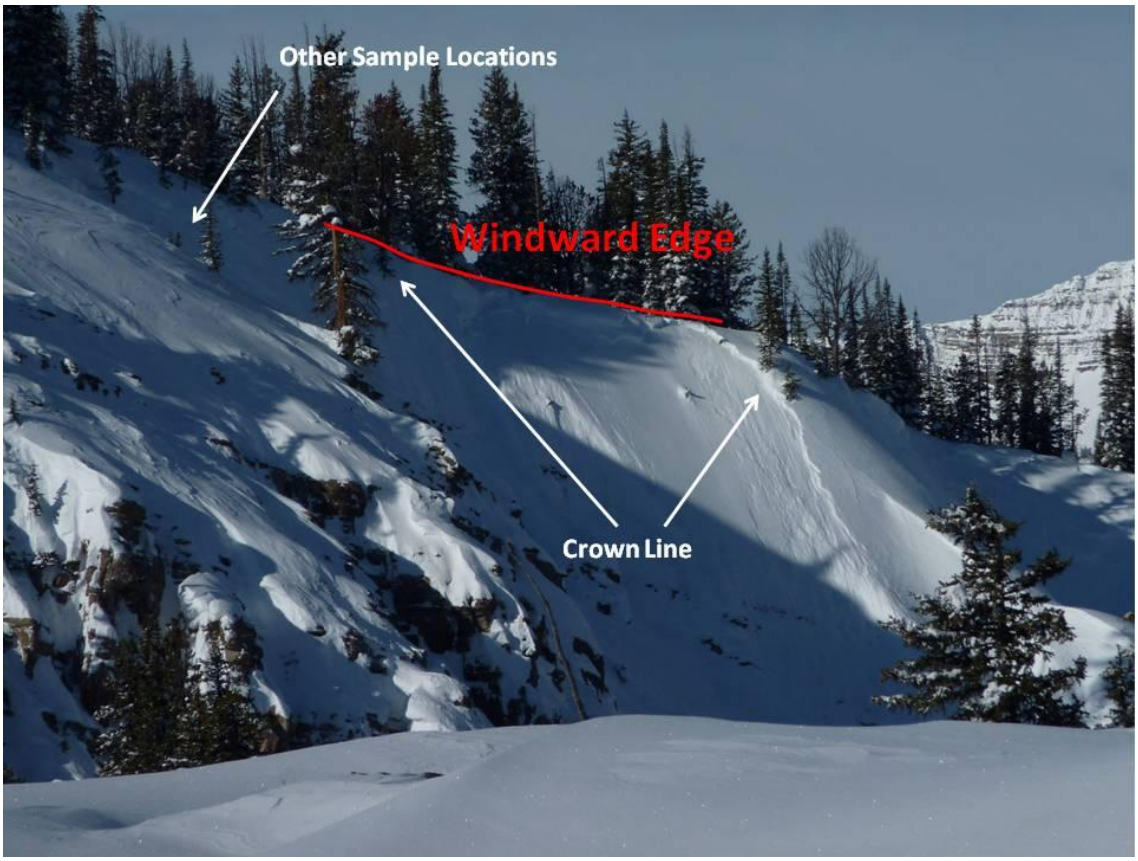

Fig. 51. Photograph of Seven Dwarves, showing the crown of an avalanche that released on a buried layer of surface hoar (SS-AS-R2-D2) on February 13, 2010 during sampling.

The results of the Granite Canyon site demonstrate how the location of PTLs can depend on complex and even opposing physical process, which are challenging to predict with terrain. The terrain that is strongly associated with PTLs for SH 4a is mostly not associated with PTLs for SH 4b, yet they were sampled at the same locations, on the same layer type, in the same season. It is evident that for some layer types recent weather and snowfall patterns have variable influences on how the terrain interacts with PTLs. Furthermore propagation propensity may be influenced by factors independent of terrain or at a finer scale than this analysis.

The second analysis in the surface hoar dataset is the presence/absence of a surface hoar layer observed in Jack Creek couloir in the Headwaters. This layer formed during a high pressure system between 12/4/10 and 12/6/10 and was subsequently buried by several light snowfalls prior to our sampling on 12/11/10. This layer of surface hoar has a fairly distinctive and clustered pattern in the topography (Fig. 52), and the models are able to predict the location of PTLs very accurately based on terrain parameters (Table 29).

One of the dominant processes describing the presence of this PTL is the destruction of the surface hoar due to sluffing. The new snow that fell after the surface hoar formed sluffed off of the steepest slopes. On Jack Creek, there are two significant rollovers that likely induced small sluffs that wiped out surface hoar on convex slopes and the slightly concave slopes below them. Slope profile and slope angle are two important parameters that associate with this process (Tables 31 and 32).

The strong positive associations between surface hoar presence and increasing wind exposure and distance from the windward edge were initially surprising (Tables 31 and 32). For the windy alpine terrain of Lone Mountain, I expect the destruction of surface hoar due to winds to be a primary driver of spatial patterns (McClung and Schaerer, 2006). The wind sheltered slopes and windward edge of this couloir could offer protection from the prevailing winds and allow more prevalent surface hoar formation or preservation after it formed. However, a possible explanation for this is a shift in wind direction after the surface hoar formed which would reverse the expected effects of wind sheltering. The wind records from the Jack Creek wind station (which is

on the ridgeline above the couloir) suggest this is a plausible explanation. In the several days following the surface hoar formation, winds were light and variable in direction, averaging 12km/hr. The day prior to our sampling, the winds strengthened from the southwest, from which Jack Creek Couloir is generally sheltered. That day, winds veered to the north and northeast for periods of time, with wind speeds exceeding 40km/hr from these directions. Thus, locations that are normally exposed to prevailing winds actually provided shelter from the powerful northeast winds (Fig. 52). This could explain why greater distance from the windward edge and a higher degree of wind exposure are all associated with presence of PTLs.

The Jack Creek surface hoar layer provides an excellent example of how relationships between terrain parameters and presence of PTLs are dynamic depending on prior weather history. It suggests that a thorough understanding of the nature of the PTL problem as well as the recent weather history are required to use terrain parameters to successfully predict PTLs, especially those at the surface.

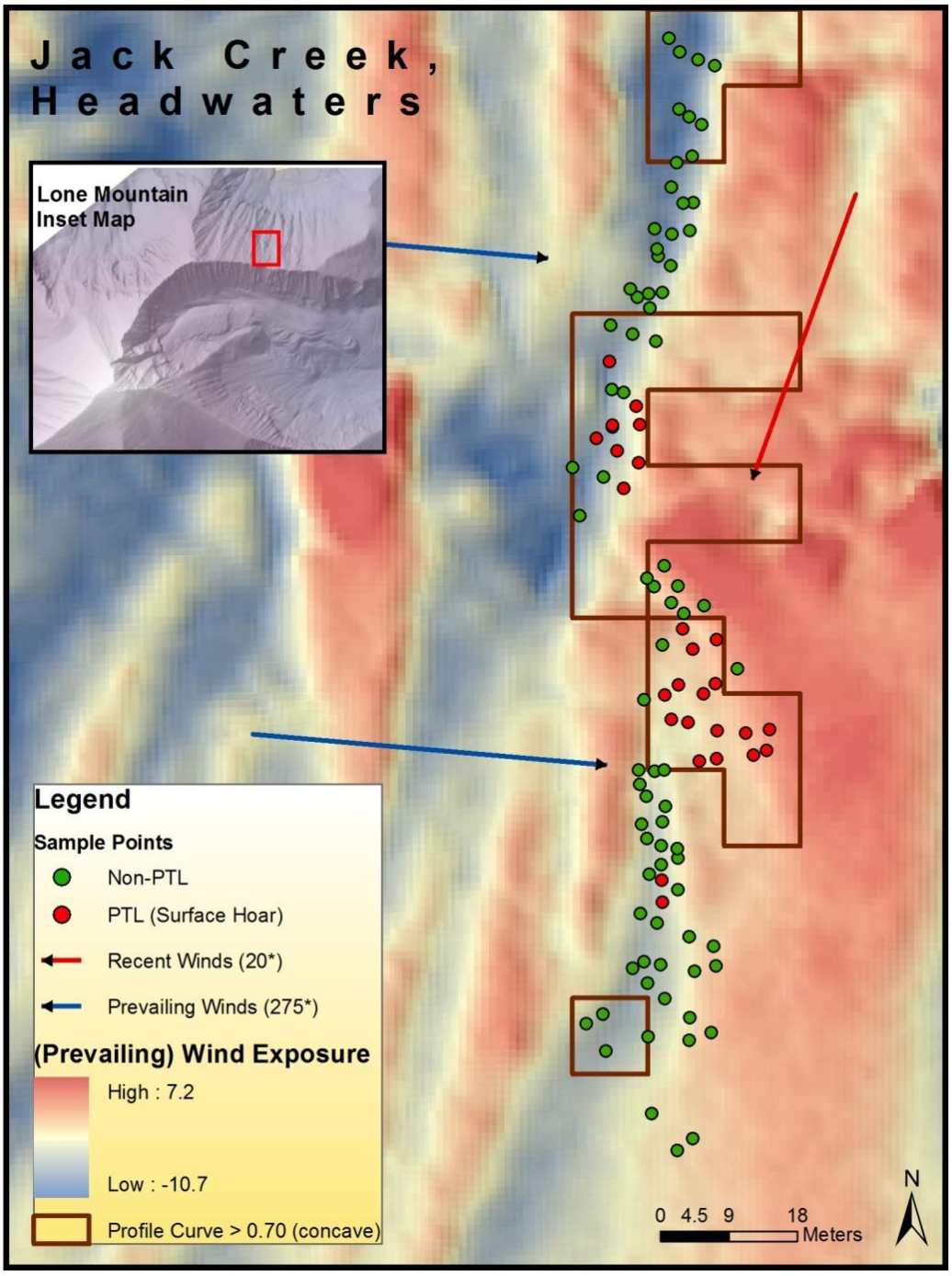

Fig. 52. Map of surface hoar PTLs on Jack Creek Couloir, showing how a shift in wind patterns after the surface hoar formation could have unexpected effects on parameters relating to wind protection. Areas that are exposed to prevailing winds (in red), offer more wind sheltering with a shift in wind direction to the northeast. Also, the association with slope profile is evident.

General Discussion

Summary

The results from modeling potential trigger locations (PTLs) of individual couloirs and geographic groups show how a wide range of parameters have varying levels of importance and varying influences on the presence of PTLs. Is there a parameter that best explains the presence of PTLs at the slope scale for steep, complex terrain? The answer is that it clearly depends on how processes occurring at a broader scale interact with the slope-scale terrain, a point that has been pointed out in previous studies (e.g., Schweizer and Kronholm, 2007; Schweizer et al., 2008), but is further emphasized in this research.

Seasonal and recent weather patterns affect how terrain parameters relate to PTLs. Near-surface weak layers are especially sensitive to short-term wind or solar patterns. This is illustrated by the surface hoar layer in Jack Creek couloir, where a change from the prevailing wind patterns over a period of less than one day changed how wind sheltering parameters interact with this fragile surface layer when compared to surface weak layers on fairly similar slopes in the North Summit cirque (Figs. 49 and 52). The changing influences of terrain as a result of weather patterns or seasonality agree with the results of Birkeland (2001), who found that the relationship between terrain parameters and regional scale stability observations was highly variable over the course of a season depending on the weather patterns leading up to the sampling day.

Regional, mountain, and cirque scale processes clearly affect how slope-scale terrain parameters interact with the snowpack. As an example, highly sheltered terrain is

related to depth hoar PTLs in the Upper A to Zs, where sheltered slopes are required for significant slab formation. However, on the opposite side of the ridge where snow loading is more prevalent in the Headwaters, highly sheltered terrain is related to absence of PTLs because the enhanced snow loading in these zones creates a snowpack that is too deep for depth hoar formation (Figs. 43 and 44). Cirque scale processes also have a strong influence on the relationship between PTLs and terrain. For example, the strong association between low elevations and an absence of PTLs in Lone Lake Cirque is due in part to the sheltering effects of the west wall of the cirque against the prevailing winds (Fig. 41).

Furthermore, couloirs in the same cirque or headwall can be surprisingly different, as evidenced by frequent poor cross-validation results between couloirs in the same cirque and decreases in modeling success rates from individual couloir models to geographic groups of couloirs in the same cirque (e.g., Figs. 38 and 39 and Tables 12). While many physical processes and their related slope-scale parameters may be operating across an entire cirque, other processes occur independently on each individual slope. These processes differ from slope to slope because each couloir has unique topographical characteristics that interact with the larger scale processes differently. An example of this is Upper AZ1: the presence of a large cliff above the slope changes how elevation relates to PTLs compared with some of the other Upper A to Z chutes (Figs. 4 and 43).

While their influences vary from couloir-to-couloir or group-to-group, some terrain parameters show the ability to discriminate PTLs better than others. For PTLs in which depth hoar is the concern, relative elevation, distance from the edge of the couloir,

degree of wind sheltering, and degree of terrain exposure are most frequently the most influential parameters in models (Table 11). KS-tests for individual couloirs show that elevation and distance from the edge are most commonly able to independently discriminate the presence of PTLs (Table 10). It is difficult to quantify the most important parameters from the logistic models because it depends on what other parameters are in the model and how uncorrelated they are from other parameters. However, the aforementioned parameters, along with profile of the slope, appear most frequently in the top logistic models (Table 11). With the depth hoar data analyzed as a whole, distance from the edge, distance from the windward edge, and the degree of wind sheltering generally fit the data best (Table 18).

Near-surface layers more frequently relate to a wider set of parameters, but the ones that describe the interactions with wind appear most frequently in the models. These include distance from the edge or windward edge, degree of exposure, the wind-sheltering index, and relative elevation. Profile curvature and slope angle are also commonly important because of their association with sluffing. The east-west aspect parameter can also be important when the other wind-related parameters are inadequate (Tables 26 and 32).

Depth hoar PTLs are generally more challenging to model with terrain parameters. Near-surface layers are related to a wider range of parameters and have improved predictability (e.g., Fig. 47). Near-surface layers are probably easier to predict in this study because they are newly formed and the processes driving formation or destruction of these layers are strongly controlled by the interaction of specific

meteorological conditions with specific terrain parameters. With the passage of time, dynamic and widely varying meteorological conditions repeatedly alter the influences of terrain on older layers: they become harder to predict. Other poorly understood processes may enhance the variability of these layers. Depth hoar layers are more consistently predicted by the same parameters because the varying influences of terrain due to dynamic meteorological processes "average" out into more common relationships. These "averaged" parameters for slow-forming depth hoar layers appear to have weaker associations than the faster-forming surface layers that are associated with specific meteorological conditions that have specific relationships with terrain parameters.

Terrain Parameter Influences

In this section I summarize the general patterns of how each of the terrain parameters affected the presence of PTLs for the entire study, and how they relate to the various physical processes. I also point out why some of the parameters are not as important in this study.

Distance from the edge is most commonly associated with depth hoar PTLs and the surface hoar ECT dataset because slab depth is highly related to proximity to the sides of couloirs (e.g., Fig. 37b). Distance from the edge is also associated with the presence of depth hoar. In relatively deeper snowpacks, the edges of couloirs are more likely to have depth hoar development because of the shallow snowpacks overlying rock and talus, whereas depth hoar formation is inhibited at greater distances from the edge due to deeper snow depths (e.g., Figs. 44 and 45). This is consistent with the findings of Arons et al. (1998) and Birkeland et al. (1995) who noted depth hoar growth and weaker snow

Table 33. Spearman rank-order correlation coefficients for terrain parameters from the entire dataset of 21 couloirs and 1662 measurements. All correlations greater than 0.048 or less than -0.048 are significant at a 95% confidence level, indicated by bold font and green shading.

	rel.elev	*slope*	*EW.aspect*	*NS.aspect*	*prof*	*plan*	*rel.solar*	*wind*	*expo*	*edge*	*rel.view*	*wind.edge*
rel.elev	**1.000**	**0.204**	-0.015	-0.010	**0.121**	-0.018	**0.179**	**-0.061**	**-0.068**	**-0.137**	**-0.051**	**-0.138**
slope	**0.204**	**1.000**	**0.390**	**-0.323**	**0.219**	-0.043	**-0.210**	**-0.494**	**-0.160**	**-0.356**	**-0.288**	**-0.334**
EW.asp	-0.015	**0.390**	**1.000**	**-0.391**	**0.138**	-0.016	**-0.059**	**-0.791**	**-0.070**	**-0.150**	**-0.334**	**-0.499**
NS.asp	-0.010	**-0.323**	**-0.391**	**1.000**	**-0.154**	0.015	**-0.112**	**0.210**	**0.058**	**0.209**	0.034	**0.226**
prof	**0.121**	**0.219**	**0.138**	**-0.154**	**1.000**	**-0.072**	**-0.109**	**-0.276**	**-0.166**	0.010	**-0.138**	**-0.055**
plan	-0.018	-0.043	-0.016	0.015	**-0.072**	**1.000**	**0.066**	**0.170**	**0.755**	0.001	**0.140**	0.027
rel.solar	**0.179**	**-0.210**	-0.059	**-0.112**	**-0.109**	**0.066**	**1.000**	**0.111**	**0.113**	0.031	**0.215**	0.027
wind	**-0.061**	**-0.494**	**-0.791**	**0.210**	**-0.276**	**0.170**	**0.111**	**1.000**	**0.297**	**0.123**	**0.455**	**0.412**
expo	**-0.068**	**-0.160**	-0.070	**0.058**	**-0.166**	**0.755**	**0.113**	**0.297**	**1.000**	-0.016	**0.240**	**0.080**
edge	**-0.137**	**-0.356**	**-0.150**	**0.209**	0.010	0.001	0.031	**0.123**	-0.016	**1.000**	-0.047	**0.456**
rel.view	**-0.051**	**-0.288**	**-0.334**	**0.034**	**-0.138**	**0.140**	**0.215**	**0.455**	**0.240**	-0.047	**1.000**	**0.282**
wind.edge	**-0.138**	**-0.334**	**-0.499**	**0.226**	**-0.055**	0.027	0.027	**0.412**	**0.080**	**0.456**	**0.282**	**1.000**

near rock outcrops or shallowly buried rocks. The interplay of slab depth and faceting near the sides of couloirs combine to form a general "sweet spot" for depth hoar PTLs around one meter from the edge of couloirs (e.g., Fig. 45). Proximity to the edge also can enhance warming on more sunlit aspects or affect the amount of wind scouring. This can have the affect of strengthening snow to prevent depth hoar or protecting or destroying near surface layers. Distance from the windward edge has similar associations as distance from edge (Table 33), but it is more appropriate where the physical processes favor one side or the other in wind-affected terrain.

The degree of wind sheltering is highly important in the many of the individual couloirs and group models for all weak layer types. Its association with PTLs varies, depending on whether it is describing the process of threatening slab development (e.g, Fig. 37d), loading of deep and stable snowpacks, or protection of weak layers from wind scouring and erosion (e.g., Fig. 49). The importance of the wind-sheltering index is consistent with the work of Gleason (1996), who found a "wind factor" was one of four most influential terrain parameters associated with natural avalanche release on Lone Mountain. My wind index is strongly correlated with *EW.aspect* (Table 33). The east/west component of aspect essentially describes the aspect as it relates to winds that typically prevail from the west, which is more comparable to Gleason's "wind factor." Including a similar wind-related parameter that modifies wind direction based on recent winds or storm events would likely improve modeling success, especially for near-surface weak layers.

Terrain exposure and plan curvature also relate to influences from wind. Exposure and plan curvature are highly correlated parameters (Table 33), but exposure appears important more frequently in the individual modeling and groupwise modeling. As with the wind index, how exposure relates to PTLs depends on numerous other variables (e.g., Figs. 43 and 44). Exposure has an advantage over the wind index in that it indicates how sheltered or exposed a cell is independent of the prevailing wind direction, so it may be more important in environments with highly variable wind directions. This could explain its importance for the Upper A to Z chutes and the Headwaters group. Exposure is also associated with warming and strengthening of snow on southerly aspects because more exposed locations are closer to low albedo rocks that readily absorb solar radiation.

At the individual couloir level, relative elevation within the couloir is the single most frequently differing and highly important parameter, supported by all models and statistical tests (Tables 10 and 11). The relationships are frequently opposing between couloirs, so it appears unimportant when couloirs are grouped together (e.g. Figs. 22 and 37a). However, the individual couloir results show that consideration of relative elevation is critical for predicting PTLs. Elevation is also documented by Gleason (1996) as one of the four most important parameters for natural avalanches on Lone Mountain. Profile curvature can be correlated with relative elevation (Table 33), but is frequently less important. However, because profile curvature relates to specific physical processes such as sluffing or wind scouring, it is a more important parameter in some cases.

Slope angles above approximately 46^{o} in the Upper A to Zs and 43^{o} in the Headwaters are associated with fewer depth hoar PTLs (e.g., Fig. 43). This can be attributed to snow sluffing which prevents the build-up of slabs (Table 17). On Jack Creek couloir, sluffing destroyed surface hoar PTLs on slopes steeper than 43^{o} (Table 31). These results are similar to those found by Gleason (1996), who cites slopes steeper than 43^{o} on Lone Mountain are associated with fewer natural slab avalanches.

Relative solar radiation only appears important in the Upper A to Z chutes and a select few other individual couloirs (Table 11 and Table 18). Other than the Upper A to Zs, the rest of this dataset is primarily north-facing, so solar radiation would likely have higher importance if more southerly aspects were studied. In the absence of a major shadowing obstruction, relative solar radiation derived from Solar Analyst in ArcMap is essentially a combination of aspect and slope angle as it relates to seasonally changing sun azimuths and angles in the sky. By changing the solar radiation to a relative measure on a scale from 1 to 100, I exaggerate what is otherwise a minimal difference between cells during the winter months on northerly slopes. I suspect that any relationships between relative solar radiation and PTLs on north facing slopes in this study is a byproduct of its correlation with slope and aspect, especially as aspect relates to wind effects (Table 33).

Relative viewshed appears to be of limited importance relative to other parameters. While I hypothesize that a parameter relating to coarse scale wind patterns is important, as illustrated with Lone Lake Cirque, relative viewshed is inadequate in characterizing these patterns for most couloirs. In the process of creating the parameter,

selecting the length of the ridge to use as the viewing platform seemed arbitrary, so I attempted to remove this guesswork by implementing the 30^{o} search width (Fig. 15). The length of the viewing platform varied tremendously due to differing lengths of couloirs, different terrain geometry, or different proximities of couloirs to the major windward ridgeline. Depending on the couloir, relative viewshed often lacked continuity as a variable, with only zero, one, or two discrete values for slopes that were directly below the major windward ridgeline and out of view. Further work could attempt to model a large scale wind process but with an improved parameter, and it could also incorporate a drift indicator, as in Winstral et al. (2002).

The two aspect parameters do not describe any physical processes that are not also modeled by other parameters; thus I am not surprised at their relative lack of importance in most of the models. Several studies cite aspect as an important terrain parameter in weak layer development (e.g., Cooperstein, 2008). Aspect itself is not driving the process, but aspect relative to the sun's position or to the wind's direction is what drives the processes. I designed a wind index, relative viewshed, and relative solar radiation to account for these processes. The use of aspect in these models is either as an indicator variable distinguishing between couloir groups, as with the full depth hoar dataset (Table 18), or to make up for inadequate wind parameters, as with the Lone Lake Cirque depth hoar layer, North Summit facet layer, or the Granite Canyon surface hoar layers. (Figs. 41 and 50; Tables 18, 27, and 32).

The one meter DEM derived from LiDAR data allowed for characterization of complex terrain that would normally not be possible over such an extensive study area.

The chutes and couloirs of this study are highly variable; the one meter resolution enabled fine scale features to be incorporated into the terrain parameters used in this study. This is especially important for parameters relating to wind exposure and sheltering, such as the wind index and exposure index. However, some of these parameters would be just as practical with a 10 m DEM, a resolution that is readily available for many mountainous regions in the United States. Distance from the edge or windward edge of the couloir do not require an elevation model, so long as the boundaries of the couloir are mapped with a GPS or can be digitized with an orthophotograph. In this study, DEM resolution was reduced to 10 m for profile curvature because it allowed identification of major rollovers and aprons. Certainly the other parameters derived at a coarser scale could still be useful, and in some cases, may even improve modeling ability if larger terrain features are controlling the physical processes. The usefulness of coarser scale terrain parameters for modeling was not tested in this study but would be worthy of future analysis.

In summary, fine scale parameters that relate to the physical processes of wind scouring, wind protection, and wind-loading are most important for predicting PTLs for couloirs in the complex alpine terrain used in this study. The strong importance of wind-related parameters in alpine terrain are in accordance with previous snow depth modeling studies that cite wind as most influential, such as Erickson et al. (2005) and Wirz et al. (2011). Parameters relating to other physical processes such as sluffing or solar effects are also related to PTLs in some cases, but they are not as frequently important for these couloirs.

Modeling Success

The success of individual and group modeling of PTLs is encouraging, especially because the parameters chosen in most of the models logically relate to physical processes. However, they do not account for all of the variability in the PTL observations. For depth hoar PTLs, success rates for individual couloirs are typically between 60% and 70% for both of the robust models (Table 11). Near-surface facet models average around 85% (Table 20). Some of the unexplained variability is attributed to error inherent in the study design (See page 162), but clearly these terrain parameters are unable to account for all of the complex processes involved in PTL spatial variability.

In the Random Forest models, the greatest decrease in success by removal of a single parameter is around 10%, and for groupwise modeling, most of the important parameters have mean decreases in accuracy between 1% to 3% (e.g., Table 18). This implies that collectively incorporating all available terrain parameters into the decision-making process will lead to the most successful decisions in avalanche terrain. For example, in the case of Upper AZ1, where *rel.elev* is clearly a very strong parameter, if you relied on a complete understanding of how relative elevation interacts with depth hoar PTLs for that slope, you would be capable of a 70% success rate (using the logistic model structure). However, if you include all of the important terrain parameters, the success rate increases to 87% (Table 11). This emphasizes the importance of incorporating the full spectrum of all of the slope scale terrain parameters and their interactions into decision making. This example from Upper AZ1 is an exceptionally well modeled layer, but it still leaves unaccounted variability. That being said, equipped with knowledge of how the large scale and meteorological processes are interacting with

the slope-scale terrain parameters, one can significantly improve their chances of finding a PTL with the appropriate slope-scale parameters, which allows for educated decision making. Furthermore, the couloirs in which I had a better understanding of the primary physical processes guiding variability, and the couloirs in which I was able to reasonably predict weak layer presence as I sampled across the slope are the ones that generally have the highest model success rates. These findings support the common practice by practitioners of probing to establish and extrapolate slope-scale patterns when assessing the variability of buried weak layers.

All of the other studies that have attempted to predict weak layer or stability characteristics from a terrain-based model have had similar unexplained variability in their modeling results because of the complexity of the snow and avalanche regime. For example, Shea and Jamieson (2010) cross validated their surface hoar model on a very similar and specific slope with 60% success rates. This is comparable to the 59% average success rate that Upper AZ3 has when cross-validating against the other Upper A to Zs for both depth hoar and facets (Table 22). Schweizer and Kronholm (2007) document an 82% success rate and 60% miss rate for a terrain-based logistic model fit to the presence of surface hoar for one region. Their rate is lower than the 92% success rate for Jack Creek Surface hoar layer and the 88% average success rates for the presence/absence of near-surface facets. This improvement may be due to different scales or the higher resolution of terrain parameters used for this study. Birkeland et al. (1995) report a 0.15 r^2 value for snow resistance modeled by snow depth and the presence of rocks on a somewhat complex slope. Birkeland (2001) explained 20% to 50% of the variability in

stability response variables with terrain parameters. These latter two are different measures of variability on different observed responses, but also demonstrate the high variability that is typical of spatial variability research in snow strength and stability.

Correlations between the parameters included in this model and total snow depth are comparable to results reported in Wirz et al. (2011) from a similar scale and similar resolution study of snow depth on a steep rock face. In their results, the maximum absolute values of Pearson correlation coefficients are: slope angle= 0.13 and curvature=0.21. For this study, Spearman correlations are much higher for some of the individual couloirs, but for the entire dataset, I get comparable correlations of: slope angle=0.27, plan curvature=0.09, and profile curvature=0.11 (Fig. 53). Correlations from *wind*, *expo*, and *rel.view* fall between these values. Comparing *edge*, which has the strongest correlation for this study, is contrived because the location of the edge depends on snow depth for many couloirs on Lone Mountain.

The two model structures, logistic regression and classification trees, frequently return different parameters that describe the same underlying process. This is inherent in the way that the models explain relationships, either linearly or with thresholds. A good example is the depth hoar group for Lone Lake Cirque, where the upper portions of the slope have a larger presence of PTLs. Relative elevation is an obvious parameter that describes this relationship. It is easy to draw a line across the two slopes showing where this transition occurred (Fig. 41). The classification tree model does so with a split at that hypothetical line. However, the linear regression explains this relationship with profile

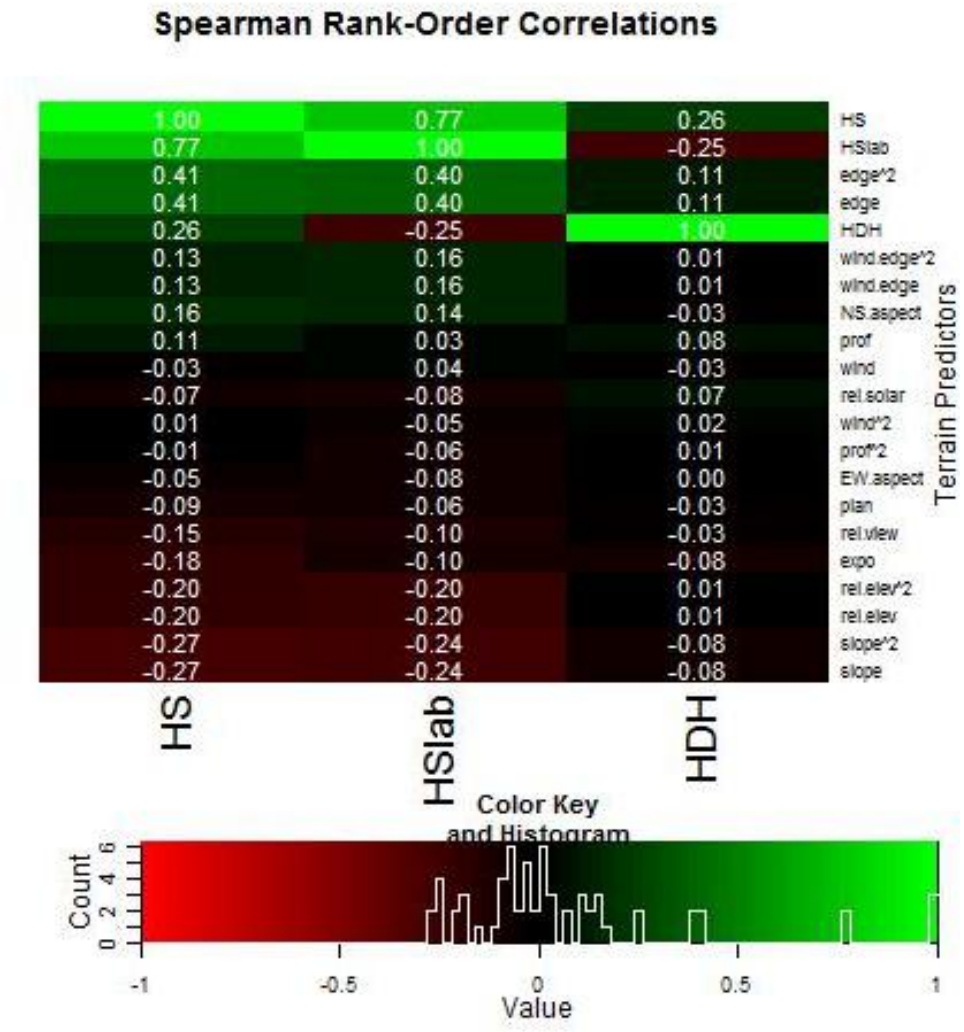

Fig. 53. Spearman rank-order correlation coefficients for the entire dataset of 21 couloirs from a sample size of 1662 measurements. All correlations greater than 0.048 or less than -0.048 are significant at a 95% confidence level.

curvature, which better describes the transition linearly (Table 18). Neither of these models is wrong. Rather, this suggests that no single "best" model is possible with statistical modeling, but there are several equally good models. We can explain the physical processes that determine the presence of PTLs using a number of parameter combinations and model structures. This agrees with the work of Birkeland (2001), who

found that different terrain parameters were selected for models of similar stability responses. "The differences between the models emphasize the underlying data complexity, and some of the difficulties that avalanche scientists face when trying to understand and predict avalanches" (Birkeland, 2001).

In general, I think that Random Forest models have advantages over logistic regression models for exploring the importance of parameters, but logistic regression models have improved modeling success. For the Random Forest model, my importance measures test the loss in predictive ability when a parameter is removed from the model. Thus, highly correlated terms that are both important, such as profile curvature and relative elevation, as described in the previous paragraph, will both be identified as important. Parameters in logistic regression are removed during the AICc reduction if they are highly correlated to other parameters with stronger relationships, and my measure of importance describes how frequently and in how good of models a parameter appears. The results can be misleading because a highly important parameter may never show up in the models if it is correlated to another parameter that describes the relationship better linearly. In the example from Lone Lake Cirque, relative elevation is completely removed from importance because profile is a better linear parameter, even though relative elevation is clearly associated with PTLs (Fig. 41). Logistic regression has several advantages such as the ability to better model linear relationships, and it predicts probabilities rather than absolute classifications.

On average, the logistic regression models have higher success rates that the Random Forest models (e.g., Table 20). There are several possible explanations: (1)

Terrain parameters associate with PTLs more often in linear form rather than thresholds. However, this is not always the case, as exemplified by Lone Lake Cirque where the Random Forest has a higher success rate using threshold relationships (Table 14). (2) I included six additional quadratic terms for logistic modeling, improving the modeling potential. (3) The model reduction techniques vary between the two models, and Random Forest models would suffer a loss of predictability if a single parameter is far superior in comparison to others because that parameter would be withheld during some of the boot-strapping iterations. (4) The success rates are calculated differently for the two model forms.

The pruned classification tree may overfit the data with very specific relationships that may not be meaningful, despite cross-validation processes aimed at refining the tree to a more robust construction. This is evident by constantly higher success rates than the more robust Random Forest model (Table 20), as well as lower nodes in the complex trees describing relationships that are not well understood. Several snow science studies have used overfit trees to describe intricate relationships in the data that are not otherwise apparent (e.g., Davis et al., 1999). This application could prove useful in discovering complex relationships between the snow and terrain for this data, but given the amount of uncertainty in data collection in this study, I interpret only the first several nodes of the pruned trees and focus on the results from the more robust models for these discussions.

Uncertainty

As with all environmental research, this study is not lacking in uncertainty, whether it be the observed input, the observed response, the model simulating the response, or the parameters.

The first major source of uncertainty is the terrain parameters derived from GIS. This includes error introduced from GPS point locations, which is described previously on page 37. LiDAR scanning also contains errors. However, root mean square errors (RMSE) typically fall below 15 cm for elevation data acquired from LiDAR (Hopkinson et al., 2009). Another source of uncertainty is resolution induced error from the one meter DEM. Parameters are measured at the resolution of one meter square grids, but the scale at which the parameter is actually influencing the snowpack may be finer. However, one meter resolution is comparable to, if not better than, what practitioners are capable of conceptualizing in the field. Another simplification is that the two wind parameters, the wind index and relative view, are based on prevailing winds averaged over the winter season, when in reality, wind patterns are much more complex.

The second major source of uncertainty is in the observed response: the snowpack measurements. Due to the challenging environment and the field methods applied, snow observations are not free of uncertainty. Snow depth measurement error was introduced when the avalanche probe was not held perfectly vertical. For *HS*, I estimate average error was less than 1 cm. Identifying the exact depth at which the moving avalanche probe punched through a slab into the depth hoar or other weak layer was often difficult. For slab thickness measurements (*HSlab*), I estimate average error was less than 2-3 cm, depending on how sharp the contrast between the slab and weak layer was. Most of the

parameters are robust to changes in slab thickness, especially on the order of several centimeters, so these errors have minimal influence on the results. The most challenging uncertainty to deal with is the presence/absence of deeply buried weak layers, which is critical for establishing the presence of a PTL. In the field, assistants and I cross-verified probing observations with repeated probe holes or hand pits when possible. Depending on the snowpack and couloir being analyzed, I estimated my certainty in identifying the presence/absence of the weak layer, which ranged from 85% to 100% (Table 2). The resolution and accuracy of probe penetration could be improved with the use of a digital snow micropenetrometer (Schneebeli and Johnson, 1998), but this would come at the cost of fewer samples, expensive instrumentation, and working with burdensome equipment in hazardous and challenging terrain.

A major source of uncertainty is the definition of a PTL for depth hoar layers. Experts do not agree on the minimum slab thickness required for a PTL, mainly because it is dependent on the strength and hardness of the slab, as well as the properties of the weak layer below it. The minimum slab criterion of 15 cm is a conservative estimate based on previous research and discussions with avalanche professionals. I address this uncertainty in the statistical analysis by allowing the minimum slab criteria to vary for both model types, and results show that most of the important parameters are robust against changes in the minimum slab criteria.

Another assumption is that the presence of a weak layer qualifies it as PTL. The probe measurements or snow surface observations do not quantify snow stability measurements typically associated with avalanche release. However, my data are simple

qualitative measures of change in snow hardness (for deep layers) or grain type (for surface layers), and both of these are closely associated with avalanche events (McCammon and Schweizer, 2002). The presence of a weak layer does not necessarily indicate instability, but I specifically use the terminology "Potential Trigger Location" because the weak layer could become unstable given the right load, and weak layers are more commonly associated with instability (Schweizer and Wiesinger, 2001).

Another source of uncertainty is the model structure and parameters. Statistical models describe processes through strict relationships, such as linear or hierarchal. It is unlikely that complex environmental processes adhere to such simple structures. I accommodate to this complexity by implementing two different model forms, but there are numerous potential models, none of which are likely to exactly replicate the true environmental process. Furthermore, the parameters used in each of the models warrant uncertainty. Models could potentially include categorical parameters, cubic parameters, two-way or three-way interactions, log-transformed parameters, or any number of increasingly complex parameters compared to the simple continuous main effects and quadratic terms used for this modeling. As described previously, I focus on the main effects for simpler interpretations and to prevent overfitting of spurious terms. Given the uncertainty in the observations, including numerous complicated terms could compound error.

In summary, uncertainty is present in this study through observed inputs and responses and the models describing them, but error and uncertainty is minimized and accounted for whenever possible. Careful cross-verification with shovel or hand pits as

well as large sample sizes guarded against erroneous field measurements. I verified that GPS recordings aligned with LiDAR data using reference points and treat the two datasets with poor GPS accuracy as outliers. I incorporated Monte-Carlo techniques to account for uncertainty in PTL slab criteria. I used two different model structures, cross-validation, multi-model averaging, boot-strapping techniques, and robust model selection techniques to optimize the validity of the statistical results. Utilizing different independent approaches that arrived at similar conclusions improved my confidence in the results.

Scope of Inference

This is an observational study of a sample of couloirs in southwest Montana and northwest Wyoming. Inferences made to larger populations of couloirs outside of the sample or different time periods are not statistically supported because the sample is not random with regard to location or time. Therefore, we can only speculate that these results can be applied to other couloirs or to other winters. However, this is the first study to show that snow weaknesses and slabs can be related to terrain parameters in this type of terrain, and it is encouraging for educated decision making in an unexplored field of snow science.

Lone Mountain has a very continental snowpack, and it is likely that weak layer patterns could vary dramatically in similar terrain for other snow climates, such as maritime or intermountain climates. The inclusion of a different snow climate, the Southern Tetons, adds a level of robustness to the results, but it is a small samples size,

and as discussed previously, data from two of the couloirs from Teton Pass contain numerous sources of error.

The scale and type of terrain should also be considered. We worked in relatively small terrain when compared to many complex avalanche chutes or couloirs around the world. Patterns observed here, and especially model coefficients or threshold values, need to be carefully considered before extrapolating them to larger or different terrain. However, given a similar snow climate and similar type of terrain, I would expect similar physical processes are associated with similar terrain parameters.

Because sampling on a single couloir disrupts the snow structure for repeated measurements, we only observed patterns in a snapshot of time when slope stability was good. The patterns of weak layers likely change throughout the season as different meteorological and metamorphic processes interact with the snowpack. Furthermore, data are from two winter seasons only. Ski patrollers have observed "sweet spots" where avalanches are commonly triggered each season, and Wirz et al. (2011) noted that snow depth distributions were similar on a steep rock face over a period of two years. Thus, we could expect to find similar patterns from year to year. However, Erickson et al. (2005) found that the significance of topographic parameters in snow depth prediction in one cirque varied over a span of seven years. Theirs is one of few studies which have studied temporal variability of snow as it relates to terrain over such an extensive time scale.

5. CONCLUSION

Summary

From a group of 21 couloirs in Montana and Wyoming, I examined the importance of terrain parameters as they relate to potential trigger locations (PTLs) of slab avalanches with exploratory analysis and robust classification tree and logistic modeling techniques.

The widely varying results from the individual couloir models demonstrate how complex and variable the influence of terrain parameters are on the presence of weak layers, slabs, and PTLs. There is a clear message from poor cross validation results from couloir to couloir: terrain interacts with the snowpack differently in each couloir, making extrapolating results from one couloir to other couloirs challenging and potentially misleading. This is true even for some closely-spaced couloirs. This does not imply that terrain patterns cannot be used to predict PTLs, but that specific thresholds and relationships from one slope are unlikely to fit well for other slopes. Rather, a more general understanding of how each slope-scale terrain parameter interacts with the snowpack under varying climatic and larger scale terrain inputs enables educated decision making. Results support that more general interactions between terrain and PTLs enable predictive success for couloirs in the same headwall or cirque, but to a lesser degree.

For these data, which were collected in steep alpine terrain, parameters relating to the physical processes of wind deposition and scouring appear to be most influential in modeling. Distance from the edge of a couloir, relative elevation in the couloir, the

degree of wind sheltering, and the degree of exposure of the terrain are the most important parameters associated with PTLs by a number of modeling standards. Other parameters are likely to be equally or more important for different topography or different snow climates, such as slope angle and solar radiation. The specific influences from these slope-scale parameters vary depending on the characteristics of the cirque or region, prior weather patterns, and seasonal trends. However, the results of this study show that the presence or absence of PTLs can be strongly associated with these parameters, with model success rates frequently reaching 80% for near surface layers and 70% for depth hoar layers. The practical implications of these findings are that the distribution of PTLs in a couloir is likely to vary depending on the influence of the above parameters, so careful consideration needs to be given when assessing the stability from a single point observation or before extrapolating the results from one couloir to the next.

Because of the high spatial variability of PTLs in complex terrain, the best strategy to successfully manage or evaluate a steep couloir requires:

(1) A complete understanding of how the larger scale terrain and meteorological conditions interact with the slope (e.g., prevailing wind and snow patterns, wind anomalies, suspect weak layers, general snowpack conditions and history).

(2) Expert intuition incorporating an understanding of how these and other important slope-scale terrain parameters interact with the snowpack for careful route selection or pit or explosive placement.

(3) A holistic approach, incorporating all possible information including current meteorological conditions, recent avalanche activity, and other signs of instability.

Future Work

The success of this study in finding meaningful relationships between terrain and potential trigger locations in such highly variable and complex terrain is encouraging for future modeling and understanding of the physical processes involved with the snowpack development and avalanche formation. Numerous possibilities exist for future work. A larger sample of couloirs from more diverse snow climates, a more diverse collection of weak layers, and data collection at different terrain scales would all expand our understanding of the system. Sampling strategies designed to allow for repeated sampling through one season would improve our understanding of how the snowpack develops over the course of a winter. Repeated sampling over numerous seasons could characterize how the influences of terrain change from year to year. Cross-validating the modeling results from these couloirs to the same couloirs but in different winters would provide interesting insights on how consistent the terrain effects are annually.

In addition to improved sampling strategies, more quantifiable techniques could increase the usefulness of future studies. Higher resolution probing methods, such as the snow micropenetrometer (Schneebeli and Johnson, 1998), more quantifiable tests relating directly to instability, such as the ECT (Simenhois and Birkeland, 2009), or more exhaustive coverage of weak layers, such as with FMCW radar (Marshall and Koh, 2008) could decrease the uncertainty of these results. Redesigning inadequate terrain parameters, such as relative viewshed, or including the same terrain parameters but at varying scales, as done by Winstral et al. (2002), could improve our ability to describe more processes at different scales. A more complex statistical model, which

incorporates hierarchal and linear relationships at different scales from slope to mountain range, could be designed for predictive purposes. Future modeling efforts could also include meteorological conditions. This research provides solid progress toward understanding the complex processes occurring in steep avalanche terrain, improving our understanding of the relationship between terrain and optimal locations for snowpits or explosive placements. This, in turn, has the potential to improve safety in complex avalanche terrain for both recreationists and avalanche professionals.

REFERENCES CITED

R Development Core Team, 2009. R: A language and environment for statistical computing. R Foundation for Statistical Computing, Vienna, Austria. ISBN: 3-900051.

Akitaya, E., 1974. Studies on Depth Hoar. Contributions from the Institute of Low Temperature Science. 26, 1-67.

Allouche, O., Tsoar, A., Kadmon, R., 2006. Assessing the accuracy of species distribution models: prevalence, kappa and the true skill statistic (TSS). Journal of Applied Ecology. 43(6), 1223-1232.

Armstrong, R.L., 1985. Metamorphism in a subfreezing, seasonal snow cover: The role of thermal and water vapor pressure conditions. PhD dissertation. Department of Geography, University of Colorado, Boulder, CO, USA, 175 pp.

Arons, E.M., Colbeck, S.C., Gray, J., 1998. Depth-hoar growth rates near a rocky outcrop. Journal of Glaciology. 44(148), 477-484.

avalanche.org, 2011. U.S. Avalanche Accidents Reports. Retrieved October 19, 2011. http://avalanche.org/accidents.php

Beven, K., Freer, J., 2001. Equifinality, data assimilation, and uncertainty estimation in mechanistic modelling of complex environmental systems using the GLUE methodology. Journal of Hydrology. 249(1-4), 11-29.

Birkeland, K., 1998. Terminology and predominant processes associated with the formation of weak layers of near-surface faceted crystals in the mountain snowpack. Arctic and Alpine Research. 30, 193-199.

Birkeland, K., 2001. Spatial patterns of snow stability throughout a small mountain range. Journal of Glaciology. 47(157), 176-186.

Birkeland, K.W., Chabot, D., 2006. Minimizing "false stable" stability test results: Why digging more snowpits is a good idea. Proceedings of the 2006 International Snow Science Workshop, Telluride, CO, USA, pp. 498–504.

Birkeland, K.W., Hansen, K.J., Brown, R.L., 1995. The spatial variability of snow resistance on potential avalanche slopes. Journal of Glaciology. 41(137), 183-190.

Birkeland, K.W., Hendrikx, J., Clark, M.P., 2010. On optimal stability-test spacing for assessing snow avalanche conditions. Journal of Glaciology. 56(199), 795-804.

Blöschl, G., Kirnbauer, R., Gutknecht, D., 1991. Distributed snowmelt simulations in an alpine catchment: 1. Model evaluation on the basis of snow cover patterns. Water Resources Research. 27(12), 3171-3179.

Bradley, C., Brown, R., Williams, T., 1977. On depth hoar and the strength of snow. Journal of Glaciology. 18(78), 145-147.

Breiman, L., 2001. Random forests. Machine Learning. 45(1), 5-32.

Breiman, L., Friedman, J.H., Olshen, R.A., Stone, C.J., 1993. Classification and Regression Trees. Chapman and Hall, New York, NY, USA.

Burnham, K.P., Anderson, D.R., 2002. Model selection and multimodel inference: a practical information-theoretic approach, second ed. Springer-Verlag, New York, NY, USA.

Calcagno, V., 2011. glmulti: GLM model selection and multimodel inference made easy. http://CRAN.R-project.org/package=glmulti

Calcagno, V., de Mazancourt, C., 2010. glmulti: An R Package for Easy Automated Model Selection with (Generalized) Linear Models. Journal of Statistical Software. 34 (12).

Campbell, C., Jamieson, B., 2007. Spatial variability of slab stability and fracture characteristics within avalanche start zones. Cold Regions Science and Technology. 47(1-2), 134-147.

Carstensen, B., Plummer, M., Laara, E., Hills, M., 2010. Package 'Epi': A package for statistical analysis in epidemiology. http://www.pubhealth.ku.dk/~bxc/Epi/

Colbeck, S., 1988. On the micrometeorology of surface hoar growth on snow in mountainous area. Boundary-Layer Meteorology. 44(1), 1-12.

Colbeck, S., 1991. The layered character of snow covers. Reviews of Geophysics. 29(1), 81-96.

Colbeck, S., 1998. Sintering in a dry snow cover. Journal of Applied Physics. 84(8), 4585-4589.

Colbeck, S.C., Jamieson, J.B., 2001. The formation of faceted layers above crusts. Cold Regions Science and Technology. 33(2-3), 247-252.

Comey, B., 2010. Season Roundup 2009/10: Bridger-Teton National Forest Avalanche Center, The Avalanche Review. 29(1), 21-22.

Conway, H., Abrahamson, J., 1984. Snow Stability Index. Journal of Glaciology. 30(106), 321-327.

Cooperstein, M.S., 2008. The effects of slope aspect on the formation of surface hoar and diurnally recrystallized near-surface faceted crystals. M.S. Thesis. Department of Earth Sciences, Montana State University, Bozeman, MT, USA, 169 pp.

Dalgaard, P., 2008. Introductory statistics with R, second ed. Springer-Verlag, New York, NY, USA.

Davis, R.E., Elder, K., Howlett, D., Bouzaglou, E., 1999. Relating storm and weather factors to dry slab avalanche activity at Alta, Utah, and Mammoth Mountain, California, using classification and regression trees. Cold Regions Science and Technology, 30(1-3), 79-89.

Davison, A.C., 2003. Statistical models. Cambridge University Press, Cambridge, England.

Deems, J., 2002. Topographic effects on the spatial and temporal patterns of snow temperature gradients in a mountain snowpack. M.S. Thesis. Department of Earth Sciences, Montana State University, Bozeman, MT, USA, 85 pp.

Dexter, L.R., 1986. Aspect and elevation effects on the structure of the seasonal snowcover in Colorado. PhD Dissertation. Department of Geography, University of Colorado, Boulder, CO, USA, 228 pp.

Elder, K., Rosenthal, W., Davis, R.E., 1998. Estimating the spatial distribution of snow water equivalence in a montane watershed. Hydrological Processes. 12(1011), 1793-1808.

Erickson, T.A., Williams, M.W., Winstral, A., 2005. Persistence of topographic controls on the spatial distribution of snow in rugged mountain terrain, Colorado, United States. Water Resources Research. 41(4), 1-17.

ESRI, 2009a. ArcGIS Desktop Help: Calculating solar radiation. ArcGIS Desktop Release 9.3, Environmental Systems Research Institute, Redlands, CA, USA.

ESRI, 2009b. ArcGIS Desktop Release 9.3, Environmental Systems Research Institute, Redlands, CA, USA.

ESRI, 2009c. Geographic (datum) transformations, parameters and areas of use. ArcGIS Desktop Release 9.3, Environmental Systems Research Institute, Redlands, CA, USA.

Feick, S., Kronholm, K., Schweizer, J., 2007. Field observations on spatial variability of surface hoar at the basin scale. Journal of Geophysical Research. 112(F2), F02002.

Fukuzawa, T., Akitaya, E., 1993. Depth-hoar crystal growth in the surface layer under high temperature gradient. Annals of Glaciology. 18, 39-45.

Föhn, P.M.B., 1988. Snow cover stability tests and the areal variability of snow strength. Proceedings of the 1988 International Snow Science Workshop, Whistler, BC, Canada, pp. 262-273.

Giddings, J.C., LaChapelle, E., 1962. The formation rate of depth hoar. Journal of Geophysical Research. 67(6), 2377-2383.

Gleason, J.A., 1996. Terrain parameters of avalanche starting zones and their effect on avalanche frequency. M.S. Thesis. Department of Earth Sciences, Montana State University, Bozeman, MT, USA, 64 pp.

Greene, E., Atkins, D., Birkeland, K., Elder, K., Landry, C., Lazar, B., McCammon, I., Moore, M., Sharaf, D., Sterbenz, C., Tremper, B., Williams, K., 2009. Snow, weather, and avalanches: observational guidelines for avalanche programs in the United States, second ed. The American Avalanche Association, Pagosa Springs, CO, USA.

Guy, Z.M., Birkeland, K.W., 2010. Spatial variability in steep couloirs: weak layer variation with respect to wind direction. Proceedings of the 2010 International Snow Science Workshop, Squaw Valley, CA, USA, pp. 88-94.

Hachikubo, A., Akitaya, E., 1997. Effect of wind on surface hoar growth on snow. Journal of Geophysical Research. 102(D4), 4367–4373.

Hageli, P., McClung, D.M., 2004. Hierarchy theory as a conceptual framework for scale issues in avalanche forecast modeling. Annals of Glaciology. 38(1), 209-214.

Harper, J.T., Bradford, J.H., 2003. Snow stratigraphy over a uniform depositional surface: spatial variability and measurement tools. Cold Regions Science and Technology. 37(3), 289-298.

Hendrikx, J., Birkeland, K., Clark, M., 2009. Assessing changes in the spatial variability of the snowpack fracture propagation propensity over time. Cold Regions Science and Technology. 56(2-3), 152-160.

Hendrikx, J., Owens, I., Carran, W., Carran, A., 2005. Avalanche activity in an extreme maritime climate: The application of classification trees for forecasting. Cold Regions Science and Technology. 43(1-2), 104-116.

Hoechstetter, S., Walz, U., Dang, L., Thinh, N., 2008. Effects of topography and surface roughness in analysis of landscape structure–A proposal to modify the existing set of landscape metrics. Landscape Online. 1, 1-14.

Hopkinson, C., Hayashi, M., Peddle, D., 2009. Comparing alpine watershed attributes from LiDAR, photogrammetric, and contour based digital elevation models. Hydrological Processes. 23(3), 451-463.

Hosmer, D.W., Hosmer, T., Le Cessie, S., Lemeshow, S., 1997. A comparison of goodness-of-fit tests for the logistic regression model. Statistics in Medicine. 16(9), 965-980.

Hosmer, D.W., Lemeshow, S., 2000. Applied logistic regression, second ed. John Wiley and Sons, New York, NY, USA.

Jamieson, B., Langevin, P., 2004. Faceting above crusts and associated slab avalanching in the Columbia Mountains. Proceedings of the 2004 International Snow Science Workshop, Jackson Hole, WY, USA, pp. 112-120.

Jamieson, J., Johnston, C., 1992. Snowpack characteristics associated with avalanche accidents. Canadian Geotechnical Journal. 29(5), 862-866.

Jamieson, J.B., 1995. Avalanche prediction for persistent snow slabs. PhD dissertation. Department of Civil Engineering, University of Calgary, Calgary, AB, Canada, 258 pp.

Jamieson, J.B., Johnston, C.D., 1993. Rutschblock precision, technique variations and limitations. Journal of Glaciology. 39(133), 666-674.

Janssen, V., 2009. Understanding coordinate reference systems, datums and transformations. International Journal of Geoinformatics. 5(4), 41-53.

Kozak, M.C., 2002. The spatial and temporal variability of snow layer hardness. M.S. Thesis. Department of Watershed Science, Colorado State University, Fort Collins, CO, USA. 162 pp.

Kronholm, K., Birkeland, K.W., 2007. Reliability of sampling designs for spatial snow surveys. Computers and Geosciences. 33(9), 1097-1110.

Kronholm, K., Schneebeli, M., Schweizer, J., 2004. Spatial variability of micropenetration resistance in snow layers on a small slope. Annals of Glaciology. 38(1), 202-208.

Kronholm, K., Schweizer, J., 2003. Snow stability variation on small slopes. Cold Regions Science and Technology. 37(3), 453-465.

Landry, C., Birkeland, K., Hansen, K., Borkowski, J., Brown, R., Aspinall, R., 2004. Variations in snow strength and stability on uniform slopes. Cold Regions Science and Technology. 39(2-3), 205-218.

Lang, R., Leo, B., Brown, R., 1984. Observations on the growth process and strength characteristics of surface hoar. Proceedings of the 1984 Snow Science Workshop, Aspen, CO, USA, pp. 188–195.

Liaw, A., Wiener, M., 2002. Classification and regression by randomForest. R News. 2(3), 18-22.

Logan, S., Birkeland, K., Kronholm, K., Hansen, K., 2007. Temporal changes in the slope-scale spatial variability of the shear strength of buried surface hoar layers. Cold Regions Science and Technology. 47(1-2), 148-158.

Lutz, E.R., Birkeland, K.W., 2011. Spatial patterns of surface hoar properties and incoming radiation on an inclined forest opening. Journal of Glaciology. 57(202), 355-366.

Maggioni, M., Gruber, U., 2003. The influence of topographic parameters on avalanche release dimension and frequency. Cold Regions Science and Technology. 37(3), 407-419.

Marienthal, A., Mancey, J., Guy, Z., Rains, F., Schwab, D., 2010. Snow avalanche research and forecasting with GIS and geospatial sciences. Proceedings of the 2010 International Snow Science Workshop, Squaw Valley, CA, USA, pp. 687-692.

Marshall, H.P., Koh, G., 2008. FMCW radars for snow research. Cold Regions Science and Technology. 52(2), 118-131.

Massey, F.R., Jr., 1951. The Kolmogorov-Smirnov test for goodness of fit. Journal of the American Statistical Association. 46(253), 68-78.

McCammon, I., Schweizer, J., 2002. A field method for identifying structural weaknesses in the snowpack, Proceedings of the 2002 International Snow Science Workshop, Penticton, BC, Canada, pp. 477-481.

McClung, D., 2003. Magnitude and frequency of avalanches in relation to terrain and forest cover. Arctic, Antarctic, and Alpine Research. 35(1), 82-90.

McClung, D., Schaerer, P., 2006. The avalanche handbook, third ed. The Mountaineers Books, Seattle, WA, USA.

McCollister, C.M., Comey, R.H., 2009. Using LiDAR (Light Distancing And Ranging) data to more accurately describe avalanche terrain. Proceedings of the 2009 International Snow Science Workshop, Davos, Switzerland, pp. 463-467.

Mock, C.J., Birkeland, K.W., 2000. Snow avalanche climatology of the western United States mountain ranges. Bulletin of the American Meteorological Society. 81(10), 2367-2392.

Morstad, B., Adams, E., McKittrick, L., 2007. Experimental and analytical study of radiation-recrystallized near-surface facets in snow. Cold Regions Science and Technology. 47(1-2), 90-101.

Ramsey, F.L., Schafer, D.W., 1997. The statistical sleuth: a course in methods of data analysis, second ed. Brooks/Cole, Belmont, CA, USA.

Savage, S., 2006. Deep slab avalanche hazard forecasting and mitigation: South Face at Big Sky Ski Area. Proceedings of the 2006 International Snow Science Workshop, Telluride, CO, USA, pp. 483-490.

Savage, S., 2010. Anatomy of a post control release: the Liberty Bowl event at Big Sky Resort. Proceedings of the 2010 International Snow Science Workshop, Squaw Valley, CA, USA, pp. 340-347.

Schaerer, P.A., 1977. Analysis of snow avalanche terrain. Canadian Geotechnical Journal. 14(3), 281-287.

Schmid, U.G., Sardemann, S., 2003. High-frequency avalanches: release area characteristics and run-out distances. Cold Regions Science and Technology. 37(3), 439-451.

Schneebeli, M., Johnson, J., 1998. A constant-speed penetrometer for high-resolution snow stratigraphy. Annals of Glaciology. 26, 107-111.

Schweizer, J., 1993. The influence of the layered character of snow cover on the triggering of slab avalanches. Annals of Glaciology. 18, 193-193.

Schweizer, J., 1999. Review of dry snow slab avalanche release. Cold Regions Science and Technology. 30(1-3), 43-57.

Schweizer, J., Jamieson, J.B., 2001. Snow cover properties for skier triggering of avalanches, Cold Regions Science and Technology. 33(2-3), 207-221.

Schweizer, J., Jamieson, J.B., Schneebeli, M., 2003. Snow avalanche formation. Reviews of Geophysics. 41(4), 1016.

Schweizer, J., Kronholm, K., 2007. Snow cover spatial variability at multiple scales: Characteristics of a layer of buried surface hoar. Cold Regions Science and Technology. 47(3), 207-223.

Schweizer, J., Kronholm, K., Jamieson, J.B., Birkeland, K.W., 2008. Review of spatial variability of snowpack properties and its importance for avalanche formation, Cold Regions Science and Technology. 51 (2-3), 253-272.

Schweizer, J., Lütschg, M., 2001. Characteristics of human-triggered avalanches. Cold Regions Science and Technology. 33(2-3), 147-162.

Schweizer, J., Wiesinger, T., 2001. Snow profile interpretation for stability evaluation. Cold Regions Science and Technology. 33(2-3), 179-188.

Shea, C., Jamieson, B., 2010. Spatial distribution of surface hoar crystals in sparse forests. Natural Hazards and Earth Systems Science. 10(6), 1317-1330.

Simenhois, R., Birkeland, K., 2006. The extended column test: A field test for fracture initiation and propagation. Proceedings of the 2006 International Snow Science Workshop, Telluride, CO, USA, pp. 79-85.

Simenhois, R., Birkeland, K.W., 2009. The extended column test: test effectiveness, spatial variability, and comparison with the propagation saw test. Cold Regions Science and Technology. 59(2-3), 210-216.

Slaughter, A.E., 2010. Numerical analysis of conditions necessary for near-surface snow metamorphism. PhD Dissertation. Department of Civil Engineering, Montana State University, Bozeman, MT, USA, 562 pp.

Slaughter, A.E., Adams, E.E., Staron, P.J., Shertzer, R.H., Walters, D.J., Munter, H., 2011. Field investigation of near-surface metamorphism of snow. Journal of Glaciology. 57(203), 441-452.

Staples, M., 2010. Season Roundup 2009/10, Gallatin National Forest Avalanche Center. The Avalanche Review. 29(1), 24-25.

Staples, M., 2011. 2010/11 Season Summary: United States, Gallatin National Forest Avalanche Center. The Avalanche Review. 30(1), 26-27.

Stewart, K., Jamieson, J., 2002. Spatial variability of slab stability in avalanche start zones. Proceedings of the 2002 International Snow Science Workshop, Penticton, BC, Canada, pp. 544-548.

Sturm, M., Benson, C., 2004. Scales of spatial heterogeneity for perennial and seasonal snow layers. Annals of Glaciology. 38(1), 253-260.

Sturm, M., Benson, C., 1997. Vapor transport, grain growth and depth-hoar development in the subarctic snow. Journal of Glaciology. 43(143), 42-59.

Therneau, T., Atkinson, B., 2010. mvpart: Multivariate partitioning, http://CRAN.R-project.org/package=mvpart

Trimble, 2008. TerraSync software and GPS Pathfinder Office software training guide. Trimble Navigation Limited, Westminster, CO, USA.

Voight, B., Armstrong, B., Armstrong, R., Bachman, D., Bowles, D., Brown, R., Faisant, R., Ferguson, S., Fredston, J., Kennedy, J., 1990. Snow avalanche hazards and mitigation in the United States. National Academy Press, Washington, DC, USA.

Warnes, G.R., 2009. gplots: Various R programming tools for plotting data, http://CRAN.R-project.org/package=gplots

Winstral, A., Elder, K., Davis, R.E., 2002. Spatial snow modeling of wind-redistributed snow using terrain-based parameters. Journal of Hydrometeorology. 3(5), 524-538.

Wirz, V., Schirmer, M., Gruber, S., Lehning, M., 2011. Spatio-temporal measurements and analysis of snow depth in a rock face. The Cryosphere Discussions. 5(3), 1383-1418.

Zar, J.H., 1972. Significance testing of the Spearman rank correlation coefficient. Journal of the American Statistical Association. 67(339), 578-580.

APPENDICES

APPENDIX A

PTLS MAPPED ON SHADED RELIEF

Depth Hoar PTLs

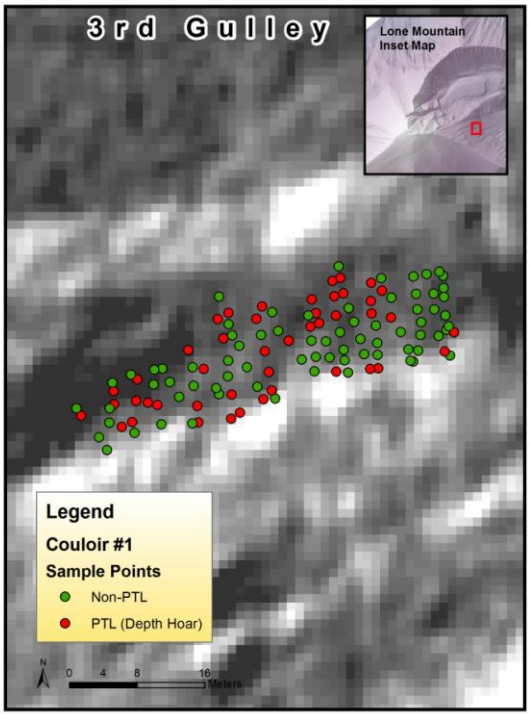

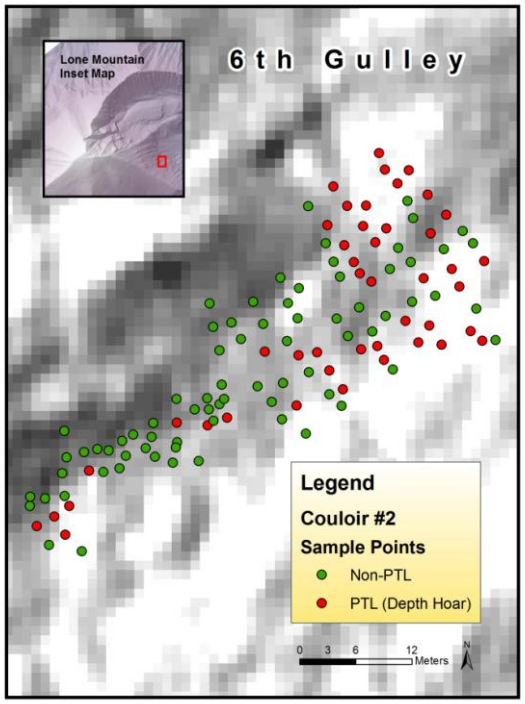

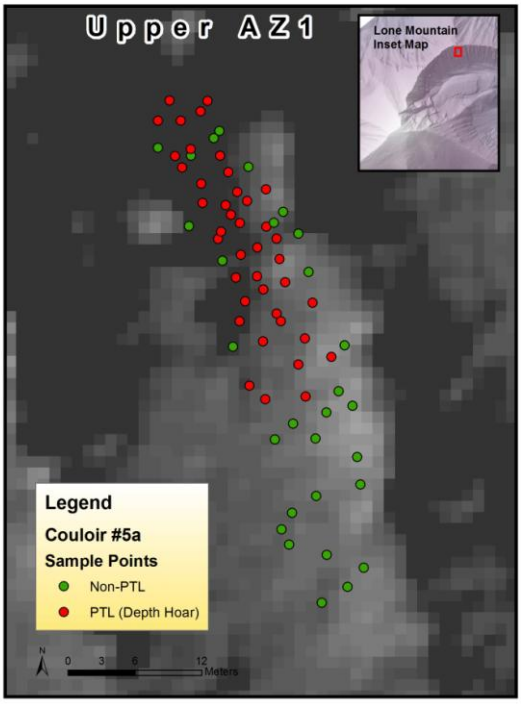

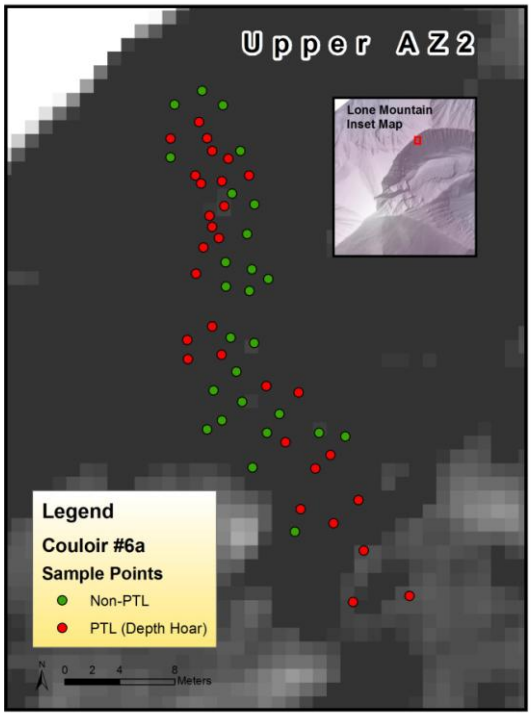

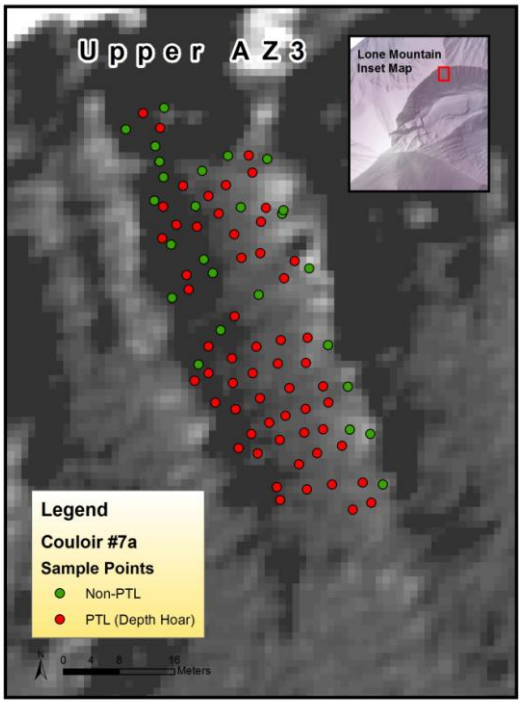
Upper AZ3
Lone Mountain Inset Map
Legend
Couloir #7a
Sample Points
Non-PTL
PTL (Depth Hoar)
0 4 8 16
Meters

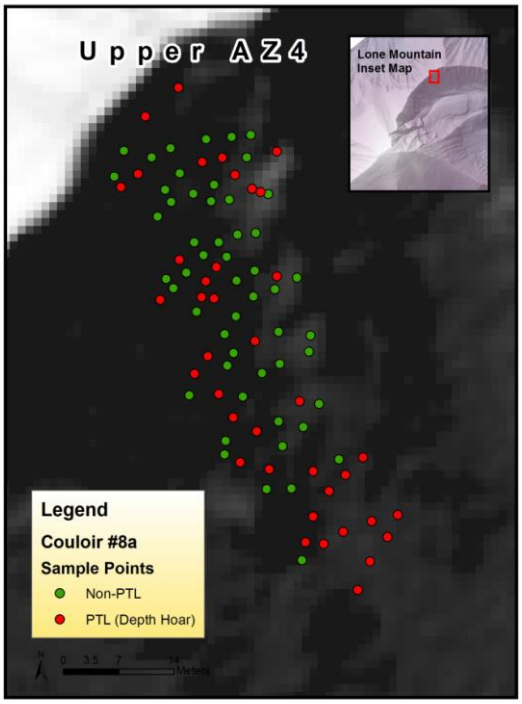
Upper AZ4
Lone Mountain Inset Map
Legend
Couloir #8a
Sample Points
Non-PTL
PTL (Depth Hoar)
0 3.5 7
Meters

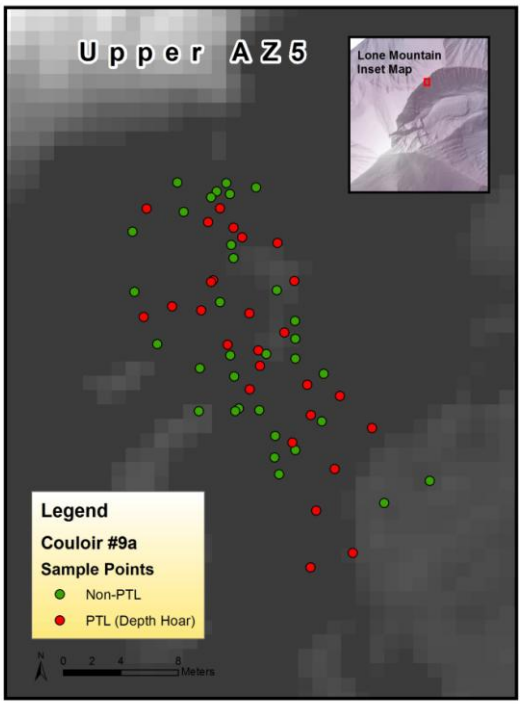
Upper AZ5
Lone Mountain Inset Map
Legend
Couloir #9a
Sample Points
Non-PTL
PTL (Depth Hoar)
0 2 4 8
Meters

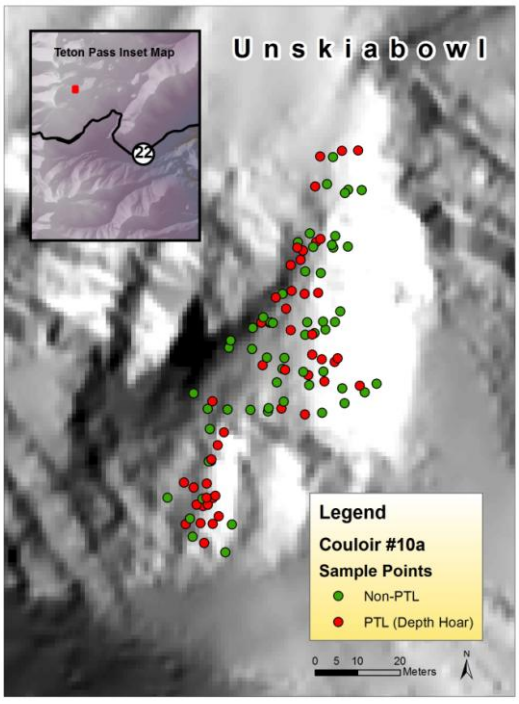
Unskiabowl
Teton Pass Inset Map
22
Legend
Couloir #10a
Sample Points
Non-PTL
PTL (Depth Hoar)
0 5 10 20
Meters
N

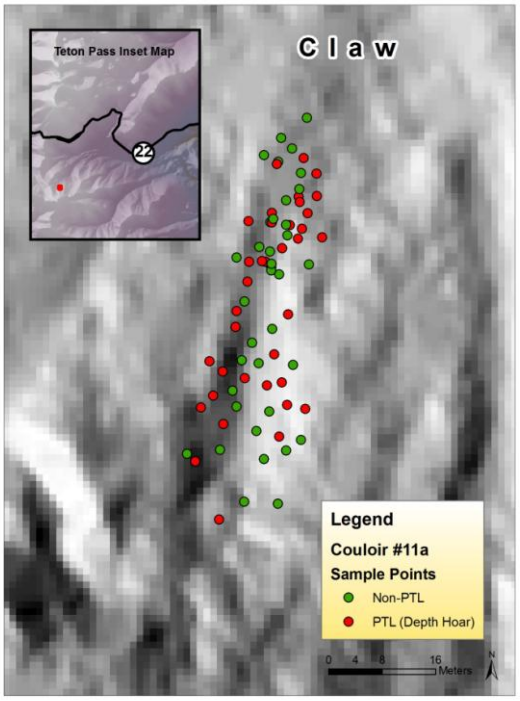
Claw
Teton Pass Inset Map
22
Legend
Couloir #11a
Sample Points
Non-PTL
PTL (Depth Hoar)
0 4 8 16
Meters
N

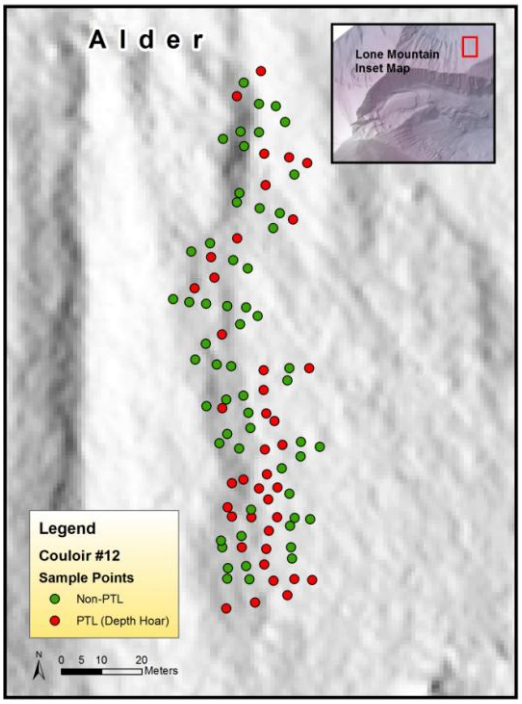
Alder
Lone Mountain
Inset Map
Legend
Couloir #12
Sample Points
Non-PTL
PTL (Depth Hoar)
N
0 5 10 20
Meters

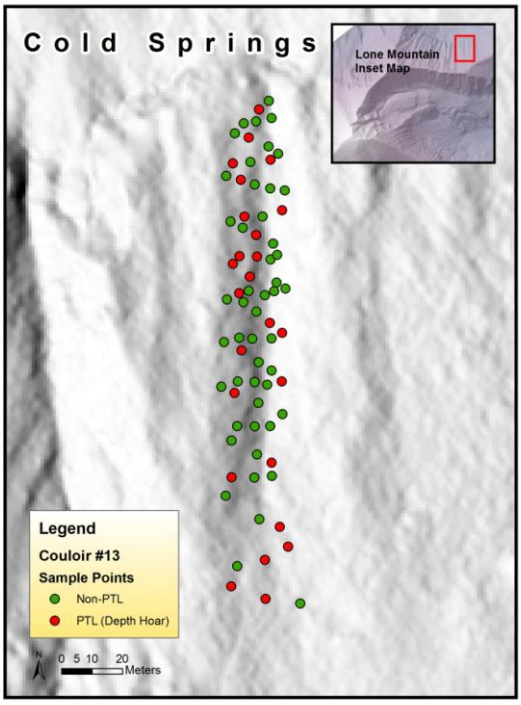
Cold Springs
Lone Mountain
Inset Map
Legend
Couloir #13
Sample Points
Non-PTL
PTL (Depth Hoar)
N
0 5 10 20
Meters

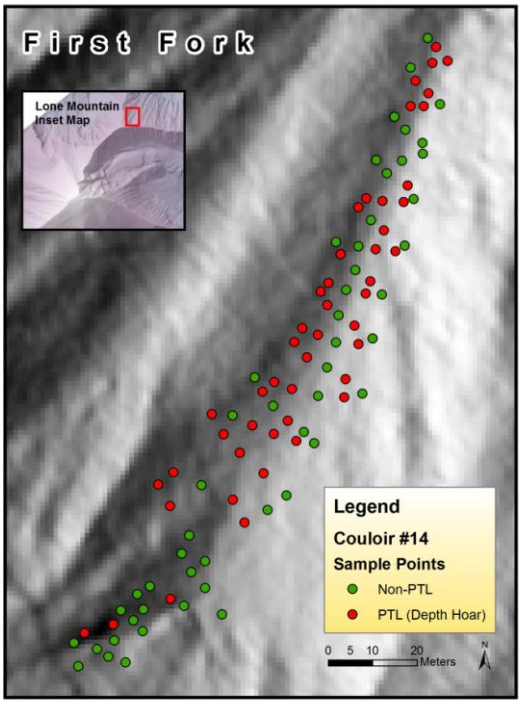
First Fork
Lone Mountain
Inset Map
Legend
Couloir #14
Sample Points
Non-PTL
PTL (Depth Hoar)
0 5 10 20
Meters
N

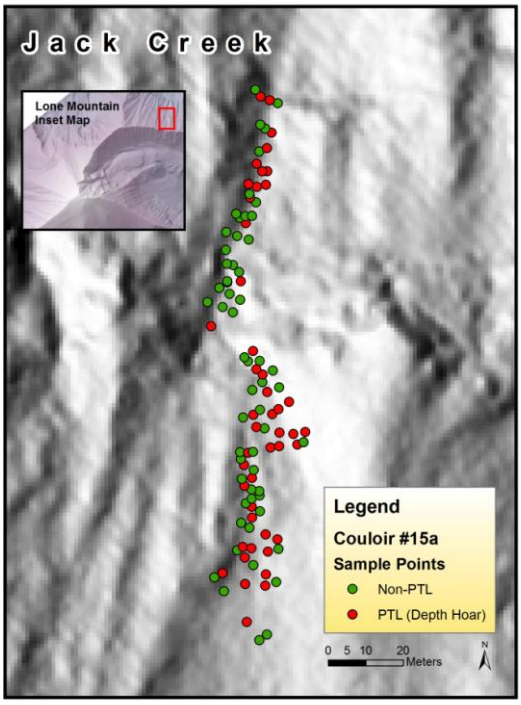
Jack Creek
Lone Mountain Inset Map
Legend
Couloir #15a
Sample Points
Non-PTL
PTL (Depth Hoar)
0 5 10 20
Meters
N

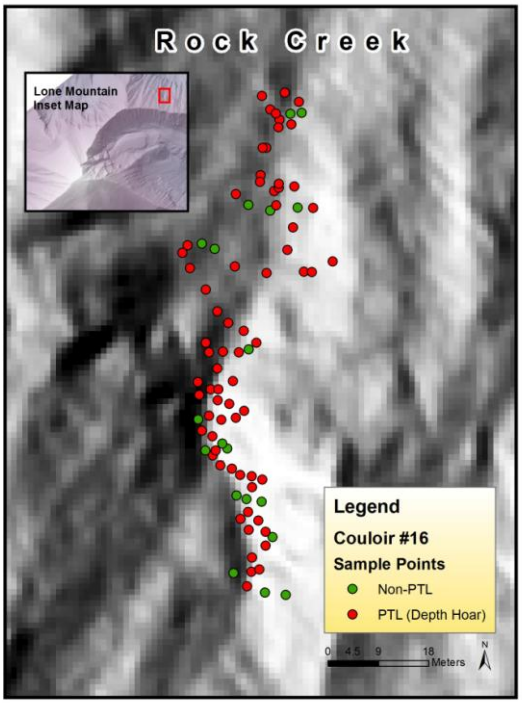
Rock Creek
Lone Mountain Inset Map
Legend
Couloir #16
Sample Points
Non-PTL
PTL (Depth Hoar)
0 4.5 9 18
Meters
N

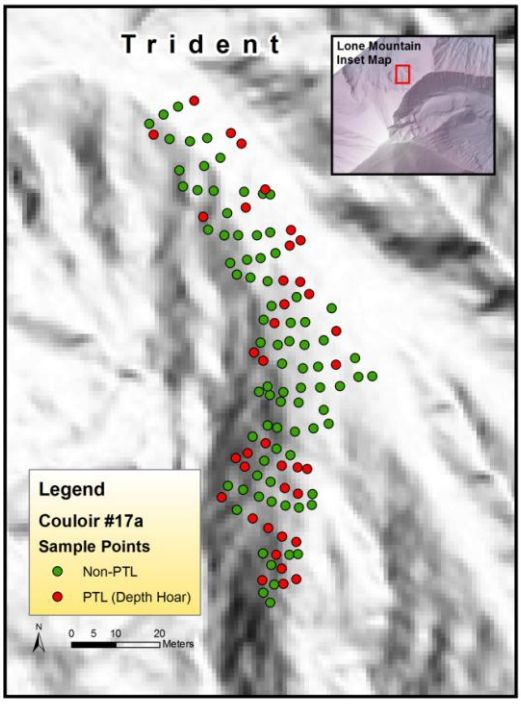
Trident
Lone Mountain Inset Map
Legend
Couloir #17a
Sample Points
Non-PTL
PTL (Depth Hoar)
N
0 5 10 20
Meters

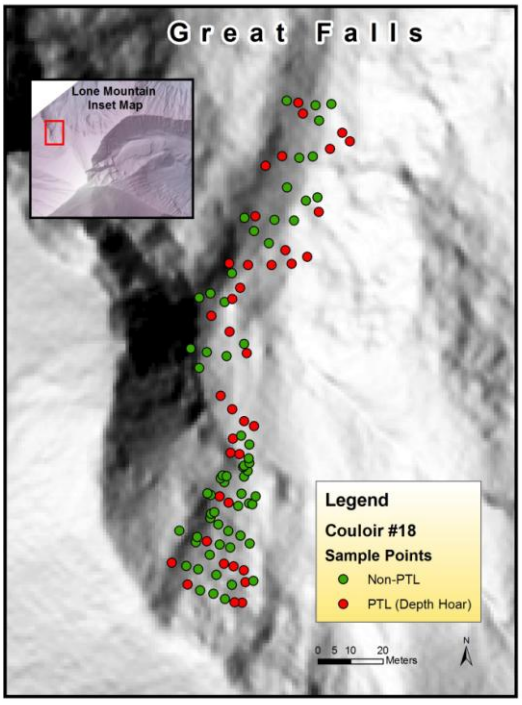
Great Falls
Lone Mountain Inset Map
Legend
Couloir #18
Sample Points
Non-PTL
PTL (Depth Hoar)
0 5 10 20
Meters
N

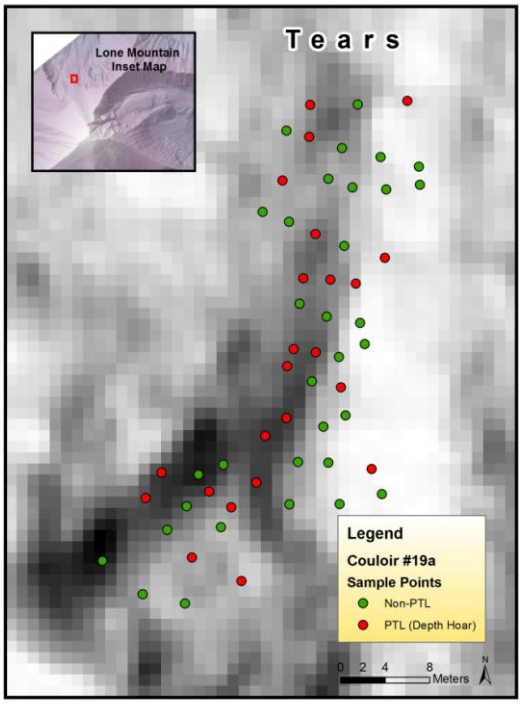
Tears
Lone Mountain
Inset Map
Legend
Couloir #19a
Sample Points
Non-PTL
PTL (Depth Hoar)
0 2 4 8
Meters
N

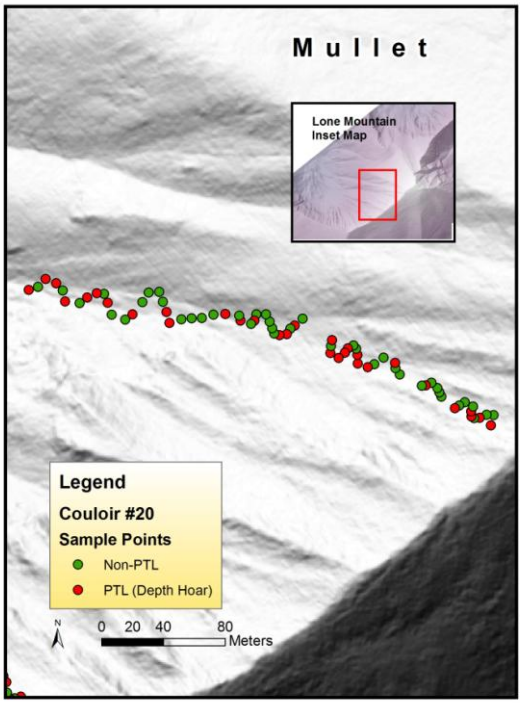
Mullet
Lone Mountain
Inset Map
Legend
Couloir #20
Sample Points
Non-PTL
PTL (Depth Hoar)
N
0 20 40 80
Meters

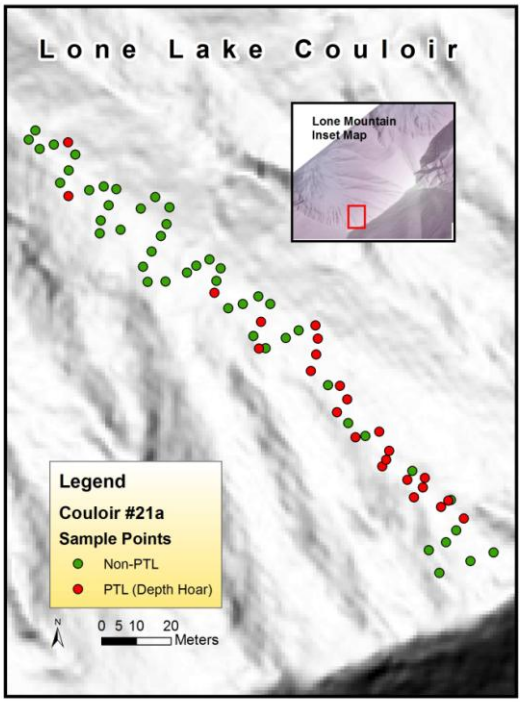
Lone Lake Couloir
Lone Mountain
Inset Map
Legend
Couloir #21a
Sample Points
Non-PTL
PTL (Depth Hoar)
N
0 5 10 20
Meters

Facet PTLs

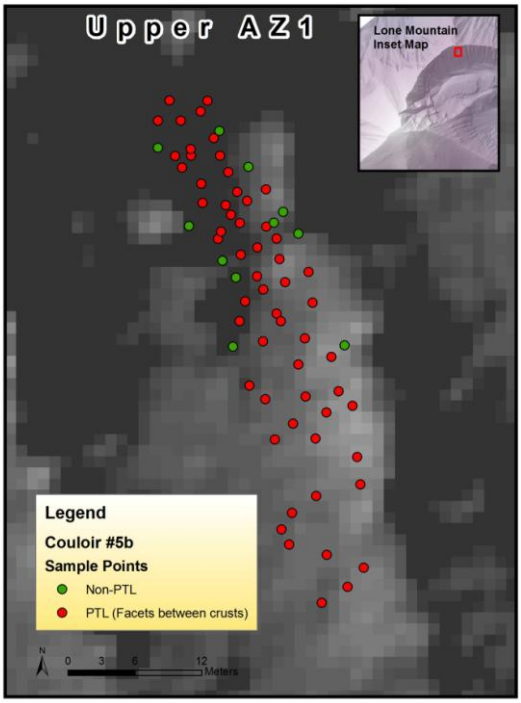
Upper AZ1
Lone Mountain
Inset Map
Legend
Couloir #5b
Sample Points
Non-PTL
PTL (Facets between crusts)
0 3 6 12
Meters

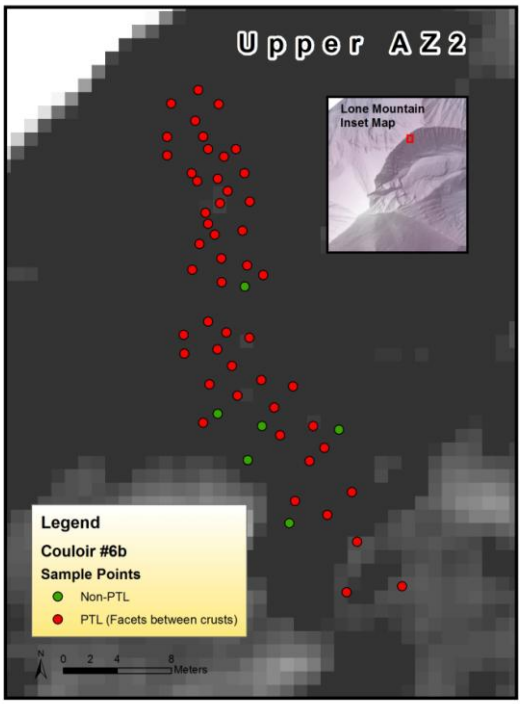
Upper AZ2
Lone Mountain
Inset Map
Legend
Couloir #6b
Sample Points
Non-PTL
PTL (Facets between crusts)
0 2 4 8
Meters

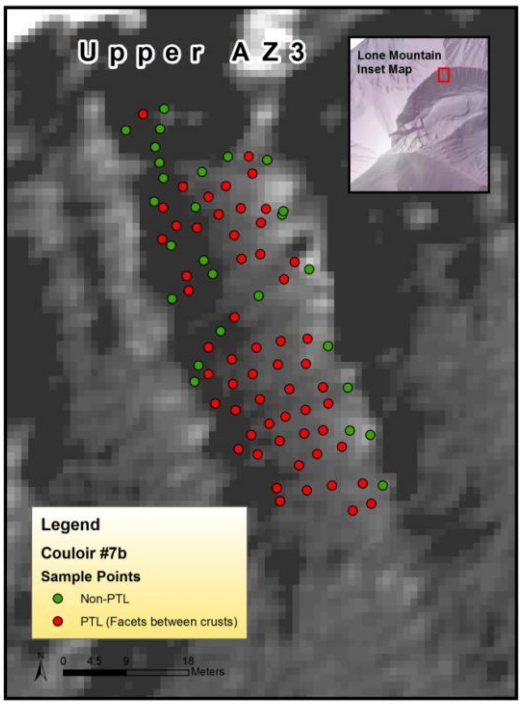
Upper AZ3
Lone Mountain
Inset Map
Legend
Couloir #7b
Sample Points
Non-PTL
PTL (Facets between crusts)
0 4.5 9 18
Meters

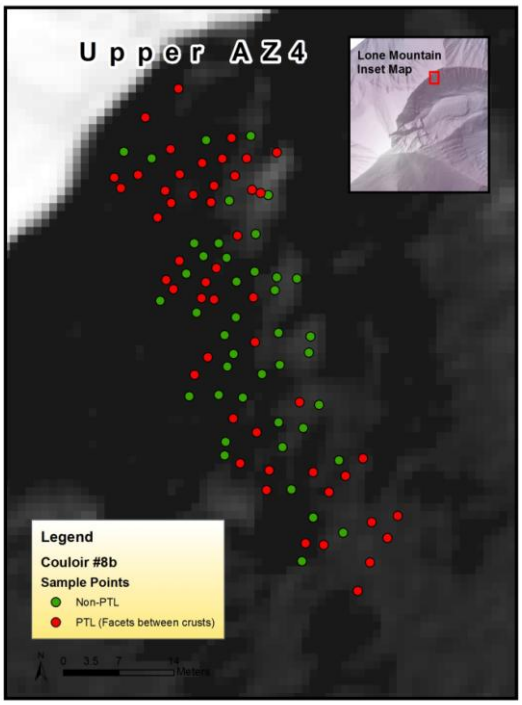
Upper AZ4
Lone Mountain
Inset Map
Legend
Couloir #8b
Sample Points
Non-PTL
PTL (Facets between crusts)
0 3.5 7
Meters

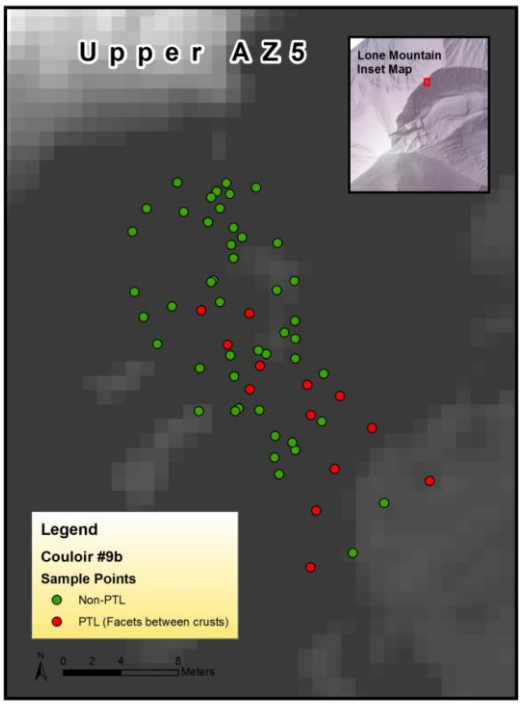
Upper AZ5
Lone Mountain Inset Map
Legend
Couloir #9b
Sample Points
Non-PTL
PTL (Facets between crusts)
0 2 4 8 Meters

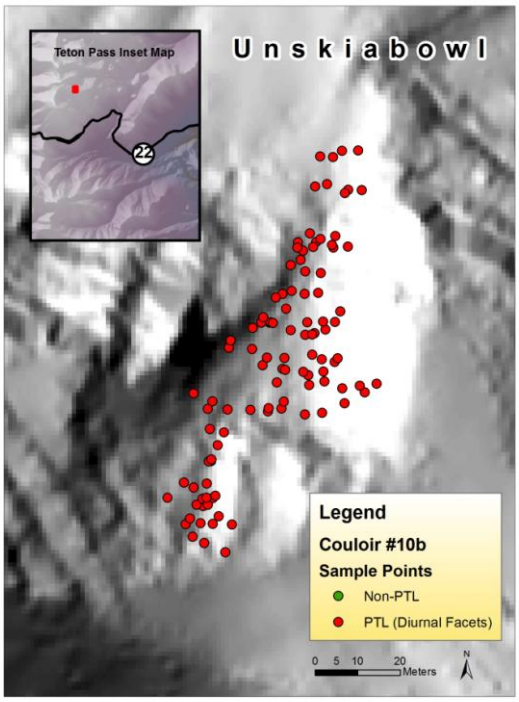
Teton Pass Inset Map
22
Unskiabowl
Legend
Couloir #10b
Sample Points
Non-PTL
PTL (Diurnal Facets)
0 5 10 20 Meters

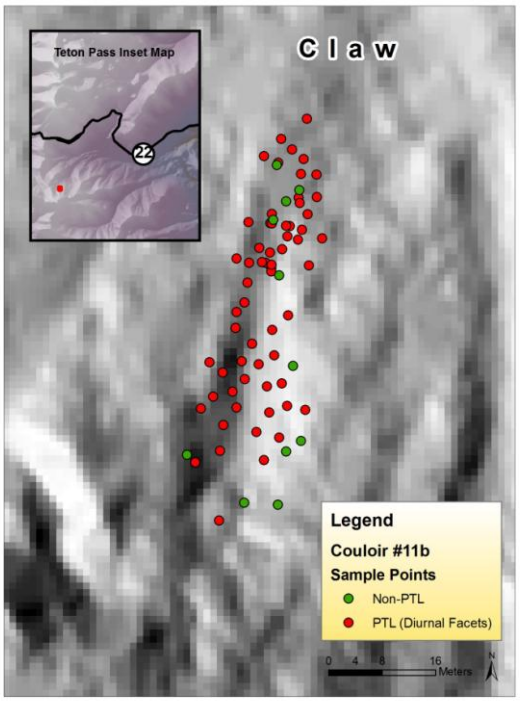
Teton Pass Inset Map
22
Claw
Legend
Couloir #11b
Sample Points
Non-PTL
PTL (Diurnal Facets)
0 4 8 16 Meters

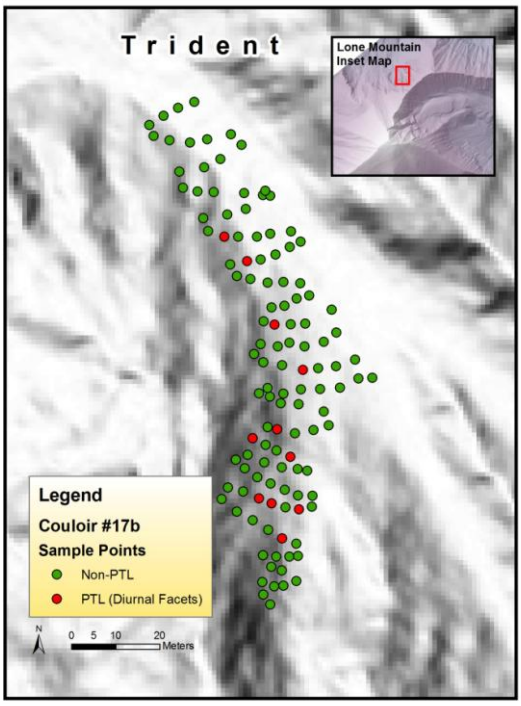
Trident
Lone Mountain Inset Map
Legend
Couloir #17b
Sample Points
Non-PTL
PTL (Diurnal Facets)
0 5 10 20 Meters

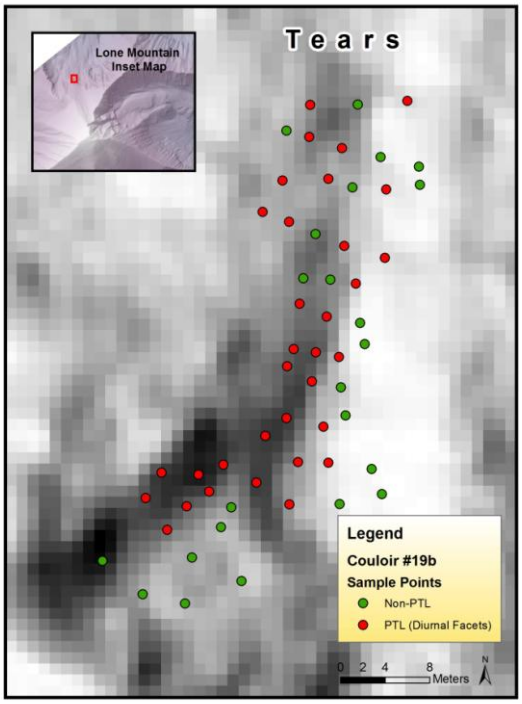
Tears
Lone Mountain
Inset Map
Legend
Couloir #19b
Sample Points
Non-PTL
PTL (Diurnal Facets)
0 2 4 8
Meters
N

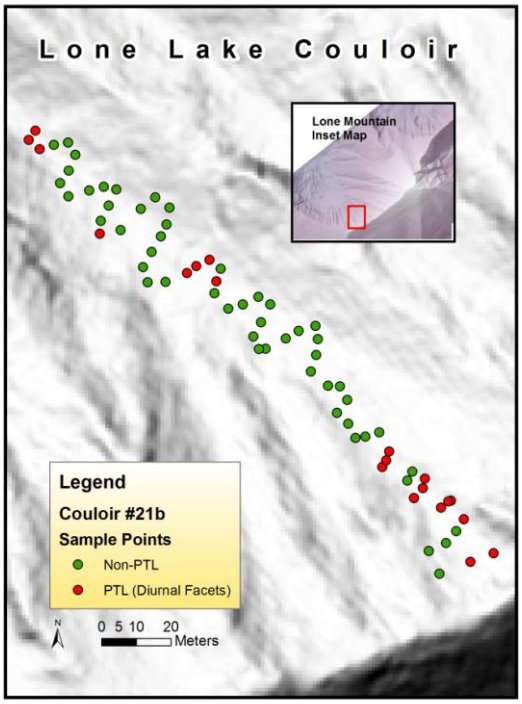
Lone Lake Couloir
Lone Mountain
Inset Map
Legend
Couloir #21b
Sample Points
Non-PTL
PTL (Diurnal Facets)
N
0 5 10 20
Meters

Surface Hoar PTLs

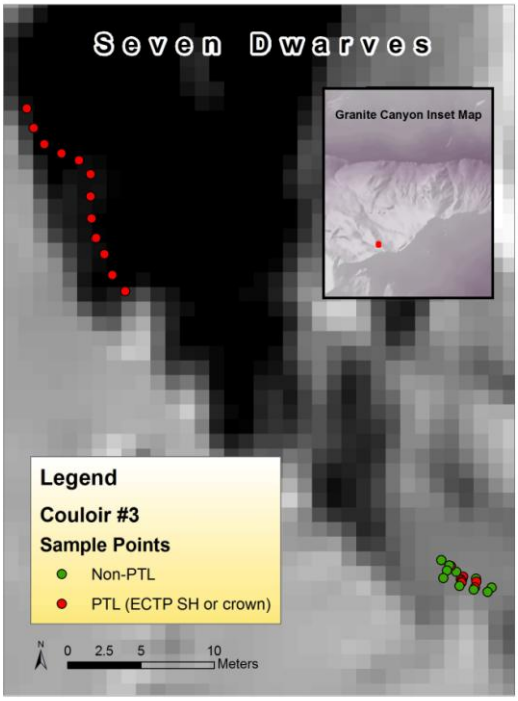

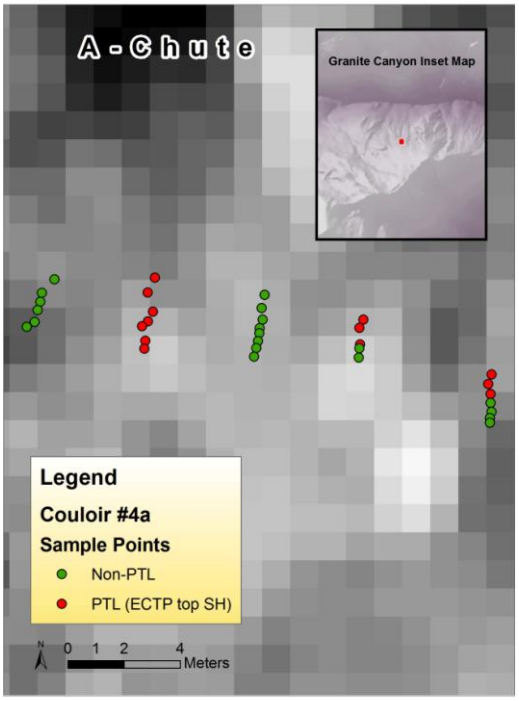

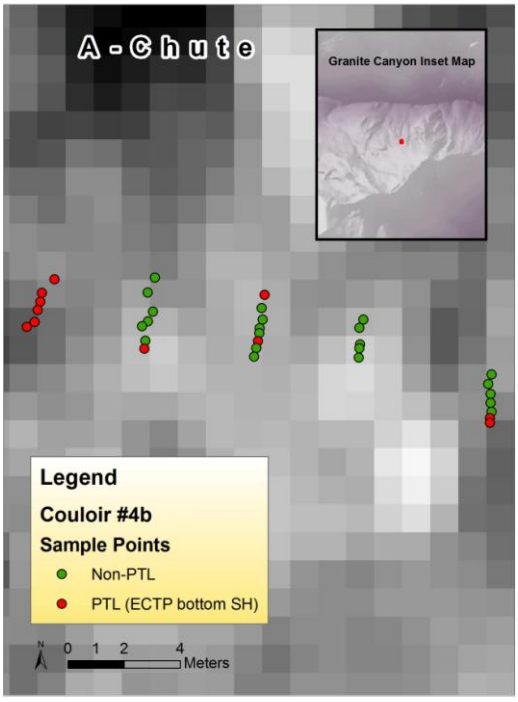

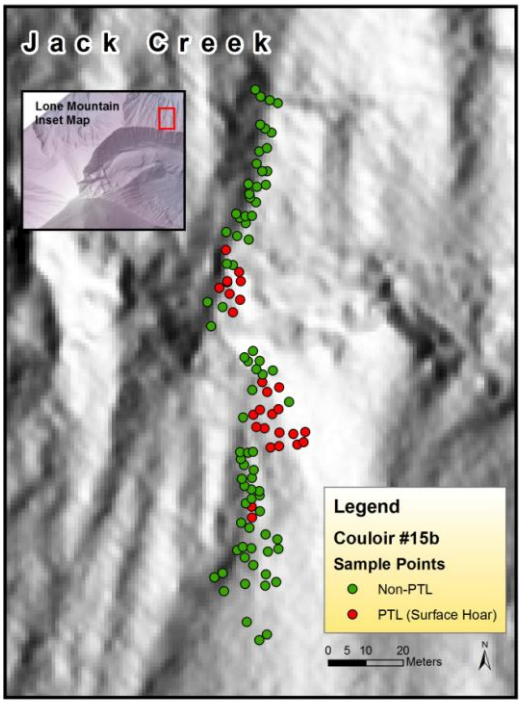

APPENDIX B

GROUPWISE MODELING STATISTICAL OUTPUTS

Appendix B contains the key figures and tables used for groupwise statistical analysis. For each group, I include: (1) Probability distribution functions for PTL and non-PTL observations for important parameters. (2) The pruned classification tree. (3) The Random Forest parameter importance for fixed PTLs (15 cm slabs) and uncertain PTLs, where the slab ranged from 0 cm to 60 cm. (4) Plots of parameter importance versus slab thickness for Random Forest modeling. (5) Logistic model parameter importance for three slab thicknesses. (6) Coefficients, odds ratios, and confidence intervals for the final logistic model.

The Gullies (Depth Hoar)

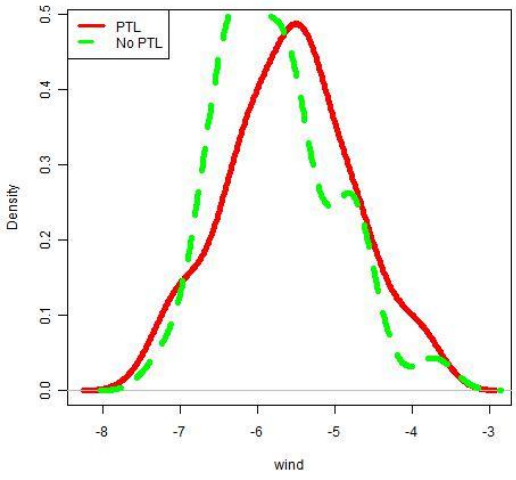

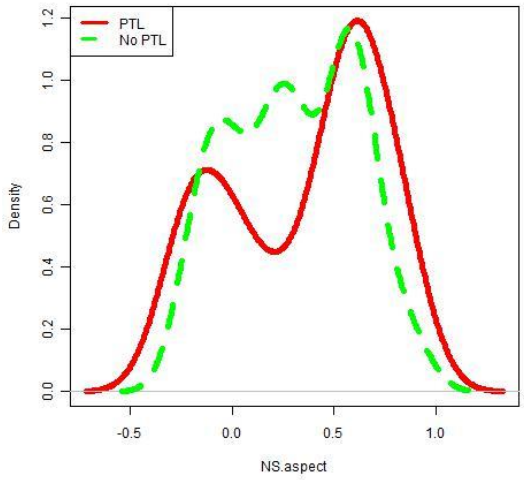

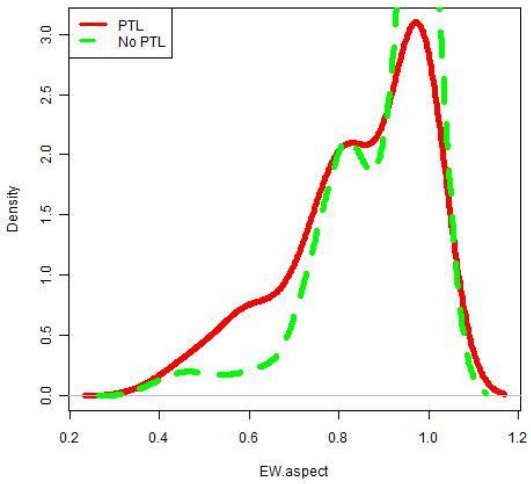
PTL
No PTL
Density
EW.aspect

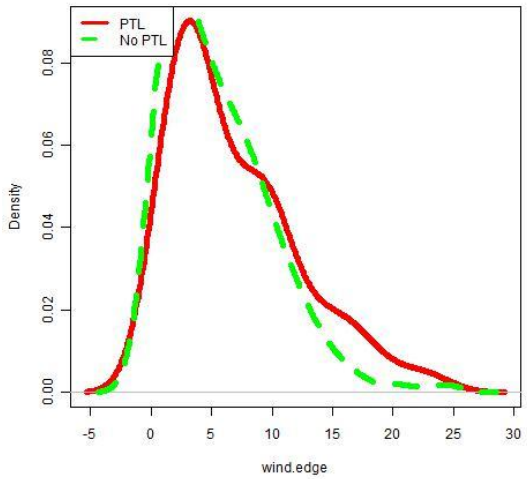
PTL
No PTL
Density
wind.edge

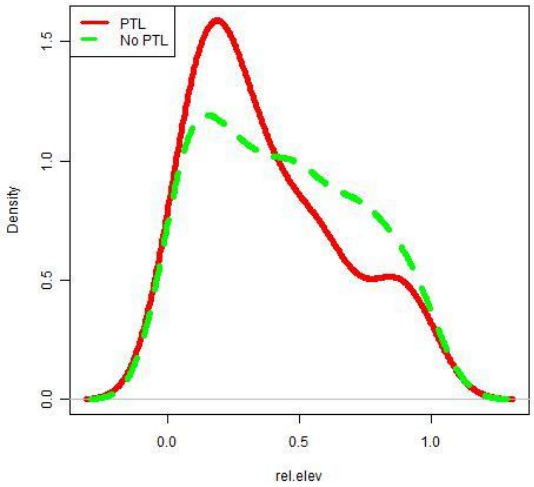
PTL
No PTL
Density
rel.elev

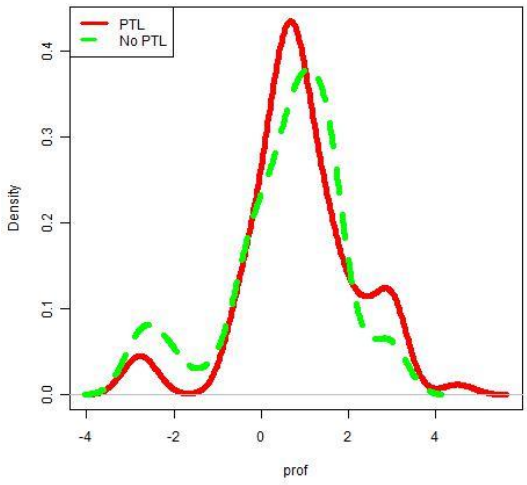
PTL
No PTL
Density
prof

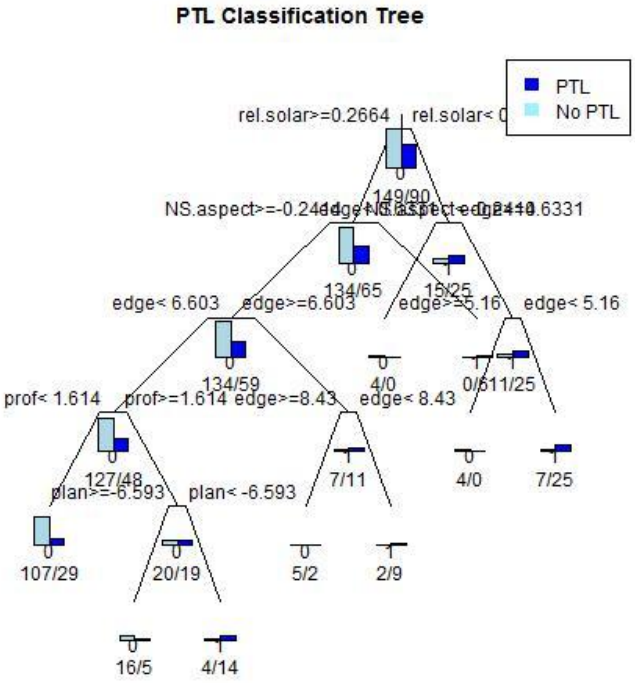
PTL Classification Tree
PTL
No PTL
rel.solar>=0.2664
149/90
NS.aspect>=-0.24
134/65
15/25
edge< 6.603
edge>=6.603
edge>=5.16
edge< 5.16
134/59
4/0
0/11
1/25
prof< 1.614
prof>=1.614
edge>=8.43
edge< 8.43
127/48
7/11
4/0
7/25
plan>=-6.593
plan< -6.593
107/29
20/19
5/2
2/9
16/5
4/14

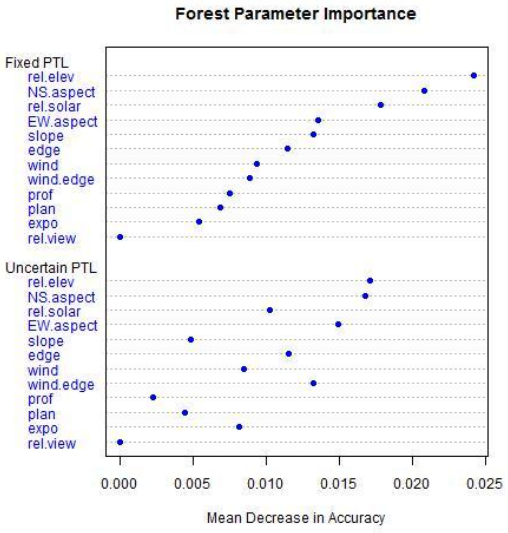
Forest Parameter Importance
Fixed PTL
rel.elev
NS.aspect
rel.solar
EW.aspect
slope
edge
wind
wind.edge
prof
plan
expo
rel.view
Uncertain PTL
rel.elev
NS.aspect
rel.solar
EW.aspect
slope
edge
wind
wind.edge
prof
plan
expo
rel.view
0.000
0.005
0.010
0.015
0.020
0.025
Mean Decrease in Accuracy

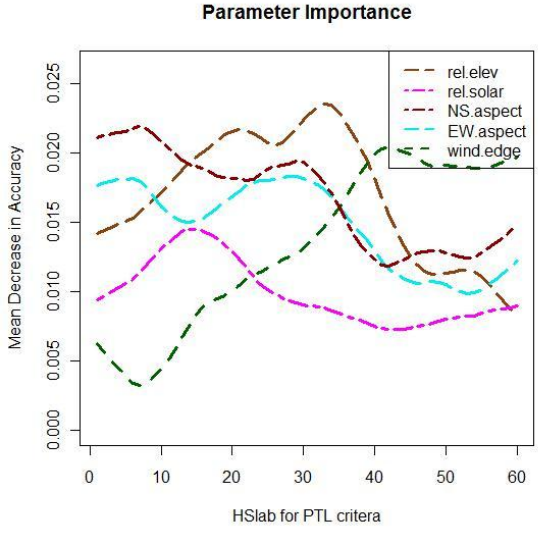
Parameter Importance
rel.elev
rel.solar
NS.aspect
EW.aspect
wind.edge
Mean Decrease in Accuracy
0.000
0.005
0.010
0.015
0.020
0.025
0
10
20
30
40
50
60
HSlab for PTL critera

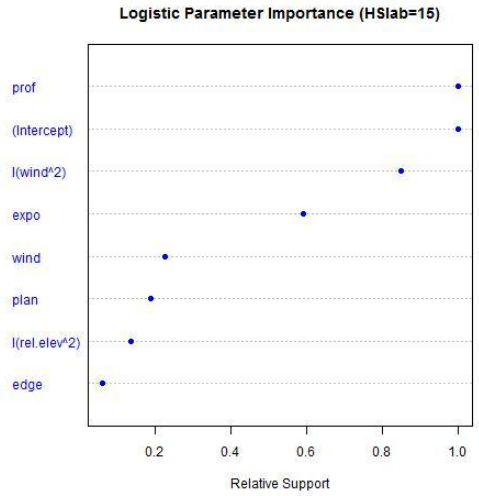

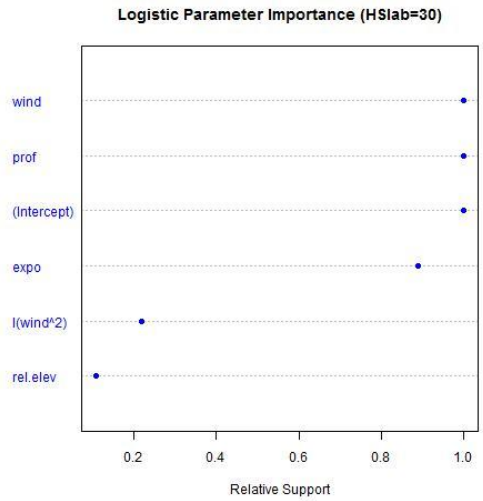

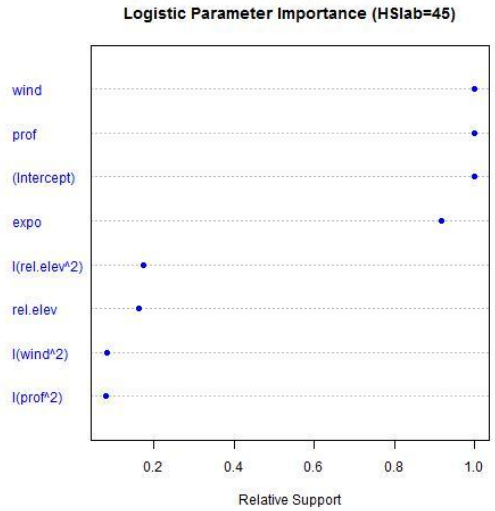

	Estimates	Lower CL	Upper CL	Odds Ratio	Upper CL Odds Ratio	Lower CL Odds Ratio	Importance
Intercept	0.92605	0.29921	1.55289	2.52452	4.7251	1.3488	1
prof	0.07176	0.02347	0.12005	1.0744	1.1276	1.0237	1
wind^2	-0.01052	-0.03274	0.0117	0.98954	1.0118	0.9678	0.849
expo	-0.28746	-0.81965	0.24472	0.75016	1.2773	0.4406	0.592
wind	0.05278	-0.1388	0.24436	1.0542	1.2768	0.8704	0.225
plan	-0.00083	-0.00366	0.00199	0.99917	1.002	0.9963	0.186
rel.elev^2	0.01922	-0.06704	0.10548	1.0194	1.1112	0.9352	0.135
edge	0.00042	-0.00224	0.00309	1.00042	1.0031	0.9978	0.059

Upper A to Zs (Depth Hoar)

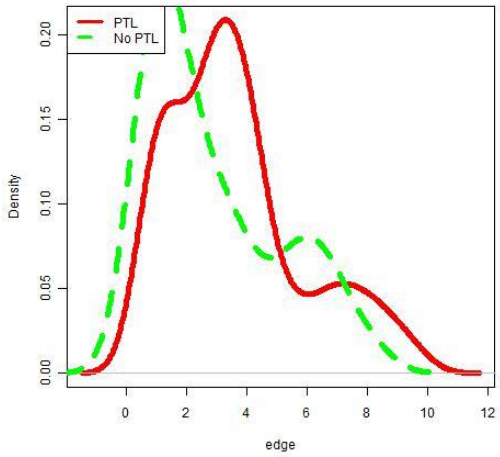

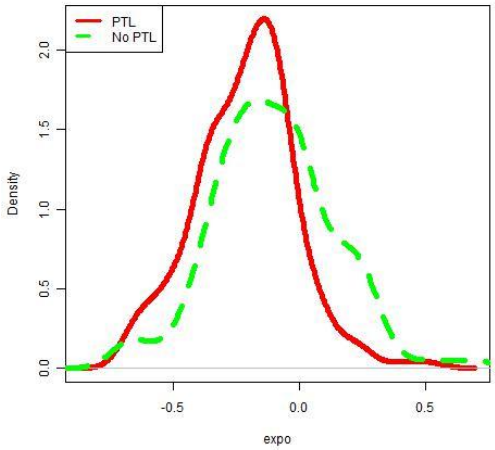

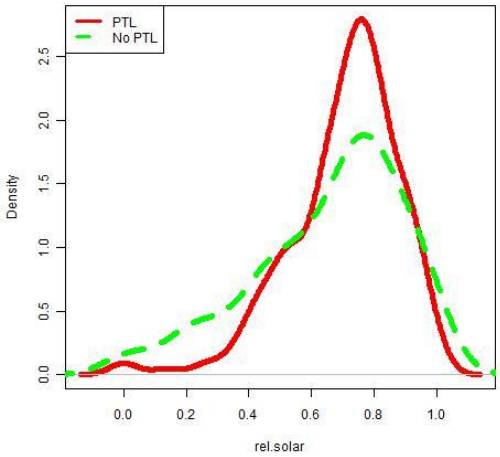

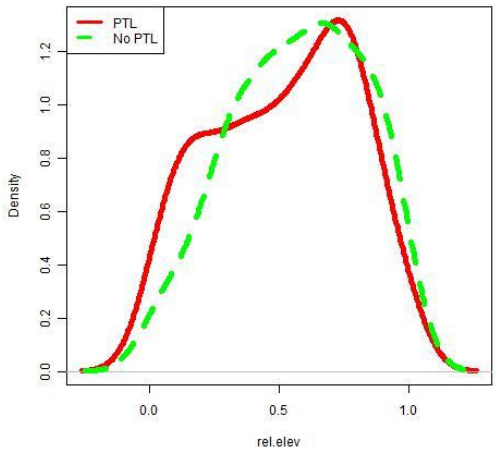

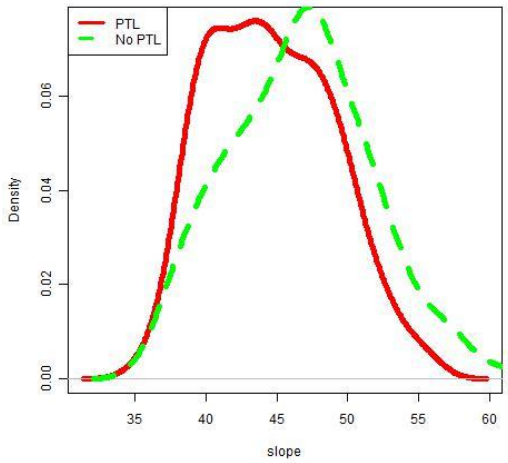

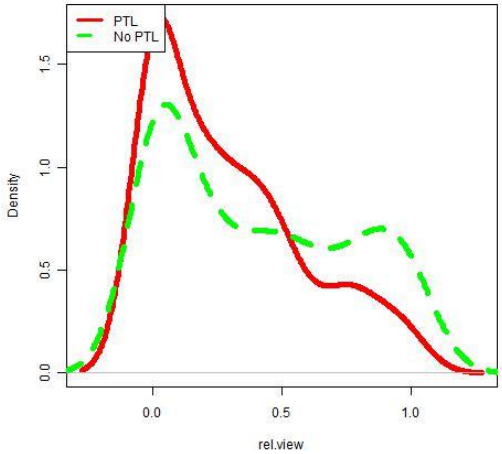

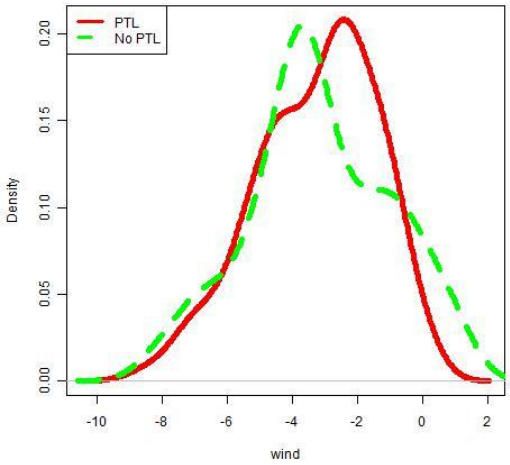
PTL
No PTL
Density
0.00
0.05
0.10
0.15
0.20
-10
-8
-6
-4
-2
0
2
wind

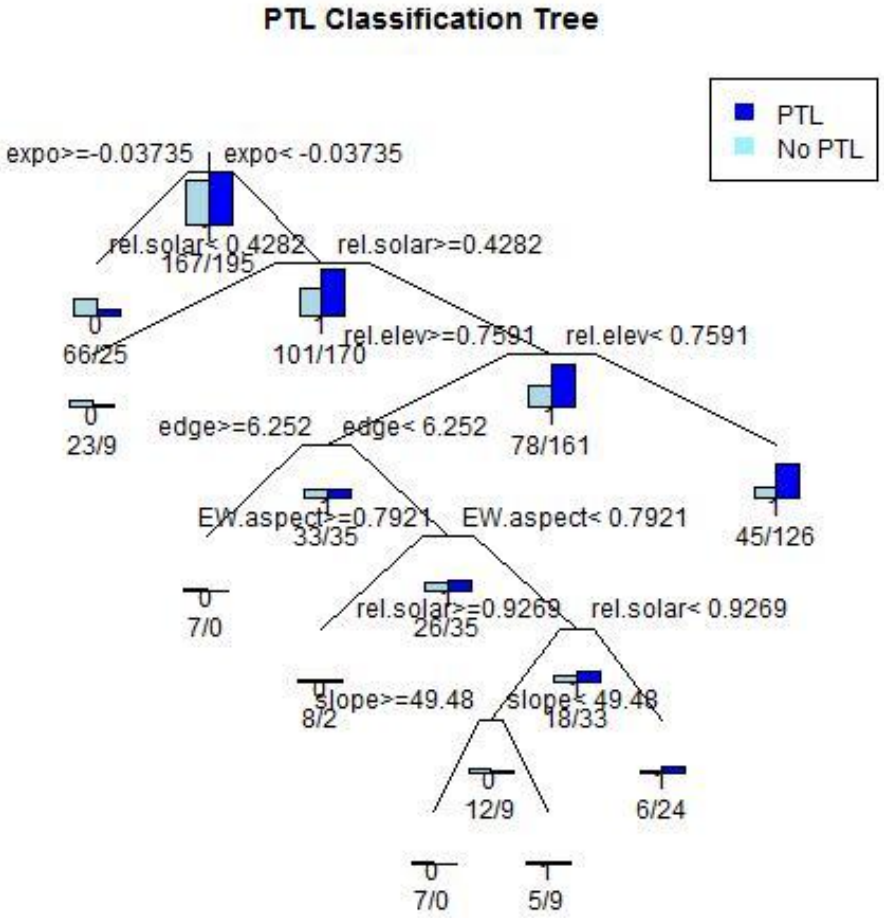
PTL Classification Tree
PTL
No PTL
expo>=-0.03735
expo< -0.03735
167/195
rel.solar< 0.4282
rel.solar>=0.4282
0
66/25
101/170
rel.elev>=0.7591
rel.elev< 0.7591
0
23/9
edge>=6.252
edge< 6.252
78/161
33/35
EW.aspect>=0.7921
EW.aspect< 0.7921
45/126
0
7/0
26/35
rel.solar>=0.9269
rel.solar< 0.9269
8/2
slope>=49.48
slope< 49.48
18/33
0
12/9
6/24
0
7/0
5/9

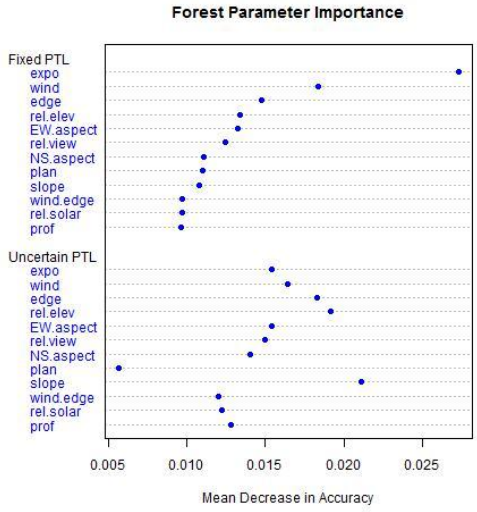
Forest Parameter Importance
Fixed PTL
expo
wind
edge
rel.elev
EW.aspect
rel.view
NS.aspect
plan
slope
wind.edge
rel.solar
prof
Uncertain PTL
expo
wind
edge
rel.elev
EW.aspect
rel.view
NS.aspect
plan
slope
wind.edge
rel.solar
prof
0.005
0.010
0.015
0.020
0.025
Mean Decrease in Accuracy

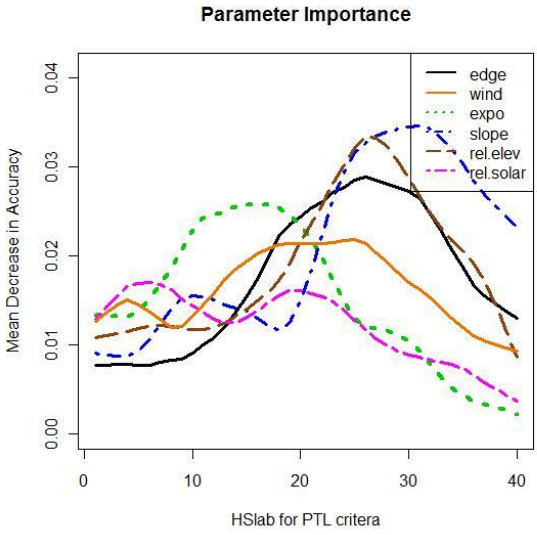
Parameter Importance
edge
wind
expo
slope
rel.elev
rel.solar
Mean Decrease in Accuracy
0.00
0.01
0.02
0.03
0.04
0
10
20
30
40
HSlab for PTL critera

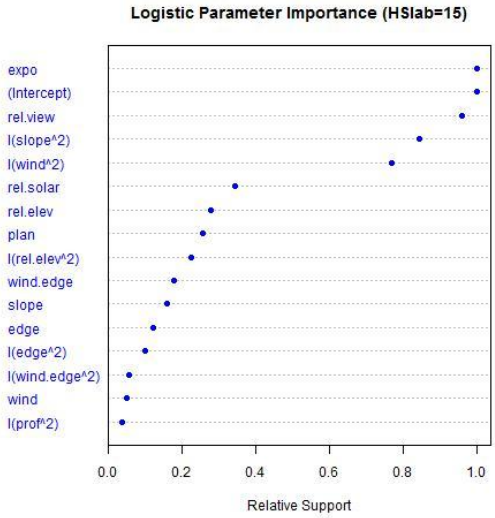
Logistic Parameter Importance (HSlab=15)
expo
(Intercept)
rel.view
I(slope^2)
I(wind^2)
rel.solar
rel.elev
plan
I(rel.elev^2)
wind.edge
slope
edge
I(edge^2)
I(wind.edge^2)
wind
I(prof^2)
0.0
0.2
0.4
0.6
0.8
1.0
Relative Support

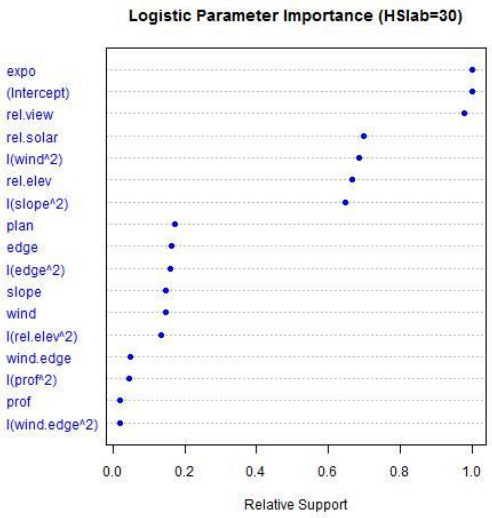
Logistic Parameter Importance (HSlab=30)
expo
(Intercept)
rel.view
rel.solar
I(wind^2)
rel.elev
I(slope^2)
plan
edge
I(edge^2)
slope
wind
I(rel.elev^2)
wind.edge
I(prof^2)
prof
I(wind.edge^2)
0.0
0.2
0.4
0.6
0.8
1.0
Relative Support

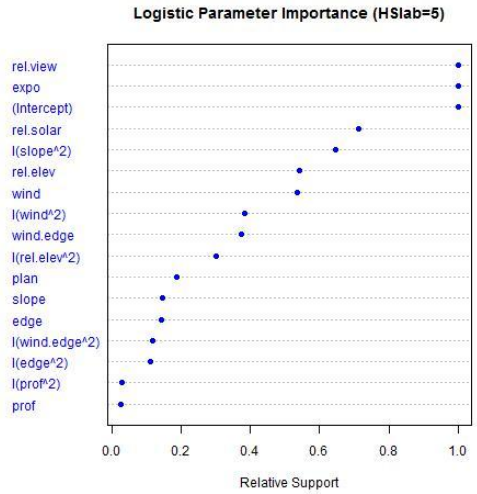

	Estimates	Lower CL	Upper CL	Odds Ratio	Upper CL Odds Ratio	Lower CL Odds Ratio	Importance
Intercept	1.25286	0.7861	1.71962	3.50033	5.5824	2.1948	1
expo	-0.61616	-0.94528	-0.28704	0.54002	0.7505	0.3886	1
rel.view	-0.31743	-0.55246	-0.08239	0.72802	0.9209	0.5755	0.961
slope^2	-0.00022	-0.00044	0	0.99978	1	0.9996	0.843
wind^2	-0.00469	-0.01121	0.00183	0.99532	1.0018	0.9889	0.768
rel.solar	0.11061	-0.20292	0.42413	1.11696	1.5283	0.8163	0.343
rel.elev	-0.07906	-0.32069	0.16257	0.92398	1.1765	0.7256	0.277
plan	0.00097	-0.0022	0.00413	1.00097	1.0041	0.9978	0.257
rel.elev^2	-0.05418	-0.23246	0.12411	0.94727	1.1321	0.7926	0.225
wind.edge	-0.0047	-0.02097	0.01157	0.99531	1.0116	0.9792	0.178
slope	-0.00319	-0.0142	0.00783	0.99682	1.0079	0.9859	0.157
edge	-0.003	-0.01436	0.00835	0.997	1.0084	0.9857	0.122
edge^2	-0.00024	-0.0012	0.00071	0.99976	1.0007	0.9988	0.098
wind.edge^2	0.00014	-0.00041	0.0007	1.00014	1.0007	0.9996	0.054
wind	0.00232	-0.0067	0.01135	1.00232	1.0114	0.9933	0.05
prof^2	-0.00003	-0.00018	0.00012	0.99997	1.0001	0.9998	0.037

Teton Pass (Depth Hoar)

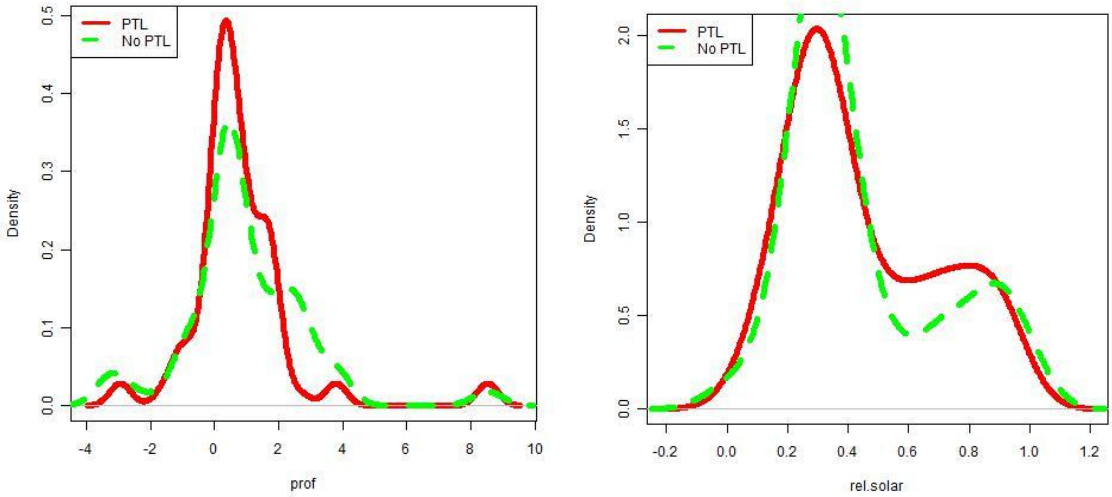

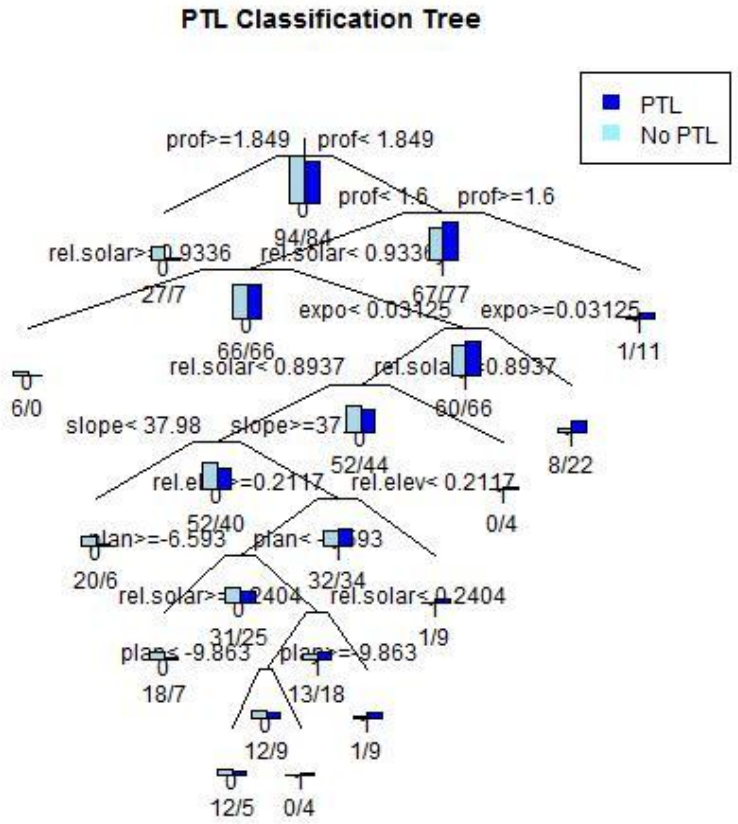

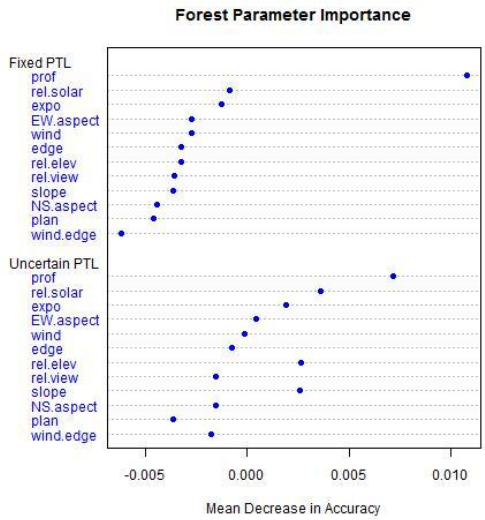
Forest Parameter Importance
Fixed PTL
prof
rel.solar
expo
EW.aspect
wind
edge
rel.elev
rel.view
slope
NS.aspect
plan
wind.edge
Uncertain PTL
prof
rel.solar
expo
EW.aspect
wind
edge
rel.elev
rel.view
slope
NS.aspect
plan
wind.edge
-0.005
0.000
0.005
0.010
Mean Decrease in Accuracy

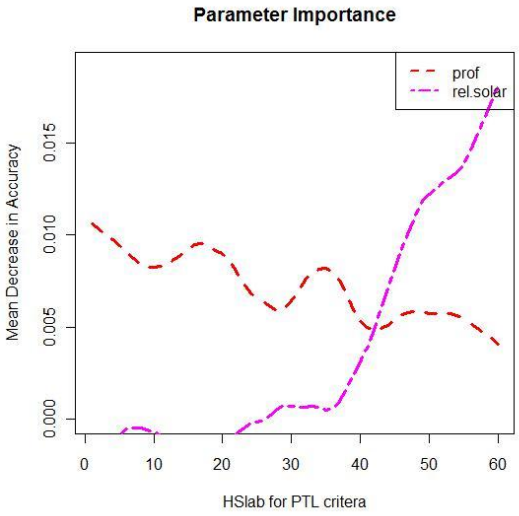
Parameter Importance
prof
rel.solar
Mean Decrease in Accuracy
0.000
0.005
0.010
0.015
0
10
20
30
40
50
60
HSlab for PTL critera

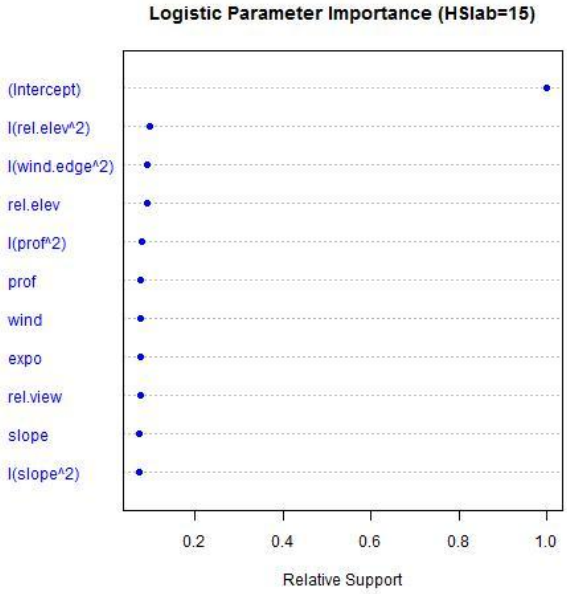
Logistic Parameter Importance (HSlab=15)
(Intercept)
I(rel.elev^2)
I(wind.edge^2)
rel.elev
I(prof^2)
prof
wind
expo
rel.view
slope
I(slope^2)
0.2
0.4
0.6
0.8
1.0
Relative Support

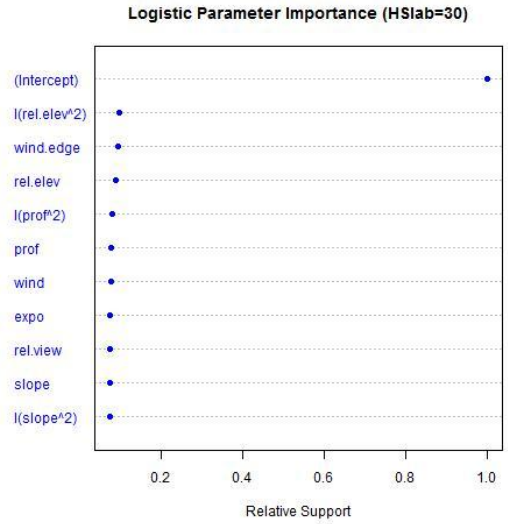

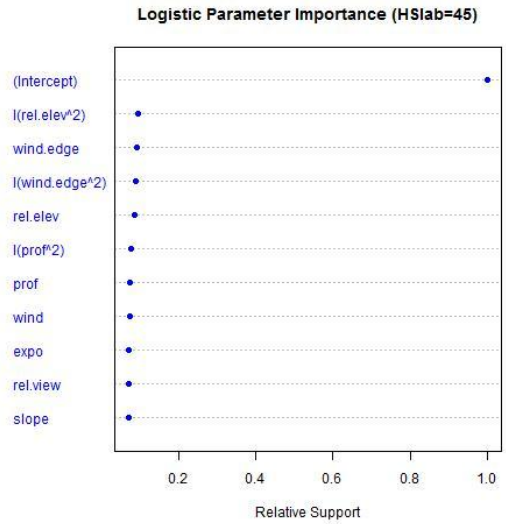

	Estimates	Lower CL	Upper CL	Odds Ratio	Upper CL Odds Ratio	Lower CL Odds Ratio	Importance
Intercept	0.44486	0.25856	0.63116	1.56027	1.8798	1.2951	1
rel.elev^2	0.01658	-0.05249	0.08566	1.01672	1.0894	0.9489	0.097
wind.edge^2	-0.00002	-0.00011	0.00007	0.99998	1.0001	0.9999	0.091
rel.elev	0.01357	-0.04588	0.07302	1.01366	1.0757	0.9552	0.089
prof^2	-0.00021	-0.00123	0.00082	0.99979	1.0008	0.9988	0.079
prof	-0.00101	-0.00651	0.00449	0.99899	1.0045	0.9935	0.076
wind	-0.00115	-0.00759	0.00529	0.99885	1.0053	0.9924	0.075
slope	0.00031	-0.00156	0.00218	1.00031	1.0022	0.9984	0.074
rel.view	-0.00502	-0.03454	0.0245	0.99499	1.0248	0.966	0.074
expo	0.00759	-0.03675	0.05194	1.00762	1.0533	0.9639	0.074
slope^2	0	-0.00002	0.00002	1	1	1	0.073

Headwaters (Depth Hoar)

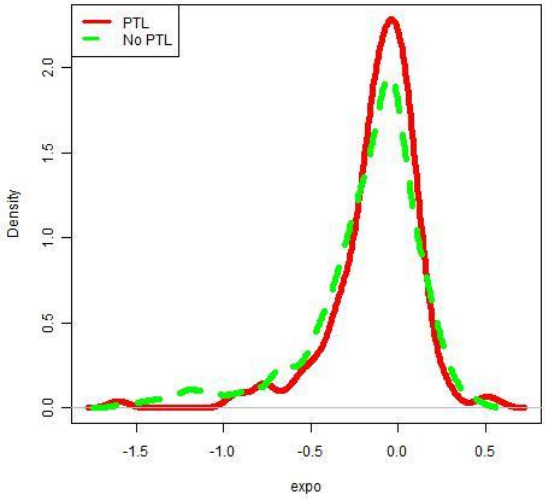

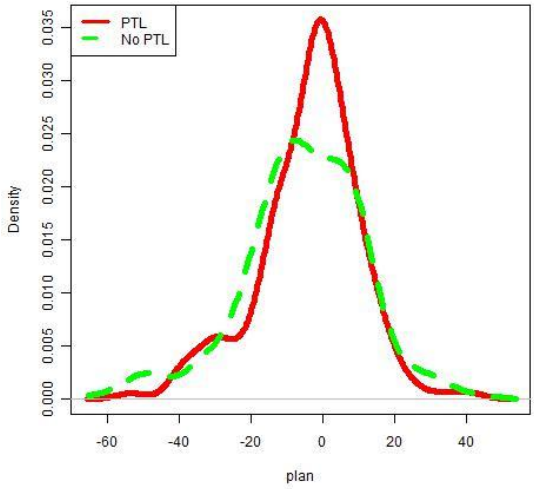

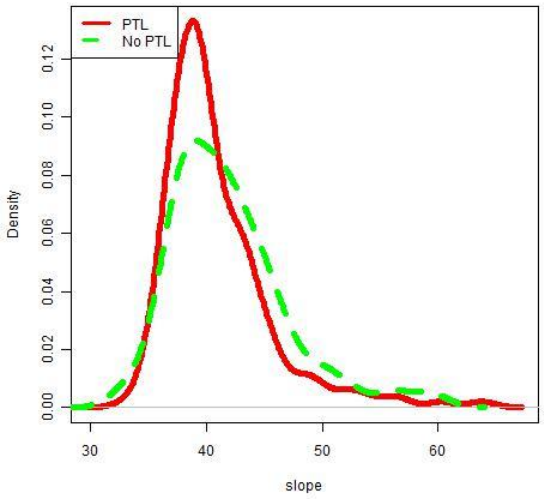

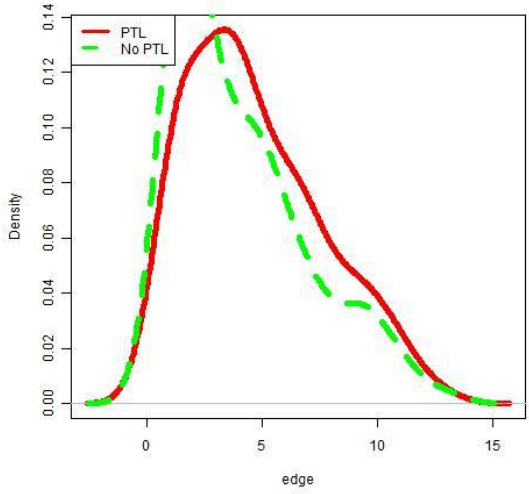

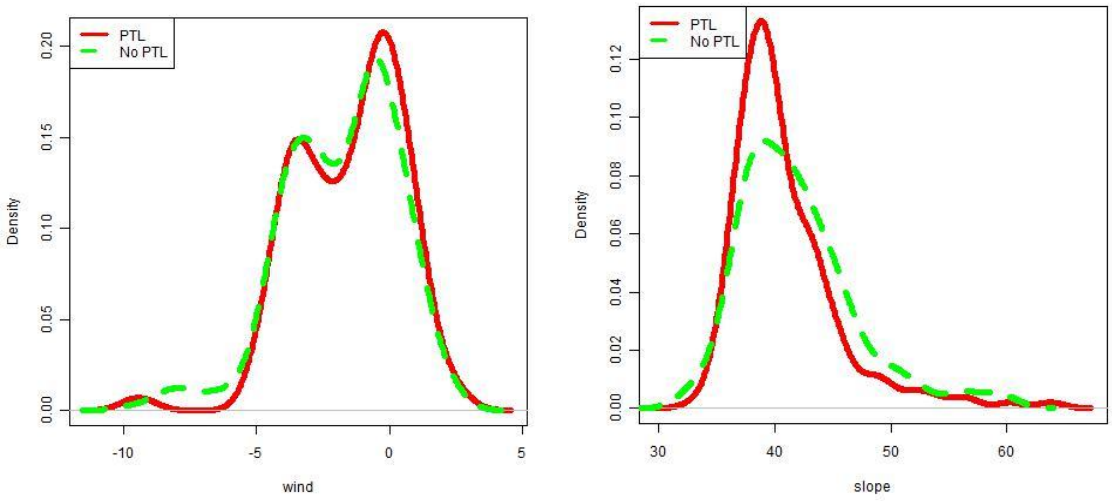
PTL
No PTL
Density
wind
slope

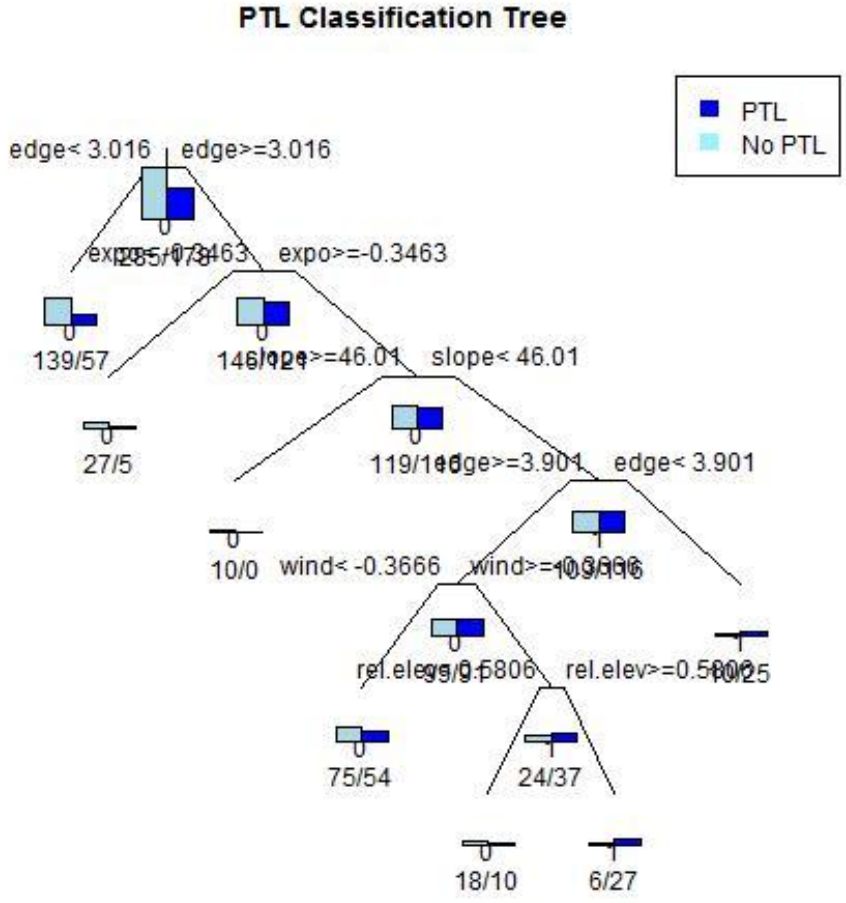
PTL Classification Tree
PTL
No PTL
edge< 3.016
edge>=3.016
expo>=-0.3463
139/57
slope< 46.01
27/5
edge< 3.901
10/0
wind< -0.3666
75/54
24/37
18/10
6/27

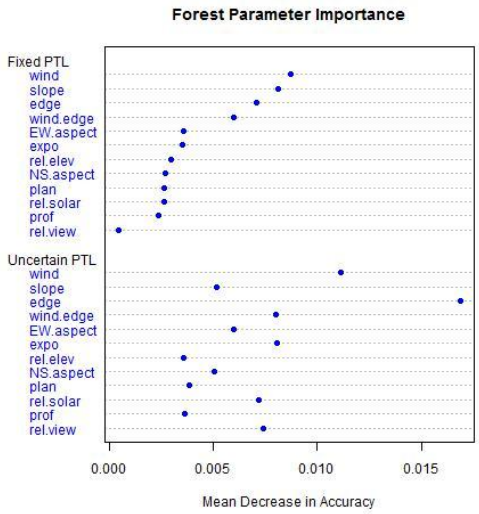
Forest Parameter Importance
Fixed PTL
wind
slope
edge
wind.edge
EW.aspect
expo
rel.elev
NS.aspect
plan
rel.solar
prof
rel.view
Uncertain PTL
wind
slope
edge
wind.edge
EW.aspect
expo
rel.elev
NS.aspect
plan
rel.solar
prof
rel.view
0.000
0.005
0.010
0.015
Mean Decrease in Accuracy

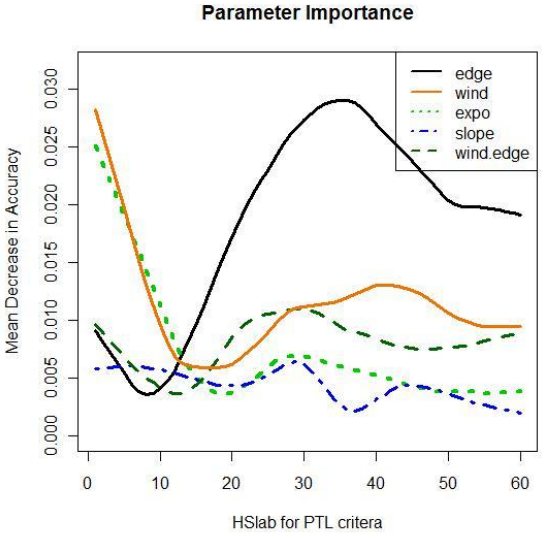
Parameter Importance
edge
wind
expo
slope
wind.edge
Mean Decrease in Accuracy
0.000
0.005
0.010
0.015
0.020
0.025
0.030
0
10
20
30
40
50
60
HSlab for PTL critera

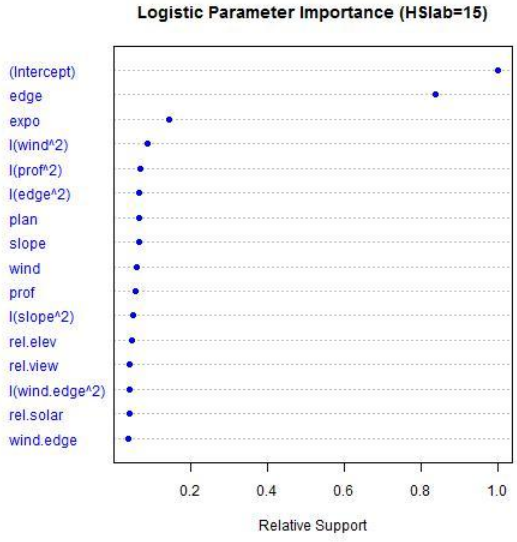
Logistic Parameter Importance (HSlab=15)
(Intercept)
edge
expo
I(wind^2)
I(prof^2)
I(edge^2)
plan
slope
wind
prof
I(slope^2)
rel.elev
rel.view
I(wind.edge^2)
rel.solar
wind.edge
0.2
0.4
0.6
0.8
1.0
Relative Support

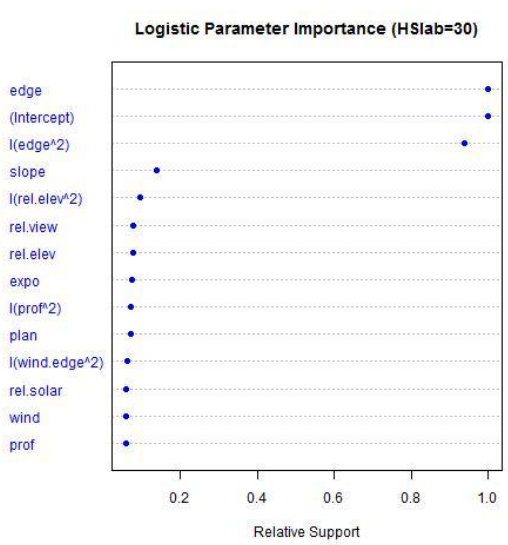

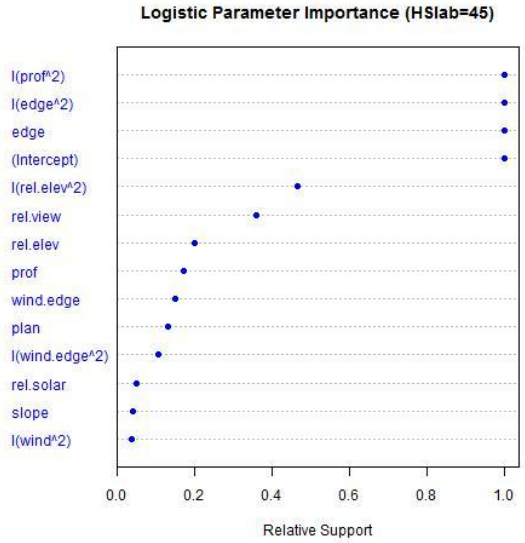

	Estimates	Lower CL	Upper CL	Odds Ratio	Upper CL Odds Ratio	Lower CL Odds Ratio	Importance
Intercept	0.34941	0.17457	0.52424	1.41822	1.6892	1.1907	1
edge	0.01763	-0.00653	0.04179	1.01779	1.0427	0.9935	0.839
expo	0.01994	-0.05351	0.0934	1.02014	1.0979	0.9479	0.143
wind^2	-0.0002	-0.00105	0.00065	0.9998	1.0006	0.9989	0.089
prof^2	-0.00039	-0.00195	0.00117	0.99961	1.0012	0.998	0.07
edge^2	-0.00025	-0.00125	0.00075	0.99975	1.0008	0.9988	0.067
plan	0.00013	-0.00039	0.00064	1.00013	1.0006	0.9996	0.066
slope	-0.00047	-0.00237	0.00144	0.99953	1.0014	0.9976	0.065
wind	0.00092	-0.00289	0.00472	1.00092	1.0047	0.9971	0.061
prof	-0.00102	-0.00533	0.00329	0.99898	1.0033	0.9947	0.058
slope^2	0	-0.00002	0.00001	1	1	1	0.052
rel.elev	0.00396	-0.01403	0.02194	1.00396	1.0222	0.9861	0.049
rel.view	0.00155	-0.00711	0.01021	1.00155	1.0103	0.9929	0.041
rel.solar	-0.00167	-0.0118	0.00846	0.99833	1.0085	0.9883	0.04
wind.edge^2	0	-0.00003	0.00002	1	1	1	0.04
wind.edge	-0.00005	-0.00046	0.00037	0.99995	1.0004	0.9995	0.039

North Summit (Depth Hoar)

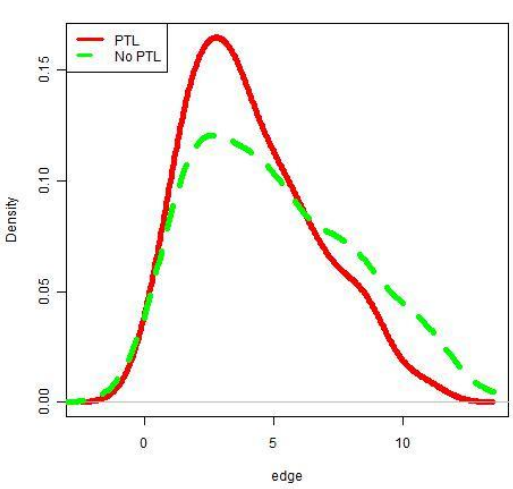

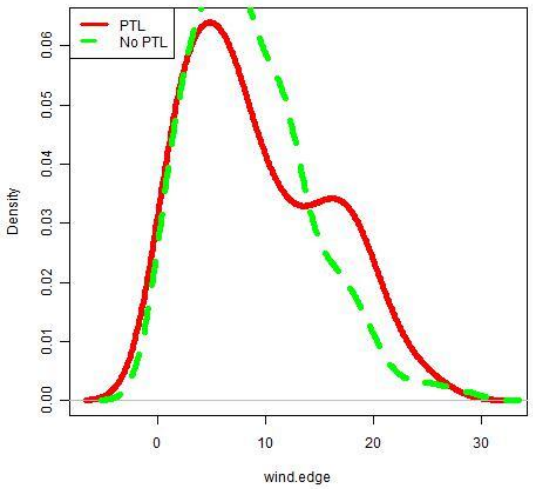

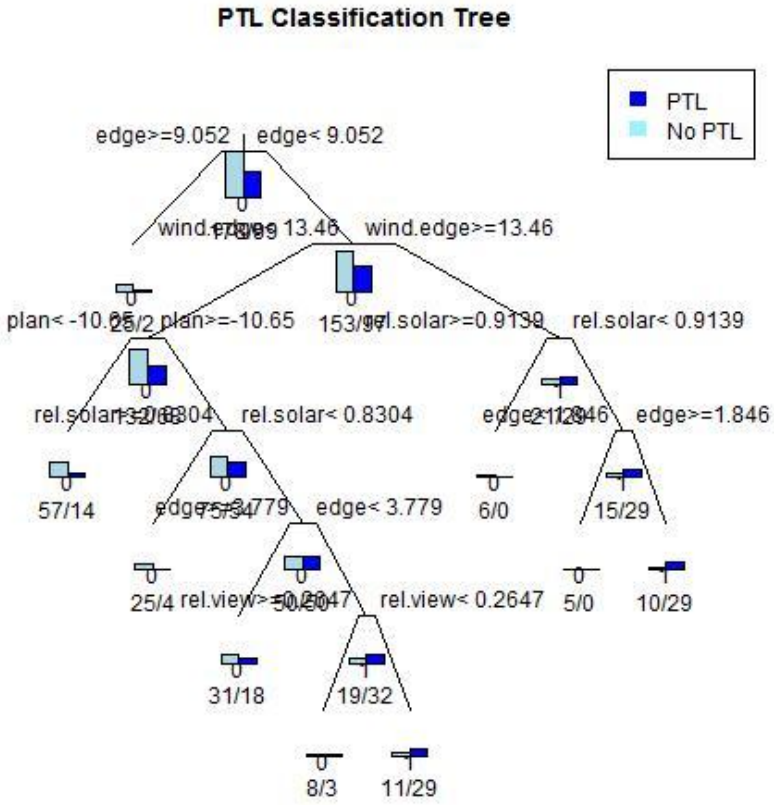

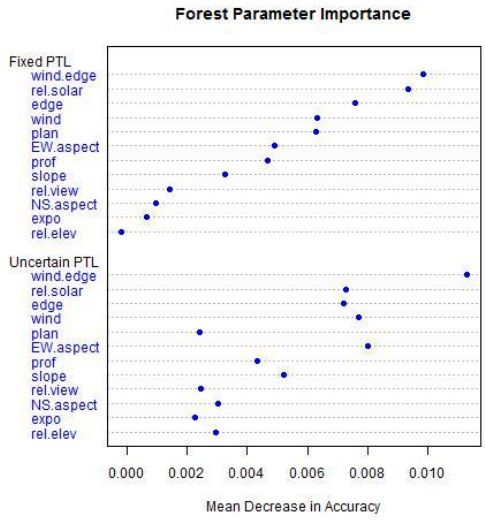
Forest Parameter Importance
Fixed PTL
wind.edge
rel.solar
edge
wind
plan
EW.aspect
prof
slope
rel.view
NS.aspect
expo
rel.elev
Uncertain PTL
wind.edge
rel.solar
edge
wind
plan
EW.aspect
prof
slope
rel.view
NS.aspect
expo
rel.elev
0.000
0.002
0.004
0.006
0.008
0.010
Mean Decrease in Accuracy

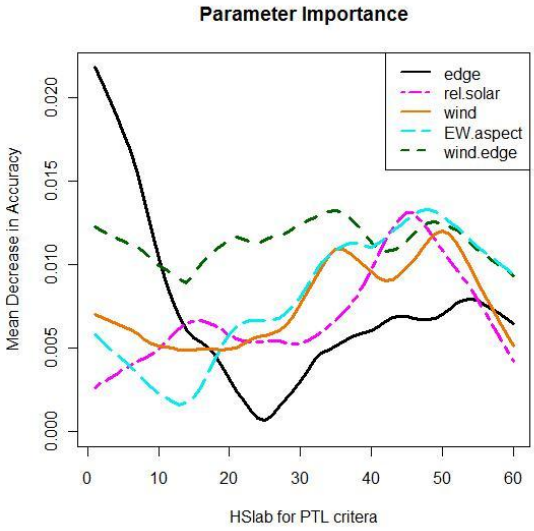
Parameter Importance
edge
rel.solar
wind
EW.aspect
wind.edge
Mean Decrease in Accuracy
0.000
0.005
0.010
0.015
0.020
0
10
20
30
40
50
60
HSlab for PTL critera

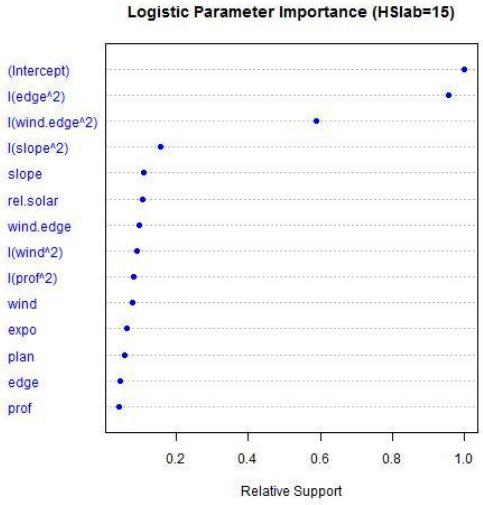
Logistic Parameter Importance (HSlab=15)
(Intercept)
I(edge^2)
I(wind.edge^2)
I(slope^2)
slope
rel.solar
wind.edge
I(wind^2)
I(prof^2)
wind
expo
plan
edge
prof
0.2
0.4
0.6
0.8
1.0
Relative Support

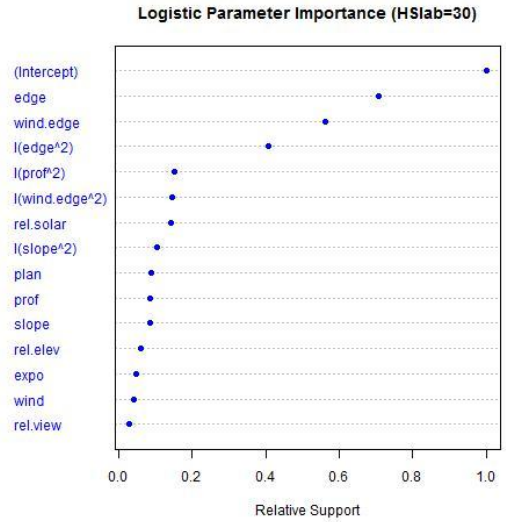

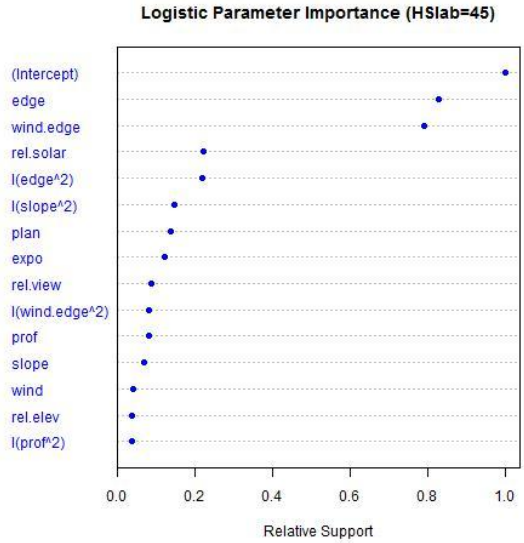

	Estimates	Lower CL	Upper CL	Odds Ratio	Upper CL Odds Ratio	Lower CL Odds Ratio	Importance
Intercept	0.35417	0.06451	0.64382	1.42499	1.9037	1.0666	1
edge^2	-0.00216	-0.00375	-0.00056	0.99784	0.9994	0.9963	0.956
wind.edge^2	0.00028	-0.00029	0.00086	1.00028	1.0009	0.9997	0.59
slope^2	0.00001	-0.00004	0.00007	1.00001	1.0001	1	0.158
slope	0.00104	-0.00297	0.00505	1.00104	1.0051	0.997	0.109
rel.solar	-0.0247	-0.12061	0.07121	0.9756	1.0738	0.8864	0.106
wind.edge	0.00106	-0.00292	0.00503	1.00106	1.005	0.9971	0.098
wind^2	-0.00018	-0.00101	0.00064	0.99982	1.0006	0.999	0.091
prof^2	-0.00012	-0.00068	0.00044	0.99988	1.0004	0.9993	0.082
wind	0.00274	-0.00788	0.01335	1.00274	1.0134	0.9922	0.079
expo	0.01223	-0.03765	0.06211	1.01231	1.0641	0.9631	0.064
plan	0.00014	-0.00045	0.00074	1.00014	1.0007	0.9995	0.058
edge	-0.00114	-0.00559	0.0033	0.99886	1.0033	0.9944	0.044
prof	-0.0004	-0.00242	0.00162	0.9996	1.0016	0.9976	0.042

Lone Lake Cirque (Depth Hoar)

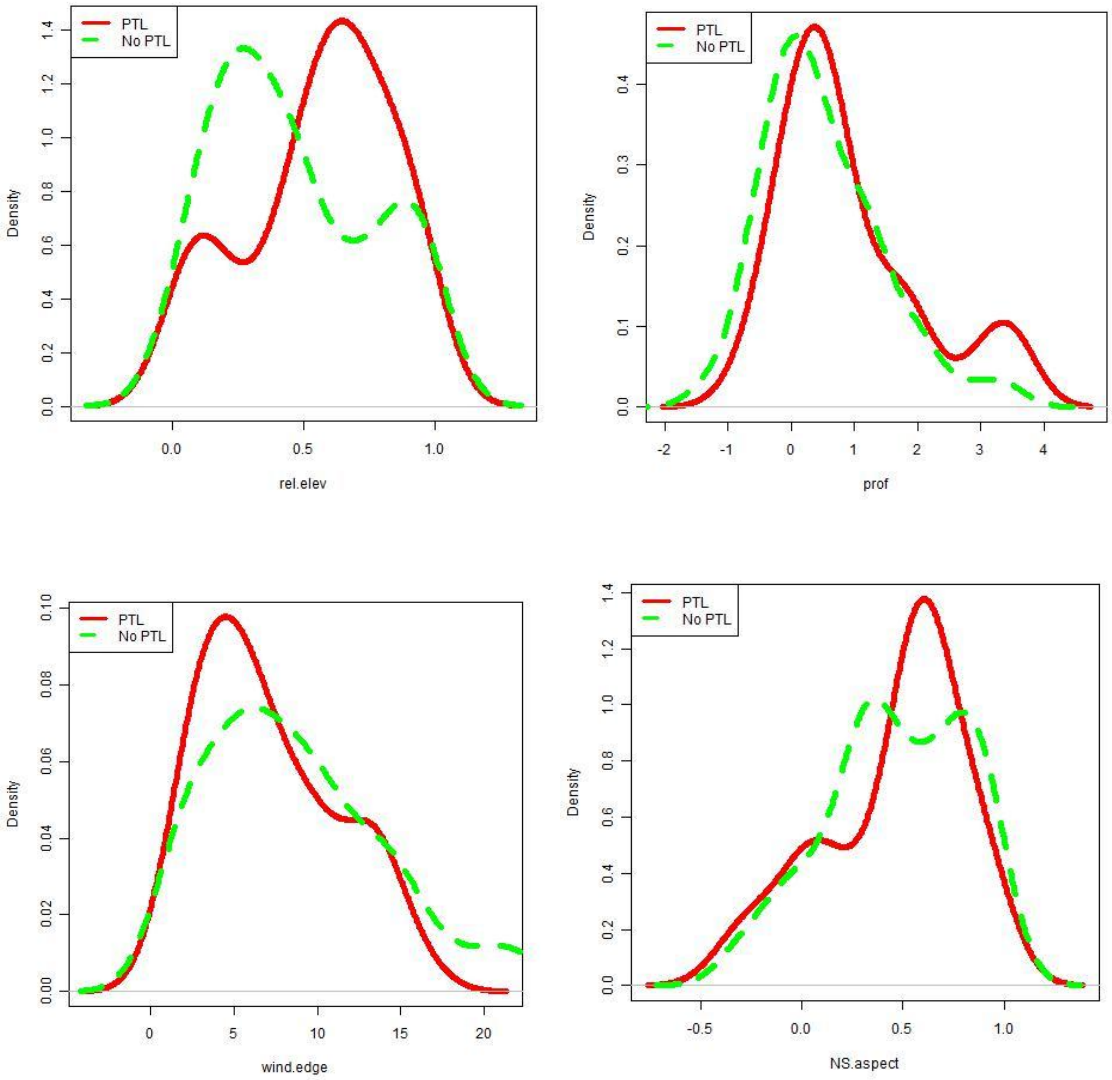

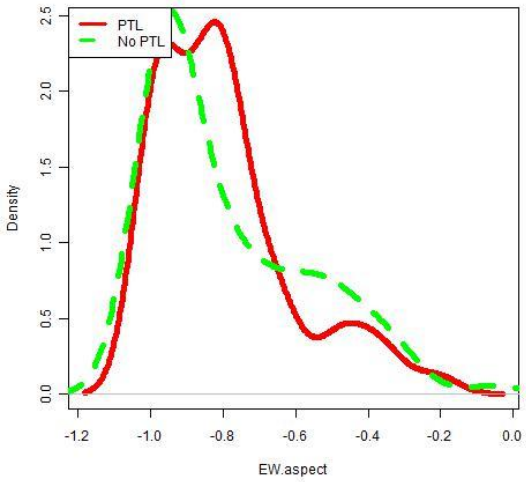
PTL
No PTL
Density
EW.aspect
0.0
0.5
1.0
1.5
2.0
2.5
-1.2
-1.0
-0.8
-0.6
-0.4
-0.2
0.0

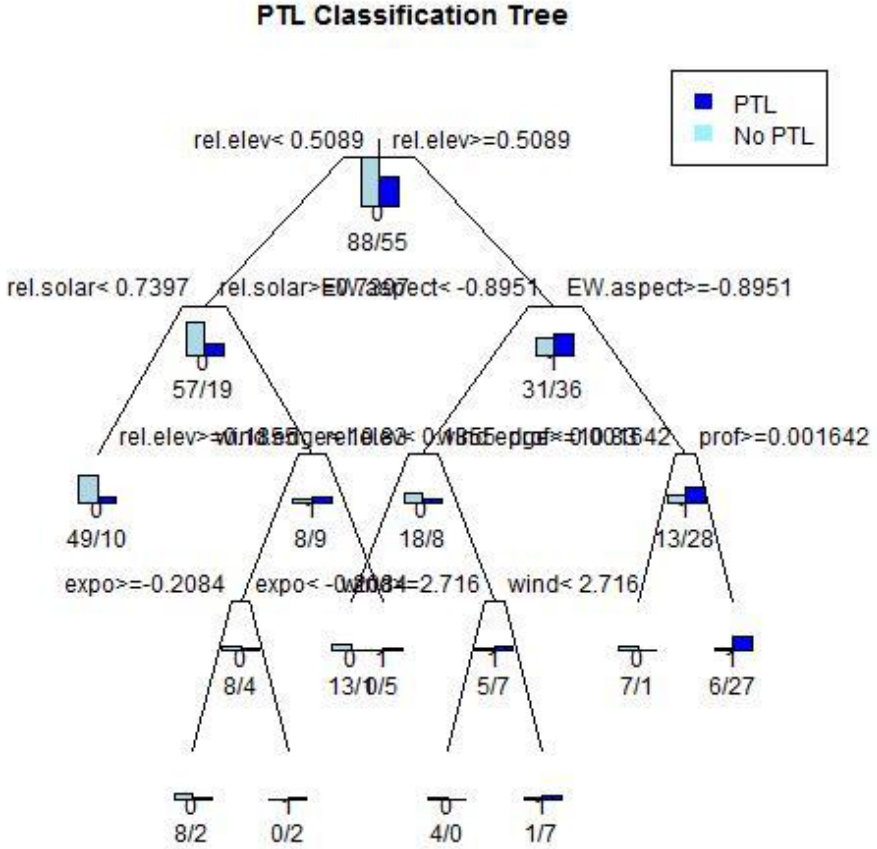
PTL Classification Tree
PTL
No PTL
rel.elev< 0.5089
rel.elev>=0.5089
88/55
rel.solar< 0.7397
EW.aspect< -0.8951
EW.aspect>=-0.8951
57/19
31/36
prof>=0.001642
49/10
8/9
18/8
13/28
expo>=-0.2084
wind< 2.716
8/4
5/7
7/1
6/27
8/2
0/2
4/0
1/7

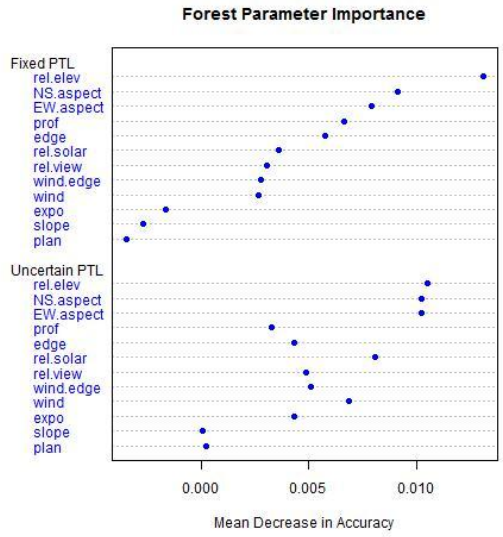
Forest Parameter Importance
Fixed PTL
rel.elev
NS.aspect
EW.aspect
prof
edge
rel.solar
rel.view
wind.edge
wind
expo
slope
plan
Uncertain PTL
rel.elev
NS.aspect
EW.aspect
prof
edge
rel.solar
rel.view
wind.edge
wind
expo
slope
plan
0.000
0.005
0.010
Mean Decrease in Accuracy

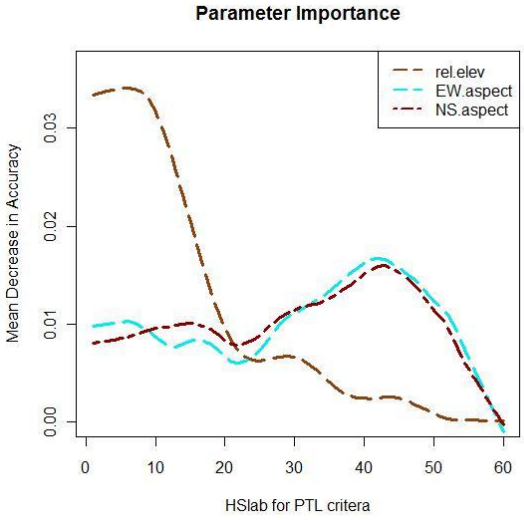
Parameter Importance
rel.elev
EW.aspect
NS.aspect
Mean Decrease in Accuracy
0.00
0.01
0.02
0.03
0
10
20
30
40
50
60
HSlab for PTL critera

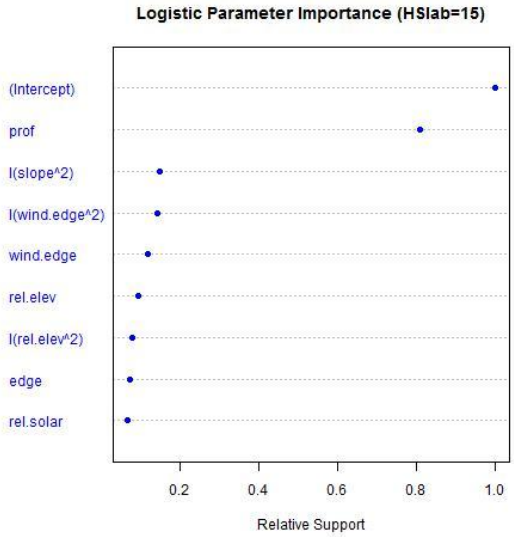
Logistic Parameter Importance (HSlab=15)
(Intercept)
prof
I(slope^2)
I(wind.edge^2)
wind.edge
rel.elev
I(rel.elev^2)
edge
rel.solar
0.2
0.4
0.6
0.8
1.0
Relative Support

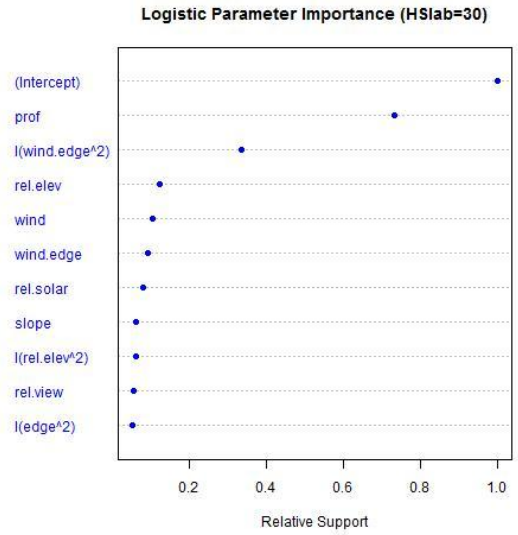

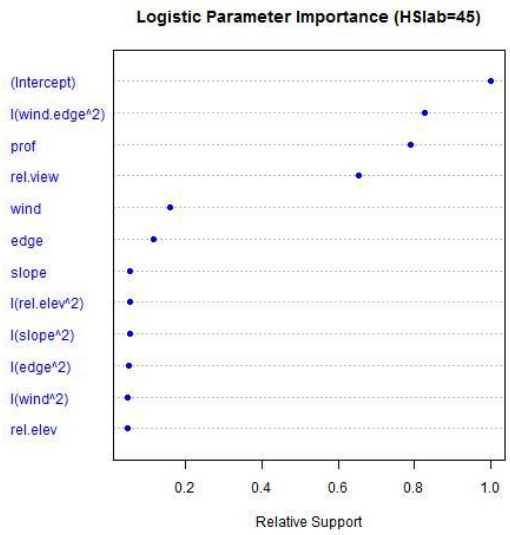

	Estimates	Lower CL	Upper CL	Odds Ratio	Upper CL Odds Ratio	Lower CL Odds Ratio	Importance
Intercept	0.30831	0.03299	0.58363	1.36112	1.7925	1.0335	1
prof	0.06342	-0.02119	0.14803	1.06548	1.1596	0.979	0.808
slope^2	0.00003	-0.00009	0.00015	1.00003	1.0001	0.9999	0.148
wind.edge^2	-0.00011	-0.00051	0.00029	0.99989	1.0003	0.9995	0.141
wind.edge	-0.0017	-0.00813	0.00473	0.9983	1.0047	0.9919	0.118
rel.elev	0.01825	-0.05555	0.09205	1.01842	1.0964	0.946	0.092
rel.elev^2	0.01177	-0.03909	0.06264	1.01184	1.0646	0.9617	0.077
edge	-0.00109	-0.00612	0.00394	0.99891	1.0039	0.9939	0.07
rel.solar	0.0091	-0.03557	0.05378	1.00915	1.0553	0.9651	0.067

All Depth Hoar Samples/Lone Mountain

*The output here is for all depth hoar samples. It is very similar to the Lone Mountain samples (the two Teton Pass couloirs are excluded, in this case), so I did not include both.

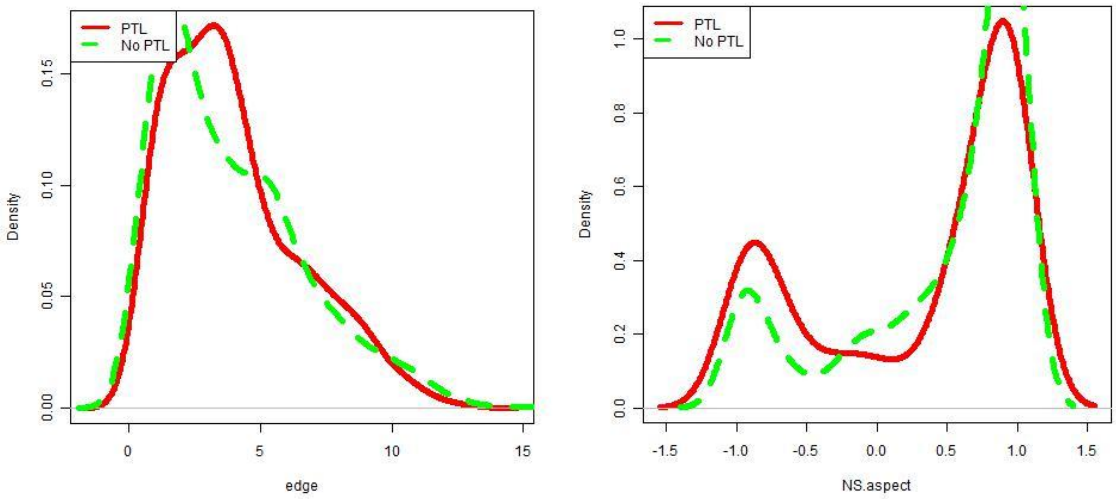

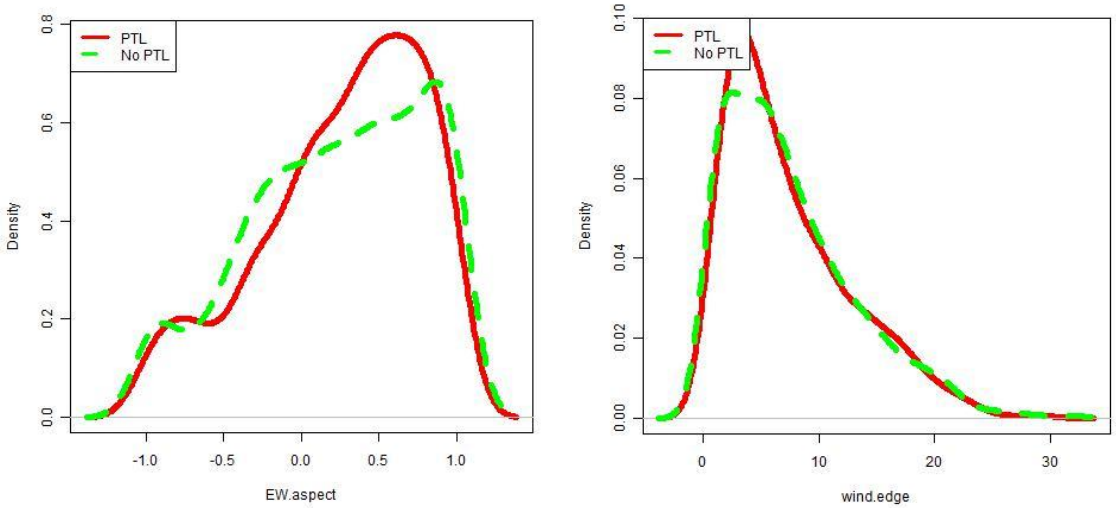

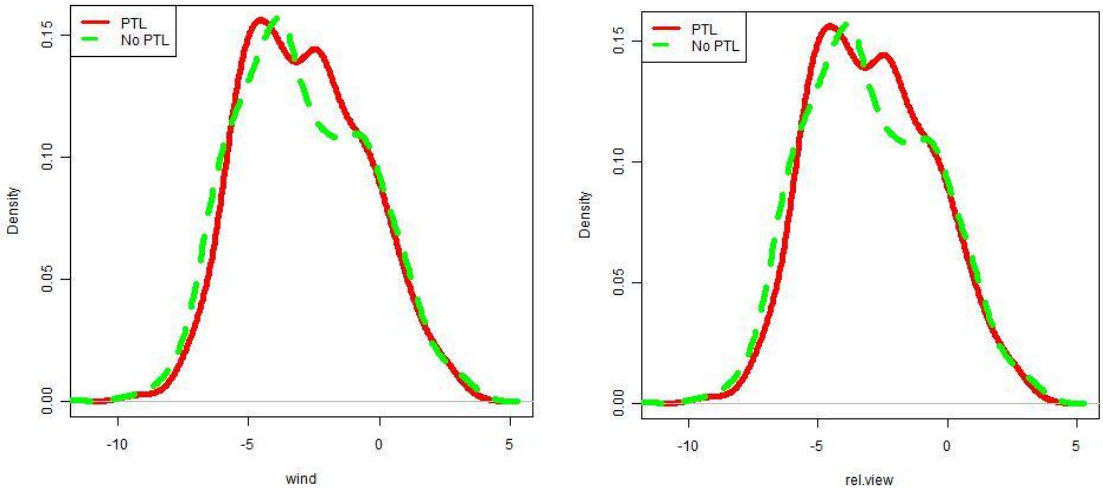
PTL
No PTL
Density
0.00
0.05
0.10
0.15
-10
-5
0
5
wind
rel.view

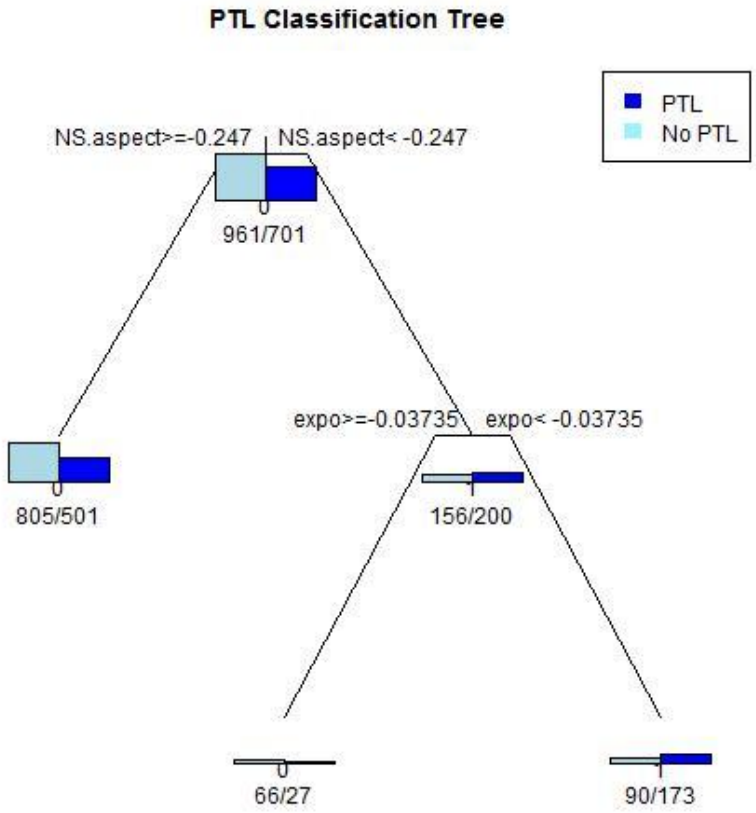
PTL Classification Tree
PTL
No PTL
NS.aspect>=-0.247
NS.aspect< -0.247
961/701
805/501
expo>=-0.03735
expo< -0.03735
156/200
66/27
90/173

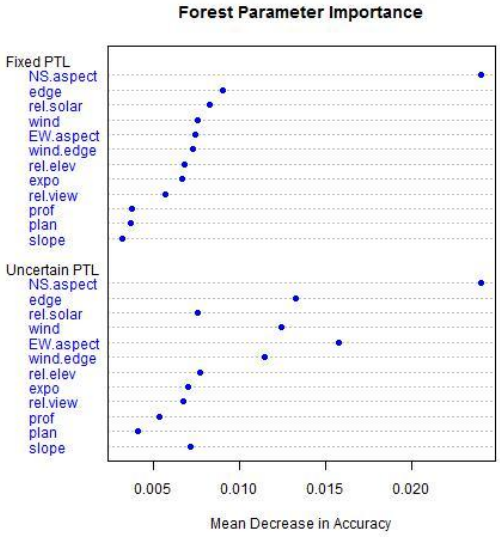
Forest Parameter Importance
Fixed PTL
NS.aspect
edge
rel.solar
wind
EW.aspect
wind.edge
rel.elev
expo
rel.view
prof
plan
slope
Uncertain PTL
NS.aspect
edge
rel.solar
wind
EW.aspect
wind.edge
rel.elev
expo
rel.view
prof
plan
slope
0.005
0.010
0.015
0.020
Mean Decrease in Accuracy

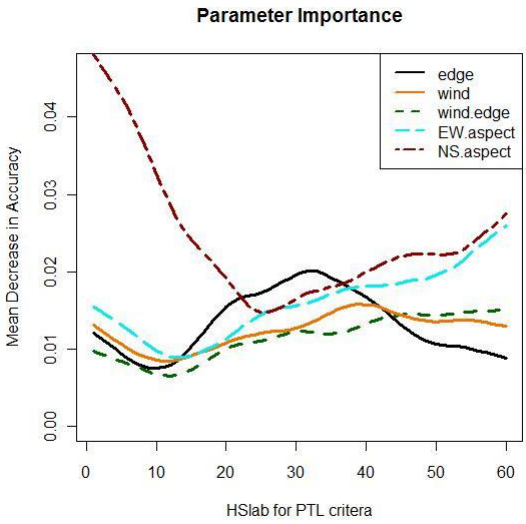
Parameter Importance
edge
wind
wind.edge
EW.aspect
NS.aspect
Mean Decrease in Accuracy
0.00
0.01
0.02
0.03
0.04
0
10
20
30
40
50
60
HSlab for PTL critera

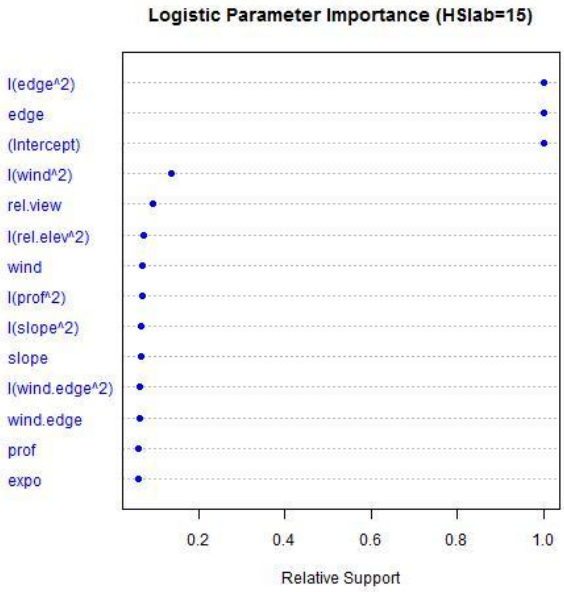
Logistic Parameter Importance (HSlab=15)
I(edge^2)
edge
(Intercept)
I(wind^2)
rel.view
I(rel.elev^2)
wind
I(prof^2)
I(slope^2)
slope
I(wind.edge^2)
wind.edge
prof
expo
0.2
0.4
0.6
0.8
1.0
Relative Support

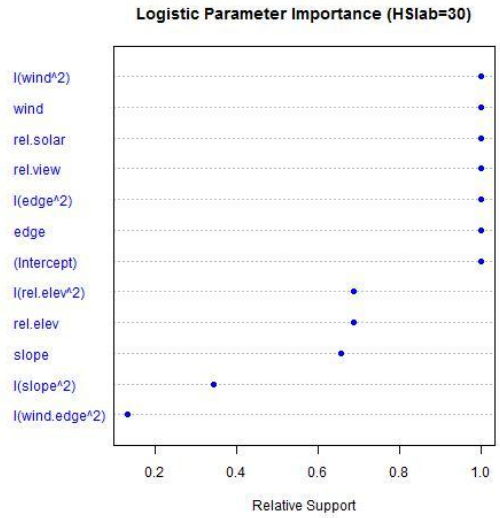

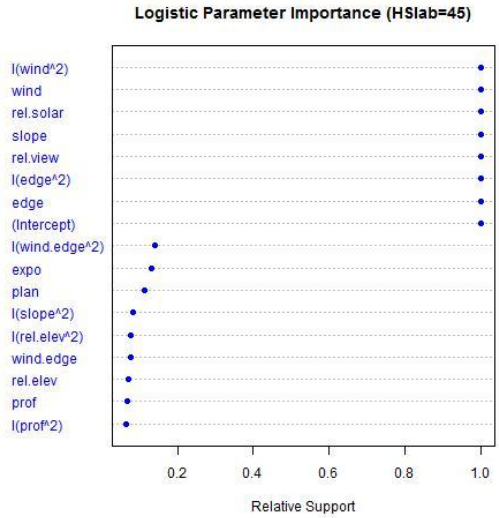

Parameter	Estimates	Lower CL	Upper CL	Odds Ratio	Upper CL Odds Ratio	Lower CL Odds Ratio	Importance
Intercept	0.34238	0.25471	0.43006	1.40830	1.53740	1.29010	1.000
edge	0.04884	0.02160	0.07609	1.05006	1.07910	1.02180	1.000
edge^2	-0.00443	-0.00689	-0.00198	0.99558	0.99800	0.99310	1.000
wind^2	-0.00020	-0.00096	0.00055	0.99980	1.00060	0.99900	0.138
rel.view	-0.00471	-0.02392	0.01449	0.99530	1.01460	0.97640	0.095
rel.elev^2	0.00241	-0.00933	0.01415	1.00242	1.01430	0.99070	0.072
wind	0.00027	-0.00108	0.00163	1.00027	1.00160	0.99890	0.071
prof^2	-0.00004	-0.00027	0.00018	0.99996	1.00020	0.99970	0.070
slope^2	0.00000	-0.00001	0.00001	1.00000	1.00000	1.00000	0.068
slope	-0.00009	-0.00060	0.00043	0.99991	1.00040	0.99940	0.066
wind.edge^2	0.00000	-0.00002	0.00002	1.00000	1.00000	1.00000	0.065
wind.edge	-0.00007	-0.00050	0.00037	0.99993	1.00040	0.99950	0.064
prof	0.00009	-0.00082	0.00100	1.00009	1.00100	0.99920	0.062
expo	-0.00039	-0.00719	0.00640	0.99961	1.00640	0.99280	0.061

Upper A to Zs (Near-Surface Facets)

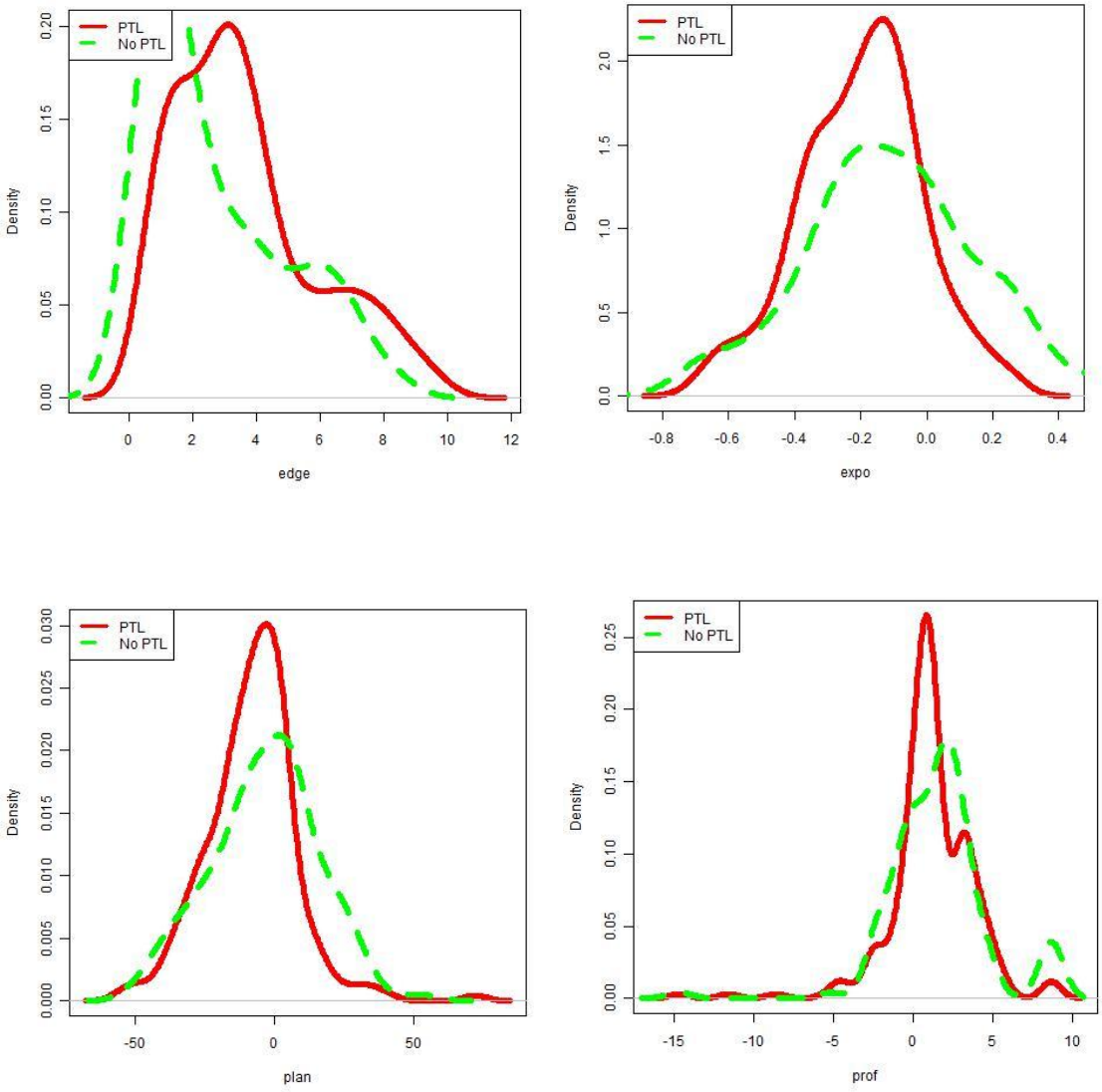

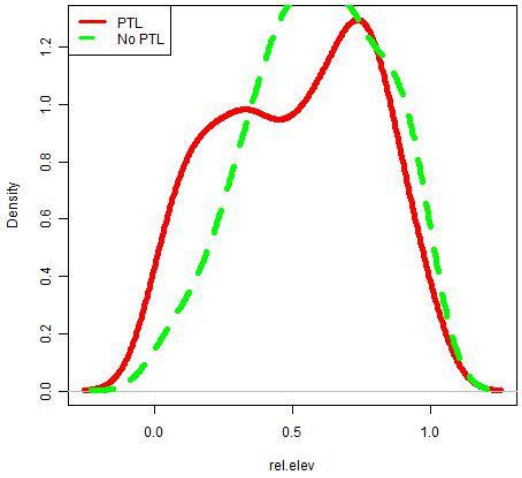
PTL
No PTL
Density
0.0
0.2
0.4
0.6
0.8
1.0
1.2
0.0
0.5
1.0
rel.elev

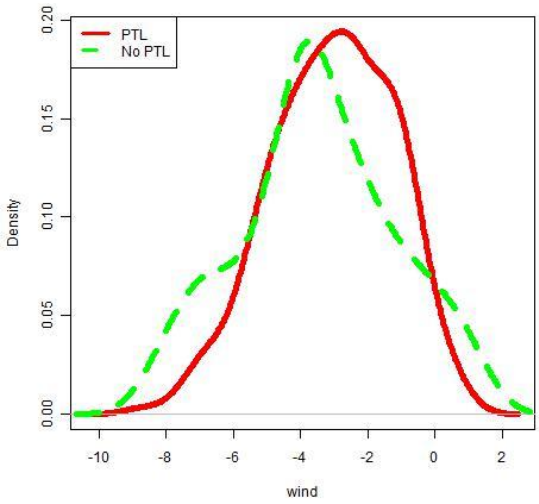
PTL
No PTL
Density
0.00
0.05
0.10
0.15
0.20
-10
-8
-6
-4
-2
0
2
wind

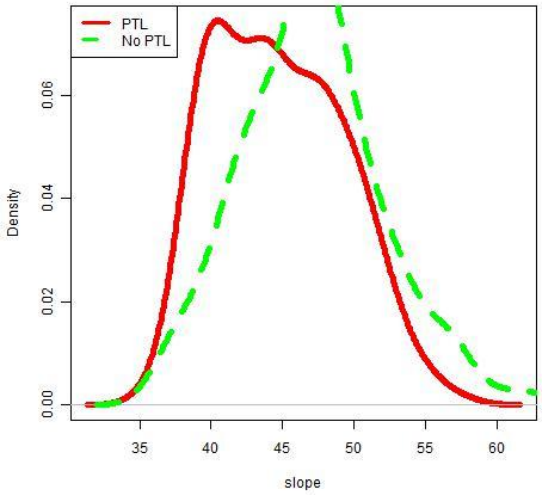
PTL
No PTL
Density
0.00
0.02
0.04
0.06
35
40
45
50
55
60
slope

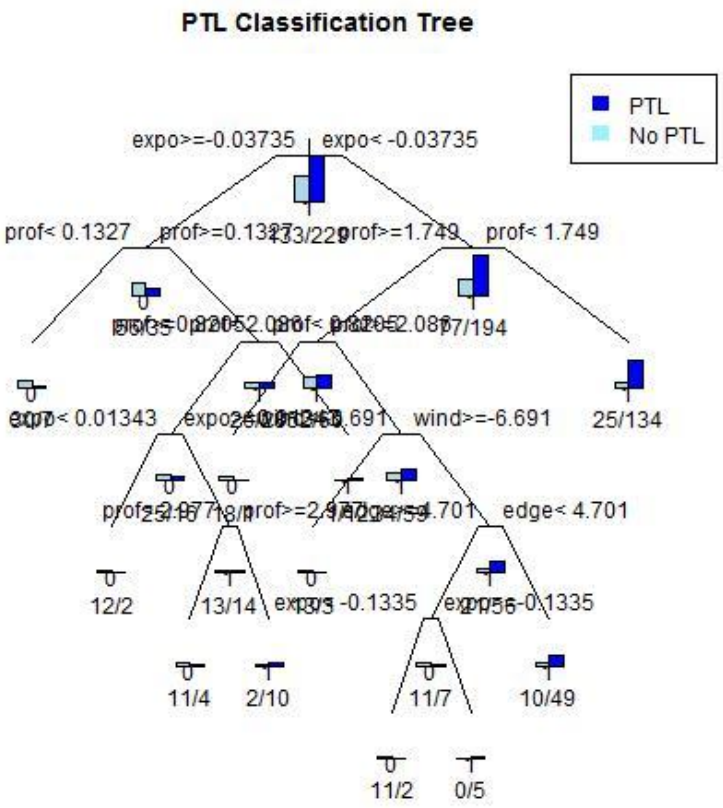
PTL Classification Tree
PTL
No PTL
expo>=-0.03735
expo< -0.03735
prof< 0.1327
prof>=1.749
prof< 1.749
97/194
wind>=-6.691
25/134
edge< 4.701
12/2
13/14
11/4
2/10
11/7
10/49
11/2
0/5

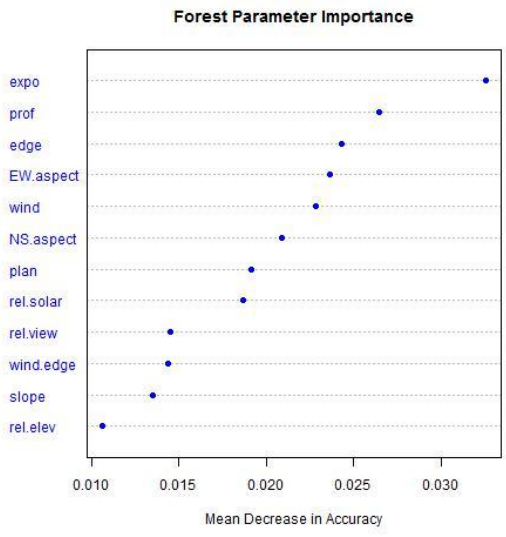
Forest Parameter Importance
expo
prof
edge
EW.aspect
wind
NS.aspect
plan
rel.solar
rel.view
wind.edge
slope
rel.elev
0.010
0.015
0.020
0.025
0.030
Mean Decrease in Accuracy

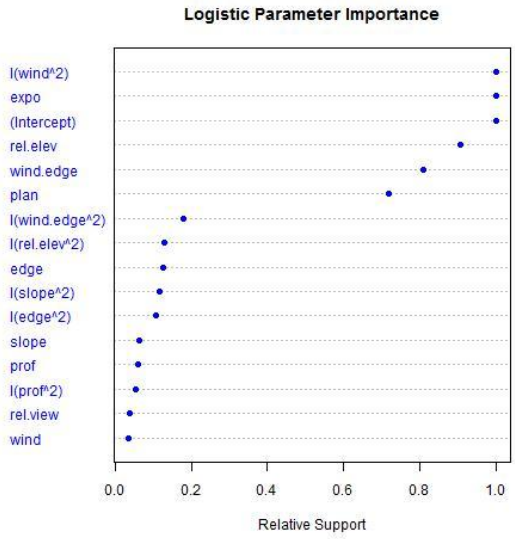
Logistic Parameter Importance
I(wind^2)
expo
(Intercept)
rel.elev
wind.edge
plan
I(wind.edge^2)
I(rel.elev^2)
edge
I(slope^2)
I(edge^2)
slope
prof
I(prof^2)
rel.view
wind
0.0
0.2
0.4
0.6
0.8
1.0
Relative Support

	Estimates	Lower CL	Upper CL	Odds Ratio	Upper CL Odds Ratio	Lower CL Odds Ratio	Importance
Intercept	0.93684	0.71237	1.16131	2.55191	3.1941	2.0388	1
expo	-0.99988	-1.36579	-0.63396	0.36792	0.5305	0.2552	1
rel.elev	-0.32672	-0.55218	-0.10127	0.72128	0.9037	0.5757	1
wind^2	-0.01306	-0.01704	-0.00908	0.98702	0.991	0.9831	1
plan	0.00343	-0.00114	0.008	1.00344	1.008	0.9989	0.837
wind.edge^2	-0.00069	-0.00158	0.00021	0.99931	1.0002	0.9984	0.831
prof	-0.00258	-0.0119	0.00674	0.99742	1.0068	0.9882	0.194
edge	0.00309	-0.0083	0.01447	1.00309	1.0146	0.9917	0.176
wind.edge	-0.00221	-0.01133	0.0069	0.99779	1.0069	0.9887	0.152
slope	-0.00073	-0.00375	0.0023	0.99927	1.0023	0.9963	0.089
prof^2	-0.00012	-0.00061	0.00037	0.99988	1.0004	0.9994	0.087
rel.elev^2	0.01404	-0.06196	0.09004	1.01414	1.0942	0.9399	0.066

North Summit/ Lone Lake (Near-Surface Facets)

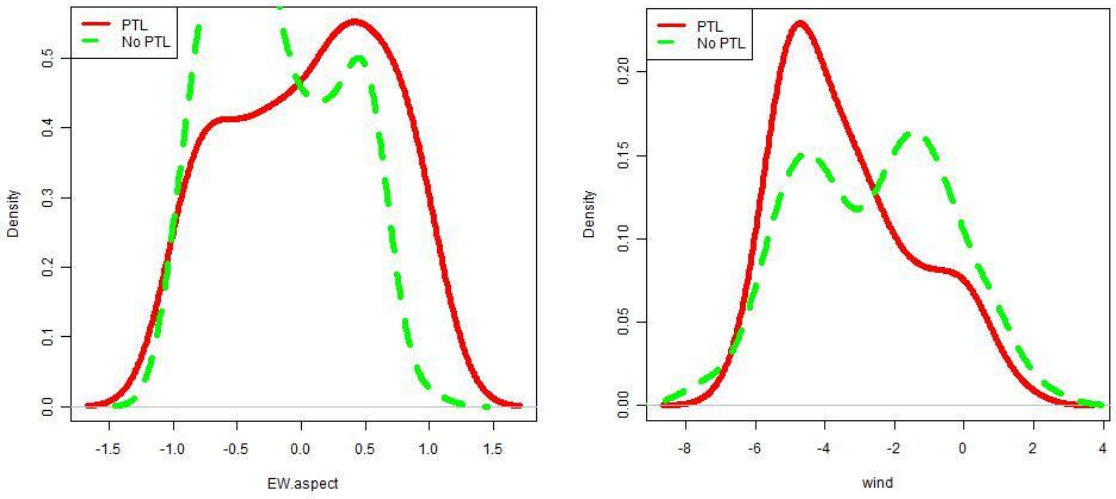

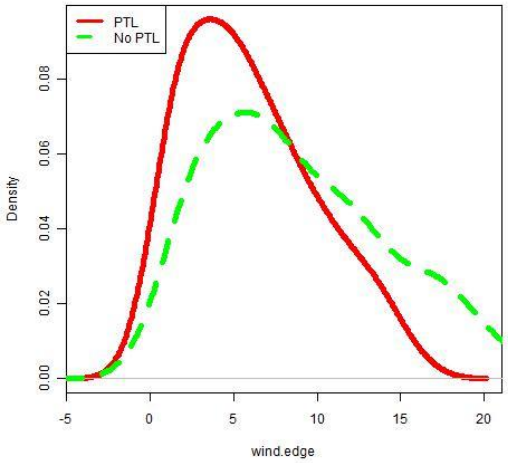
PTL
No PTL
Density
0.00
0.02
0.04
0.06
0.08
-5
0
5
10
15
20
wind.edge

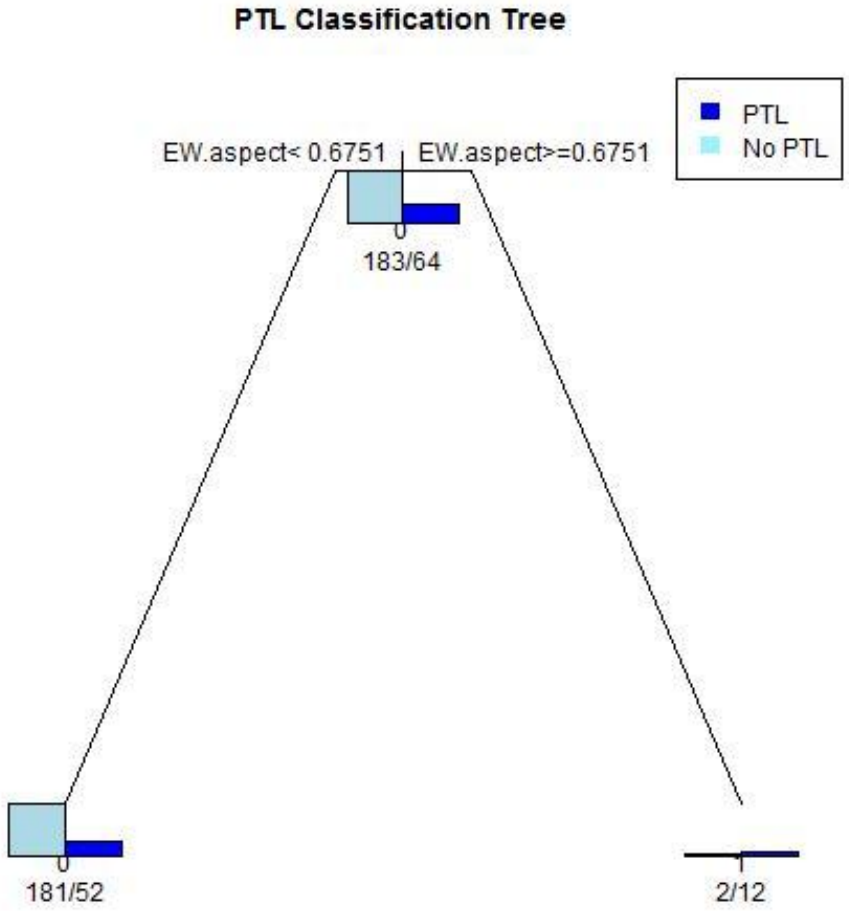
PTL Classification Tree
PTL
No PTL
EW.aspect< 0.6751
EW.aspect>=0.6751
0
183/64
0
181/52
2/12

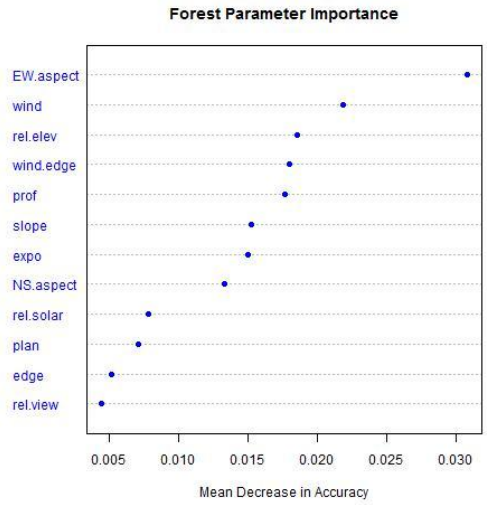

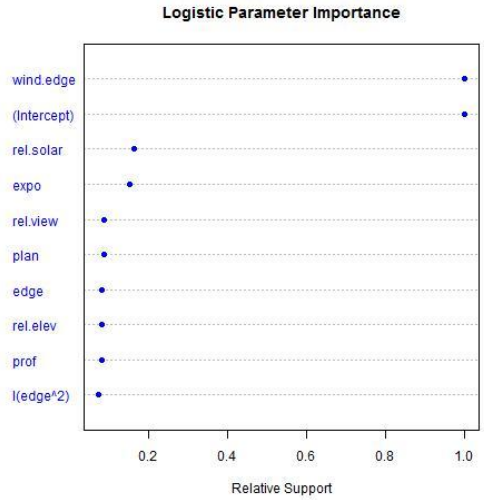

	Estimates	Lower CL	Upper CL	Odds Ratio	Upper CL Odds Ratio	Lower CL Odds Ratio	Importance
Intercept	0.37127	0.21145	0.53109	1.44958	1.7008	1.2355	1
wind.edge	-0.02287	-0.03597	-0.00977	0.97739	0.9903	0.9647	1
rel.solar	0.09977	-0.18466	0.38419	1.10491	1.4684	0.8314	0.344
rel.view	0.04383	-0.10208	0.18974	1.0448	1.2089	0.903	0.279
expo	-0.05859	-0.25078	0.13359	0.94309	1.1429	0.7782	0.24
plan	-0.00013	-0.00071	0.00045	0.99987	1.0005	0.9993	0.074
rel.elev^2	0.00578	-0.0216	0.03315	1.00579	1.0337	0.9786	0.071
rel.elev	0.006	-0.02234	0.03433	1.00601	1.0349	0.9779	0.071
prof	-0.0008	-0.00471	0.00311	0.9992	1.0031	0.9953	0.069

Granite Canyon (Surface Hoar)

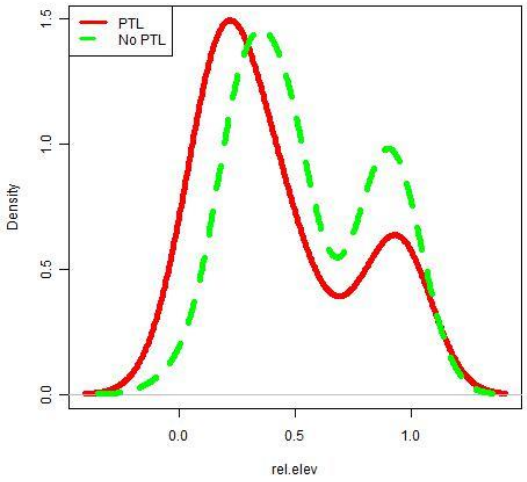

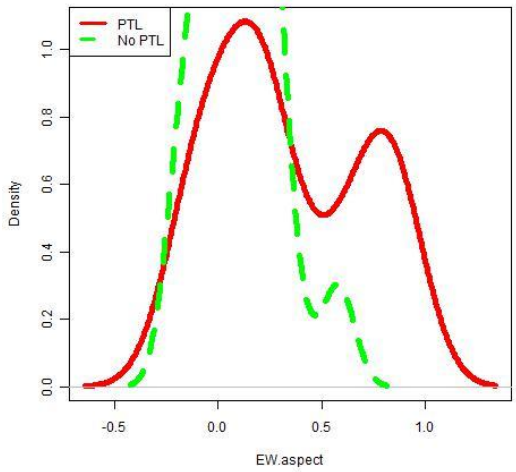

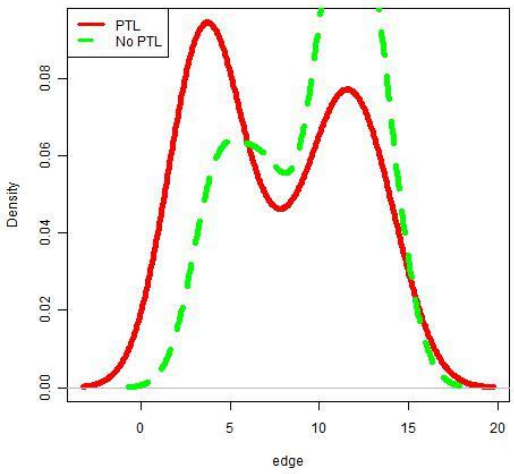

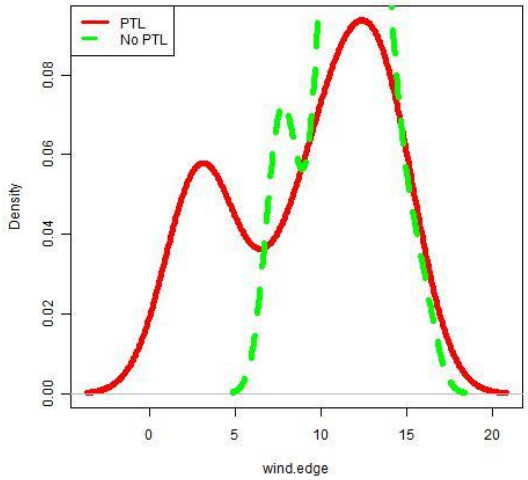

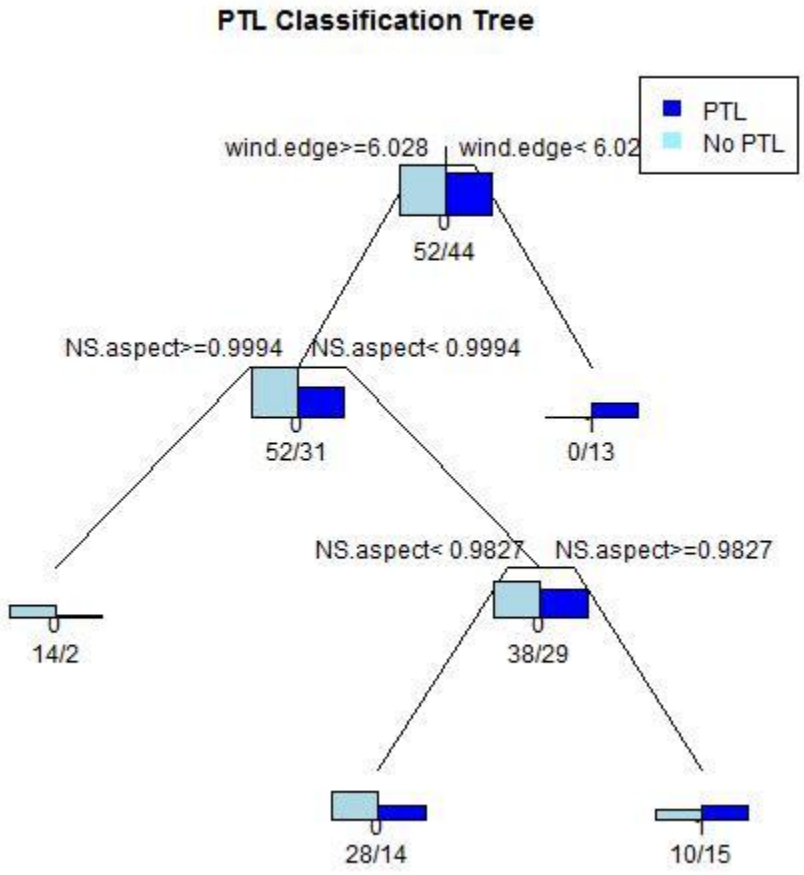
PTL Classification Tree
PTL
No PTL
wind.edge>=6.028
wind.edge< 6.02
52/44
NS.aspect>=0.9994
NS.aspect< 0.9994
52/31
0/13
NS.aspect< 0.9827
NS.aspect>=0.9827
14/2
38/29
28/14
10/15

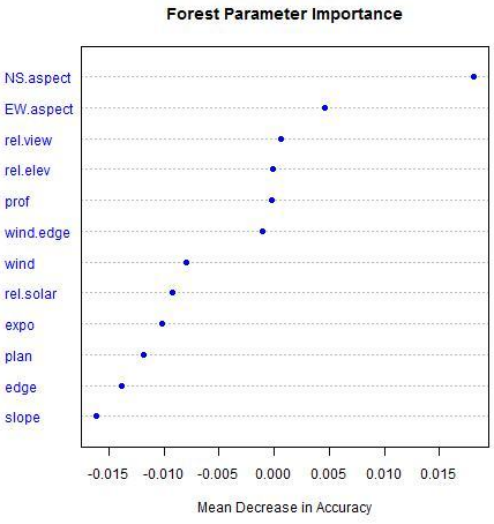
Forest Parameter Importance
NS.aspect
EW.aspect
rel.view
rel.elev
prof
wind.edge
wind
rel.solar
expo
plan
edge
slope
-0.015
-0.010
-0.005
0.000
0.005
0.010
0.015
Mean Decrease in Accuracy

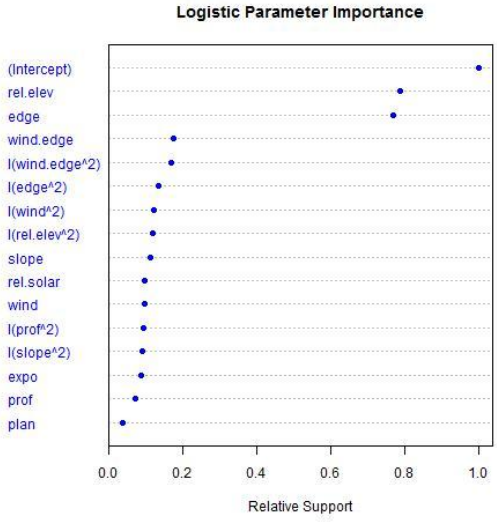
Logistic Parameter Importance
(Intercept)
rel.elev
edge
wind.edge
I(wind.edge^2)
I(edge^2)
I(wind^2)
I(rel.elev^2)
slope
rel.solar
wind
I(prof^2)
I(slope^2)
expo
prof
plan
0.0
0.2
0.4
0.6
0.8
1.0
Relative Support

	Estimates	Lower CL	Upper CL	Odds Ratio	Upper CL Odds Ratio	Lower CL Odds Ratio	Importance
Intercept	1.25459	0.63266	1.87652	3.50641	6.5308	1.8826	1
rel.elev	-0.47196	-1.10701	0.16309	0.62378	1.1771	0.3305	0.789
edge	-0.04533	-0.10544	0.01479	0.95569	1.0149	0.8999	0.77
wind.edge	-0.02714	-0.12219	0.06792	0.97323	1.0703	0.885	0.177
wind.edge^2	0.00117	-0.00303	0.00537	1.00117	1.0054	0.997	0.17
edge^2	-0.0002	-0.00174	0.00133	0.9998	1.0013	0.9983	0.136
wind^2	0.00536	-0.01612	0.02685	1.00538	1.0272	0.984	0.122
rel.elev^2	-0.02305	-0.21074	0.16464	0.97721	1.179	0.81	0.117
slope	-0.00065	-0.00524	0.00395	0.99935	1.004	0.9948	0.111
wind	-0.01506	-0.07527	0.04515	0.98505	1.0462	0.9275	0.097
rel.solar	0.01021	-0.04733	0.06776	1.01026	1.0701	0.9538	0.097
prof^2	0.00081	-0.00261	0.00423	1.00081	1.0042	0.9974	0.094
slope^2	-0.00001	-0.00008	0.00005	0.99999	1.0001	0.9999	0.09
expo	-0.03161	-0.1616	0.09838	0.96888	1.1034	0.8508	0.088
prof	0.00542	-0.02128	0.03212	1.00543	1.0326	0.9789	0.072
plan	-0.00002	-0.00029	0.00024	0.99998	1.0002	0.9997	0.038

Jack Creek (Surface Hoar)

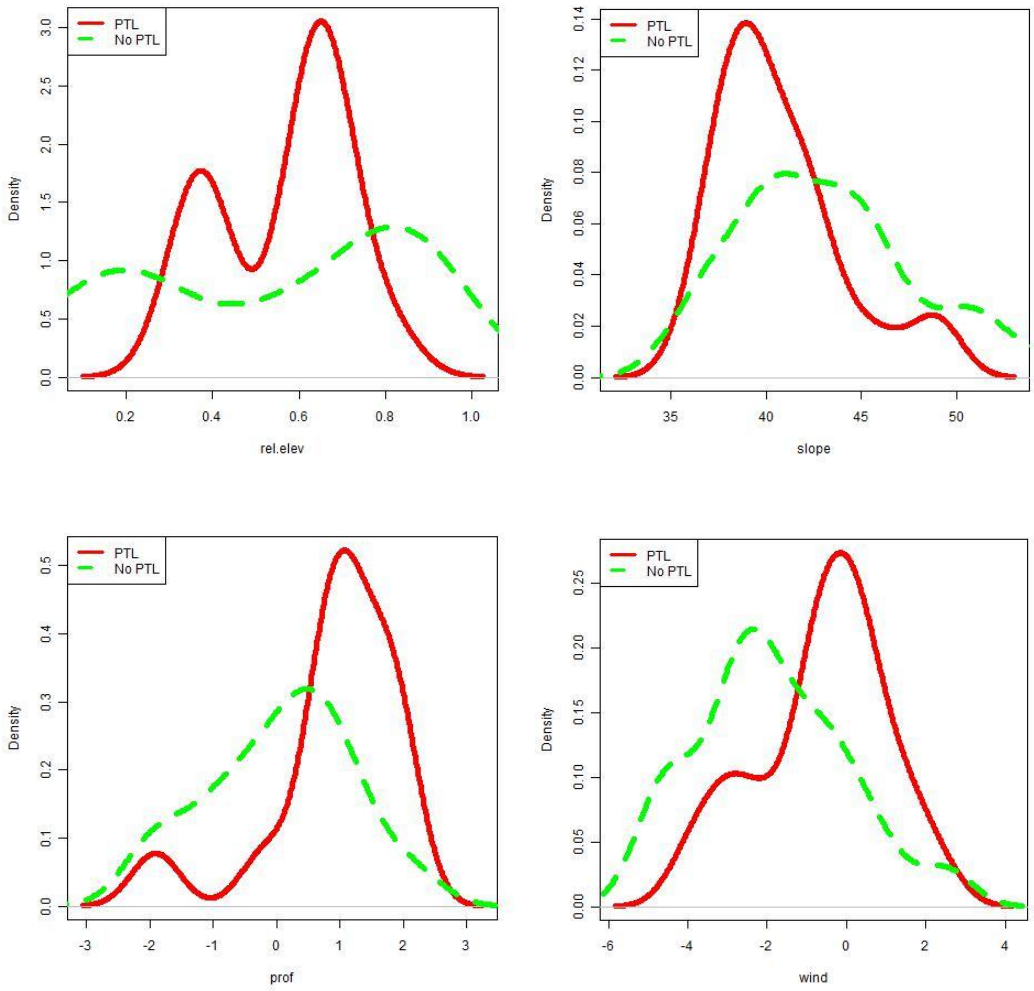

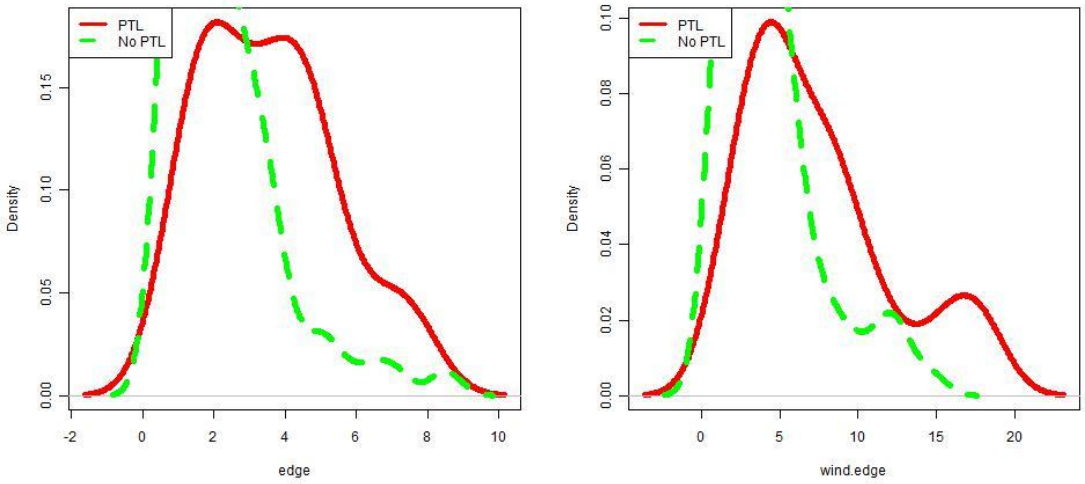
PTL
No PTL
Density
edge
wind.edge

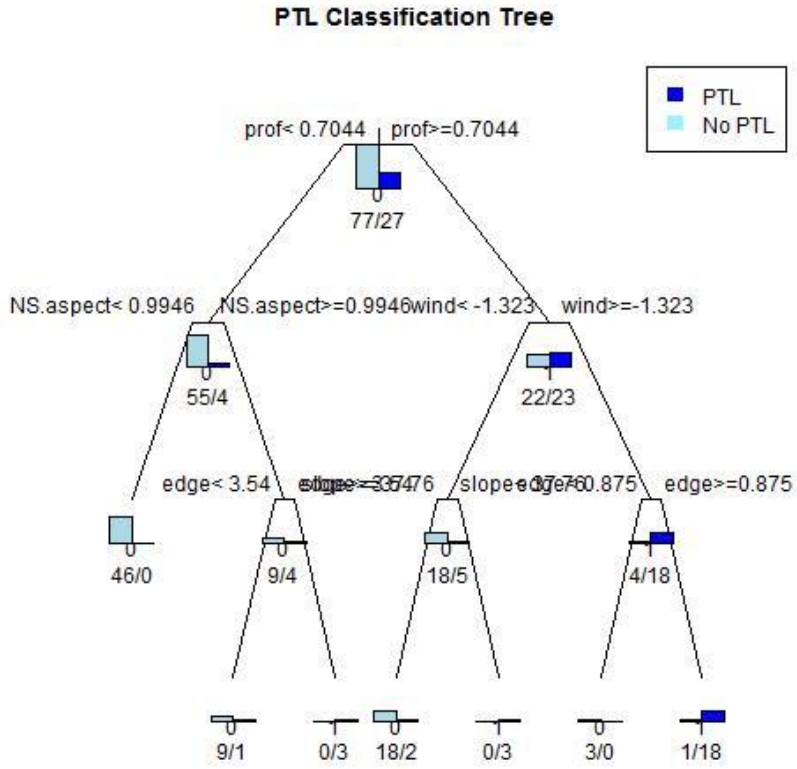
PTL Classification Tree
PTL
No PTL
prof< 0.7044
prof>=0.7044
77/27
NS.aspect< 0.9946
NS.aspect>=0.9946
wind< -1.323
wind>=-1.323
55/4
22/23
edge< 3.54
edge>=0.875
46/0
9/4
18/5
4/18
9/1
0/3
18/2
0/3
3/0
1/18

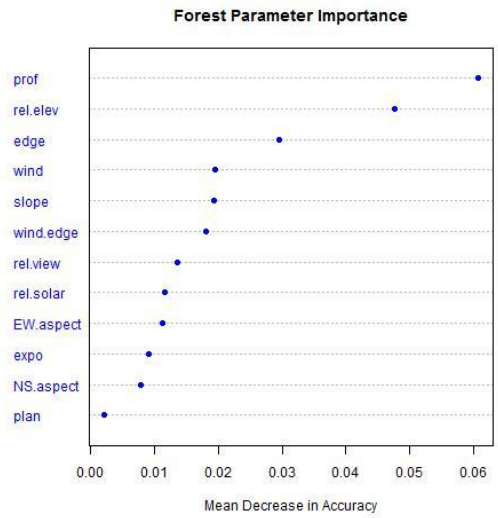

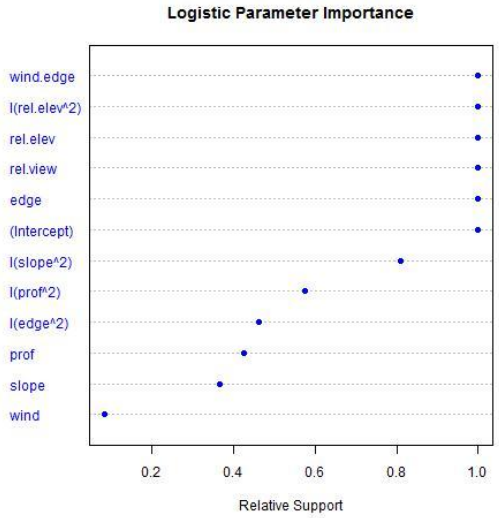

	Estimates	Lower CL	Upper CL	Odds Ratio	Upper CL Odds Ratio	Lower CL Odds Ratio	Importance
Intercept	-28.0749	-65.7923	9.6425	0.000000	1.541E+04	0.00000	1
edge	1.64693	-0.59869	3.89255	5.191040	49.03590	0.54950	1
rel.view	-5.35346	-10.287	-0.41992	0.004730	0.65710	0.00000	1
rel.elev	103.0932	37.05732	169.1291	5.926E+44	2.830E+73	1.241E+16	1
rel.elev^2	-96.775	-155.882	-37.6675	0.000000	0.00000	0.00000	1
wind.edge	0.47467	0.10713	0.84221	1.607490	2.32150	1.11310	1
slope^2	-0.00638	-0.02399	0.01122	0.993640	1.01130	0.97630	0.81
prof^2	-0.08401	-0.26715	0.09914	0.919430	1.10420	0.76560	0.574
edge^2	-0.10815	-0.41009	0.1938	0.897500	1.21380	0.66360	0.461
prof	0.29019	-0.46322	1.0436	1.336690	2.83940	0.62930	0.426
slope	0.26007	-1.20673	1.72687	1.297020	5.62300	0.29920	0.365
wind	-0.02505	-0.15358	0.10349	0.975260	1.10900	0.85760	0.083

APPENDIX C

SUPPLEMENTARY 3D MAPS

Appendix C contains a selection of three-dimensional maps to supplement text and maps in the main document. The graphics were created in ArcScene.

Terrain Parameter Grids for Lone Lake Couloir

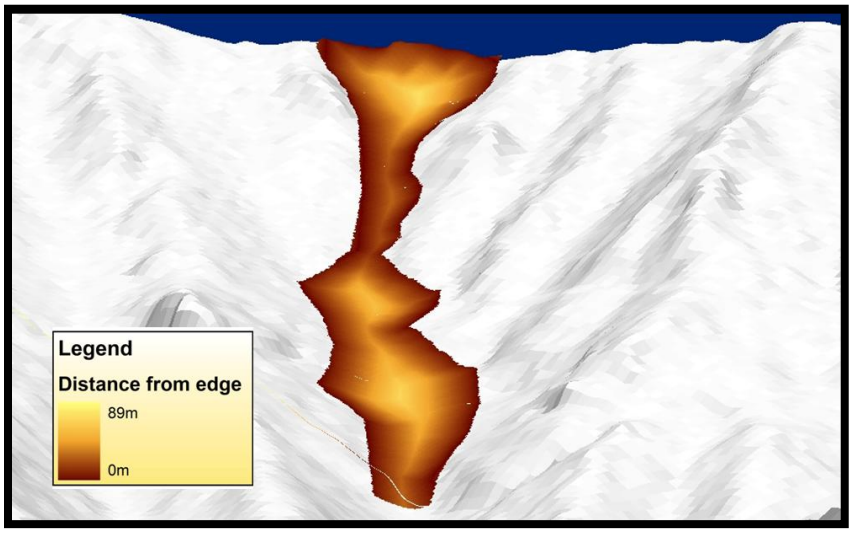

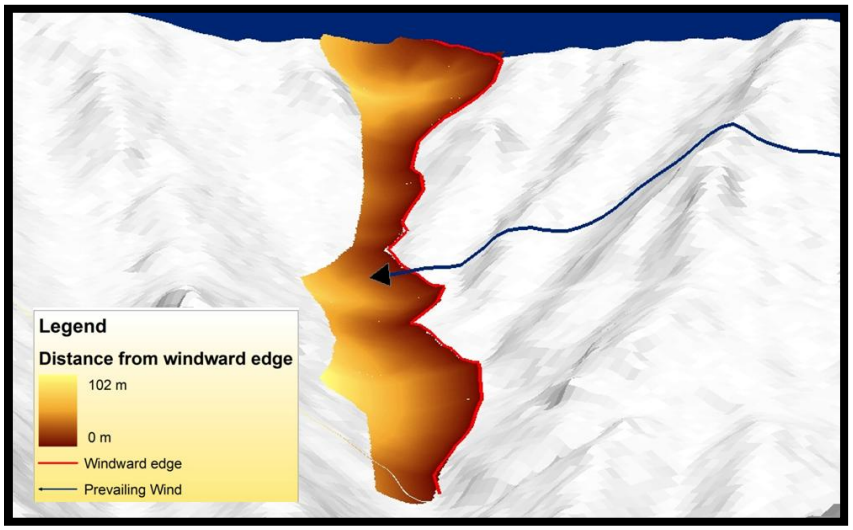

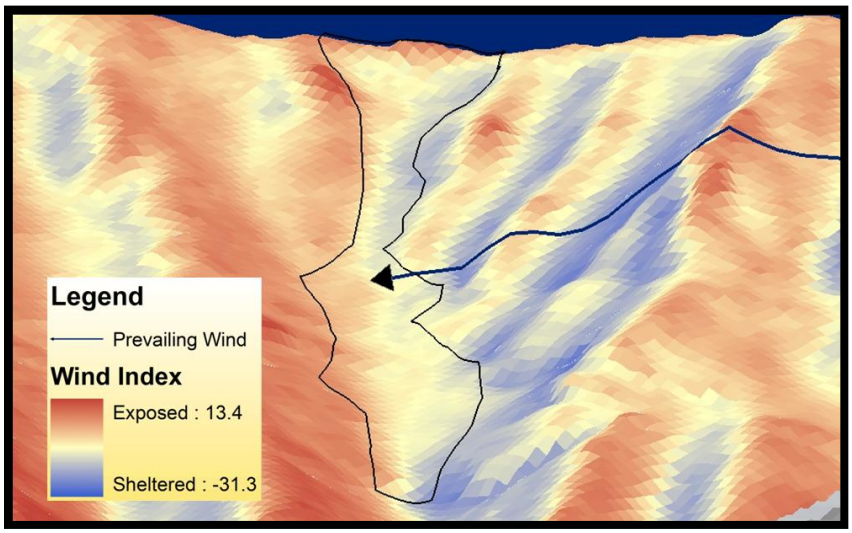
Legend
Prevailing Wind
Wind Index
Exposed : 13.4
Sheltered : -31.3

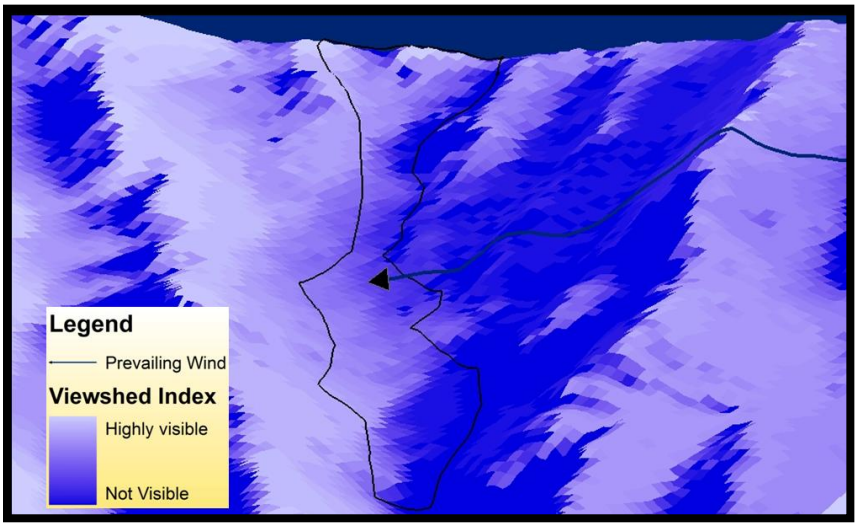
Legend
Prevailing Wind
Viewshed Index
Highly visible
Not Visible

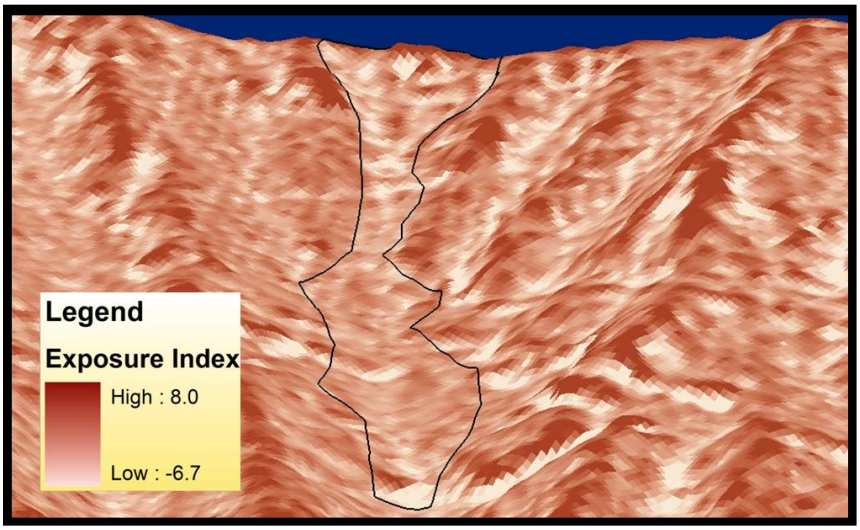
Legend
Exposure Index
High : 8.0
Low : -6.7

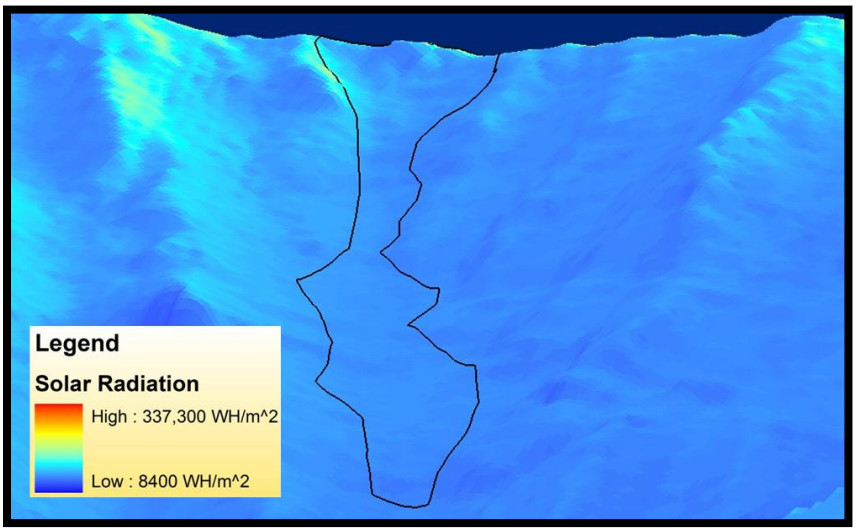
Legend
Solar Radiation
High : 337,300 WH/m^2
Low : 8400 WH/m^2

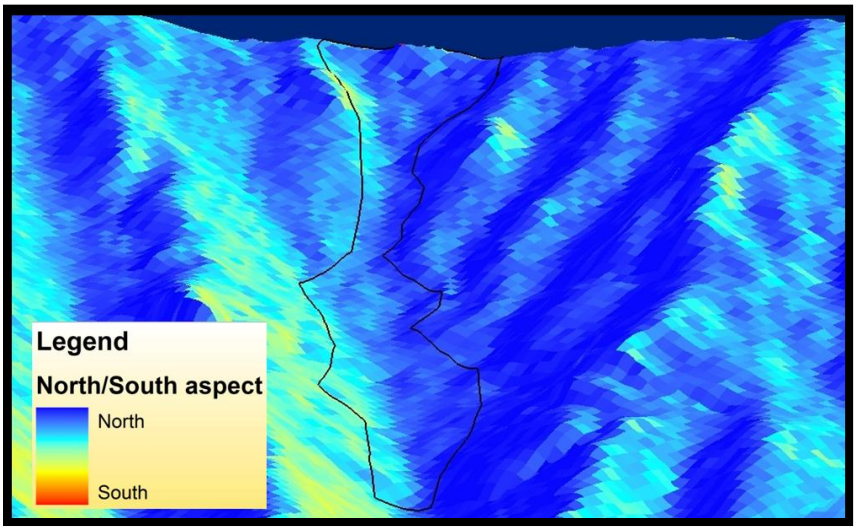
Legend
North/South aspect
North
South

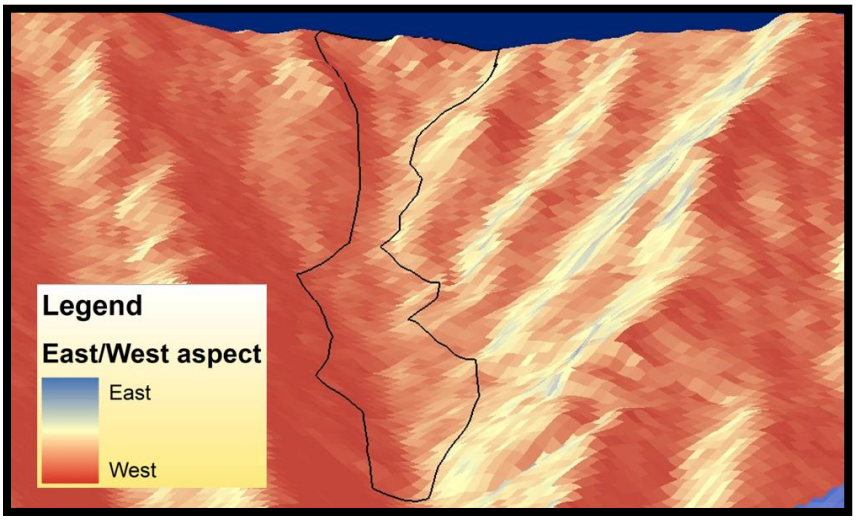
Legend
East/West aspect
East
West

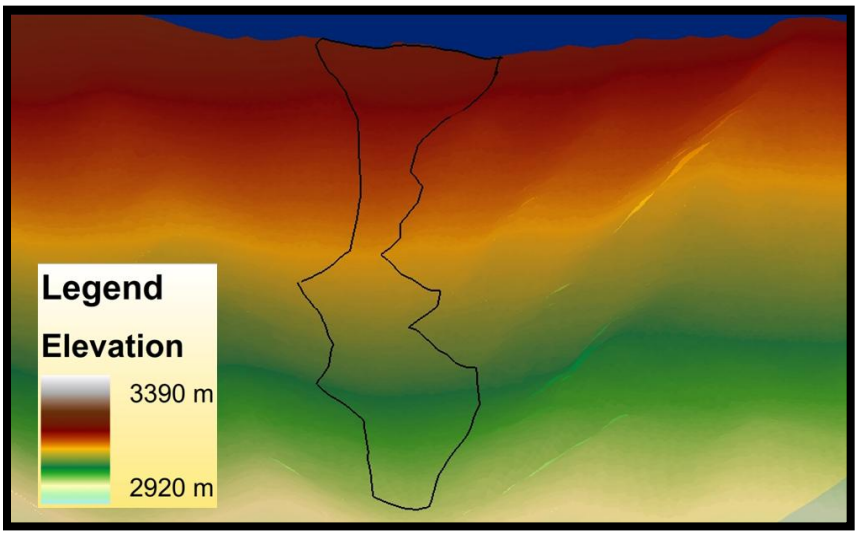
Legend
Elevation
3390 m
2920 m

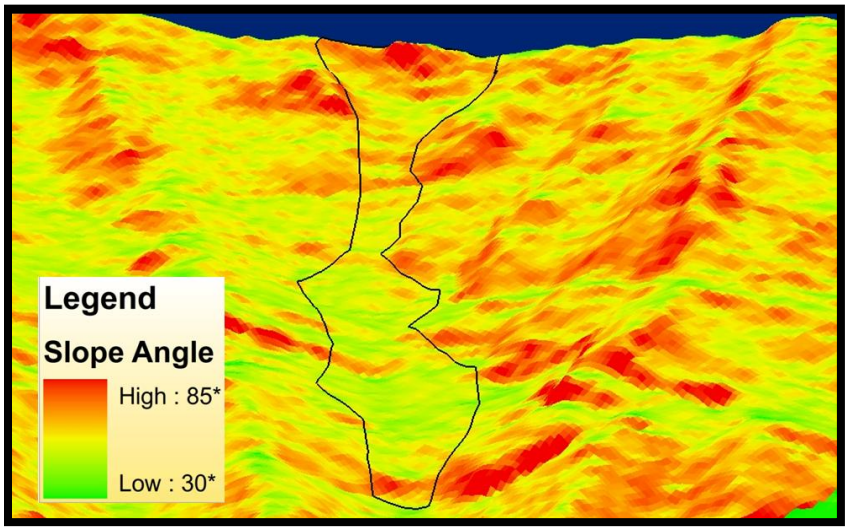
Legend
Slope Angle
High : 85*
Low : 30*

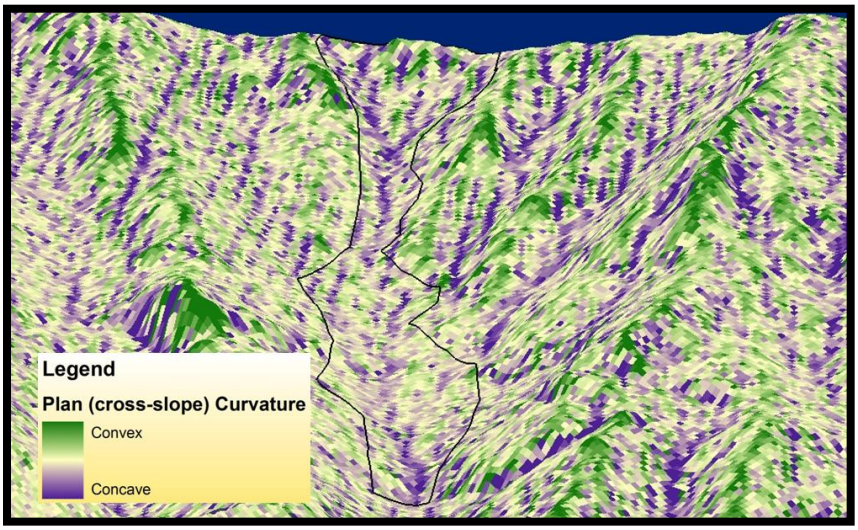
Legend
Plan (cross-slope) Curvature
Convex
Concave

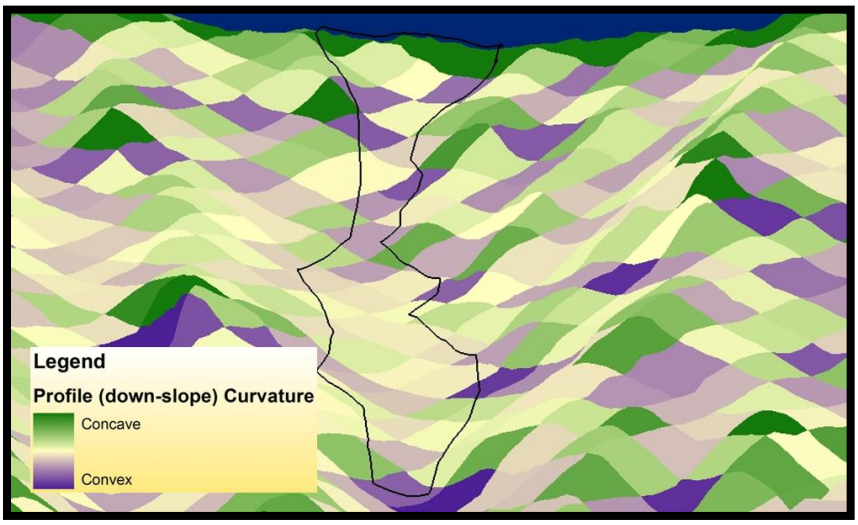
Legend
Profile (down-slope) Curvature
Concave
Convex

Main Document Supplementary Figures

The following are 3D maps re-illustrating a selection of figures presented in the main body of this document to aid in visualization. Below each figure in this appendix is a caption noting which figure(s) in the document the graphic refers to.

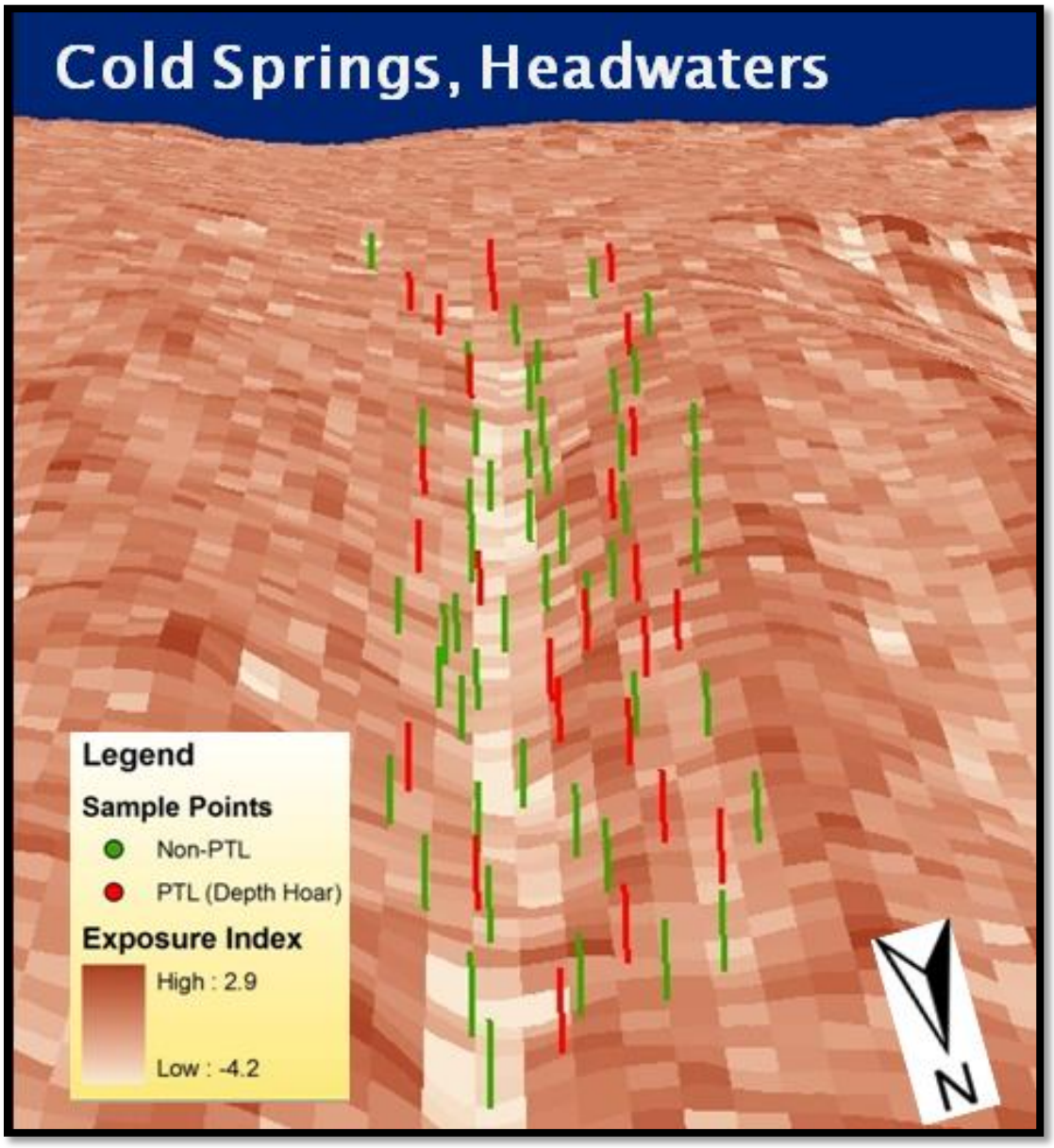

Fig. 37c

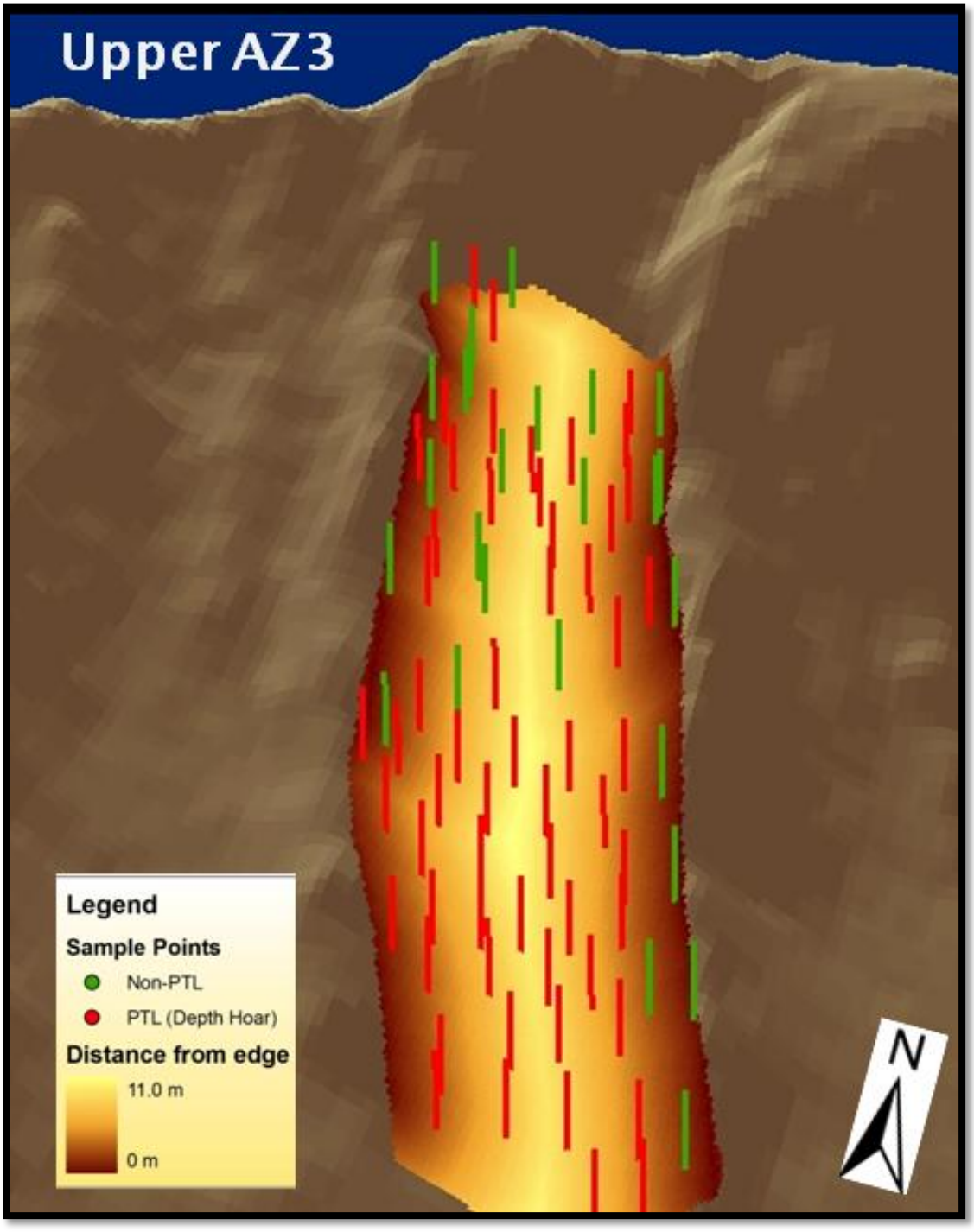
Upper AZ3
Legend
Sample Points
Non-PTL
PTL (Depth Hoar)
Distance from edge
11.0 m
0 m
N

Fig. 37b

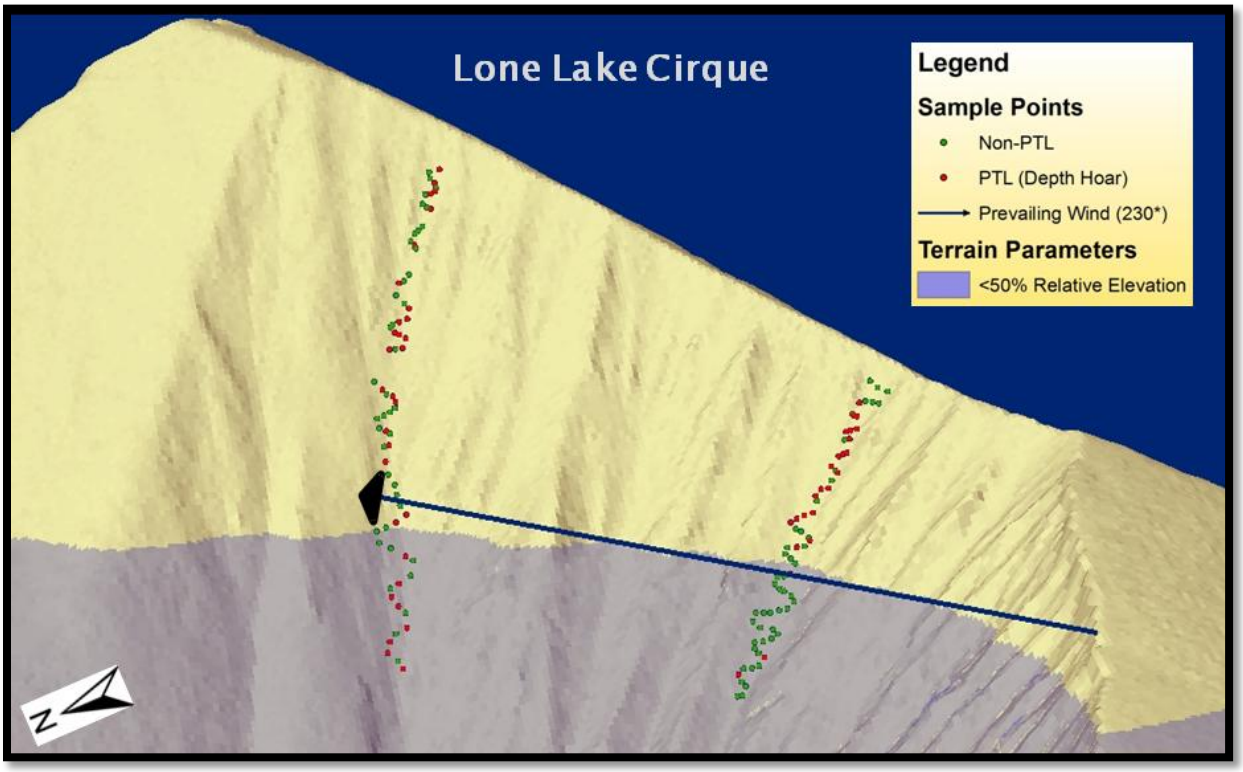
Lone Lake Cirque
Legend
Sample Points
Non-PTL
PTL (Depth Hoar)
Prevailing Wind (230*)
Terrain Parameters
<50% Relative Elevation
N

Fig. 41

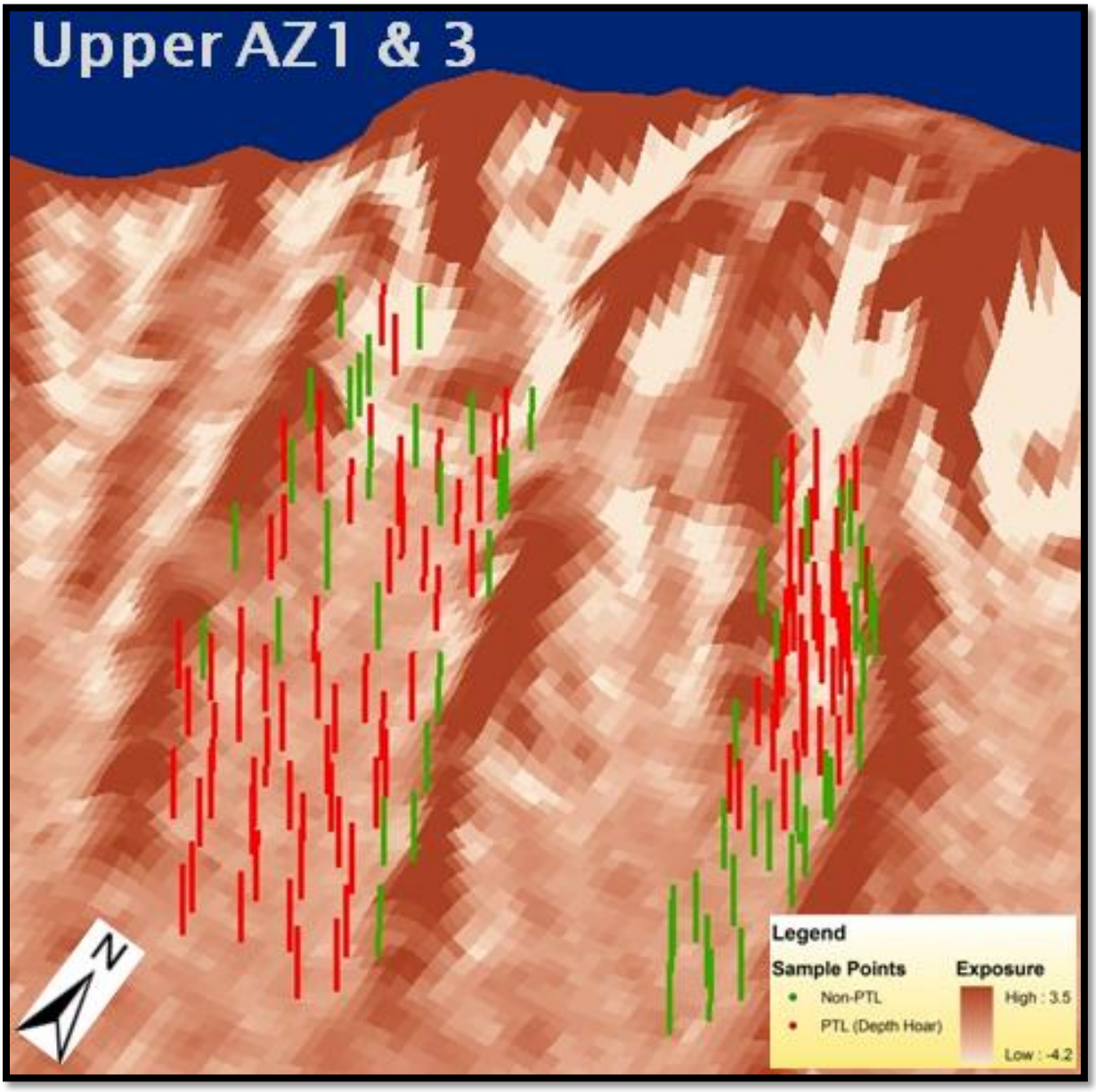

Figs. 22 and 43

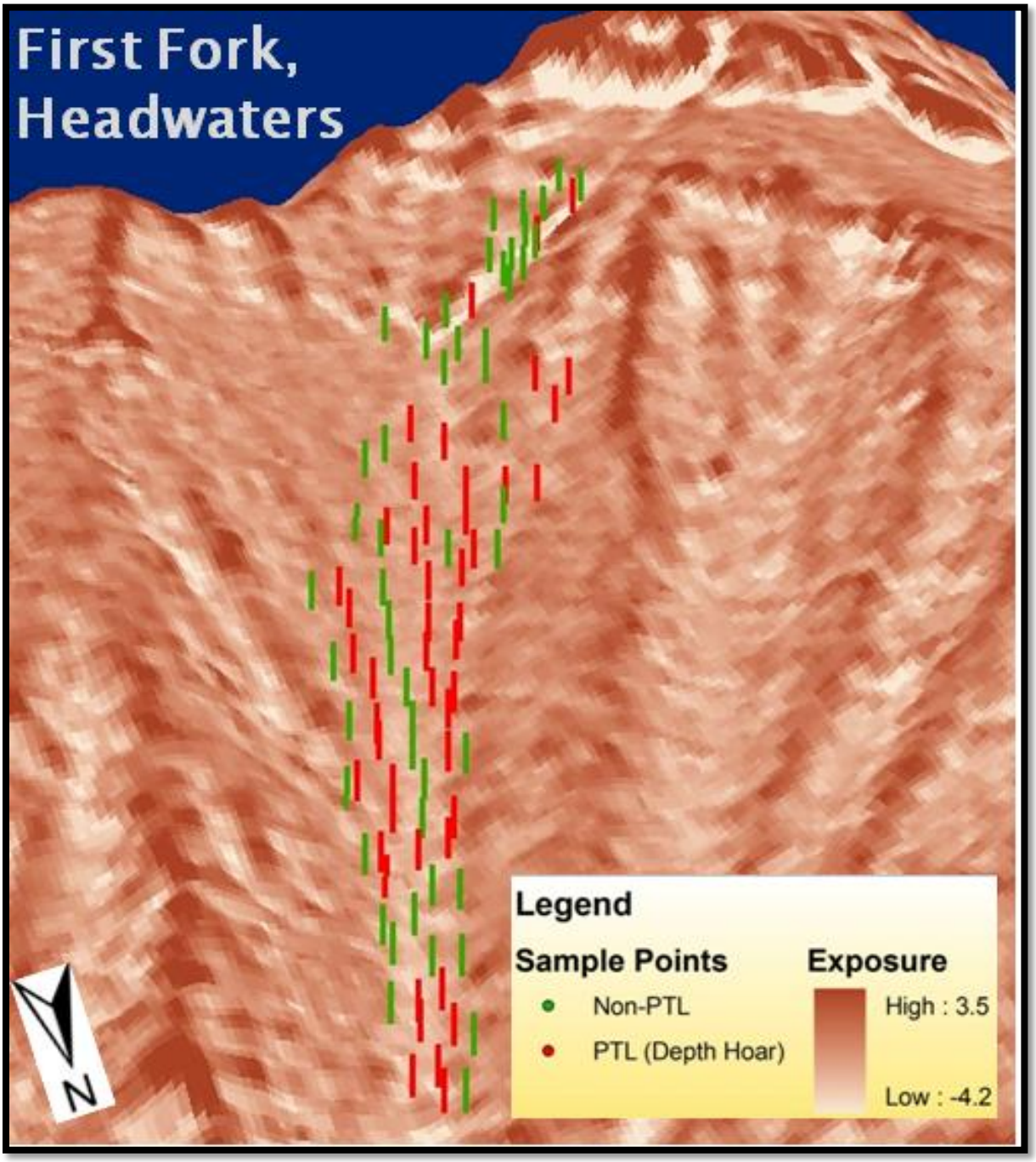
First Fork,
Headwaters
Legend
Sample Points
Non-PTL
PTL (Depth Hoar)
Exposure
High : 3.5
Low : -4.2
N

Fig. 44

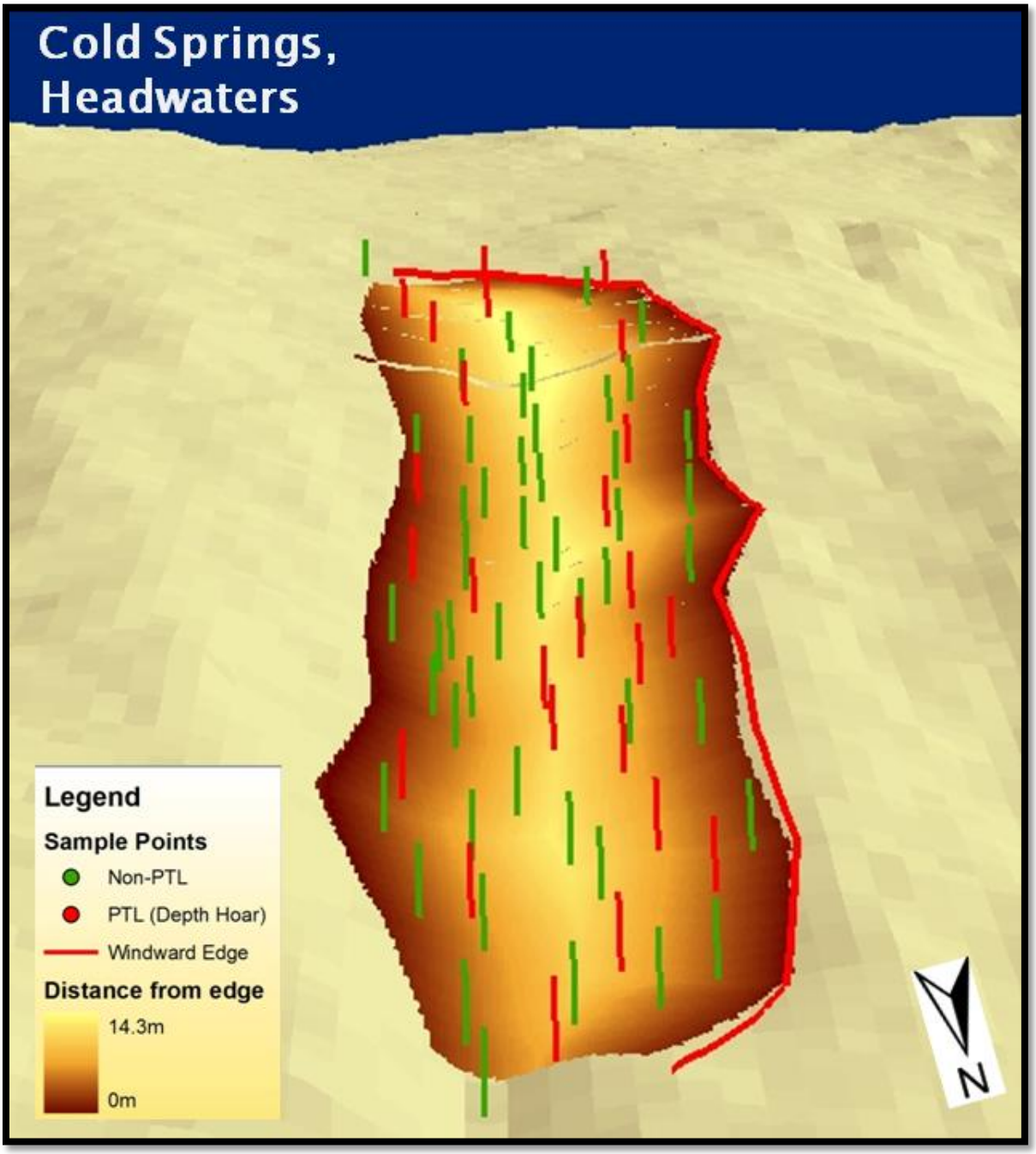
Cold Springs,
Headwaters
Legend
Sample Points
Non-PTL
PTL (Depth Hoar)
Windward Edge
Distance from edge
14.3m
0m
N

Fig. 45

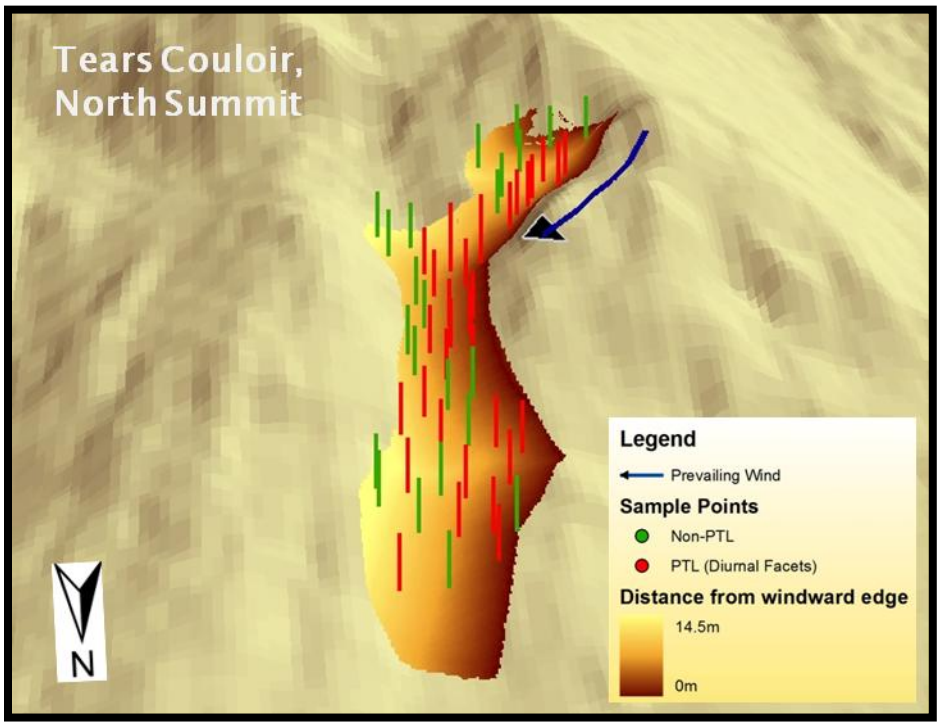
Tears Couloir,
North Summit
Legend
Prevailing Wind
Sample Points
Non-PTL
PTL (Diurnal Facets)
Distance from windward edge
14.5m
0m
N

Fig. 49

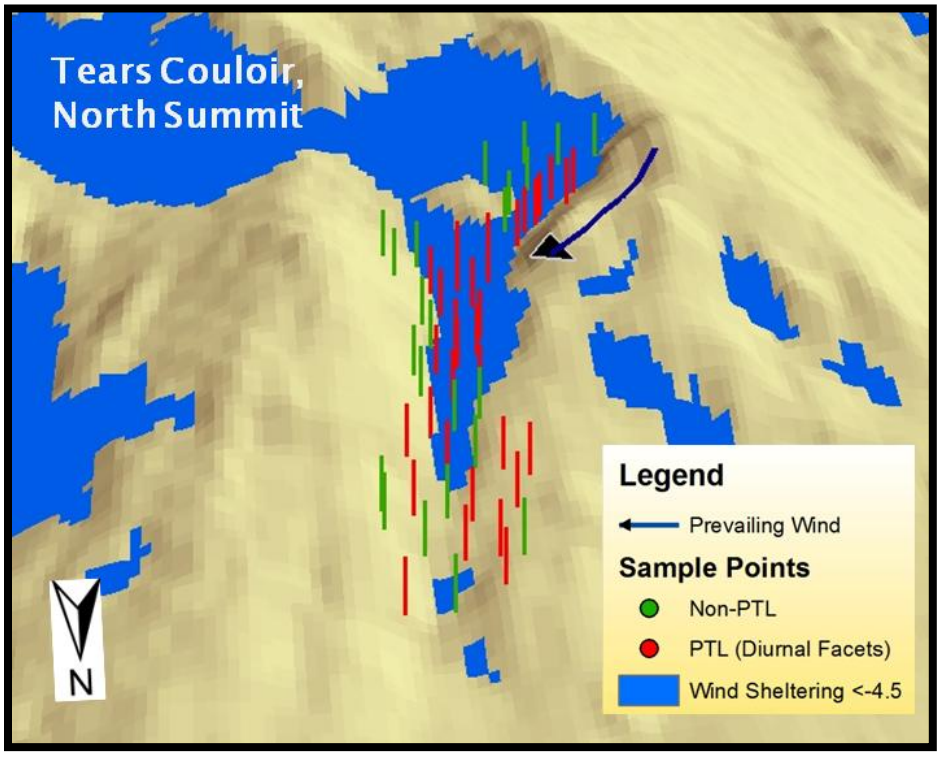
Tears Couloir,
North Summit
Legend
Prevailing Wind
Sample Points
Non-PTL
PTL (Diurnal Facets)
Wind Sheltering <-4.5
N

Fig. 49

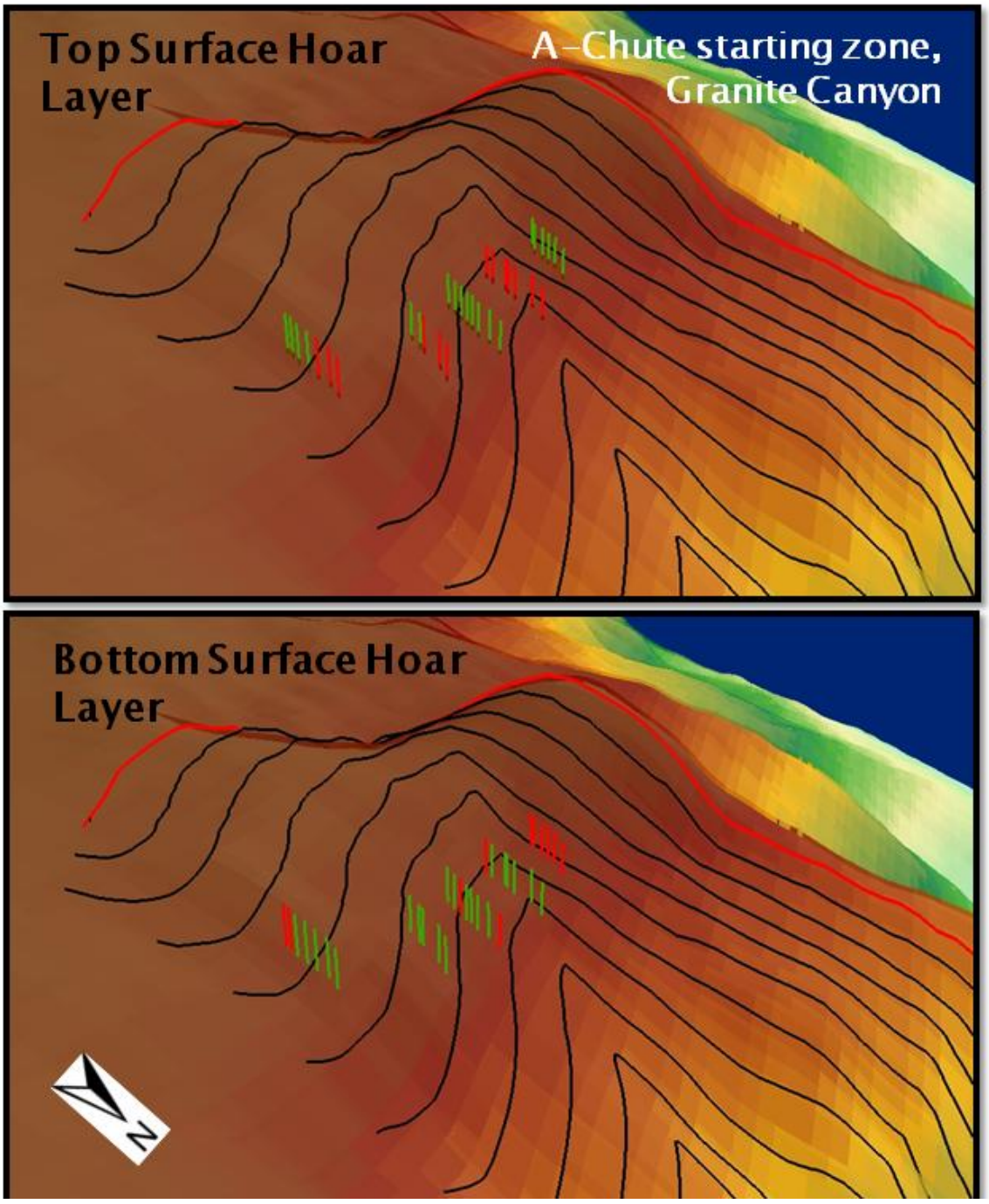
Top Surface Hoar Layer
A-Chute starting zone, Granite Canyon
Bottom Surface Hoar Layer
N

Fig. 50

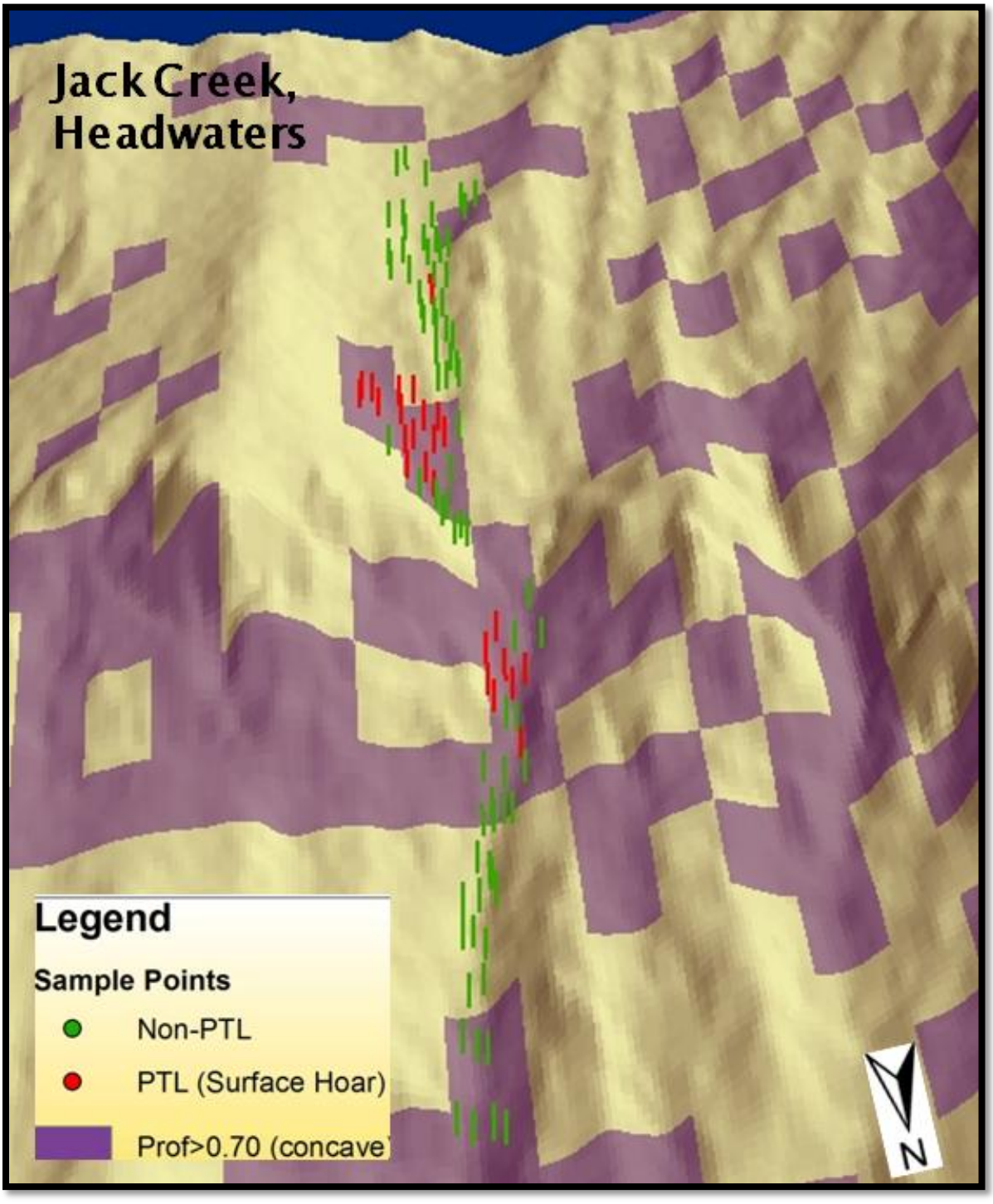
Jack Creek,
Headwaters
Legend
Sample Points
Non-PTL
PTL (Surface Hoar)
Prof>0.70 (concave
N

Fig. 52

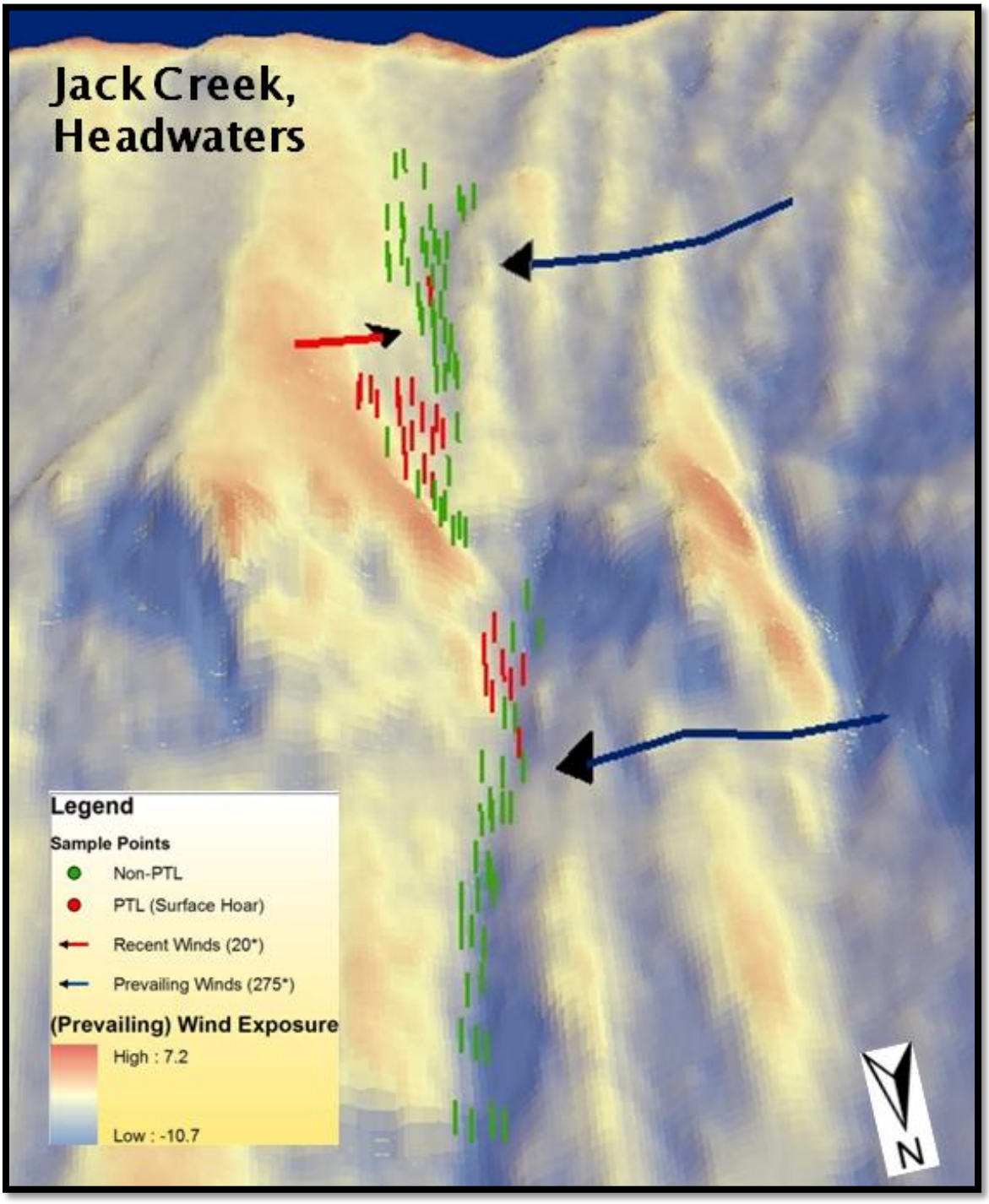
Jack Creek,
Headwaters
Legend
Sample Points
Non-PTL
PTL (Surface Hoar)
Recent Winds (20°)
Prevailing Winds (275°)
(Prevailing) Wind Exposure
High : 7.2
Low : -10.7
N

Fig. 52